INVESTIGATIONS ON THE REMOVAL OF IRON FROM ILMENITE

THESIS SUBMITTED TO
THE UNIVERSITY OF KERALA
IN FULFILMENT OF THE REQUIREMENTS
FOR THE DEGREE OF

DOCTOR OF PHILOSOPHY

IN CHEMISTRY
UNDER THE FACULTY OF SCIENCE

BY
E. JEYA KUMARI

BEACH SAND MINERALS RESEARCH
REGIONAL RESEARCH LABORATORY (CSIR)
TRIVANDRUM-695 019, KERALA, INDIA

JANUARY, 2001

DEDICATED TO
MY PARENTS AND TEACHERS

DECLARATION

I hereby declare that, the thesis entitled "***INVESTIGATIONS ON THE REMOVAL OF IRON FROM ILMENITE***" embodies the results of the investigations carried out by me at the Beach Sand Minerals Research of the Regional Research Laboratory (CSIR), Trivandrum, under the supervision of ***Dr .P. N. Mohan Das*** and the same has not been submitted elsewhere for a degree.

E. Jeya Kumari

January, 2001

Dr. P. N. MOHAN DAS, M.Sc., Ph.D.
DEPUTY DIRECTOR
HEAD, BSMR

REGIONAL RESEARCH LABORATORY (CSIR)
TRIVANDRUM - 695 019, INDIA
Phone : (0471) 515250
Fax : (0471) 491712, 490186
E mail : pnmd@rrlt.csir.res.in
daspnm@rediffmail.com
Residence : Steinberg
Trivandrum - 695 019
Phone : (0471) 490720

25-1-2001

CERTIFICATE

This is to certify that the work embodied in the thesis entitled **"Investigations on the Removal of Iron from Ilmenite"** is an authentic record of the research work carried out by **Ms. E. Jeya Kumari** under my supervision and guidance at Beach Sand Minerals Research Unit, Regional Research Laboratory (CSIR), Trivandrum in the fulfillment of the requirements for the degree of Doctor of Philosophy in Chemistry of the Kerala University and further that no part thereof has been presented before for any other degree

Dr. P. N. Mohan Das
(Research Supervisor)

Acknowledgements

I take this opportunity to express my deep sense of gratitude and obligation to my research supervisor ***Dr. P. N. Mohan Das*** *for suggesting this investigative topic, his constant encouragement and inspiration.*

I express my sincere thanks to ***Dr. G. Vijay Nair,*** *Director, RRL Trivandrum, for providing the necessary facilities for conducting the research.*

I am grateful to Dr. Peter Koshy, Scientist, RRL for introducing me to my research supervisor. I take this opportunity to thank him for his advice and help in carrying out the SEM studies. I thank all the members of BSMR namely, Mr. K. H. Bhat, Mrs. M. E. K. Janaki, Mr. S. Velusamy, Mr. S. Sasibhooshanan and Mr. Prakash for their cooperation and help. I would like to thank Dr. Syamprasad, Scientist and Mr. Gurusamy for helping in the XRD studies.

I would like to thank Dr. Sheela Berckman, Scientist, CECRI, Karaikudi for helping me in the cyclic voltametric studies. A special word of thanks to Mr. J. Vinosh Babu, for assisting me in writing the computer program for the modelling studies.

I would like to thank all my teachers for all the help and blessings I received from them throughout my career. I thank all my friends and colleagues in RRL who assisted me in carrying out this work.

Financial assistance from CSIR, New Delhi is greatly acknowledged.

Finally I would like to express my deepest sense of gratitude to my family members, who remain the constant source of encouragement and inspiration throughout my academic career.

E. Jeya Kumari *January, 2001*

CONTENTS

CHAPTER 2

MATERIALS AND EXPERIMENTAL METHODS

CHAPTER 4

STUDIES ON RUSTING OF REDUCED ILMENITE USING MIXTURES OF CARBONYL COMPOUNDS ALONG WITH NH_4Cl

CHAPTER 6

DEVELOPMENT OF A STRUCTURAL MODEL FOR RUSTING REACTIONS CARRIED OUT USING REDUCED ILMENITE

CHAPTER 7

AN ELECTROCHEMICAL INVESTIGATION ON RUSTING REACTION USING CYCLIC VOLTAMMETRY

PREFACE

Ilmenite, which is the ore of titanium, is one of the major mineral resources of India. In terms of reserves India stands first in the world. Conventional processes employed commercially at present suffer from major pollution problems. This is especially true in the case of manufacture of synthetic rutile, which is the intermediate product for production of TiO_2 pigment and titanium metal. A recent process developed at RRL, Trivandrum is more envirofriendly where the iron present in ilmenite is converted to solid iron oxide, which can be easily separated instead of leaching out with acid in the conventional process. In this process ilmenite is reduced with coal and the metallic iron is catalytically oxidized to solid iron oxide, which is separated using methods like hydrocyclone. This process also has the draw back that the catalytic oxidation step, which is called rusting, is very slow which takes up to 16 hrs. Increasing the efficiency of the reaction will help in improving the economy of the process. Hence it was thought worthwhile to take up detailed investigations to find out the feasibility of accelerating the rusting reaction by using better catalysts.

A few organic compounds were used along with NH_4Cl as catalysts and it is observed that the reaction can be completed in less than half of the normally required time and the product obtained was better quality. Attempts were made to understand the mechanism of the reaction by different methods. The results of these investigations are described in this thesis. Major portion of this work has been patented and published.

PATENT

An improved process for the production of high-grade synthetic rutile.

P.N.Mohan Das, **E.Jaya Kumari** and S.Sasibhushanan

Indian Patent No. 317/98

LIST OF PUBLICATIONS

1. Catalytic removal of iron from reduced ilmenite

   E.Jaya Kumari, K.H.Bhat, S.Sasibhooshan & P.N.Mohan Das

   Minerals Engineering (in press)

2. Investigations on the effect of certain carbonyl compounds on the removal of iron during the rusting of reduced ilmenite

   E. Jaya Kumari, Peter Koshy and P.N.Mohan Das

   Trans. I.I.M. (Accepted)

3. Morphological changes occuring during the rusting of ilmenite.

   E.Jaya Kumari, Peter Koshy and P.N.Mohan Das

   Presented at the National Conference on Electron Microscopy, Dec. 1 - 3, 1999, Kanpur.

4. processing of Ilmenite – A New Approach

   E.Jaya Kumari and P.N.Mohan Das

   Presented at the National Seminar on Materials Processing and Characterisation – Challenges and Prospects, Feb. 3-4, 2000 at Trivandrum

5. Investigations on the Removal of Iron from Ilmenite

   E.Jaya Kumari and P.N.Mohan Das

   Presented at the Third National Symposium of Research Scholars on Metals and Materials, Sep. 8-9, 2000 at IIT, Madras

POSTER PRESENTATION

1. Scanning Electron Microscopic Studies on the Removal of Iron from Ilmenite

   E.Jaya Kumari, Peter Koshy and P.N.Mohan Das

   Presented at the National Conference on Electron Microscopy, Nov. 14-16, 1998 Hyderabad

CHAPTER 1

INTRODUCTION

1.1. History and occurrence of Titanium

Titanium is the ninth most abundant element by weight in nature. An English Mineralogist Rev.William Gregor discovered the element in 1870. It occurs in the IV B group of the periodic table. The atomic number and the atomic weight of the element are 22 and 47.88 respectively. The boiling point of the metal is 3260°C and the melting point 1668°C. Its density is 4.51-g/ ml. The element has two oxidation states +4 and +3 respectively.

The chief minerological occurence of titanium is as oxides, titanates and silico titanates. As an oxide mineral titanium occurs in the form of rutile, brookite and anatase. Ilmenite ($Feo.TiO_2$) and Arizonite ($Fe_2O_3.\ 3TiO_2$) are the main titanates, while Sphene ($CaTiO_3$) is the major occurence as silico titanate. Titanium minerals have got high specific gravity and stability. The mineral deposits are found in India, USA, Malaysia, Srilanka, Japan and many countries in Europe. In India it occurs in nature mainly as ilmenite and rutile. Large deposits are found at Quilon (Kerala), Manavalakurichi (Tamil Nadu) and Orissa coasts. A few properties [1] of the major minerals of titanium are given in table 1.1.

Table1.1 Properties of Titanium Minerals

Mineral	Chemical Formula	% TiO_2	Crystal Form	Hardness	Mode of occurrence
Rutile	TiO_2	92 -96	Tetragonal Prisms, Terminated by Pyramids	6 - 7	a) As segregations in igneous rocks. b) As pregmatic dykes, associated with ilmenite. c) In detrital deposits as a constituent of beach sands or streambeds.
Ilmenite	$FeTiO_3$	35- 60	Hexagonal Trigonal	_	a) As disseminated grains in basic igneous rocks. b) As ilmenite / magnetite/ haematite segregations. c) In coastal or beach sand deposits.
Leucoxene	TiO_2	60- 90	Mixture of rutile, anatase, ilmenite, etc.	_	As weathered product of ilmenite, in coastal or beach sand deposits.

1.2 World Reserves of Titanium Minerals

The reserves of titanium minerals are widespread throughout the world. It is estimated that the total unproven world reserves of various titanium minerals are about 340 million tones. About 216 million tones of these are considered to be economic reserves, which could be exploited commercially. Out of this 160 million tones are ilmenite. Details of the economic reserves [2] are given in table 1.2

Table 1.2: Economic World Deposits of Titanium Minerals

(Unit: Tonne X 1000)

Country	Ilmenite	Rutile & Anatase	Total
North America			
Canada	15,000	-	15,000
USA	10,000	1000	11,000
South America		40,000	41,200
Brazil	1200	(Anatase)	
Europe			
Finland	2000	-	2000
Norway	31,000	-	31,000
USSR	4000	1600	5600
Africa			
Sierra-Leone	-	1800	1800
South Africa	34,000	3300	37,300
Asia			
India	13,000	2000	15,000
China	20,000	-	20,000
Sri Lanka	13,000	3000	16,000
Oceanea			
Australia	15,000	5300	20,300
Total	**158,200**	**58,000**	**216,200**

The total reserves of titanium minerals [3] are given in table 1.3

Table 1.3 Total Reserves of Titanium Minerals

Minerals	Total Reserves in Million Tones	
	India	World
Ilmenite	146	1722
Rutile	8	225
Leucoxene	6	NA

The estimated Indian deposits of titanium minerals [4] are given in table 1.4

Table 1.4 Total Indian Deposits of Ilmenite & Rutile

(In Million Tonne)

Location	Deposits	
	Ilmenite	Rutile
All India	146.31	8.20
Andhra Pradesh Visakhapatnam/ East & West Godavari/ Krishna/ Guntur/ Nellore	9.34	0.32
Bihar / Ranchi	0.74	0.01
Kerala Coast (Quilon) Lake & Sea beds	27.54	2.02
Maharashtra Ratnagiri	1.80	-
Orissa Ganjam	35.90	1.34
Tamil Nadu Kanya Kumari, Tirunelveli, etc.	68.08	4.32
W.Bengal	2.91	0.19

Ilmenite occurs in nature in the form of beach sands or as deposits. Unlike rutile this mineral cannot be directly used for the production of titanium tetrachloride, which is an intermediate, formed during the production of titanium metal or titanium dioxide pigment through the chloride route. As the demand for $TiCl_4$ increases with diminishing reserves of rutile, ilmenite has to be beneficiated to synthetic rutile (> 92 % TiO_2).

The trend for titanium application to move from military to civilian, from aerospace to terrestrial and from high cost to low cost has continued apace. In Europe and Japan it is apparent that these trends, particularly in non-aerospace applications have proceeded further than the United States.

1.3 Titanium dioxide

Titanium dioxide (TiO_2) is a white pigment used in paints and also as an opacifier to make coloured paint opaque. The pigment is also used in photography, manufacture of fluxes for welding rods, ceramic industry, artificial silk, dyeing of leather, cloth, etc. This is due to its high refractive index and whiteness. $TiCl_3$ is an important Zeigler Natta catalyst for making polythenes and other polymers. Due to the hardness and high melting point titanium carbide is used in cutting tools. The profile of world consumption of TiO_2 [5] is given in table 1.5

Table 1.5 Profile of TiO_2 Consumption

(Unit: Percentage)

Total Consumption	USA	Western Europe	Rest of the World
	35	30	35
Coatings	51	62	75
Paper	24	9	4
Plastics	14	18	8
Others	11	11	13

The demand for TiO_2 in India is estimated to increase and hence there is necessity for increasing production.

1.4 Metal Titanates

Titanium forms extensive series of titanates with the alkali, alkaline earth and heavy base metals in which it appears as the acidic constituent. Generally metal titanates are prepared by heating the corresponding oxide, hydroxide, carbonate or neutral salts with an intimate mixture of TiO_2 at elevated temperatures to bring about a direct reaction. In rare earths, the mono and dititanates of lanthanum, praseodymium, neodymium, samarium

and yittirium have been prepared by fusing the corresponding oxide with TiO_2 in stoichiometric propotions [6].

Titanium metal is produced on tonnage basis using Kroll's process [7], which was developed in 1940.

A detailed survey of literature reveals that a number of research workers have attempted to beneficiate ilmenite by looking at its properties from different angles. A large number of reports have appeared on investigations for the production of synthetic rutile [8-9]. Some of the very important methods reported prior to this time are referred in brief. Out of these some have been used on commercial scale, a few are in pilot plant stage and all others have been confined to the laboratory and are of only academic interest.

Processes for the beneficiation of ilmenite for the production of synthetic rutile can be broadly classified as follows

- ❖ Reduction followed by catalytic aeration and removal of the solid iron oxide formed.
- ❖ Reduction smelting of ilmenite with carbon with a suitable flux resulting in titania rich slag and pig iron.
- ❖ Direct leaching of ilmenite with acids under atmospheric or high pressure resulting in preferential dissolution of iron.
- ❖ Reduction of ilmenite with suitable reductants in solid state followed by the removal of iron by physical or chemical methods.
- ❖ Halogenation of ilmenite by halogenating agents for the preferential formation of iron halide leaving behind enriched TiO_2

- ❖ Conversion of iron oxide or titania of ilmenite into easily leachable compounds such as sulphates, sulphides, etc.

A study of recovery of granular titanium dioxide has been reported by Bernard [10]. Here ilmenite was directly chlorinated in a vertical column and the iron chloride vapours were flushed off with a neutral gas.

Raymond et al [11] reported that the addition of Mg compounds to the ore during the reduction with coke followed by leaching increased the yield of TiO_2.

Pressure leaching experiments were carried out by Tikkanen et al [12] under reducing conditions to determine the optimum conditions for selective leaching of iron from ilmenite concentrate using waste solution containing 5 - 25% H_2SO_4 from the pigment process.

Williams et al [13] prepared a concentrate containing 75 - 90% TiO_2 by reducing pre-oxidised ilmenite with hydrogen at 700°C followed by leaching. Kino and co-workers [14] prepared a high grade titanium concentrate containing above 93% TiO_2 from ilmenite by the oxidation-reduction-leach process. Ilmenite was subjected to solid state reduction and the metallic iron obtained was oxidised to a soluble Fe (II) complex, which was then separated as solid Fe_2O_3 by oxidation [15].

Samanta et al [16] studied the separation of iron from ilmenite. Crushed ilmenite was heated with coke at 1200°C for 2-4 hours and quenched in water containing NH_4Cl. Air or oxygen was bubbled through the suspension with agitation for 12 - 16 hours and the hydrated Fe_2O_3 formed was removed.

A two stage process had been developed by Becher et al [17] for upgrading ilmenite to a product containing around 90% TiO_2. It consists of

roasting ilmenite with solid carbon, followed by agitating the reduced mass in aerated water in presence of catalysts to rust away the iron from the grains.

A concentrate containing more than 90% TiO_2 was obtained from ilmenite by roasting in air at 800 – 1200°C followed by reduction with a mixture of CO and H_2 gas at 750 – 1250°C and leaching with $FeCl_3$ to dissolve iron as $FeCl_2$ which was then regenerated [18]. In another process ilmenite or rutile was directly chlorinated in presence of reducing agent like coal or coke and the resulting $TiCl_4$ was oxidised to TiO_2 with a gas containing oxygen [19].

Ilmenite was directly treated with HCl at elevated pressure and temperature with counter current flow to obtain a TiO_2 concentrate and a solution consisting primarily of $FeCl_2$ and residual HCl [20]. By leaching ilmenite in two steps with different concentrations of HCl at 105 – 110°C at high pressures Lo et al could remove more than 95% iron from it [21]. Akio Yamaguchi [22] studied the kinetics of reduction of ilmenite ore by H_2 at 650 – 800°C and the rate of the reaction was calculated. Khairy [23] studied the effect of pretreatment on reducibilities of Egyptian ilmenite and found that pre oxidised ore was more susceptible to reduction up to certain temperatures.

Sehra et al [24] upgraded Quilon ilmenite to a product containing 97.28% TiO_2 by a single stage HCl leaching at about 250°C for 48 hours without stirring or for 24 hours with stirring. A process for recovering HCl was developed. Preparation of a residue containing 94% TiO_2 and small quantities of Fe from ilmenite by reducing it in a fluidised bed with

hydrogen at 595 – 760°C followed by leaching with 10% H_2SO_4 solution was reported [25]. The reduction of Egyptian ilmenite, which occurred in three distinct stages with respect to temperature of reduction, was studied by Kammal Hussein [26] with H_2. Below 600°C the reduction was slow and corresponded to the reduction of Fe_2O_3 to lower oxidation stages and partially to iron. During the second stage extending upto 800°C, the partial reduction of TiO_2 to lower oxides takes place.

When ilmenite was heated with 30% by volume H_2SO_4 a concentrate containing 80 -90% TiO_2 was obtained. All Fe^{3+} was converted to Fe^{2+} using iron scarp. TiO_2 was precipitated [27] with Na_2CO_3. Sinha and co-workers [28] proposed an improved method in which ilmenite was subjected to oxidation roast before partial reduction and leaching with 20% HCl. The product contained 95-97% TiO_2. Aramendia and co-workers [29] beneficiated ilmenite ore to yeild a concentrate suitable for chlorination. Ilmenite was oxidised at 600- 1000°C for 1-2 hours and then reduced at 600-750°C with hydrogen under pressure. After magnetic separation and leaching with dilute acid TiO_2 with 95.3% purity was obtained. Roasting was found to increase the TiO_2 content.

Madhavan Pillai [30] beneficiated ilmenite by heating at 900 – 1000°C without fusion. It was then suddenly chilled and separated magnetically. The addition of charcoal during heating improved the yield. O'Brien and co-workers [31] studied the effect of temperature and time on spheroidization of the iron during the reduction of ilmenite and found out the optimum conditions. Above 1200°C, spheroidization and separation of Fe

from gangue was inhibited by the formation of reduced titanium compounds. In a continuous method [32] for the production of synthetic rutile, the ferric oxide present in ilmenite was first reduced to ferrous state at 950°C with coke, followed by gaseous reduction at 950-1100°C with CO and H_2 where reduction to about 95% metallic iron took place. It was then subjected to acid leaching.

Safiullin et al [33] have prepared TiO_2 with 92.6% purity from ilmenite using the method of alkali decomposition. The ore was heated with Na_2CO_3, leached with H_2O and then with 20% HCl. TiO_2 was recovered from the solution.

O'Brien et al [34] studied the conversion of New Zealand ilmenite to high titania products and spheroidal iron. Ilmenite was reduced with char at 1200°C, followed by ball milling and magnetic separation to give a material containing about 80% TiO_2. Suchil'nikov [35] studied the reduction of kusinsk ore, which is a mixture of ilmenite and magnetite, using coke at different temperatures. At about 1220°C, and above reduction was fast, but at 1100°C the process slowed down with changes in the composition of the product gases. Oster et al [36] reported another process where finely powdered ore was refluxed with HCl to dissolve the iron and the residue was washed and calcined to give a product containing 92.2% TiO_2.

The selective chlorination of iron from ilmenite with hydrogen chloride gas was studied by Sankaran et al [37]. Mathew Pullimootil [38] studied the recovery of titanium values from ilmenite or rutile by fusing the ore with KNO_3 or $NaNO_3$ followed by leaching. The residue was treated to recover titanium values. Gokarn et al [39] studied the reduction of Indian

ilmenite using different industrial reductants. It was found that charcoal when used in excess also gave a reduction up to 73.3% which increased when 2% Na_2CO_3 was used as a flux. When oxidised ilmenite was used, the rate of reduction by carbon was faster. Reduction upto 85.5% was achieved using large excess of city gas and hydrogen. In the continuous moving bed experiments, higher reduction percentages were obtained using coke.

Reeves et al [40] studied the preparation of rutile from ilmenite using lignite, anthracite, etc. as reductants and various factors affecting the reduction of ilmenite were investigated. The reduced mass was leached with ammoniacal ammonium carbonate solution in presence of oxygen and Fe_2O_3 and TiO_2 were separated by floatation. Honchar and co-workers [41] studied the continuous leaching of metallised ilmenite ore with an acid to produce a TiO_2 concentrate suitable for chlorination feed material in the production of $TiCl_4$. Chen et al [42] prepared rutile by leaching out the iron present in ilmenite with hydrochloric acid at about 143°C with pressure after giving a HCl vapour treatment. A product containing 96% TiO_2 and about 0.5% Fe was obtained by reducing a pre oxidised powdered ilmenite with methane in a fluidized bed [43,44]. The Fe (II) formed was extracted with HCl. Hi'eser et al [45] prepared rutile from ilmenite by heating in a stream of gaseous SO_2 and CO and then leaching with aq. H_2SO_4. The residue was roasted in air to remove the S as SO_2, leaving rutile.

Bade and co-workers [46] prepared TiO_2 concentrates with 94.1% purity from ilmenite by subjecting it to reduction roasting followed by iron oxide separation. Ilmenite was subjected to reduction with carbon like petroleum coke in two stages in presence of alkali or alkaline earth salt. In

the first stage at about 800- 950°C ferric iron was converted to ferrous, while in the second, metallic iron was formed at about 1070°C. The product was leached with H_2SO_4 to give a concentrate with 98.5% TiO_2 [47]. Leaching of ilmenite with HCl was used for beneficiation [48]. The ore was first reduced with coke and then leached with preheated HCl solution at about 145°C. Almost 97.5% TiO_2 was recovered from ilmenite by this process.

Jain et al [49] studied the preparation of TiO_2 from ilmenite by selective sulphidisation. Ilmenite was sulphidised with H_2S gas at 1000°C for 5 hours or at 1100°C for 4 hours and was leached with 20% excess of boiling HCl. The residue contained about 91% TiO_2. Meyer et al [50] prepared TiO_2 from ilmenite by reduction followed by leaching. Sponge iron was recovered from the iron oxide by further reduction. Henkel and co-workers [51] prepared TiO_2 concentrates from ilmenite by heating it with steam in a non reducing atmosphere at 600-900°C followed by acid leaching at elevated temperatures. Naguib [52] reduced ilmenite with H_2 to metallic Fe and/ or magnetic Fe oxides. This was magnetically separated before dilute acid leaching of non-magnetic fraction which gave concentrate with 93-98% TiO_2.

In a patented process reported by Soverini et al [53] rutile containing more than 90% TiO_2 was prepared by dilute acid leaching of ilmenite to dissolve the FeO present in it. The residue was subjected to reduction with hydrogen or CO at about 650 – 900°C, followed by dilute acid leaching at higher temperatures. They also reported a different method in which the preheated ore was reduced with hydrogen or CO or their mixtures which was then leached with HCl to remove iron [54]. In a continuous process

developed by Dunn [55] ilmenite was treated with chlorine to convert iron oxide to ferric chloride. The volatile ferric chloride was removed and TiO_2 was obtained from the residue.

Ilmenite was subjected to reduction at a temperature when 90-98% of Fe^{3+} was converted to Fe^{2+}, which was then leached, with H_2SO_4 containing a Ti^{4+}salt and a colloidal hydrated oxide accelerator. A material containing around 85% TiO_2 was obtained [56]. A product containing 92.7% TiO_2 and 1.4% Fe_2O_3 was obtained from ilmenite by feeding ilmenite together with 25% coke in a fluidized bed reactor and treating with a mixture of 42% Cl_2, 10% O_2 and 48% N_2 at 900°C for 2-3 hours [57]. Fukushima and co-workers [58] reported a process for the preparation of rutile in which the pre oxidized ore was chlorinated at 800-950°C in presence of coke. TiO_2 was separated after proper treatments. Synthetic rutile containing 95-97% TiO_2 was prepared by chlorination of ilmenite in presence of petroleum coke in a fluidised bed at 1000°C when iron was removed as ferric chloride giving TiO_2 with less than 1% Fe_2O_3 [59].

In a patented process [60] by Chen, ilmenite was treated at 815-1095°C with reducing agents like petroleum coke or fuel oil in presence or absence of materials containing sulphur. Ferrous oxide or sulphide formed was leached out with dilute mineral acid. Stickney et al [61] recovered rutile from the reduced titaniferous slag obtained in the reduction smelting by oxidation at about 650°C followed by heating at about 1200°C in presence of compounds like phosphorous oxides. The rutile crystals formed were separated from the glassy matrix.

Marshall and co-workers [62] prepared TiO_2 80.7% from powdered ilmenite by leaching with HCl in presence of $SnCl_2$, Fe or Cu as reducing agents. In another process ilmenite was subjected to reduction smelting with coal and flux at 1100 – 1200°C for 2 hours. The metallic Fe and TiO_2 formed were separated magnetically or by floatation [63]. Iqubal et al [64] reported the thermodynamics of chlorination and various methods of enrichment of ilmenite. Camara [65] reported that at 60°C, after direct treatment for 2 hours with Con.HCl, a product with 91.4% TiO_2 was obtained from ilmenite of Espirito Santo. In another patented process reported by Moklebust [66], reduction followed by smelting was employed. Ilmenite was reduced with carbon to convert the iron oxides to metallic iron. After magnetic separation, the magnetic part was smelted in an arc furnace at 1730 – 1810°C when the oxides of titanium got separated as slag, while all the iron remained in the molten state. In another process synthetic rutile with 92% TiO_2 was prepared from ilmenite [67] by roasting in presence of oxidizing or non-reducing gases followed by reduction at 550-750°C with gases like CO or H_2. The reduced iron was dissolved out with dil.HCl at 80-110°C. Ilmenite was reduced at 815 – 1095°C with carbonaceous materials in presence of traces of sulphur, which helped in the conversion of ferric oxide to FeO and FeS. The product was cooled and leached with dil. HCl at higher temperatures and pressures. Rutile thus obtained had a purity of 92-93% [68]. Various aspects of processing as well as demand of ilmenite and TiO_2 were reviewed by Iammartino et al [69]. Samanta et al [70] studied the thermochemical beneficiation of Indian Ilmenite by first reducing the iron

oxide to iron followed by reoxidation to Fe_2O_3 which was removed by physical methods.

Lilach and co-workers [71] had patented a process for the preparation of TiO_2 concentrates in which powdered ilmenite after pre-reduction at 900-1200°C was subjected to low temperature reduction using carbon. Metallic iron formed was leached out. A rutile sample with more than 95% TiO_2 was prepared from ilmenite by Kataoka and co-workers [72]. Ilmenite was subjected to partial reduction using coke followed by magnetic separation and leaching with waste acid. The titanium salts present in the leach solution were reprecipitated and calcined. Othmer et al [73] prepared TiO_2 of 95-99.5% purity by fractional chlorination of ilmenite in presence of powdered coke in a reactor. The $TiCl_4$ so formed was reacted with iron oxides when TiO_2 got precipitated. Synthetic rutile containing about 95% TiO_2 was prepared from ilmenite by reduction in a fluidized bed followed by leaching with dil.HCl at about 105°C to remove iron [74].

Rutile containing 89-92% TiO_2 was prepared by Tittle and co-workers [75] by treating ilmenite with HCl gas in presence of coal at 1220 - 1320K where 75-80% iron could be removed. The metallic iron formed due to reduction was leached with dilute acid. In the Murso process [76] which is one of the important routes for the production of synthetic rutile, crushed ilmenite after giving an oxidative roasting at 900-950°C was subjected to reduction with H_2 or mixtures of hydrogen, CO, CO_2 and steam, around 850 – 900°C. The ferrous iron formed was leached with dil.HCl at about 110°C. HCl was regenerated from the product. Ilmenite was subjected to repeated cycles of oxidation and reduction in presence of Na_2SO_3 in one or three

stages at different temperatures [77]. NH_4HCO_3 was added to the mass before the third stage. The product was subjected to magnetic separation after grinding. The concentrate thus obtained contained about 85% TiO_2. Different methods available for separating Fe from TiO_2 in ilmenite were reviewed by Jena et al [78]. TiO_2 with 95-98% purity was made by treating finely divided ilmenite with H_2S or a H_2S containing gas and leaching with 20% HCl or H_2SO_4 [79].

Slags with TiO_2 contents of 80% had been prepared by reduction smelting of Manavalakurichi ilmenite in electric arc furnace with various fluxing agents where pig iron was obtained as by-product. The effect of uniform distribution of carbon had been studied by giving a carbon coating to ilmenite [80]. Mackey [81] had reported a modified acid leaching technique where the reduced ilmenite was leached with excess HCl in a rotating jar under high pressure and temperature. The residue gave a rutile sample with more than 90% TiO_2 content. Rutile with more than 99% purity was prepared by Hiester et al [82] from ilmenite in which high temperature sulphidisation with H_2S followed by magnetic separation and leaching was used.

Mackey et al [83] developed a laboratory method for converting ilmenite to synthetic rutile in a short time and leaching at moderate pressure. Kurata et al [84] reported that the iron oxide present in ilmenite was reduced to ferrous form using H_2 which was leached out with 20% HCl at 105°C, giving a product with 96.2% TiO_2 and 0.6% iron. Effects of various factors like concentration of acid, presence of coagulants and flow velocity on leaching have been studied. Ilmenite ore was subjected to reduction using

carbon as reductant at 1200-1250°C in a furnace, which was then smelted in an electric arc furnace where TiO_2 could be separated. Energy saving was reported in this pilot plant scale studies [85].

A product containing around 96% TiO_2 and 3% Fe_2O_3 was obtained by heating ilmenite with carbon or CO gas at 1000 – 1200°C while $FeCl_3$ vapour was introduced into it to remove iron as $FeCl_2$ [86]. Pogorelov et al [87] improved the production of TiO_2 concentrate from ilmenite by leaching. 1-2% KCl was added to the ilmenite which was reacted with HCl in presence of titanium sponge with bubbling of a Cl_2-air mixture. Allan and Mori [88,89] reported two processes for the beneficiation of ilmenite, which were more or less the same in principle. Ilmenite was reduced to convert the iron oxide to metallic iron, which was then dissolved out electrolytically in a cell. Pollard [90] beneficiated ilmenite by reducing it with carbon in presence of NaCl in a molten salt bath upto 1300°C. The powdered product after washing with water and magnetic separation gave a non-magnetic part with 85.4% TiO_2. Rutile was prepared from ilmenite by Shiah [91] by reducing ilmenite with H_2 in presence of $CaSO_4$ to convert the iron oxide in ilmenite to metallic iron and $CaSO_4$ to CaS. After magnetic separation of the product the magnetic fraction was leached with $FeCl_3$ solution and rutile was recovered from the residue by further treatment. In a process reported by Kurata et al [92] ilmenite after oxidation roasting at 950°C was reduced with hydrogen. The ferrous iron was then leached with dil.HCl counter currently and concurrently. The product obtained contained 93.2% TiO_2 and 2.8% iron. Various workers [93-96] had reviewed the procedures and processes for the beneficiation of ilmenite for the production of synthetic rutile.

In another process ilmenite was beneficiated to 96.72% with a recovery of 97.6% by the process of reduction followed by leaching [97]. The ore was first reduced with heavy fuel oil followed by leaching with dil.HCl containing sulphate ions. A slag containing titanium in lower valence states was obtained from ilmenite by heating calcined pellets of powdered ilmenite in a mixed gas plasma with hydrocarbon at 1800 – 2500°C in a water cooled copper crucible [98]. Preston et al [99] prepared a rutile sample containing 93.2% TiO_2 by treating a reduced ilmenite sample with waste H_2SO_4 containing Ti^{4+} ions which was obtained from the ilmenite leaching process. Ilmenite sample from Kutubdin island in Bangladesh was upgraded to 98% by direct leaching of powdered ore with excess of commercial HCl [100]. It was also reported that reduction of the ilmenite at 1000°C for 1 hour followed by dil. HCl leaching gave good concentrations. A pilot plant scale study was carried out by Elger et al [101] by reduction smelting of ilmenite with coke and lime in electric arc furnace at 1600°C. The slag after proper treatment and leaching with dil.H_2SO_4 gave a rutile with 88% TiO_2. An evaluation of the economy of the process was also carried out.

Synthetic rutile containing 85-95% TiO_2 was obtained by oxidation of ilmenite followed by reduction and aeration leaching [102]. Hashimoto et al [103] prepared high purity rutile concentrate from ilmenite employing reduction with carbon and leaching with HCl followed by calcination in presence of a reductant at high temperature in a gas containing Cl_2. A titania enriched product was obtained by the process of reduction followed by leaching [104]. Ilmenite was reduced in presence of a Cl_2 containing

compound like NaCl and S or sulphur containing compounds to convert iron oxide to metallic iron. The product was washed and leached with dilute acid to obtain the concentrate. Lakschevitz and co-workers [105] prepared rutile containing 93-97% TiO_2 by heating ilmenite with reducing gases in presence of H_2S or SO_2 followed by leaching with 20% HCl. The reagents were recovered from the product and recycled.

Jones et al [106] had reported a detailed analysis of the reduction process of ilmenite using techniques like optical microscopy and EPMA. The metallic iron formed was etched out before analyzing the oxide phases. Complete reduction of Fe^{2+} was hindered at temperatures below 1000°C by an enrichment zone formed during reduction. But at higher temperatures, metallic iron got segregated to the peripheries of the grains. During pre oxidation of the ore, the single crystal ilmenite grain was converted to sub-grains causing simultaneous faster topochemical reduction.

In the pilot plant scale [107] studies reported for upgrading New Zealand ilmenite, it was reduced in a tunnel kiln at 1200°C with coal. The powdered product on magnetic separation gave a non-magnetic part containing about 70% TiO_2 and a magnetic part with about 80% Fe. A review of different methods of preparation of synthetic rutile was reported by Burastero [108]. Ilmenite was subjected to reduction roasting using H_2-CO mixture followed by leaching with Con.HCl. Iron was removed as $FeCl_2$ and TiO_2 precipitated by addition of Fe_2O_3 [109,110]. In another process, which was claimed to be more effective, ilmenite was subjected to reduction roasting below 900°C followed by HCl leaching at 80-110°C. $FeCl_2$ was

separated by saturation with HCl gas. TiO_2 was precipitated from the hot solution.

Jain et al [111] investigated the selective leaching of Gopalpur ilmenite under different conditions. The influence of conditions like concentration of the acid, its quantity and temperature of leaching on the extent of iron removed from ilmenite was studied. It was reported that repeated leachings were required. But with partially reduced ilmenite, leaching was faster and more efficient. Synthetic rutile was prepared by the selective chlorination of ilmenite in a chlorinator with certain amount of air or oxygen. Various conditions affecting chlorination have been studied. Pilot plant scale as well as industrial trials were carried out [112].

Burastero [113] applied acid leaching for the preparation of synthetic rutile with 95.4% purity. He observed that when the ore was subjected to oxidation or reduction, leaching was more efficient. Rutile was prepared from Uruguay ilmenite [114] by roasting it in a fluidised bed at 1000°C followed by reduction with charcoal at 950°C. The reduced sample was then leached with 20% HCl. The residue after calcination and magnetic separation gave a concentrate containing around 95% TiO_2.

Hussein et al [115] studied the effect of pre oxidation and pre reduction on the removal of iron from ilmenite on leaching with HCl. It was observed that pre oxidation retarded iron removal while reduction with H_2 improved the removal of iron giving a product with about 95% purity. Various factors affecting the reduction-roasting of pre oxidised ilmenite namely charcoal/ ilmenite ratio, variable factors of reducing agents, temperature and duration were studied by Situmorang et al [116]. It was reported that the optimum conditions for reduction roasting were 25% wood

charcoal at 1010°C for 90 min. and those for the aeration stage were stirring with 0.5% aq. NH_4Cl at 1100 rpm for 6.5 hour at 45°C. Negoiu et al [117] studied the leaching conditions of ilmenite with HCl. He obtained a product containing 80% TiO_2 for an ilmenite-HCl azeotropic ratio 1: 8 and leaching time 9 hours which were found to be optimum.

A rhombohedral ilmenite phase and an orthorhombic pseudo brookite phase formed were observed by Quaida et al [118] when Australian ilmenite was heated in an inert atmosphere at temperatures above 1500°C. On heating in a reducing atmosphere like H_2 or CH_4, 95% of the iron oxide present was reduced to metallic state. Swinden et al [119] carried out the smelting of ilmenite ore in arc furnace to give metallic Fe and a titaniferous slag. They found that there was no difficulty in producing slags with a TiO_2 concentration upto 95% from Western Australia beach sand ilmenite, but the reduction kinetics suggested that it would be uneconomical to process beyond 85% TiO_2 concentration.

Synthetic rutile was also prepared from ilmenite by multi-stage procedure [120]. Fe_2O_3 present was first reduced to Fe (II) and metallic iron. The metallic iron was then oxidized under controlled conditions to Fe (II) which on leaching with acid gave a product containing about 92% TiO_2. Tolley [121] prepared rutile by reduction roasting of ilmenite at 650-1000°C with reducing gases followed by leaching with HCl containing phosphoric acid. Bracanin and co-workers [122] reported a process for the production of synthetic rutile, ferutile and sponge iron. Ilmenite was reduced with coal in a rotary kiln when Fe_2O_3 was converted to metallic iron. From the reduced mass, Fe_2O_3 was precipitated by agitation in aerated water in presence of

catalysts. Rutile was separated from this after giving a mild acid leach. Negoiu et al [123] obtained TiO_2 from Rumanian ilmenite concentrates by reacting powdered ilmenite with 96% H_2SO_4 at higher temperatures followed by leaching with water at pH 1.5. TiO_2 was precipitated from the Ti $(SO4)_2$ solution using hydrazine.

Borowiec [124] prepared synthetic rutile from weathered ilmenite by hydrometallurgical method. Egyptian ilmenite after leaching with 15% HCl was oxidised at 750°C and was again leached to yield synthetic rutile containing 78.7% TiO_2. It was observed that the temperature of oxidation and reduction of ilmenite affected the leaching rate of iron [125], which increased with increase in oxidation temperature. The optimum oxidation and reduction temperatures were found to be 950°C and 850°C. The leaching rate increased with HCl concentration as well as the addition of $FeCl_2$. When a mixture of HCl and $FeCl_2$ solutions was used for leaching, the rate of leaching was dependent on the total Cl^- ion concentration and not on acid concentration.

In another process, the ferric iron present in ilmenite was electrolytically reduced to ferrous form, which was dissolved out giving beneficiated ilmenite [126]. Synthetic rutile from Egyptian black sand was prepared by reduction followed by leaching [127]. Ilmenite was reduced with hydrogen. TiO_2 contents of the rutile were 85% and 96.2% when leaching was carried out with 25% HCl and 20% HCl with a coagulant respectively. Leaching of the powdered sample with azeotropic HCl by refluxing increased TiO_2 content from 85 to 92.2%. A concentration of 93% was achieved using 12% H_2SO_4. Some of the parameters affecting the

leaching process were optimised. Ilmenite was also upgraded to a rutile enriched product containing 86% TiO_2 by high temperature borate fusion followed by H_2SO_4 leaching [128].

Canadian ilmenite was subjected to reduction roasting in H_2-CO atmosphere at 775°C for 75 mts. and was leached with Con.HCl at 100°C + 10 mv potential [129]. TiO_2 concentrate was prepared from primary ilmenite by reduction smelting in arc furnace followed by Con.H_2SO_4 leaching at slightly higher temperatures [130]. Tsuchida et al [131] reported the kinetic study of the leaching of powdered ilmenite using highly concentrated HCl. With the help of X-ray diffraction and electron microscopic techniques, the changes in shape and grain size of the ore particles during leaching were studied. Duncan and co-workers [132] studied the structure and composition of New Zealand ilmenite before and after leaching with 1-10 M HCl solution at 70°C, using X-ray, EPMA and optical mineralogical studies. They reported that extensive pores were formed parallel to the basal plane due to acid leaching. The rapid dissolution in the initial stages was attributed to the removal of iron rich surface phase and to channel formation. The decline in the reaction rate during the later stages was due to the polymerization and transport of dissolved Ti within the porous solid structure. These prevented the diffusion of reaction products outwardly making the reaction slow.

Ilmenite was subjected to selective chlorination with N_2-Cl_2 mixture in a fluidised bed at 800-1300°C. Fe volatilized as $FeCl_3$ and the non-volatile residue contained 97.7% pure TiO_2 [133]. A residue containing mainly TiO_2 with only 0.9% Fe was obtained from ilmenite by selectively reducing it with vegetable charcoal at 1300°C for 3 hrs and leaching with aq. $FeCl_3$

solution [134]. Brandstatter [135] studied the carburisation of ilmenite or slags premixed with powdered carbon at 1200-2300°C. The TiC obtained after magnetic separation of Fe, was suitable for the manufacture of pigment grade TiO_2 and low temperature chlorination to $TiCl_4$.

Solov'ev et al [136] separated a titanomagnetite concentrate and an ilmenite concentrate from the ores of Maly-Tagul deposit in Western Siberia and the concentrates were electro-smelted. Ti slags with 91% and 65% TiO_2 were obtained from ilmenite and titano magnetite respectively. They also found the reducibility of ilmenite concentrate was higher than that of magnetite ore, the reason for which was also discussed. Yin [137] studied the reaction mechanism for selective chlorination of ilmenite for the preparation of rutile and its physical and chemical properties and structure were established using microscopy, X-ray diffraction and scanning electron microscopy. Ismail et al [138] prepared synthetic rutile having 90-95% purity from Sri Lankan ilmenite through the process of reduction-leaching. Ilmenite after oxidation above 900°C was reduced at 1100°C using sawdust reductant, leached with HCl and calcined.

The slag obtained on smelting the magnetically concentrated mineral in an electric arc furnace was roasted with Na_2CO_3. TiO_2 was recovered using H_2SO_4 [139]. Various methods available for the conversion of ilmenite to rutile had been reviewed by Girgin [140]. Levin and co-workers [141] observed that agitation of the solution during leaching made the iron removal faster. At optimum conditions with 20% HCl about 94.6% titanium was recovered as rutile, giving a product with 95% TiO_2 and 0.79% iron. Poniatowski and co-workers [142] prepared slags containing about 80% TiO_2 from ilmenite by reduction smelting in an arc furnace using coke

breeze and coal. Ilmenite was subjected to partial reduction with gaseous or solid reductants at 800°C, which was chlorinated with gaseous chlorine and washed with water to give a concentrate containing 93% TiO_2 by Joedden et al [143].

Jaffrey A. Khan [144] reviewed the methods for the production of synthetic rutile from ilmenite and leucoxene, which could be used as feed stocks for the production of $TiCl_4$. Sinha [145] studied the hydrochloric acid leaching which consists of an oxidation followed by reduction, which increased the reactivity of ilmenite towards leaching. It was observed that the leaching of iron was affected by various parameters like temperature of leaching, speed of stirring, concentration of acid and addition of ferrous chloride. TiO_2 was prepared from the solution. The reduction of ilmenite with H_2 at 500-1200°C followed by 18% HCl leaching at 45°C gave a rutile product with about 90% TiO_2. A synthetic rutile containing 2.5% Fe_2O_3 was prepared by Moles [146] by reducing ilmenite at 600-1000°C followed by 15-20% HCl leaching using an autoclave. In this case, iron removal was found to be faster than the normal leaching.

A residue containing 95% TiO_2 was obtained from ilmenite by sulphidisation using a mixture of H_2S and CO and then leaching with dil.HCl [147]. In another process, titanomagnetite was sulphidised with SO_2 in presence of carbon at about 800°C followed by leaching with 1M HCl, which gave a synthetic rutile product. The parameters affecting the reaction like temperature, time and amount of carbon were optimised [148]. Elger and co-workers [149] reported the reduction smelting of ilmenite with carbon and soda ash. The Ti containing slag on treatment with SO_2 and air

followed by leaching to remove soluble impurities finally gave a product containing about 85.5% TiO_2. The experiments were carried out in pilot plant and large scale.

Lemi et al [150] investigated the leaching of Norway ilmenite with HCl and mixed aqueous HCl-alcohol solutions at boiling temperatures. It was found that the alcohols methanol, ethanol and ethylene glycol all substantially increased the leach rate and in the case of methanol and ethanol this was achieved at lower boiling temperatures compared with aqueous HCl. Synthetic rutile is manufactured from titaniferous material by chlorinating in a fluid bed after pre-heating which is a patented process [151].

Ismail Girgin [152] studied the leaching of Norway ilmenite concentrate in $HCl\text{-}H_2O$, $HCl\text{-}CH_3OH\text{-}H_2O$ and $HCl\text{-}CH_3OH$ solutions at 3M HCl concentrations at temperatures between 25°C and 65°C. It was observed that $HCl\text{-}CH_3OH$ showed better dissolution of iron in ilmenite compared to $HCl\text{-}H_2O$ and $HCl\text{-}CH_3OH\text{-}H_2O$ solutions.Grey et al [153] obtained rutile by reducing titaniferous ores followed by two stage acid leaching or aqueous aeration and acid leaching.

Damodaran et al [154] investigated the batch scale and continuous rotary kiln carbothermic metallisation of ilmenite followed by different down stream treatments such as catalytic rusting, acidic chloride leaching, oxidation leaching, etc. has given rise to a high grade synthetic rutile (98% TiO_2). Warner [155] prepared TiO_2 pigment from titaniferous material by contacting ilmenite with carbon to reduce iron oxide to iron and to form titania slag with lower content of oxide. Hoecker [156] produced synthetic rutile by reducing ilmenite with a reducing agent, which gave metallic iron

along with TiO_2. This reduced ore is contacted with aqueous solution through which a gas is passed which contained atleast one oxidizing gas selected from O_2 and O_3 to oxidize atleast a part of the metallic iron.

A detailed study was carried out by Mohan Das et al [157] to examine the possibility of producing synthetic rutile from Indian ilmenite using a similar method followed in Australia. Ilmenite is first reduced and then subjected to oxidation by air in aqueous medium using NH_4Cl as catalyst. Rusted ilmenite was leached with dil.HCl to produce synthetic rutile containing 2.5% iron.

Mohan Das et al have developed many patented processes for the production of synthetic rutile. A novel process for the production of high grade synthetic rutile [158] is one among them.

An improved process for the production of high grade synthetic rutile was another patent by the same group [159]. An alternate process for the production of titania rich slag and pig iron is yet another patented process by them [160, 161, 162, 163, 164, 165, 166].

Mohan Das et al [167] have developed another patented process in which better rusting was found to occurfaster.

Nagamouri et al [168] developed a two-site model for the carbothermic reduction of ilmenite in an arc furnace at 1900 – 2000K. A comprehensive mathematical model was developed to simulate the reduction of ilmenite ore with C in an electric furnace. Two distinct reaction sites were assumed to exist in open arc furnace.

- Bubbling surface
- Bulk bath of TiO_2

The model takes into account physical features as sorrounding temperature, viscosity, density and equilibrium mass balances incorporating thermodynamic properties of TiO_2 – Ti_2O_3 – TiO – FeO – SiO_2 – Al_2O_3 – MgO slag and explains all known observations including interdependence of the TiO_2 content of slag and carbon content of pig iron and its variation with temperature and electric power consumptions. The model also provides partial explanations for foaming and permanent CO gas boiling of the slag.

Application to the direct reduction of ilmenite concentrate was developed by Bazin et al [169]. The application led to a significant reduction in product variability and operating cost of ilmenite furnaces.

Chen et al [170] have found that increased dissolution of ilmenite is induced by high energy ball milling. High energy ball milling treatment leads to full dissolution of ilmenite sands containing both $FeTiO_3$ and $Fe_2Ti_3O_9$ phases in a H_2SO_4 solution at 100°C. Complete dissolution of iron on milling ilmenite for 200 hrs in an oxygen free atmosphere takes place. This occurs as a result of gradual reduction of Fe^{3+} phase ($Fe_2Ti_3O_9$) to relatively more soluble Fe^{2+} phase ($FeTiO_3$) on milling in vacuum.

Applications of microwave heating in minerals processing was developed by Bradshaw [171]. Many minerals are effective absorbers of microwave energy. Many mineral processing applications have been tested including ilmenite on lab scale.

Another patented process was developed by Yang [172]. TiO_2 and Fe_2O_3 are manufactured from ilmenite by electrophoresis in dil. H_2SO_4 or HCl. The electrophoresis trough consists of an anode chamber and a cathode chamber that are separated by an anionic diaphram. Fe is selectively leached from ilmenite in the anodic chamber; the Fe ions migrate under electrostatic

force of the electric field through the anionic diaphram into the cathode chamber and is separated there from the electrolyte solution.

Sahoo et al [173] prepared TiO_2 rich slag by plasma smelting of ilmenite. Ilmenite concentrates from eastern coast of India have been treated by plasma smelting to produce TiO_2 containing slag and pig iron. Petroleum coke has been used as reductant and parameters such as amount of reductant, effect of power input and slag characteristics have been varied. In some cases the slag was flowable. The presence of suboxides of titanium (Ti_2O_3) hindered the flowability.

1.5 Existing Methods for Processing Ilmenite

The primary consumer of all forms of titanium concentrates is the pigment industry which uses either sulphate or chloride routes of processing.

In the sulphate route of processing, finely ground ilmenite is heated with strong H_2SO_4 (92%) to give a black solution containing titanyl sulphate, $FeSO_4$ and $Fe_2(SO_4)_3$. Ferric iron is reduced to ferrous by the addition of iron scrap into the acidic solution. The reduced liquor is clarified, concentrated and then boiled by injecting live steam so that the hydrated titania gets precipitated. The precipitate is filtered and mixed with certain additives in small quanities and fed into rotary kiln. Crystalline titanium dioxide, as anatase or rutile gets discharged depending on the additives given to the calciner feed. It is then fine milled to give titanium dioxide pigment. M/S Travancore, Titanium Products Limited, Trivandrum, India is following this method for anatase grade pigment manufacture. One major disadvantage of this process is the environmental pollution created by the highly acidic effluent containing ferrous sulphate and dil.H_2SO_4. Moreover

for the manufacture of H_2SO_4, sulphur has to be imported. The earlier method was to discharge the effluent into sea, where the alkalinity of seawater could take care of the acidity. But with increase in awareness of pollution problems, stringent regulations were promulgated in the industrialised countries, which prohibited such marine disposal. In order to avoid these problems, various new routes of processing have been developed and tried, out of which chloride route is one of the most important.

In the chloride process, which is followed by most of the modern industries, rutile is chlorinated to give titanium tetrachloride. Chlorides of iron present in small quantities are removed by condensation. Purified $TiCl_4$ is burnt in presence of oxygen to produce titanium dioxide pigment in the rutile form. The chlorine set free is recycled, thus avoiding pollution. M/S. Kerala Minerals and Metals, Quilon adopts this technology for TiO_2 pigment production.

Traditionally, rutile, which has got a higher titanium dioxide content than ilmenite or titano magnetite is the feedstock of choice, used in the production of rutile and titanium metal. Rutile deposits are very scarce in nature and they are becoming increasingly more expensive to mine. Consequently the cost of natural rutile is many times higher compared to ilmenite. Synthetic rutile, which is prepared from the cheaper and more abundant mineral ilmenite, by the removal of iron present in it, is found to be a good substitute for the costly and scarce natural rutile as the starting material in the processing. M/S. Dhrangadhara Chemical Works Limited, Sahupuram, Tamil Nadu, India is one of the large scale producers of synthetic rutile in India.

There are three main technical routes for the production of synthetic rutile in major quantities. One of the routes commercially practised at the present time involves reduction of the iron oxide present in ilmenite either partially to the ferrous state or to the metal. The iron is then removed by dissolution.

In the second route, the iron present in ilmenite is removed by selective chlorination. Since iron exhibits a greater affinity towards chlorine than titanium, it may be preferentially removed in a fluidized bed chlorinator leaving a highly TiO_2 enriched matrix. Under proper conditions the extraction of iron is essentially complete before $TiCl_4$ production commences.

The third method is the reduction smelting usually carried out using an electric arc furnace. The high titania slag obtained is used as the raw material for further processing.

1.6 Ilmenite as Welding Electrode Flux Material

Welding electrodes are rods used for combining two metallic pieces through welding. The core of the welding rods consists of the metal to be welded, which will be covered by a flux material. The functions of the flux material in a welding rod are lowering of welding temperature and to protect the welding electrode and the weld from oxidation. A material containing around 65-70% TiO_2 and around 25-30% metallic iron is used as the flux material in special type of welding electrodes. The commonly used flux materials are rutile, ilmenite, feldspar, kaolin, etc. The presence of rutile coating gives ductility and the presence of metallic iron reduces the carbon content of the weld and improves the sulphur distribution. It also resists the

formation of solidification cracks. The advantages of using reduced ilmenite as flux material is that it is cheaper and it is directly prepared from the raw material and the product has a better uniformity as metallic iron is distributed throughout the TiO_2 particles.

As the demand for titanium and its compounds increases and the reserves of rutile mineral dimnish, ilmenite has to be beneficiated to synthetic rutile to replace natural rutile. Five different processes were developed for the manufacture of synthetic rutile. They are Benilite, Murso, Ishihara, Becher and Summit processes. All these processes involve partial or complete reduction of the iron oxide in the ilmenite lattice by roasting with coal followed by selective leaching of the iron with HCl, H_2SO_4, $FeCl_3$ or aerated NH_4Cl solution. However Benilite and Becher processes employing the hydrometallurgical route have proved commercially successful. A comparison of the iron removal strategies followed in the above processes is described schematically in Fig 1.1.

Fig 1.1 Ilmenite ($FeO.\ TiO_2$)

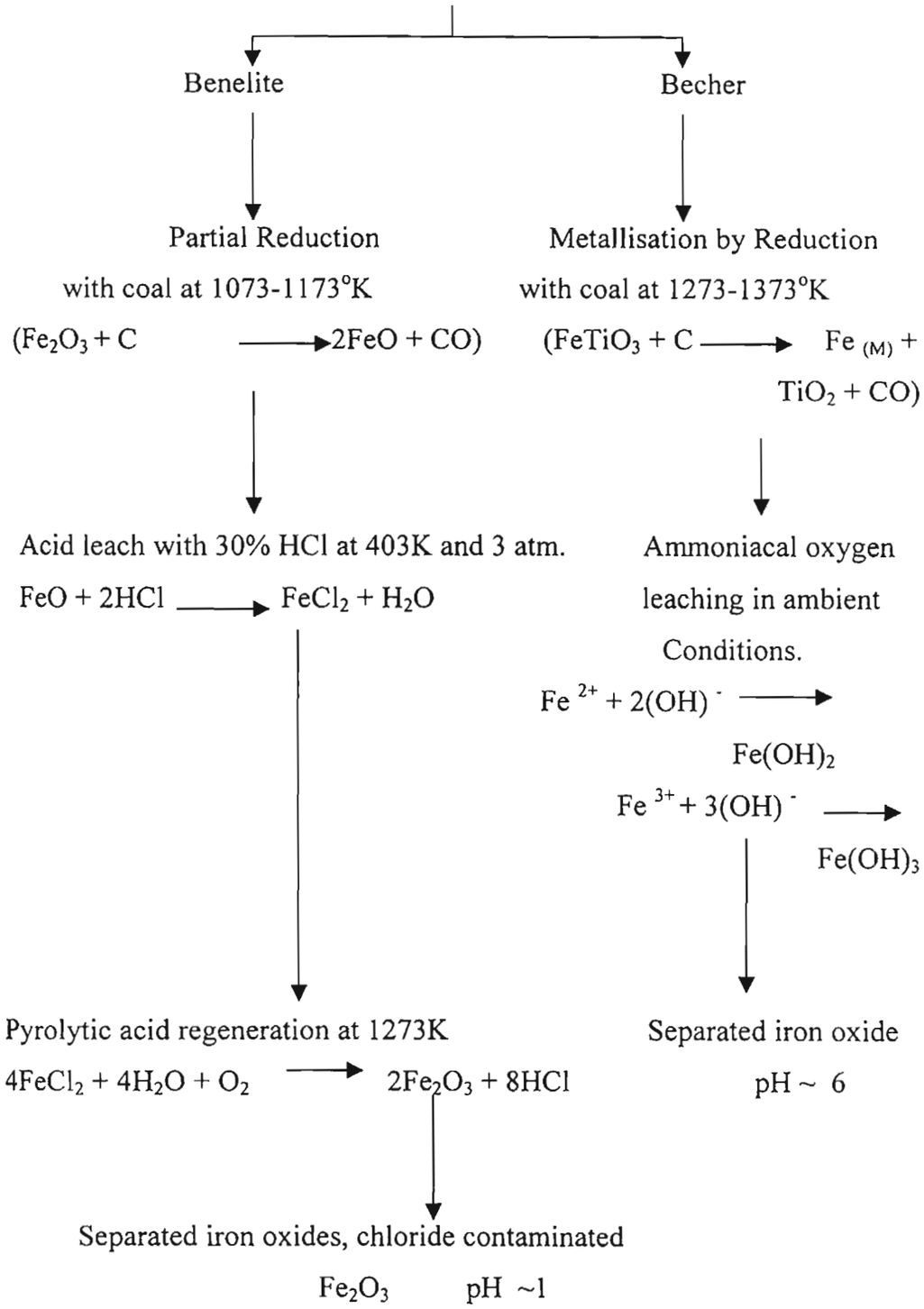

The Becher process has found worldwide acceptance due to its environmental advantages as well as the reduced capital and operating costs since the conversion of metallic iron to iron oxide is carried out in a single step at ambient conditions.

The most important disadvantage of the above process is that it takes upto 14-16 hrs for the complete conversion of metallic iron to iron oxide.

A new patent (Mohan Das et al) [158] developed by RRL – Trivandrum has the folllowing steps. Reduction, rusting or catalytic aeration, rutilation and acid leaching. Rusting or catalytic aeration step involves the aeration reaction of reduced ilmenite in the presence of a catalyst like NH_4Cl and the metallic iron gets converted to solid iron oxide, which can be separated. But this step also is very slow which takes about 14-16 hrs for completion which affects the productivity and hence economy. Any improvement in the catalytic aeration step will enhance the productivity.

This thesis highlights the attempts carried out to increase the rate of the catalytic aeration step using a few organic compounds along with NH_4Cl as catalyst. Also the effects of these catalysts when partially reduced ilmenite was used are also investigated.

1.7 Background of the Work

In the Becher process as well as the new process developed by RRL, Trivandrum, the major steps involved are

- Carbothermic reduction of ilmenite
- Catalytic removal of iron
- Acid leaching

a) Carbothermic reduction

The major reactions taking place during the reduction of ilmenite with carbon are

$$FeO.TiO_2 + C \longrightarrow Fe + TiO_2 + CO$$
$$Fe_2O_3.TiO_2 + 3C \longrightarrow 2Fe + TiO_2 + 3CO$$
$$FeO.TiO_2 + CO \longrightarrow CO_2 + Fe + TiO_2$$
$$Fe_2O_3.TiO_2 + 3CO \longrightarrow 3CO_2 + 2Fe + TiO_2$$
$$C + O \longrightarrow CO$$
$$CO_2 + C \longrightarrow 2CO$$

In the reduction both solid state as well as gaseous reactions are taking place. The temperatures used are usually 1000-1100°C. The reduced ilmenite is sieved and magnetically separated from coal and ash and is used for further processing.

b) Catalytic removal of iron

The reactions taking place is essentially aeration rusting as given below.

$$Fe \longrightarrow Fe^{2+} + 2e^-$$
$$Fe \longrightarrow Fe^{3+} + 3e^-$$
$$\tfrac{1}{2} O_2 + H_2O + 2e^- \longrightarrow 2(OH)^-$$
$$Fe^{2+} + 2(OH)^- \longrightarrow Fe(OH)_2$$
$$Fe^{3+} + 3(OH)^- \longrightarrow Fe(OH)_3$$

In the process reduced ilmenite is suspended in a solution of NH_4Cl, which is the catalyst and is aerated. The major functions of the catalyst are [158].

- acts as a buffer
- removal of iron from the particle by the formation of complexes

- Breaking up of the iron oxide film formed on the surface of the particle

The major factors affecting the reaction are

- ❖ pH of the solution
- ❖ Dissolved oxygen present in the system
- ❖ Temperature of the slurry
- ❖ Concentration of the catalyst
- ❖ Solid liquid ratio

Most of these parameters have already been optimised in the case of NH_4Cl as catalyst [157].

C) Acid leaching

The rusted ilmenite may contain small quantities of iron unremoved, which is leached out using dilute acids. The leaching is done before or after a rutilation step. The product thus obtained is usually high grade synthetic rutile with 94-96% TiO_2.

Even though this process is more environment friendly there is necessity for improving the catalytic aeration step which is at present very slow with NH_4Cl as catalyst.

1.8 Scope of the present investigation

The review of the literature shows that out of the available commercial processes for the production of synthetic rutile the Becher process only is environment friendly. However it also suffers from the fact that the catalytic rusting process is very slow which will be the main bottleneck in the process. This warrants the necessity for developing better catalysts, which can complete the reaction in considerably lesser time, which will be highly beneficial for the industries. Hence a detailed investigation

was under taken to find out the catalysts that can accelerate the rusting reaction. As NH_4Cl helps to serve the three basic functions it was retained as the basic catalyst and the effect of new compounds were evaluated in combination with NH_4Cl. Different types of compounds namely acids, alcohols, aldehydes, ketones, sugars, etc. either alone or as mixtures with NH_4Cl were evaluated. Attempts to understand the effects of various parameters affecting the reaction, kinetics, electrochemical investigations, structural and morphological changes as well as simulation of the reaction were carried out. The results of these investigations are presented in the next few chapters of this thesis.

CHAPTER 2

MATERIALS AND EXPERIMENTAL METHODS

This chapter deals with the description of the raw materials and chemicals used; experimental and analytical methods employed and the properties of the raw materials used for the present investigation.

2.1 Materials

The raw material used for the present study is Kerala ilmenite. The chemical composition of the Kerala ilmenite is given in table 2.1 [174].

Table 2.1 Chemical Analysis of Kerala Ilmenite

Constituent	Content (%)
TiO_2	60.60
Fe_2O_3	26.10
FeO	9.60
MnO	0.50
Cr_2O_3	0.40
V_2O_5	0.12
MgO	0.15
P_2O_5	0.50
ZrO_2	0.15
SiO_2	0.40
Rare Earths	0.80

Kerala ilmenite is reduced with carbon in a commercial rotary kiln. The reduced ilmenite is used as the stock material throughout the study. The material thus obtained had an iron metallisation of 83%. The chemical composition of the reduced ilmenite is given in table 2.2.

Table 2.2 Chemical Composition of Reduced Ilmenite

Constituent	Content (%)
TiO_2	62.64
Total Iron	28.32
Metallic Iron	24.03
P	0.12
C	1.00
S	0.15
MgO	2.80
Cr_2O_3	0.80
Al_2O_3	1.50
MnO	0.45
SiO_2	1.00
Others (V, Zr, etc.)	0.26

2.1.1 Properties of the Material Used

Ilmenite is a black shiny powdery material having particles of various sizes. The particle size ranges from 75μ to 385μ. The specific gravity of ilmenite is reported to be 4.39.

Reduced ilmenite contains black particles of various sizes. The sieve analysis of reduced ilmenite is given in table 2.1.1. The specific gravity was measured to be 4.467.

Table 2.1.1 Sieve Analysis of Reduced Ilmenite

Sl.no	Particle Size (mm)	Weight of fraction	%
1	1.4	-	-
2	1	-	-
3	-1 to 0.71	0.066	0.132
4	-0.71 to 0.5	4.414	8.84
5	-0.5 to 0.355	9.107	18.23
6	-0.355 to 0.25	12.629	25.28
7	-0.25 to 0.18	13.321	26.67
8	-0.18 to 0.125	9.401	18.82
9	-0.125 to 0.09	0.911	1.82
10	-0.09 to 0.063	0.091	0.182
11	-0.063	0.01	0.02
	Total	49.95	

Total weight taken = 50 g

2.1.2 Chemicals Used

The chemicals used for the experiments were of commercial grade and for the analysis were of AR grade. The AR grade chemicals used were of MERCK or s.d.fine chem. Ltd. The chemicals used in the experiment and analysis were NH_4Cl, Con.HCl, CH_3OH, C_2H_5OH, CH_3COCH_3, CH_3CHO, HCHO, HCOOH, CH_3COOH, Glyoxal, Glucose, Sucrose, Starch, Urea, Saccharin, H_2O_2, $Na_2S_2O_3$, Pyrogallol, Anthraquinone 2-sulphonic acid sodium salt, $K_2Cr_2O_7$, Ferric Ammonium Sulphate, $SnCl_2$, $HgCl_2$, Con.H_2SO_4, Phosporic acid, Zimmermann solution, Barium diphenyl amine sulphonate, Ammonium Thiocyanate, Potassium bisulphate, N-Phenylanthranilic acid, $NaHCO_3$, $KMnO_4$, Diphenyl Carbazide, Standard Manganese, Potassium periodate, Nitric acid, Carbon powder (electrolytic grade) and Tri butyl phosphate.

2.2 Experimental Methods

2.2.1 Seive Analysis

Sieve analysis of reduced ilmenite was carried out using a standard set of BSS sieves as per ISI method, IS 460 – (1962). Specific gravity was found out using a specific gravity bottle as per standard procedure [175].

A weighed amount of sample was placed on the top most sieve in the sieve set. Switched on the sieve set and made to run for definite period of time. The fraction of sample present in each sieve was collected and weighed, from which percentage of various sizes were calculated.

2.2.1 Rusting

2.2.1.1 Rusting Vessel

One litre plastic beaker was used as the rusting vessel. Three baffles were given as lining inside the vessel. Three inlets were given at the bottom

of the beaker to admit air during the rusting reaction. Air was admitted into the rusting vessel by means of rubber tubing, which in turn was connected, to a compressor. The experimental set up is shown in Fig 2.1

2.2.1.2 Mechanical Stirrer

Universal Motors (Remi Motor), India mechanical stirrer was used to stir the system throughout the experiment. The rotation was fixed as 800 per minute.

2.2.1.3 Compressor

An Elgi air compressor was used to pass air at the rate of 4-5 litres per minute during the reaction.

2.2.1.4 pH Meter

A Toshniwal Instruments pvt. Ltd, (Ajmer) pH meter was used to monitor the changes in pH throughout the reaction.

2.2.1.5 Dissolved Oxygen

A digital Oxygen Meter (Hi-Tech Accessories, India) was used to monitor the amount of oxygen dissolved during the course of the reaction.

2.2.1.6 Thermostat

Siskin Jublabo VPC Fab. No 07 thermostat was used to study the effect of temperature on rusting reaction.

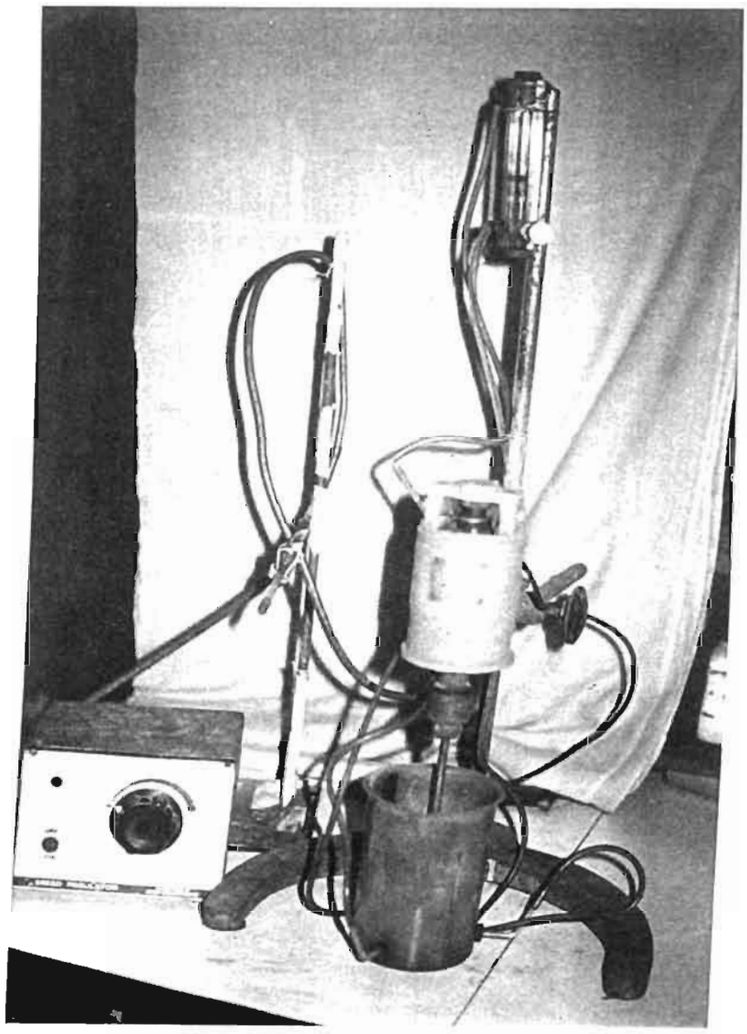

Fig. 2.1 Experimental set up for the rusting reaction

2.3 Experimental Procedure

125 gms of reduced ilmenite was suspended in 500 ml of 1.5 % ammonium chloride solution (1:4 w/w ratio). 1-2% of the new compounds were added and the pH was adjusted to 4 with Con.HCl if needed. The system was stirred using a mechanical stirrer and the r.p.m. was fixed as 800. Air at the rate of 4-5 lit/min. was passed through the suspension. The experiment was carried out for a period of 8 hrs. Samples were withdrawn at regular intervals of time and analysed for total iron. During rusting the metallic iron present in the reduced ilmenite is converted to solid iron oxide. After 8 hrs of reaction the rusted ilmenite and solid iron oxide were separated, washed well with water and dried in an air oven at 110°C for 2 hrs.

2.3.1 Effect of temperature

Effect of temperature on rusting reaction was studied using a temperature controlled circulating water bath (thermostat). A stainless steel reaction vessel fabricated with clamping facilities and set of baffle lining inside was used for the experiments. Along the baffle lining glass tubes were inserted and clamped to pass air. The temperatures selected for the studies were 25, 30, 35 and 40°C. All the experimental conditions were maintained as explained in section 2.2.1. Samples were withdrawn at regular intervals of time and analyzed for total iron.

2.3.2 Solid-Liquid Ratio

Experiments were carried out to optimize the solid-liquid ratio. Maintaining the volume of ammonium chloride solution constant the weight of ilmenite was varied from 25 – 175 g and the solid liquid ratio has been optimized as 1:4.

2.3.3 Rotations per Minute

Experiments were carried out by changing the rpm from 600 to 900 to fix the optimum rpm for the rusting reaction.

2.4 Rutilation

Rutilation, which is an oxidation step, was carried out by heating the rusted ilmenite in an electric furnace in the presence of air at about 700 or 800°C for 30 minutes.

2.5 Leaching set up

A three necked round bottom flask of 250 ml volume was used for carrying out the leaching experiments. A teflon stirrer was introduced into the flask through one neck while a thermometer was fitted in the second neck to measure the temperature. A water condenser was fitted to the third neck to avoid the evaporation of the acid. A heating mantle with controls was used for heating the solution. A Remi mechanical stirrer was used for agitating the solution.

Rusted ilmenite and 20% HCl in the ratio 1:2 w/v were taken in the flask. 20% HCl was used as this forms a constant boiling azeotrope. Leaching temperature was fixed at 80-90°C as this was reported to be optimum [176]. Leaching was carried out continuously for 3 hrs. Stirring rate was adjusted to about 100 rpm. After leaching the synthetic rutile formed was washed well with water, dried in an air oven at 110°C and used for analysis.

2.6 Chemical Analysis

2.6.1 Estimation of Total Iron

Standard chemical analysis procedure was followed for the estimation of total iron in ilmenite [177].

2.6.2 Estimation of Metallic Iron

Metallic iron was estimated using the method [178] as given below.

Approximatley 6 g of $HgCl_2$ was boiled with 150 ml water. About 0.5g of exactly weighed sample was added to this boiled solution, boiled for a few minutes and filtered. The residue was again boiled with water till free from iron. Presence of iron was tested by placing a drop of the filtrate on pottassium ferricyanide solution. Formation of a green precipitate showed the presence of iron. The solution was then titrated against std. $K_2Cr_2O_7$, after adding 20 ml of dil. Phosphoric acid – sulphuric acid mixture, 10 ml of Zimmermann solution and 2 drops of N-phenyl anthranilic acid as indicator. Appearance of pink colour gave the end point. The amount of iron present in the solution was calculated from the titration data.

2.6.3 Estimation of Ferrous Iron

Ferrous iron present in the sample was estimated using the standard procedure followed in metallurgical analysis [179] as given below.

Weighed accuratley 0.5 g of the sample and transfered into a 500 ml conical flask fitted with Bunsen valve. Moistened the sample with 10 ml water and added 1 g $NaHCO_3$, 50 ml of Con.HCl and 4 drops of HF. The contents were digested for 5-10 mts with Bunsen valve in position. Carefully washed and removed the valve, and diluted the contents of the flask to 250 ml with distilled water. Added 10 ml of Con. H_3PO_4 and 5 ml of barium diphenylamine sulphonate indicator. Titrated against std.$K_2Cr_2O_7$ solution to a purple colour.

A Bunsen valve consists of a glass tube at one end of which is attached to a short rubber tubing. The upper end of the rubber carries a short glass rod. The rubber tube has a vertical slit about 1-2 cm long, which forms the valve. This allows the gas or vapour from inside to pass out but closes by atmosphere pressure when evolution ceases and thus prevents the entry of air.

2.6.4 Estimation of TiO_2

About 0.5 g of the sample was fused with excess of potassium bisulphate. Cooled the mass and dissolved in 150 ml of 20% H_2SO_4 and made upto 250 ml in a standard measuring flask. Pipetted out 20 ml of the made up solution in an Erlenmeyer flask and added 30 ml of Con.HCl to the above solution. Boiled the solution well and removed from the mantle. Attached 2 gms of high purity Aluminium foil to the end of the glass rod of the reductor. Immediatley inserted the rubber stopper carrying the glass rod with Aluminium foil and the delivery tube into the flask. Placed the other end of the delivery tube below the level of sodium bicarbonate taken in a beaker. The reaction between the Aluminium foil and the solution was rapid. Towards the end of the reaction swirled the flask to ensure complete mixing and reduction. When all the Aluminium foil appeared to be dissolved, gently boiled the solution for 3-5 mts keeping the delivery tube immersed in sodium bicarbonate solution.

Cooled the sample to less than 60°C. As the sample was cooled, the sodium bicarbonate solution was drawn inside the Erlenmeyer flask and the carbon dioxide evolved gave the necessary protective atmosphere. When the solution was cooled, the stopper was removed and rinsed the glass rod and the delivery tube with distilled water. Added 2 ml of 24% Ammonium

thiocyanate indicator. Titrated with standard ferric ammonium sulphate solution.

% TiO_2 = ml of titrant X factor X 250 X 100 / Weight of the sample (g) X Volume of the sample pipetted

2.7 Instrumental Methods Used

2.7.1 X–ray diffraction

The X-ray diffraction studies were carried out by the powder diffraction technique using a Philip's x-ray diffractometer (Model no. PW – 1140). Results were analysed by comparing with standard values available in the literature.

2.7.2 Scanning Electron Microscopy (SEM)

The SEM studies of the samples were carried out using a JSM 5600. The samples were fixed on an adhesive tape pasted over the stud. Gold was sputtered and the pictures were taken at the required magnification depending on the surface selected for the studies.

2.7.3 Cyclic Voltammetric Studies

Cyclic Voltammetric studies were carried out using a potentio scan Wenking POS – 88 (Germany) with X, Y/t recorder (Rikadenki, Japan)

The cyclic voltammetric studies were carried out using a three electrode cell containing platinum counter electrode, saturated calomel electrode as the reference electrode (E = + 0.2422) and ilmenite carbon paste capillary as working electrode.

High anodic potentials were observed and the current increased in a non-linear way when reduced ilmenite (RI): Carbon paste (CP) weight ratio was high. Hence the electrode was prepared with relatively low ratios. RI

and CP were mixed in a ratio of 1:4 with tri - n – butyl phosphate as binder and packed in a 1.5mm diameter capillary tube and used as the working electrode after compacting.

2.7.4 UV-Visible Spectrophotometer

Trace elements such as manganese and chromium were analysed using UV-Visible Spectrophotometer.

Manganese was analysed by oxidising Mn to permanganic acid using potassium per iodate solution and the absorbance measured at 545nm and value obtained from calibration graph [180].

Chromium was analysed by developing colour with 0.25% diphenyl carbazide solution and the absorbance measured at 546nm and the value obtained from calibration graph [180].

2.7.5 Thermo Gravimetric Analyser

The oxidation studies of synthetic rutile were carried out using Shimadzu TGA-50H. The heating rate was $10^{o}C$/ min. A minimum quantity of synthetic rutile was taken in a platinum cell and heated in N_2 atmosphere. The rate of flow of N_2 was adjusted to 20 ml/ min.

2.7.6 Surface Area Analyser

The surface area of the reduced ilmenite as well as rusted ilmenite were analysed using a Micromeritics 2360 Surface Area Analyser.

2.7.7 Optical Microscopy

The optical microscopic studies were carried out by using a Leitz Metallo Plan, Germany.

CHAPTER 3

STUDIES ON RUSTING OF REDUCED ILMENITE USING ADDITIONAL COMPOUNDS ALONG WITH NH_4Cl

In the newly developed process for synthetic rutile rusting of ilmenite is carried out in presence of NH_4Cl. As rusting reaction is very slow with NH_4Cl, certain additional compounds were added along with it to accelerate the rusting reaction. This chapter describes the results of experiments carried out using certain additional compounds, which were added during rusting.

3.1 Rusting Reaction Carried out using NH_4Cl alone

About 200 g of ilmenite was suspended in 500ml of 2.5% (w/v) NH_4Cl solution. HCl was added in drops to bring the pH of the solution to 4. Air at the rate of 4-5 lit/ min.was passed and the rpm was fixed at 900. Samples were withdrawn at regular intervals of time and analyzed for total iron. The results of analysis are given in table 3.1.

Table 3.1 Chemical analysis data of reaction using NH_4Cl alone

Time (hrs)	% Total Iron	% Iron Removal
0	28.47	0.0
1	26.32	7.55
2	24.15	15.17
3	22.60	20.62
4	19.78	30.52
5	18.20	36.07
6	18.00	36.78
7	16.83	40.88
8	16.60	41.69
9	16.61	41.66
10	16.58	41.76

3.2 Rusting Reaction using CH_3CHO along with NH_4Cl

10 ml of 20% CH_3CHO was added to the NH_4Cl solution which was used for rusting reaction. The experiment was carried out as described earlier. The results are given in table 3.2.

Table 3.2 Chemical Analysis Data of Rusting of Reduced ilmenite using $NH_4Cl + CH_3CHO$

Time (hrs)	% Total Iron Remaining	% Iron Removal
0	28.47	0.0
1	22.89	19.60
2	20.57	27.75
3	16.00	43.80
4	13.83	51.42
5	12.60	55.74
6	10.80	62.07
7	10.66	62.55
8	10.21	64.17
9	10.18	64.24
10	10.02	64.80

A comparison of the results obtained is given in Fig. 3.1

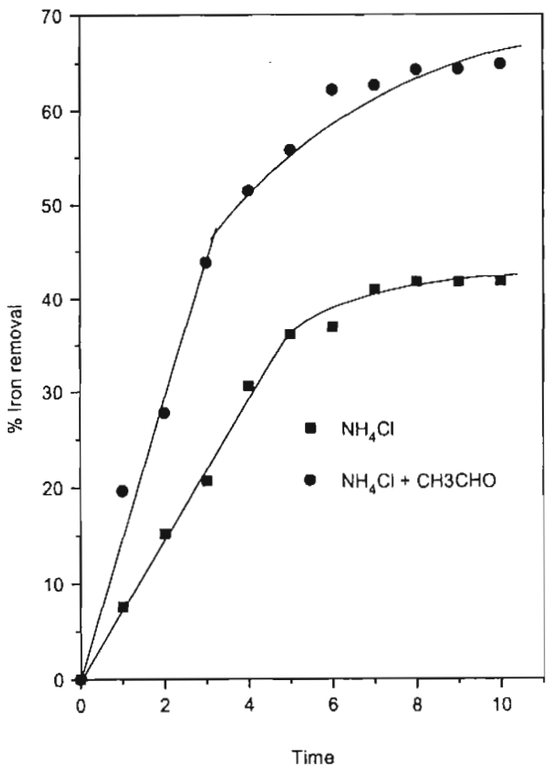

Fig 3.1 % Iron removal using NH_4Cl and $NH_4Cl + CH_3CHO$

After 10 hrs of rusting with NH_4Cl alone the total iron left unremoved was 16.6% while with $NH_4Cl + CH_3CHO$, it was 10%. Passivation of the reaction was observed after 7 hrs in the case of NH_4Cl alone and after 6 hrs in the case of $NH_4Cl + CH_3CHO$. So, it was decided to carry out all the reactions for 8 hrs.

Before studying the effects of individual new compounds, the rusting parameters such as solid-liquid ratio, concentration of catalyst, effects of temperature and rpm used were optimised.

3.3 Optimisation of solid-liquid ratio

Experiments were carried out with different quantities of ilmenite ranging from 25-175 gms in 500 ml of the solution. Fig. 3.2 gives the results of these investigations.

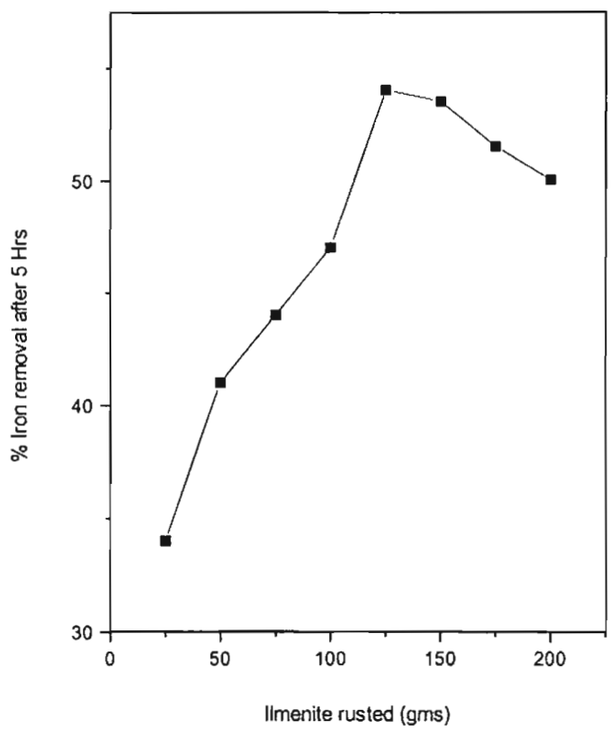

Fig. 3.2 Optimisation of solid-liquid ratio

From the figure it is evident that the optimum solid liquid ratio is 1:4

As NH_4Cl is the basic catalyst in the rusting reaction the optimisation of the amount of NH_4Cl is highly essential. Experiments were carried out to optimise the amount of NH_4Cl needed for the rusting reaction. The concentrations were changed from 1 to 2% (w/v) in the system. The results are given in Fig. 3.3 where the values after 5 hrs of rusting is plotted against concentration. It is observed that the trend is the same at any time upto 8 hrs where the reaction gets stabilised.

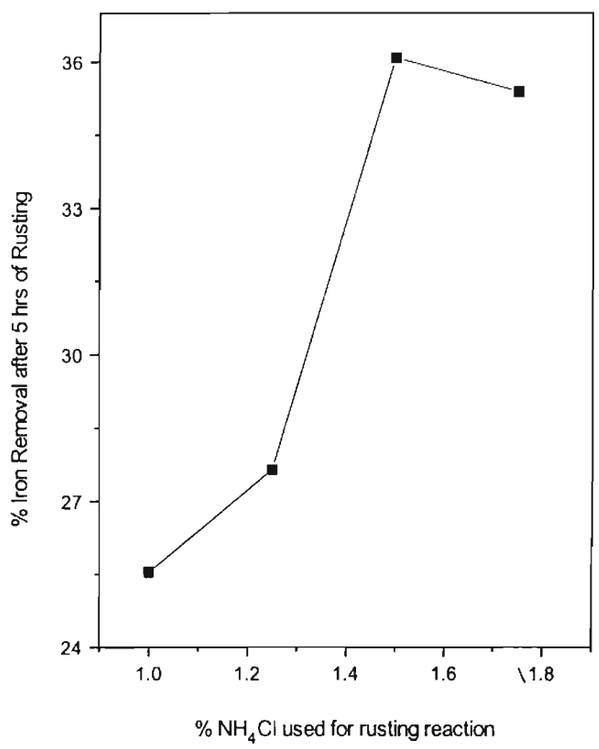

Fig. 3.3 Optimisation of concentration of NH_4Cl

From the above figure it is clear that 1.5% NH_4Cl is optimum for the reaction.

3.5 Optimisation of the concentration of the additional compounds

3.5.1 Addition of CH_3CHO

Experiments were carried out to optimise the quantity of the new compounds added to 500ml of NH_4Cl solution during the rusting of ilmenite. The volume of CH_3CHO added was 0 to 15 ml of commercial solution. The results of the studies are shown in Fig. 3.4. It is found that 10 ml of CH_3CHO was sufficient for maximum iron removal.

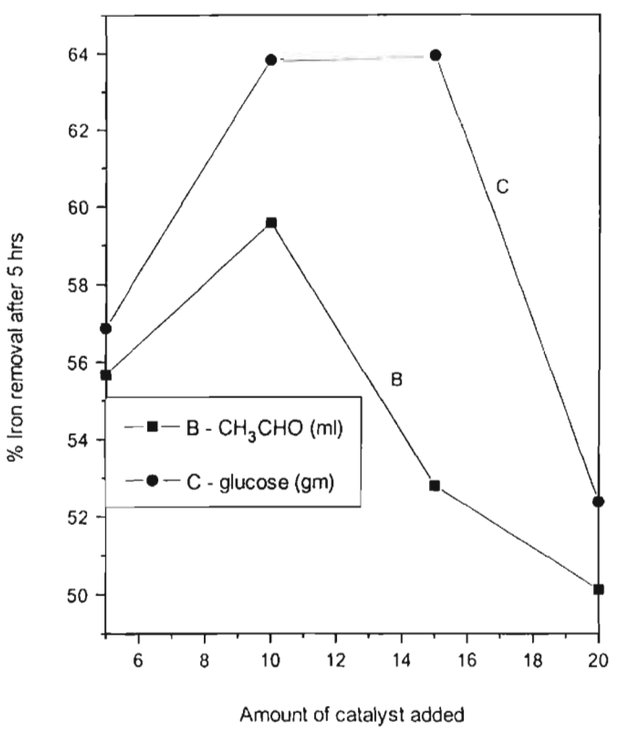

Fig. 3.4 Optimisation of catalysts like CH_3CHO and glucose

3.5.2 Addition of Glucose

The results of the experiments carried out using glucose are given in Fig. 3.4. Experiments were carried out as in the case of CH_3CHO. Quantity of glucose used was 0 – 20 g in 500 ml of NH_4Cl solution. The graph shows that the optimum quantity of glucose for the reaction is 10 – 15 g in 500 ml.

From the above experiments it is found that adding 10 ml of CH_3CHO or 10 gm of glucose was essential for rusting.

3.6 Effect of temperature

Experiments were carried out to find out the effect of temperature on the rusting reaction. The temperatures selected were 25,30,35 and 40°C. When NH_4Cl alone was used the rusting reaction increased with temperature. It was observed that the rusting reaction was found to be very slow above 30°C when additional organic compounds were added along with NH_4Cl. The rusting reaction was maximum at 35°C in the case of CH_3CHO whereas maximum rusting reaction was observed at 30°C in the case of HCHO, CH_3CHO, CH_3OH, CH3COCH3, C_2H_5OH, CH_3COOH, glucose, sucrose, starch and urea. Above these temperatures the reaction was very slow. Because of this reason the above four temperatures were selected for the study. The temperature effects will be discussed in detail under kinetics. Fig. 3.5 shows the increase in rusting with temperature in the case of NH_4Cl alone whereas Fig. 3.6 shows that there is a decrease in rusting as temperature is increased above 30° when methanol, glucose, sucrose, starch and urea were used as catalyst along with NH_4Cl.

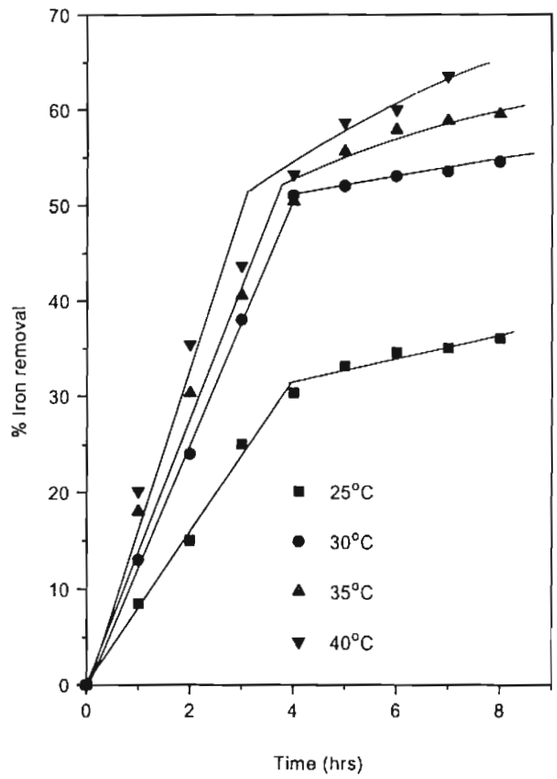

Fig.3.5 Variation in rusting with temperature when NH_4Cl alone is used

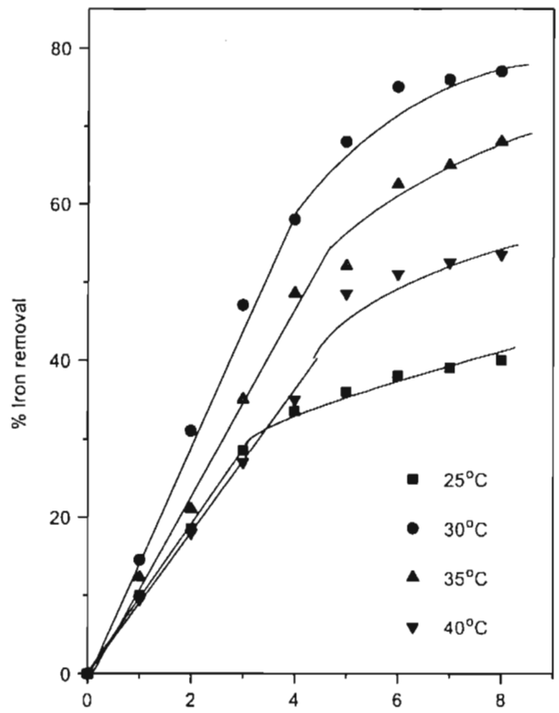

Fig·3.6 Variation in iron removal with temperature using $NH_4Cl + CH_3OH$

3.7 Optimisation of stirring rate of suspension

Suspension of the solid in the liquid medium is a major requirement for rusting to take place. Suspension of solids is directly related to the rpm of the stirrer. Hence experiments were carried out to optimise the rpm of the stirrer during rusting. The rpms selected were 600, 700, 800 and 900 respectively. The effect of rpm on iron removal after 2 hrs of rusting is

shown in Fig. 3.7. From the figure it is evident that the optimum rpm for iron removal is 800.

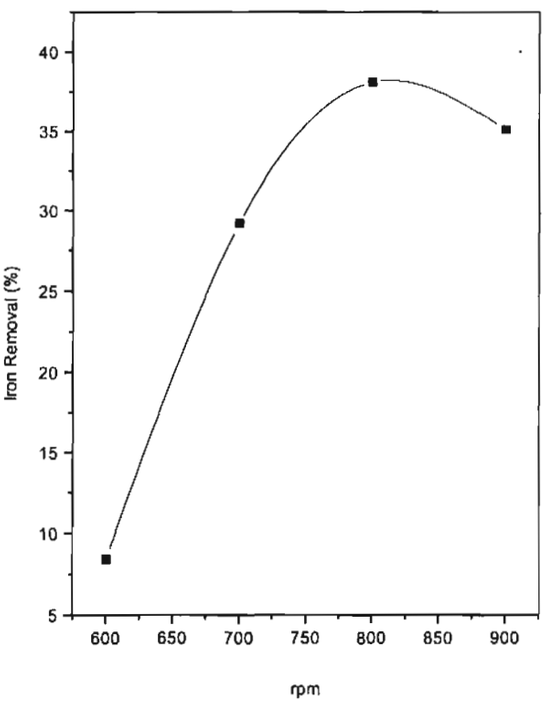

Fig. 3.7 Optimisation of rpm

After optimising the above parameters experiments were carried out at the optimised conditions. Separate experiments were carried out with NH_4Cl alone and NH_4Cl + additional compounds and the results were compared. While carrying out the rusting reaction pH of the system and dissolved oxygen present were measured after every hour and plotted.

3.8 Optimised rusting reaction using NH_4Cl alone

Experiments were carried out as described in section 2.3. Reduced ilmenite used 125 g, NH_4Cl 1.5% in 500 ml, Con.HCl for pH adjustment, rpm – 800 and airflow 4 –5 lit/min. The results of the experiments are given in table 3.3

Table 3.3 Rusting reactions using NH_4Cl alone under optimised conditions

Time (hrs)	% Total Iron remaining	% Iron Removal
0	28.47	0.0
1	24.77	13.00
2	21.64	24.00
3	17.65	38.12
4	13.95	50.98
5	13.67	52.01
6	13.38	53.13
7	13.24	53.5
8	12.95	54.5

3.8.1 pH of the reaction

As pH 4 was favourable for rusting reaction, Con.HCl was added to bring down the pH to 4. The change in pH after every hour during the progress of the reaction is given in table 3.4.

Table 3.4 Variation of pH during rusting

Time (hrs)	pH
0	4.0
1	5.4
2	5.4
3	5.7
4	5.8
5	5.7
6	5.7
7	6.2
8	6.2

3.8.2 Dissolved Oxygen

As rusting is an oxidation reaction, presence of dissolved oxygen in the system will have a major influence on its progress and hence was monitored every hour. The values are given in table 3.5. It is seen that the dissolved oxygen in the system decreases during the progress of the reaction.

Table 3.5 Variation of dissolved Oxygen during rusting

Time (hrs)	Dissolved Oxygen (ppm)
0	6.8
1	4.6
2	3.7
3	4.0
4	3.9
5	3.7
6	3.7
7	3.7
8	3.7

3.9 Rusting reactions carried out using NH_4Cl + additional compounds

In order to increase the rate of the rusting reaction certain organic and inorganic compounds were added along with NH_4Cl to see if the reaction was improved. The results of the experiments using each individual compound will be discussed by comparing with NH_4Cl alone when used as the catalyst.

3.10 Results and discussion

3.10.1 Rusting reaction using methanol, acetone or CH_3COOH along with NH_4Cl

Rusting was carried out at the optimized conditions with 2% methanol or 2% acetone or 1% CH_3COOH along with NH_4Cl added to the system. As pH was already 4 on adding methanol or acetone or CH_3COOH, HCl was not added. When 2% (v/v) acetic acid was used, the reaction was uncontrollable due to foaming, so the amount of acid added was reduced to 5ml ie 1% only. Rusting was very fast and the results are as given in Fig. 3.8.

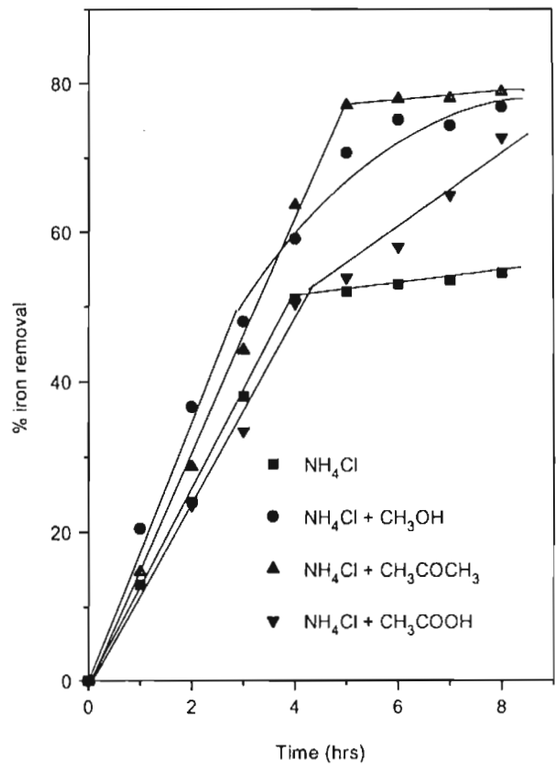

Fig-3.8 % Iron removal vs-time

3.10.2 Rusting with acetic acid, methanol or acetone + NH_4Cl

It was observed that when NH_4Cl alone was used as the catalyst the rusting reaction was quite fast up to 4 hrs where about 45% of iron was removed after which a passivation was observed and only 54.5% iron removal was obtained in 8 hrs. When acetic acid was used along with NH_4Cl up to 4 hrs there was no change in the rate of the reaction. However after 4

hrs there was still considerable reaction resulting in 70% removal in 8 hrs. There was lot of foaming during the initial 4 hours.

When methanol was added along with NH_4Cl during the rusting, the reaction was faster up to 5 hrs where about 71% was removed, after which the reaction got passivated ending up in about 77% iron removal after 8 hrs.

When acetone was added along with NH_4Cl during the rusting the reaction was very fast and more than 75% iron removal was observed at 5 hrs after which the reaction was slow giving only 80% of iron removal in 8 hrs.

From Fig 3.8, it is clear that the efficiency of iron removal decreased in the order acetone > methanol > acetic acid > NH_4Cl.

3.10.3 Variation in pH against time

The variations in pH observed for the above three systems against time during the progress of the reaction are plotted in Fig. 3.9

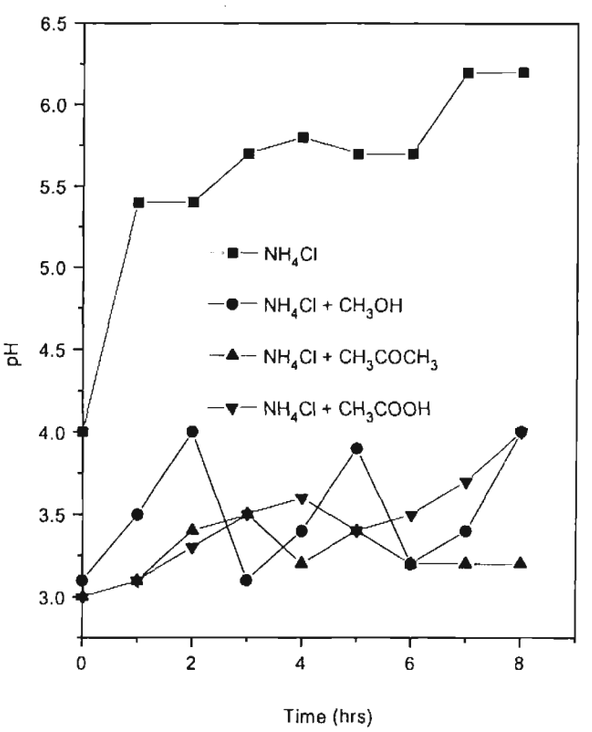

Fig-3.9 Variations in pH during rusting

When NH_4Cl alone was used the initial pH was adjusted to 4, as the rusting reaction was found to be favourable at pH 4. In the 1st hr of rusting the pH increased up to 5.4 and then increased gradually up to 6.5 in 8 hrs.

When acetic acid was added the pH measured initially was 3 and a gradual increase in pH was observed up to 4 hrs. The pH measured at the 4th hr was 3.5, which then increased to 4 till 8 hrs.

In the case of methanol the pH initially was 3.1, which then increased to 4 till 2 hrs fluctuating afterwards, till 8 hrs. At 8^{th} hr the pH measured was 3.9.

On adding acetone to the system the initial pH was 3, which slightly fluctuated till 8 hrs ending up at 3.2.

3.10.4 Variation of Dissolve oxygen against time

The dissolved oxygen measured during the progress of the reaction with time for the above three systems are plotted in Fig. 3.10.

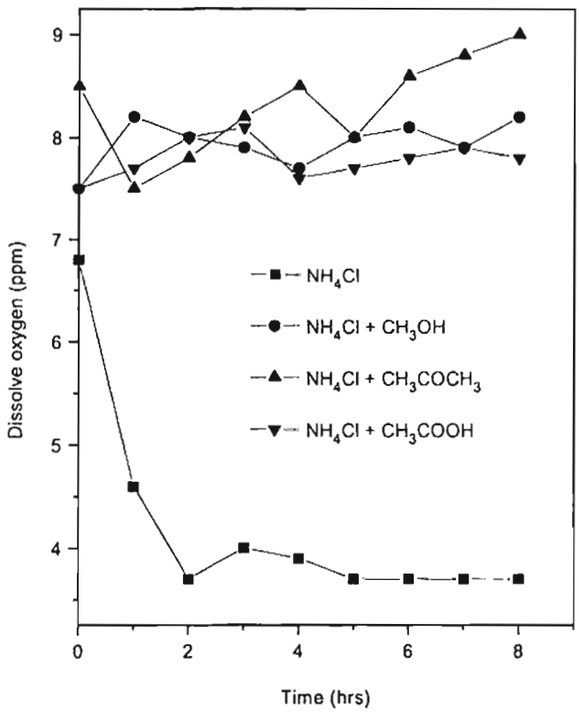

Fig·3.10 Variation in dissolved oxygen during rusting

When NH_4Cl alone was used the dissolved oxygen present initially was 6.9 ppm, which decreased gradually and then stabilised at 3.7 ppm from 5th hr onwards.

In the case of acetic acid the dissolved oxygen present initially was 7.5 ppm, which increased up to 8.1 ppm till 3 hrs and then slightly decreased to 7.9 ppm at 8 hrs.

When methanol was added the dissolved oxygen initially was 7.5 ppm, which then increased to 8.2 ppm in the 1st hr after which minor increase and decrease were observed reaching a value of 8.1 ppm at 8 hrs.

When acetone was added to the system the dissolved oxygen initially was 8.5 ppm, which decreased up to 7.5 ppm in the 1st hr, after which it gradually increased up to 8.5 ppm up to 4 hrs. The value then decreased to 8 at 5 hrs and then increased to 9 ppm till 8 hrs.

Figs 3.8, 3.9, 3.10 show that the rusting reaction was very fast with NH_4Cl + acetone and about 80% iron removal was observed in 8 hrs. The dissolved oxygen was also quite high and fluctuated up to 9 ppm. The pH was comparatively low and varied from 3 to 3.5 till 8 hrs of reaction.

3.11 Reaction using glucose, sucrose or starch + NH_4Cl

Fig. 3.11 gives the iron removal behaviour when NH_4Cl + glucose or sucrose or starch when added during the rusting reaction. The pH was adjusted to 4 using HCl. The amount of glucose, sucrose or starch added was 2% (w/v). Rusting improved to some extent on the addition of glucose, sucrose or starch.

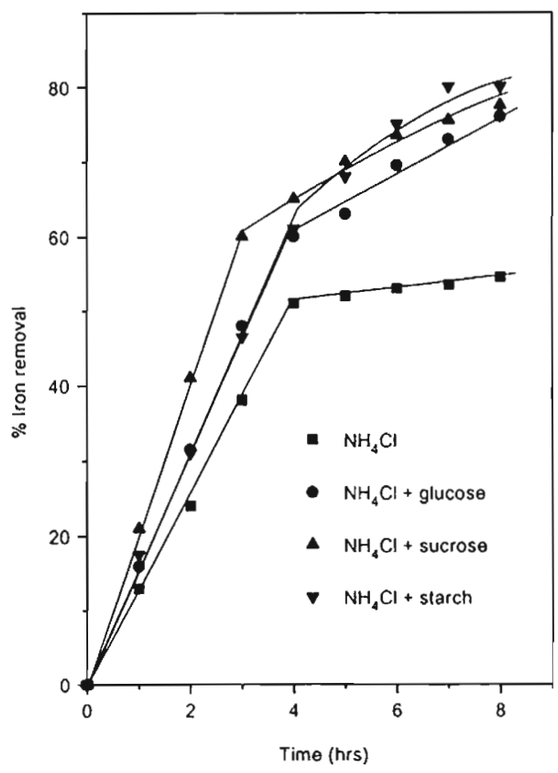

Fig-3.11 % Iron removal vs-time

3.11.1 Rusting with Glucose, Sucrose or Starch along with NH_4Cl

Fig. 3.11 gives the iron removal behaviour when using catalysts such as glucose, sucrose and starch along with NH_4Cl. When glucose was added along with NH_4Cl rusting reaction was very fast till 4 hrs and about 60% of the iron was removed. After that the reaction became comparatively slow with a final removal of 75% after 8 hrs of rusting which could be due to the

scarcity of metallic iron on the surface of the particles necessitating diffusion of iron from the interior of the particles to the surface.

When sucrose was added along with NH_4Cl the rusting reaction was quite fast up to 3 hrs when 60% of the iron was removed after which it slowed down giving a value of 77% after 8 hrs.

When starch was added, initially the rusting reaction was slow till 5 hrs compared to NH_4Cl alone. After 5 hrs the iron removal progressed further and increased up to 8 hrs giving a removal of 76% compared to 54% for NH_4Cl alone after 8 hrs.

3.11.2 Variation in pH

The variations in pH observed, when the rusting reaction was carried out using starch along with NH_4Cl is shown in Fig. 3.12. Since the other systems namely glucose and sucrose had the similar type of pH behaviour only pH obtained on adding starch is plotted and shown here.

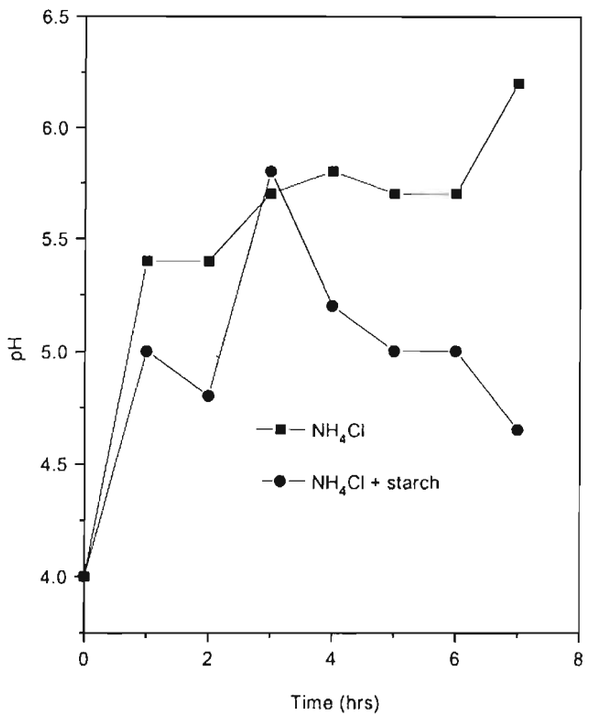

Fig.3.12 Variation in pH during rusting

In the case of NH_4Cl alone the pH increased with the reaction while in the case of starch the pH increased from 4 to 5.75 in 3 hrs after which it decreased indicating that the medium was acidic even after 8 hrs. The same trend was observed in the case of other compounds also.

3.11.3 Variation in Dissolved Oxygen

Variations in dissolved oxygen measured for the above three systems namely glucose, sucrose or starch along with NH_4Cl is shown in Fig. 3.13

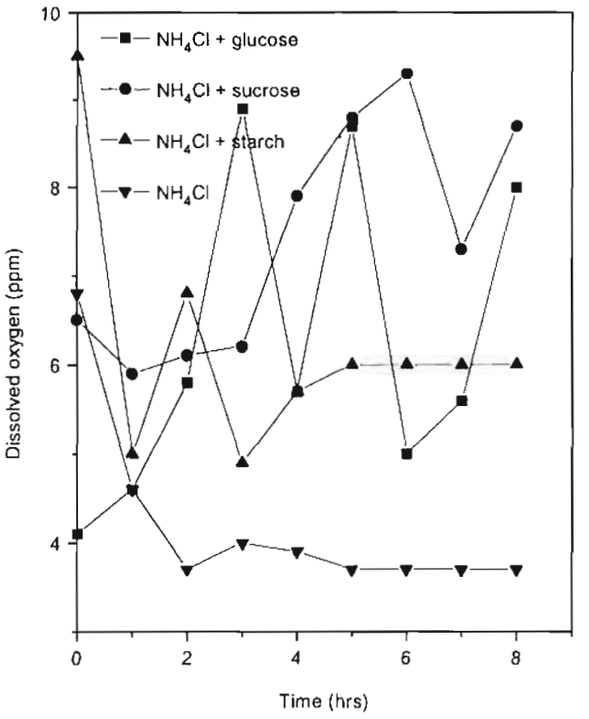

Fig·3.13 Variation in dissolved oxygen during rusting

In the case of glucose and sucrose the dissolved oxygen varied in an irregular manner between 5 and 10 ppm whereas in the case of starch the variation was observed initially for 4 hrs after which it remained more or less steady. This is quite different from the behaviour of NH_4Cl alone where the dissolved oxygen decreases drastically during the initial 2 hrs after which it remains more or less constant at about 3.7 ppm.

3.12 Rusting reaction carried out using Glyoxal or urea or saccharin + NH_4Cl

Rusting reaction was carried out by adding glyoxal or urea or saccharin along with NH_4Cl. Amount of glyoxal added was 2% (v/v), 2% (w/v) in the case of urea and 2% (w/v) in the case of saccharin. pH was not adjusted since the pH was already 4 on adding glyoxal, while adding urea and saccharin the pH was adjusted using HCl. The results of rusting are shown in Fig. 3.14.

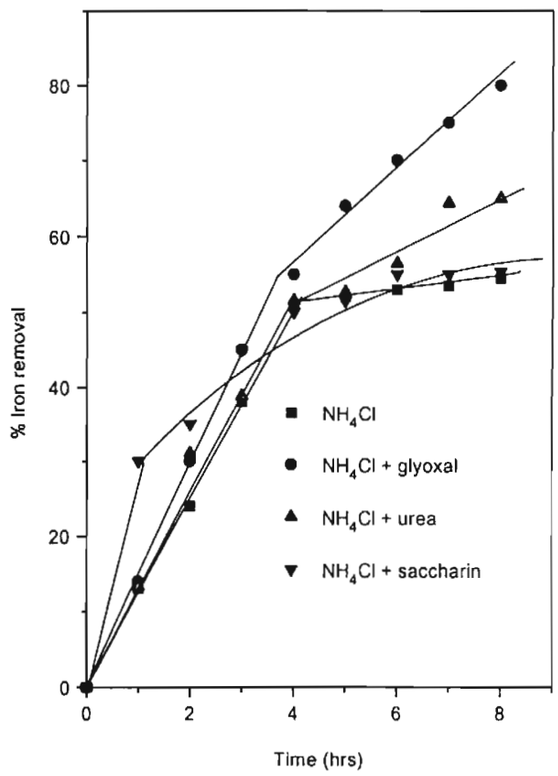

Fig-3.14 % Iron removal vs-time

3.12.1 Rusting reaction carried out by adding glyoxal, urea or saccharin + NH_4Cl

Fig. 3.14 shows the rusting behaviour of reduced ilmenite when catalysts such as glyoxal, urea and sacchrin were added along with NH_4Cl. When glyoxal was added along with NH_4Cl the rusting reaction was very fast up to 4 hrs where about 55% total iron removal was observed. Afterwards the reaction proceeded in a regular manner reaching a value of 80% iron removal in 8 hrs.

When urea was added along with NH_4Cl the iron removal was quite fast till 4 hrs where about 50% of iron removal was observed. After 4 hrs the reaction became slow reaching a value of 67% iron removal in 8 hrs. The presence of iron oxide film over the grains may be the reason for less iron removal after 4 hrs.

When saccharin was added along with NH_4Cl the rusting reaction was very fast during the 1^{st} hour. About 30% iron removal was observed in the 1^{st} hour itself. Afterwards the reaction became very slow giving about 52% iron removal in 8 hrs. This may be due to the deposition of iron oxide over the particles, which does not allow the exposure of metallic iron to the rusting environment.

3.12.2 Variation in pH

Variation in pH measured during the rusting reaction is plotted in Fig. 3.15. As the trend in pH of urea and saccharin was almost the same, only pH measured using saccharin is plotted.

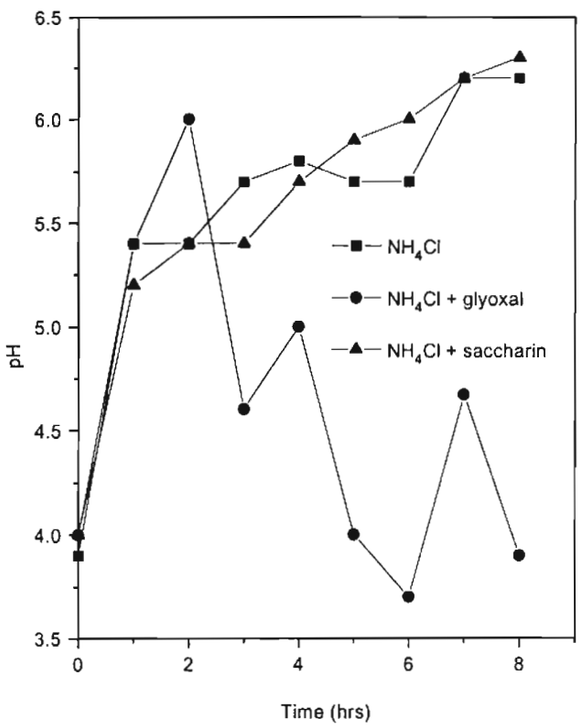

Fig·3.15 Variation in pH during rusting

The variation in pH measured during the rusting reaction carried out by adding glyoxal and saccharin along with NH_4Cl is plotted in Fig 3.15. When glyoxal was added along with NH_4Cl even though the initial pH was 4, the pH increased up to 6 in the 2^{nd} hour and then gradually decreased and came down up to 3.7 and then fluctuated between 3 and 4. This may be due to the oxidation of glyoxal to oxalic acid because of continuous aeration throughout the reaction. Formation of oxalic acid during the reaction was

confirmed through proper tests. That may be the reason for the decrease of pH during the course of the reaction.

When saccharin was added along with NH_4Cl the pH increased from 4 to 5.5 in the 1st hour itself. The pH started increasing in a regular manner and went up to 6.3 during the progress of the reaction. That may be the reason for less rusting when saccharin was added.

3.12.3 Variation in dissolved oxygen

Variation in dissolved oxygen observed during the rusting reaction is plotted in Fig. 3.16. The dissolved oxygen measured by adding glyoxal and saccharin is plotted.

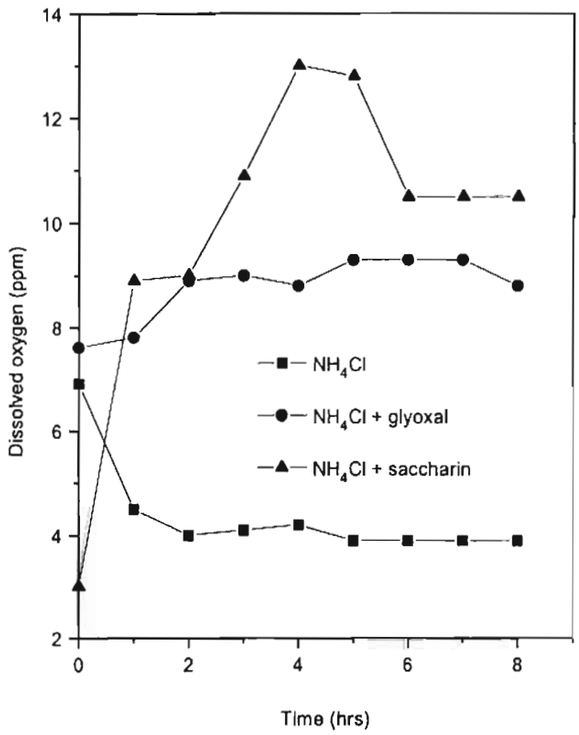

Fig-3.16 Variation in dissolved oxygen during rusting

When glyoxal was added along with NH_4Cl the dissolved oxygen fluctuated in a zigzag manner from 7.5 ppm to 9 ppm. When saccharin was added along with NH_4Cl the dissolved oxygen increased from 3 ppm to 8.8 ppm in the 1st hour and then increased up to 13 ppm after which it decreased in a narrow manner up to 10 ppm. From this experiment it is evident presence of oxygen alone in the environment does not favour the rusting reaction.

3.13 Rusting reaction carried out by adding H_2O_2 or pyrogallol or Anthraquinone 2- sulphonic acid sodium salt along with NH_4Cl

Rusting reaction was carried by adding H_2O_2 or pyrogallol or anthraquinone 2 – sulphonic acid sodium salt along with NH_4Cl. The results are plotted in Fig. 3.17. The amount of H_2O_2 added was 2% (v/v) while that of pyrogallol and anthraquinone 2- sulphonic acid sodium salt were 2% and 3% (w/v) respectively.

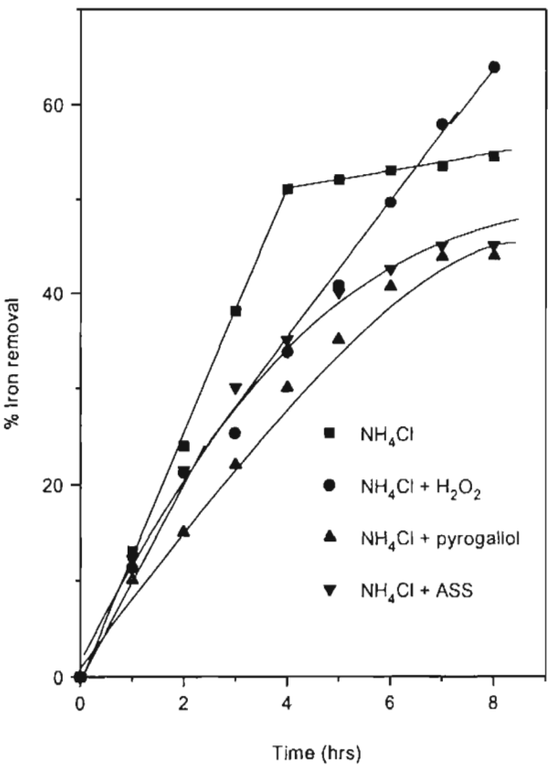

Fig-3.17 % Iron removal vs-time

3.13.1 Rusting reaction carried out using H_2O_2, pyrogallol or anthraquinone 2-sulphonic acid sodium salt along with NH_4Cl

The rusting behaviour of reduced ilmenite when compounds such as H_2O_2, pyrogallol or anthraquinone 2-sulphonic acid sodium salt along with NH_4Cl are added, are plotted in Fig-3.17. When H_2O_2 was added along with NH_4Cl, the rate of rusting was less as compared to NH_4Cl during every hour.

But the rusting reaction proceeded in a steady manner reaching a value of 65% iron removal in 8 hrs.

When pyrogallol was added along with NH_4Cl the rusting reaction was very slow, where about 40% of iron removal was observed in 7 hrs and finally 42% in 8 hrs. Moreover the rate of rusting of NH_4Cl is also suppressed when this compound was added.

When anthraquinone 2-sulphonic acid sodium salt was added along with NH_4Cl the reaction was very slow and at any time the rate of rusting was very less than NH_4Cl alone. About 43% iron removal was observed in 8 hrs.

3.13.2 Variation in pH

The pH measured when pyrogallol or anthraquione 2-sulphonic acid sodium salt was added along with NH_4Cl. The results are plotted in Fig. 3.18.

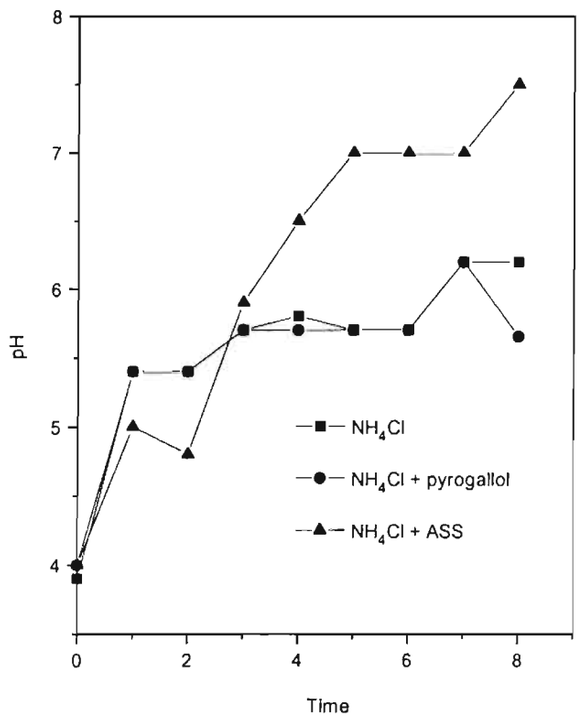

Fig·3.18 Variation in pH

The pH plot of pyrogallol + NH_4Cl and NH_4Cl alone almost had typical behaviour. But even then the rate of rusting with pyrogallol was less than NH_4Cl alone. When anthraquinone 2-sulphonic acid sodium salt was added along with NH_4Cl the pH increased as reaction proceeded up to 7.5 in 8 hrs. The rusting rate usually becomes less when pH is increased. The rusting rate when anthraquinone 2-sulphonic acid was added along with NH_4Cl is also very less.

3.14 Rusting reaction carried out by adding $Na_2S_2O_3$ or HCHO or CH_3CHO along with NH_4Cl

The results of rusting reaction carried out by adding $Na_2S_2O_3$ or HCHO or CH_3CHO along with NH_4Cl are plotted in Fig. 3.19. The quantity of $Na_2S_2O_3$ added was 1% (w/v) while that of HCHO and CH_3CHO was 2% (v/v).

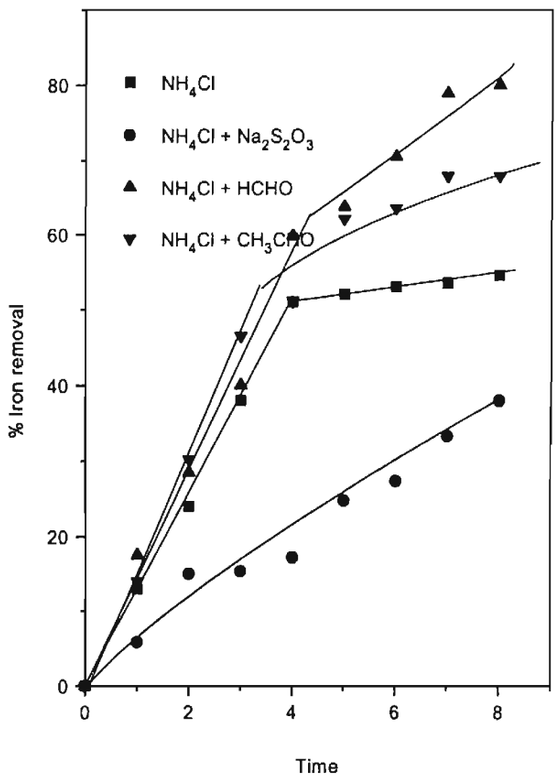

Fig-3.19 % Iron removal vs-time

3.14.1 Rusting reaction carried out by adding $Na_2S_2O_3$, HCHO or CH_3CHO along with NH_4Cl

When $Na_2S_2O_3$ was added along with NH_4Cl the rate of rusting was very slow and in 8 hrs about 35% of iron removal was obtained. The addition of $Na_2S_2O_3$ along with NH_4Cl suppresses the reaction rate to lesser than that with of NH_4Cl alone.

When HCHO was added along with NH_4Cl the rusting reaction was fast, and the rusting rate increased steadily with an iron removal of 83% was obtained in 8 hrs. As the reaction proceeded known quantity of solution from the system was withdrawn every hour and the amount of acid generated during the reaction was estimated. The amount of acid generated during the reaction varied which could be the reason for good rusting.

When CH_3CHO was added along with NH_4Cl the rusting reaction was fast up to 4 hrs, which decreased and finally an iron removal of 65% was obtained in 8 hrs.

3.15 Estimation of acid during the rusting of ilmenite

When carbonyl compounds were used in the rusting reaction considerable enhancement in rusting has taken place. Also the pH measurements indicate that acid formation was taking place as the reaction proceeded. Hence the concentration of acid was estimated every hour. The results of experiments using HCHO and CH_3CHO are given in table 3.6

Table 3.6 Acid concentrations during rusting reaction

Time (hrs)	% Acid concentration using HCHO	% Acid concentration using CH_3CHO
0	0.2873	0.0579
1	0.2509	0.0869
2	0.3281	0.0869
3	0.3378	0.0965
4	0.2316	0.0676
5	0.2895	0.0676
6	0.2316	0.0483
7	0.2220	0.0772
8	0.1737	0.0676

From the above results it is evident that the carbonyl compounds produce acids on getting themselves oxidized in presence of air which is further responsible for the enhancement in rusting.

The acid formed during rusting using glyoxal was found to be oxalic acid, which was proved through appropriate reactions like titration with permanganate. When starch was used with NH_4Cl for rusting reaction it was observed that starch was absent in the system after one hour of the reaction, which was established through potassium iodide test. It is well known that starch on hydrolysis produces reducing sugars. The solution after one hour gave positive test for glucose (oxime test), which shows that starch gets converted to glucose during the reaction. Afterwards the glucose gets converted to corresponding acid, which was proved by titration with alkali.

All the above tests confirm that the organic compounds get consumed during the reaction to give products, which are favourable for the rusting reaction, and hence an improvement in rusting is obtained.

3.16 X – ray diffraction studies

X – ray diffraction studies of the rusted ilmenite were carried out to find out the phase changes taking place during rusting. Samples withdrawn at regular intervals of rusting were studied using Kα radiation with a scan speed of 2°/min. Diffraction lines for each constituent was selected which had high relative intensity and did not interfere with lines of other constituents. The XRD data of reduced ilmenite is shown in table 3.7

Table 3.7 XRD data of reduced ilmenite

Sl. no	d- value	Relative Intensity (%)	Assignment
1	3.45	12.41	Anatase
2	2.67	7.26	Pseudobrookite
3	2.37	8.12	Rutile
4	2.11	15.51	Rutile
5	1.96	100.00	Metallic iron
6	1.83	2.75	Anatase

XRD data of 8 hrs rusted ilmenite using NH_4Cl + glyoxal is given in table 3.8

Table 3.8 XRD data of 8 hrs rusted ilmenite using NH_4Cl + glyoxal

Sl.no	d- value	Relative Intensity (%)	Assignment
1	3.49	31.50	Anatase
2	3.2	90.77	Rutile
3	2.73	16.13	Pseudobrookite
4	2.47	65.78	Rutile
5	2.18	48.01	Rutile
6	2.01	10.35	Metallic iron
7	1.96	6.35	Pseudobrookite
8	1.88	8.04	Anatase
9	1.75	4.61	Pseudobrookite
10	1.68	100.00	Rutile
11	1.63	28.67	Rutile

In reduced ilmenite the maximum intensity peak is that of metallic iron. The other major phases present were anatase and pseudobrookite. But in the rusted ilmenite the maximum intensity peak is that of anatase while the metallic iron peak becomes very weak. The prominent peaks observed in the rusted samples were of anatase, rutile and pseudobrookite. The XRD data clearly shows the removal of metallic iron from the reduced ilmenite during rusting. The presence of small quantities of metallic iron observed in

XRD of rusted ilmenite is also confirmed through chemical analysis. The concentrations of anatase and rutile increased in the rusted samples as metallic iron got removed.

3.17 Scanning Electron Microscopy

The morphology of the reduced ilmenite before and after rusting was investigated using scanning electron microscopy. The SEM photographs are shown in Fig 17.1, 17.2, 17.3, 17.4 and 17.5 respectively. The surface of reduced ilmenite is uneven with globular structures formed as a result of reduction and sintering. After rusting with NH_4Cl the morphology changed to a porous noncontinuous surface formed as a result of removal of metallic iron from the particle. The particle becomes highly porous like a honeycomb after rusting for 8 hrs with carbonyl compounds along with NH_4Cl. The mechanical strength of the particle was very much reduced as a result of which the particles crumble very easily. The porosity of the particle after rusting with carbonyl compounds was very high compared with NH_4Cl alone.

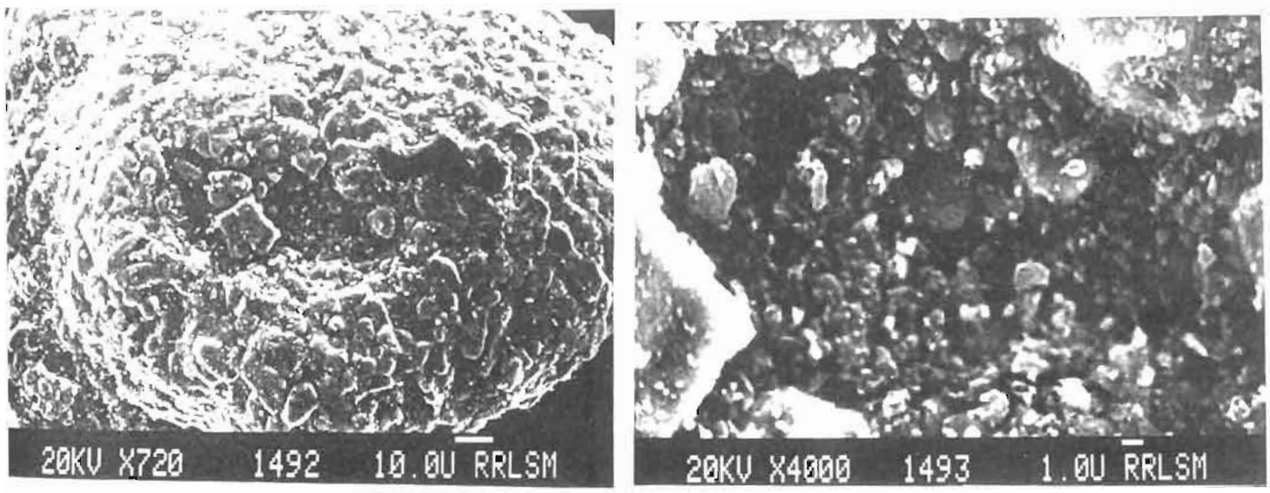

Fig. 17.1 SEM photograph of Reduced ilmenite

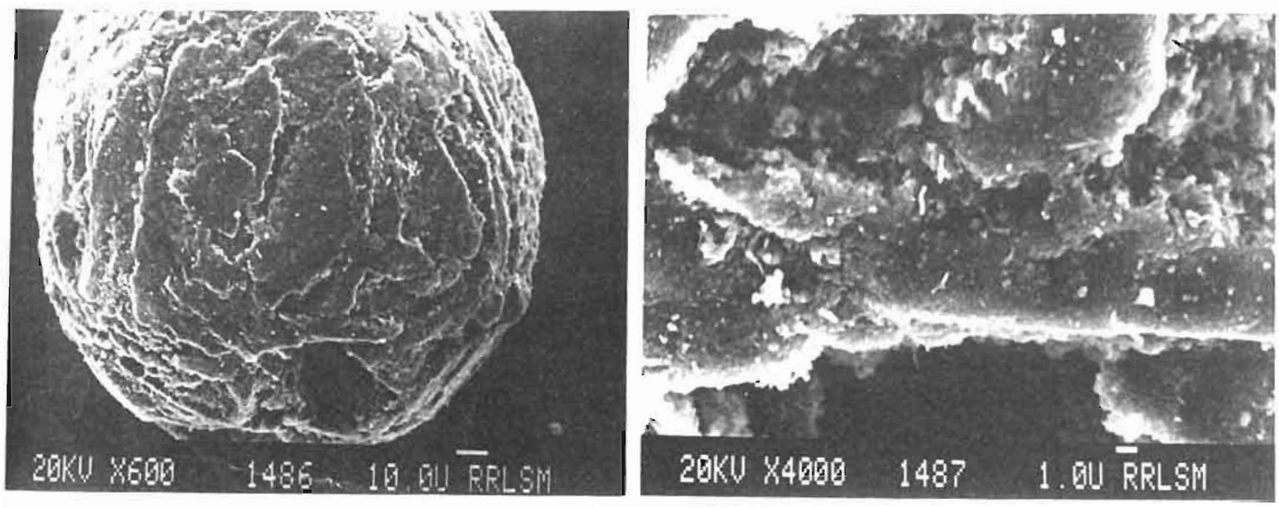

Fig. 17.2 (a)

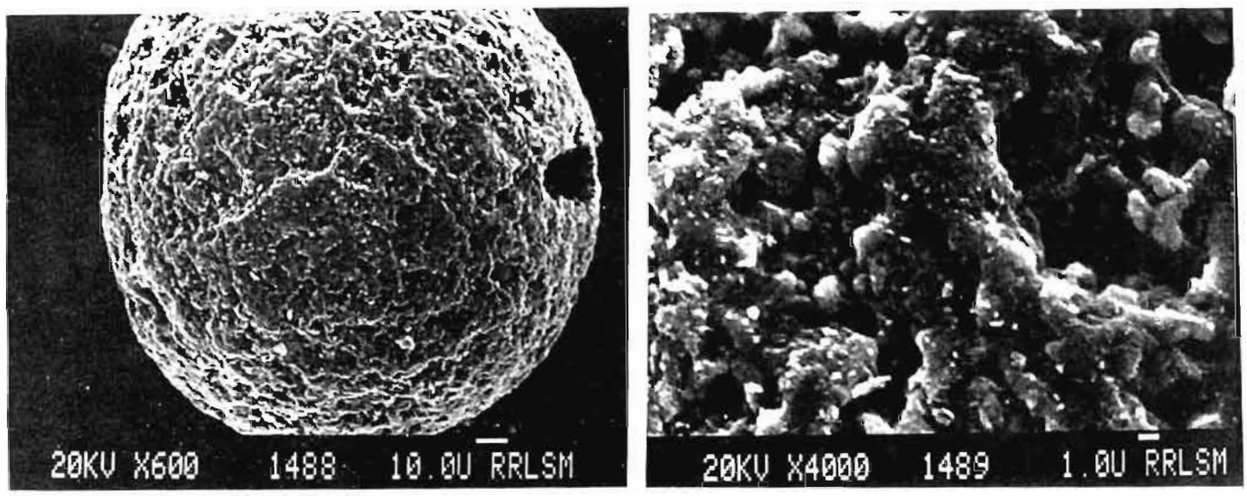

Fig. 17.2 (b)

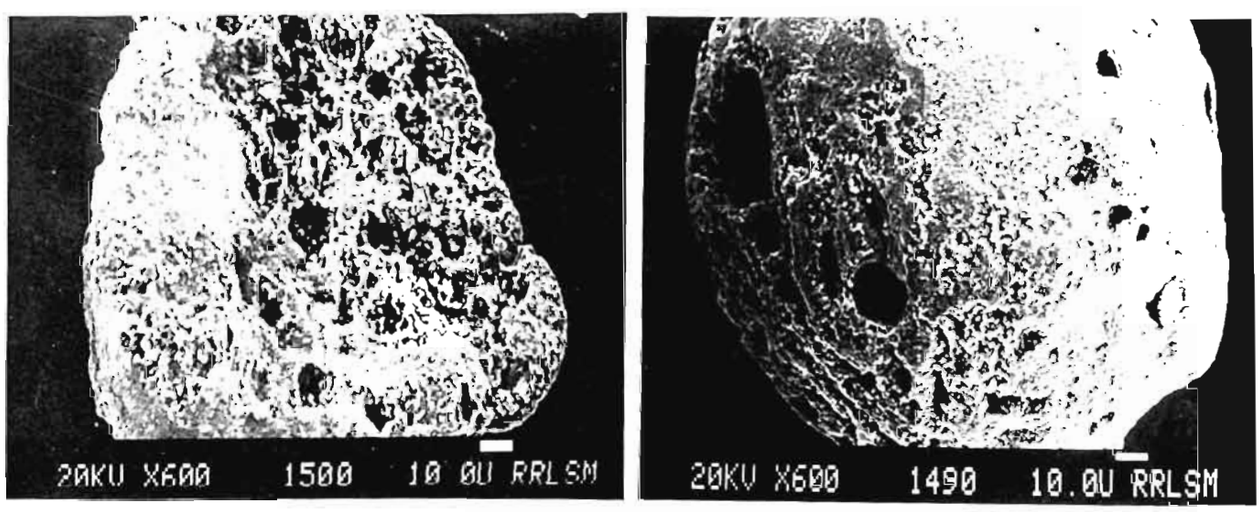

(c)

Fig 17.2 SEM photograph of Rusted ilmenite using NH_4Cl
(a) 3 hrs. (b) 5 hrs. (c) 8 hrs.

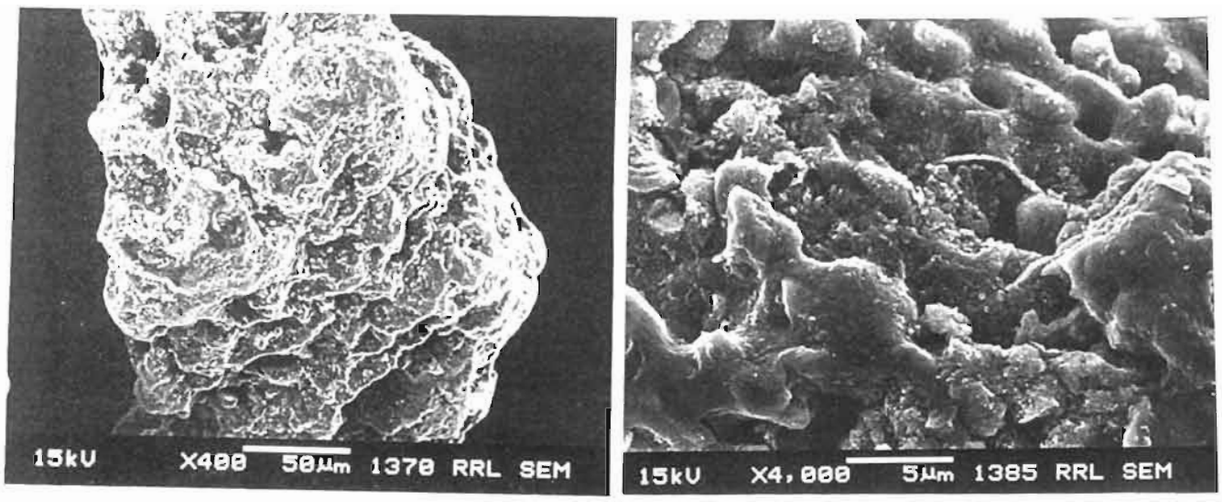

Fig. 17.3 (a)

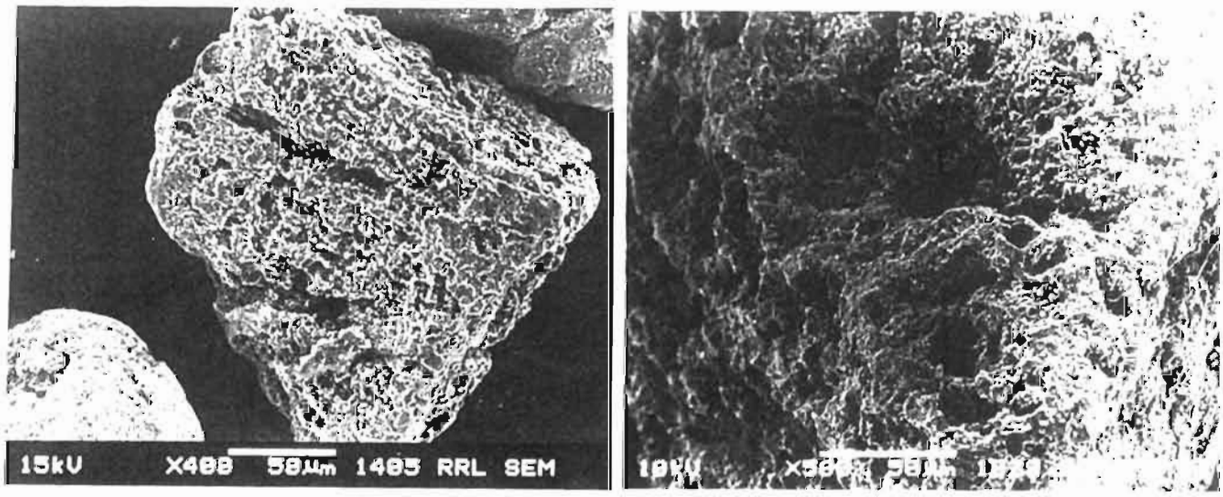

Fig. 17.3 (b)

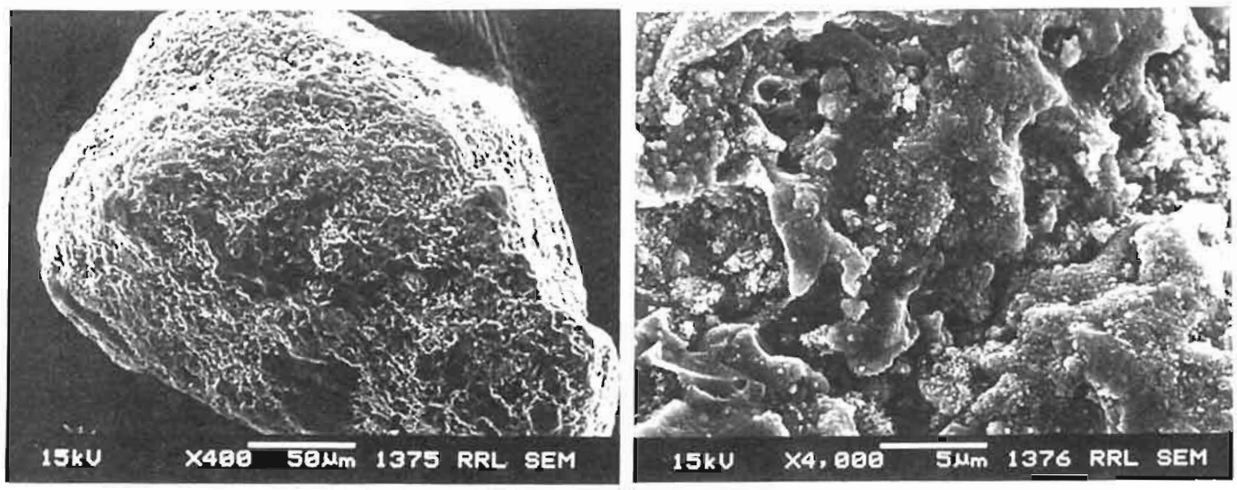

(c)

Fig. 17.3 SEM photograph of Rusted ilmenite using NH_4Cl + saccharin
(a) 3 hrs. (b) 5 hrs. (c) 8 hrs.

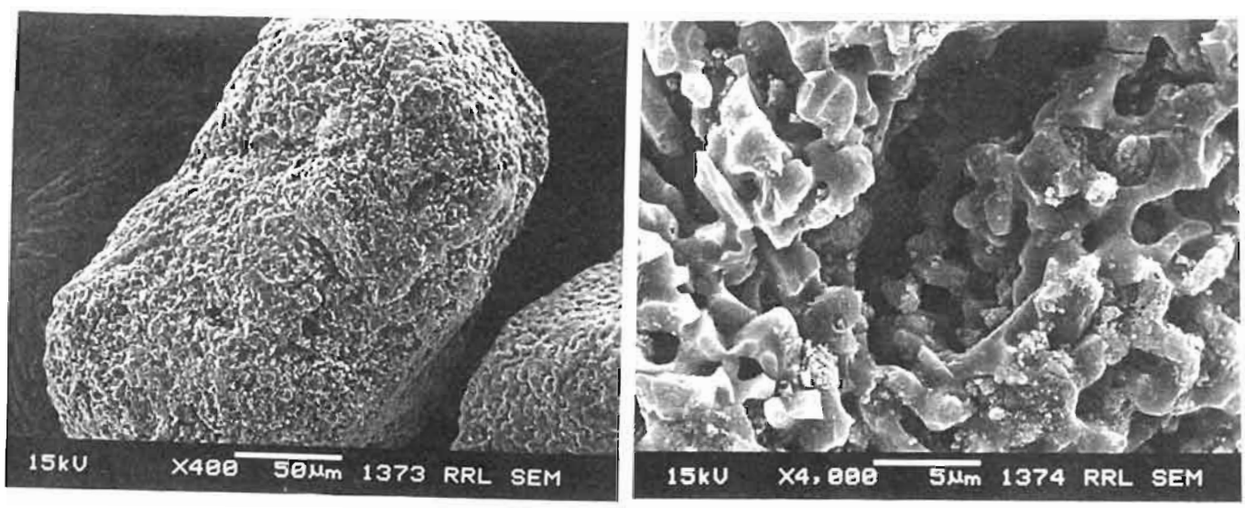

Fig. 17.4 SEM photograph of Rusted ilmenite using NH_4Cl + starch (8 hrs.)

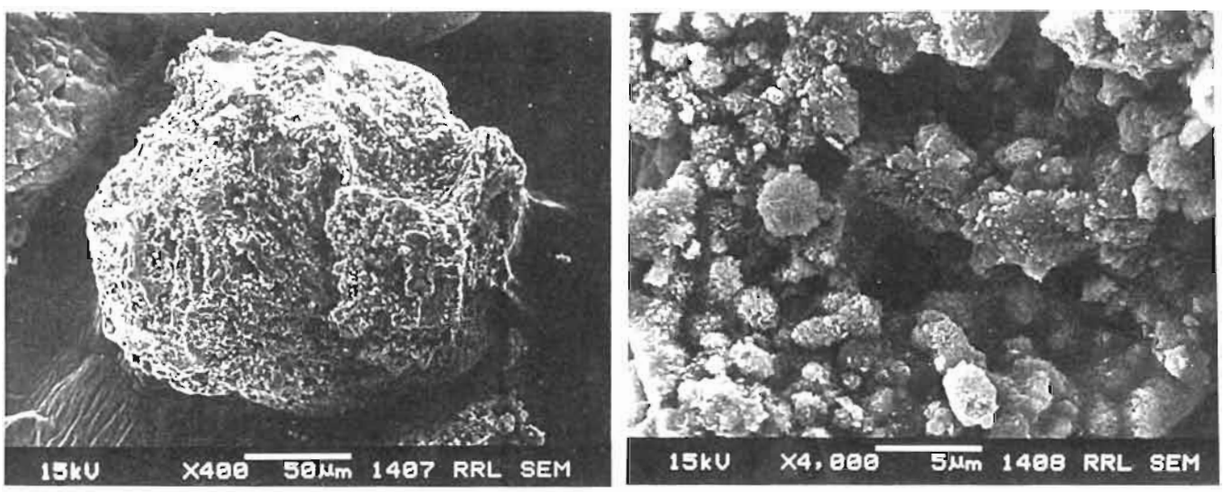

Fig. 17.5 (a) SEM photograph of Rusted ilmenite using NH_4Cl + acetic acid (8 hrs.)

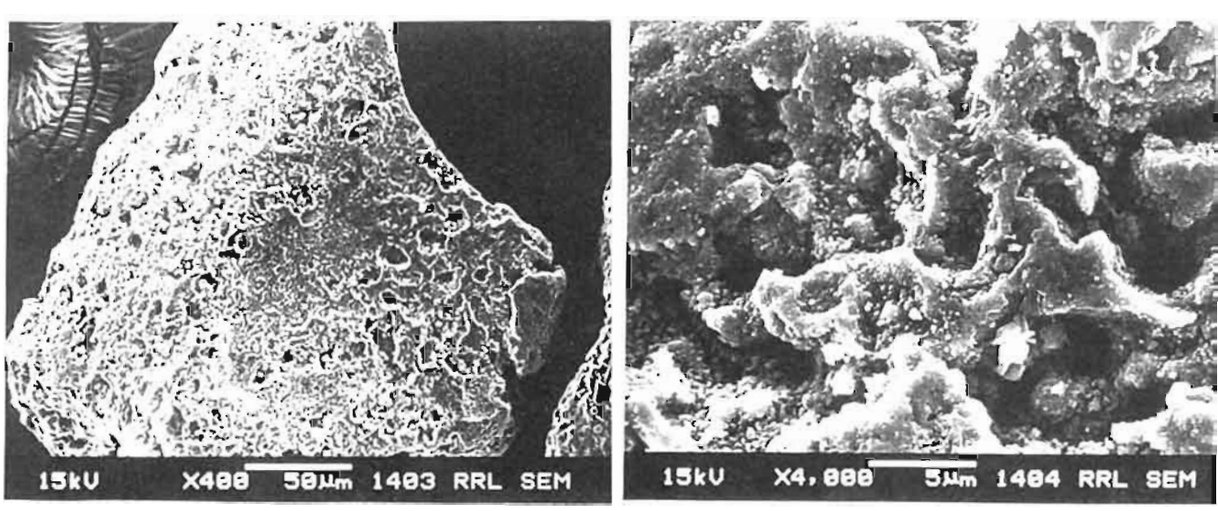

Fig. 17.5 (b) SEM photograph of Rusted ilmenite using NH_4Cl + sucrose (8 hrs.)

3.18 Surface Area Measurments

The SEM studies clearly indicated that major morphological changes take place during rusting as a result of which the particles become highly porous. This should result in major changes in the surface area of the particles due to rusting. Hence surface area measurements of reduced and rusted ilmenite were carried out using a surface area analyzer. The results of the measurements are given in table 3.10.

Table 3.9 Surface area measurements

Sample	Surface area m^2/ g
Reduced ilmenite	2.8757
Rusted ilmenite with NH_4Cl	3.012
Rusted ilmenite with starch + NH_4Cl	3.2259
Rusted ilmenite with sucrose + NH_4Cl	3.157
Rusted ilmenite with methanol + NH_4Cl	3.2462
Rusted ilmenite with acetone + NH_4Cl	3.2622

Reduced ilmenite has a surface area of 2.8757m^2/ g, which increases slightly due to rusting. The increase in surface area is expected as more pores are developed due to the removal of iron during the reaction. This is in agreement with the results of the SEM studies, which clearly indicated the formation of pores on the surface.

3.19 Effect of temperature

Detailed investigations were carried out to find out the effect of temperature on rusting. In the case of NH_4Cl alone an increase in

temperature was found to favour the reaction. Experiments carried out at 25, 30, 35 and 40°C show that the iron removal increases with temperature giving maximum at 40°C. Even though higher iron removal was observed at higher temperatures in the case of NH_4Cl alone, experiments were carried out only up to 40°C for comparison as the optimum in the case of the carbonyl compounds were found to be below 40°C.

3.19.1 Kinetics of chemically controlled reactions

A reaction generally involves several steps. In the case of heterogeneous reactions, the reactions occur at the interface between different phases and may also and may also require heat transfer in addition to mass transfer steps [182]. The kinetic models are postulated on the basis of some idealized schemes of reaction mechanism and actual kinetic data are matched against them. The chemical reaction at the interface takes place through

- ❖ Adsorption of reactant species
- ❖ Chemical reaction
- ❖ Desorption of reaction products species

When reaction steps are in series then the slowest step becomes the rate controlling if other steps are comparatively fast.

Let us consider a solid reacting with surrounding fluid. We assume that the solid remains at constant temperature throughout and hence the heat of the reaction is negligible. We assume that there is excess of fluid at all times throughout the reaction. The following assumptions should be taken into account.

- ❖ Diffusion of reactant in bulk fluid towards the outer surface.
- ❖ Diffusion of reactant through product or residue layer.
- ❖ Adsorption of reactant at the reaction interface.

- ❖ Reaction at the reaction interface.
- ❖ Desorption of the product gases
- ❖ Nucleation and growth of new phases formed.
- ❖ Diffusion of product fluids outward through the product or residue layer.
- ❖ Diffusion of product fluids outward from the outer surface.

The reaction interface need not always be sharp. It may be diffused when the solid is porous and the fluid is able to penetrate before being consumed. If the solid is so porous the fluid penetrates entirely with reaction occurring simultaneously everywhere so that there is no unreacted core as such at any time. The concentration profile of the diffusing species will depend on the rate controlling step and the porosity of the solid. If the chemical reaction at the interface is rate controlling then the diffusion process through the product layer is rapid. A kinetic law has been derived considering the ilmenite particles as spheres.

$$Kt = 1-(1-x)^{1/3}$$

Calculations were carried out to find out the activation energies of the reaction. The equations used for the calculations were

$$1-(1-x)1/3 = K't \quad \text{----------(1)}$$

$$K' = 1/R_o \quad \text{----------(2)}$$

$$K' = C_A K_C/\rho R_o \quad \text{----------(3)}$$

Where x is the fraction of the iron reacted, C_A, the concentration of the dissolved oxygen, Kc the rate constant, ρ the specific gravity of the reduced ilmenite and R_o is the average particle size. The values of $1-(1-x)^{1/3}$ calculated for NH_4Cl alone and NH_4Cl + individual compounds at different temperatures were plotted against time. All the plots gave straight lines. This

shows that the rate-determining step is controlled by the surface chemical reaction.

The activation energies are calculated from the Arrhenius plots. Calculation of activation energies for the system NH_4Cl + starch is shown below as a typical example.

$Kc = m\rho R_o/C_A$

m - slope

ρ - density of reduced ilmenite

R_o - average particle size

C_A - Concentration of the dissolved oxygen in the system

Slope at 25°C = 3.54×10^{-4}

Slope at 30°C = 9.88×10^{-4}

Slope at 35°C = 8.54×10^{-4}

Slope at 40°C = 6.14×10^{-4}

Kc at 25°C = $3.54 \times 10^{-4} \times 4.467 \times 0.2 \times 10^{-4} / 1.094 \times 10^{-4}$

= 2.89×10^{-4}

Kc at 30°C = 9.88×10^{-4} x4.467 x 0.2 x 10-4/ 1.25×10^{-4}

= 7.06×10^{-4}

Kc at 35°C = $8.54 \times 10^{-4} \times 4.467 \times 0.2 \times 10^{-4} / 1.5 \times 10^{-4}$

= 5.086×10^{-4}

Kc at 40°C = $6.14 \times 10^{-4} \times 4.467 \times 0.2 \times 10^{-4} / 2.344 \times 10^{-4}$

= 2.34×10^{-4}

1/ T for temperatures 25°, 30°, 35° and 40°C

3.35×10^{-3}

3.3×10^{-3}

3.25×10^{-3}

3.2×10^{-3}

log Kc for 25°C = -3.54

log Kc for 30°C = -3.4

log Kc for 35°C = -3.29

log Kc for 40°C =-3.63

Slope = $-0.15 / 0.105 \times 10^{-3}$

= -1428.57

m = - Ea/ RT

Ea - Activation energy

R - Gas constant

T - Temperature (K)

M - Slope

Ea = - (mRT)

- (- 1428.57 x 8.314 x 2.303)/ 1000

27.35KJ/ mol

The activation energy for all the systems are calculated as described above and are given in table 3.10

Fig. 3.20 shows the plot of time *vs.* $1-(1-x)^{1/3}$ at different temperatures in the case of rusting with NH_4Cl alone. The straight lines obtained in the graph at different temperatures confirm that the kinetics of the reaction was surface chemical. In the case of reaction with NH_4Cl alone the removal of iron increased with temperature, which is evident from Fig. 3.20. The activation energy calculated was 63.82KJ/ mol.

Fig. 3.21 shows the plot of time *vs.* $1-(1-x)^{1/3}$ when a mixture of NH_4Cl and glucose was used. From the plot it is clear that the optimum iron removal in the case of NH_4Cl + glucose mixture was 30°C. The activation energy calculated was 41.78KJ/ mol.

Fig. 3.22 shows the plot of time *vs.* $1-(1-x)^{1/3}$ when NH_4Cl + glyoxal was used for the rusting reaction. The optimum temperature for maximum iron removal was found to be 30°C. The activation energy of the reaction was 28.07KJ/ mol.

Fig. 3.23 shows the plot of time *vs.* $1-(1-x)^{1/3}$ when NH_4Cl + sucrose was added during rusting reaction. The optimum temperature for maximum iron removal was 30°C and the activation energy was found to be 46.36KJ/ mol.

Fig. 3.24 gives the plot of time *vs.* 1-(1-x)1/3 when NH_4Cl + starch was used for the rusting reaction. The optimum temperature for maximum iron removal was 30°C and the activation energy was 27.35KJ/ mol.

When NH_4Cl + HCHO were added during the rusting reaction, the optimum temperature observed for maximum iron removal was 30°C which is evident from Fig. 3.25. The activation energy for the reaction was 42.80KJ/ mol.

When NH_4Cl + acetaldehyde were added during the rusting reaction, the maximum iron removal was found to be at 35°C which is evident from Fig. 3.26. This may be due to the evaporation of acetaldehyde as temperature is increased above 35°C. Once the acetaldehyde gets exhausted in the system it may follow the rusting reaction in presence of NH_4Cl. The activation energy calculated for the system was 54.71KJ/ mol.

Fig. 3.27 shows the plot of time vs $1-(1-x)^{1/3}$ when NH_4Cl + acetone were added during the rusting reaction. The optimum temperature for maximum iron removal was found to be 30°C and the activation energy calculated was 28.22KJ/ mol.

When NH_4Cl + methanol were added during the rusting reaction, maximum iron removal was observed at 30°C which is evident from Fig. 3.28. The activation energy calculated was 17.78KJ/ mol.

Fig. 3.29 shows the plot of time vs 1-(1-x)1/3 when NH_4Cl + acetic acid were added during the rusting reaction. The maximum iron removal was observed at 30°C and the activation energy calculated was 45.26KJ/ mol.

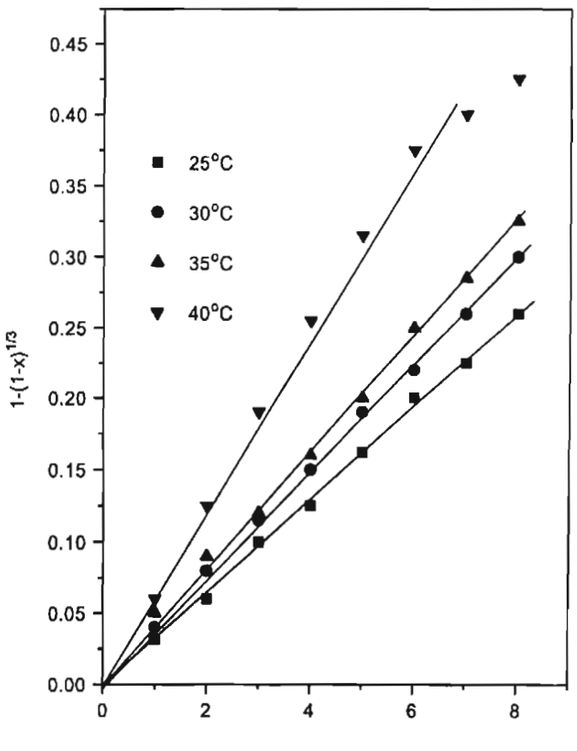

Fig-3.20 Plot of time vs-1-(1-x)$^{1/3}$ using NH_4Cl alone

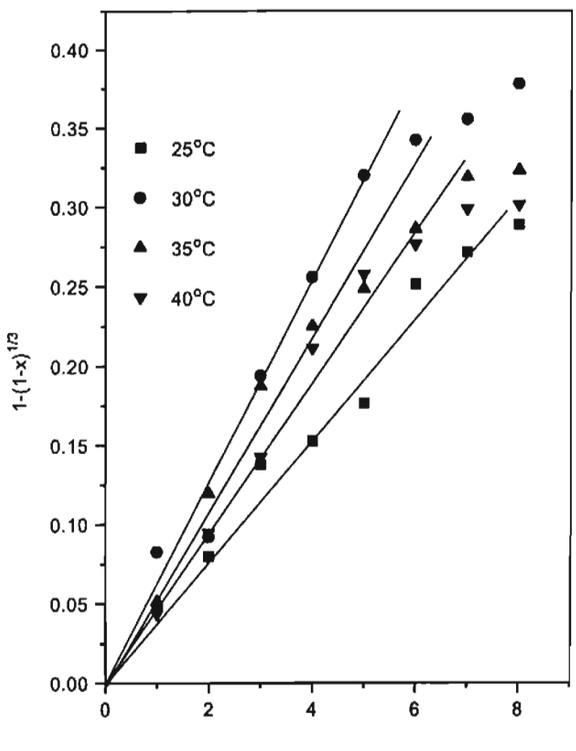

Fig·3.21 Plot of time vs·1-(1-x)$^{1/3}$ using NH_4Cl + glucose

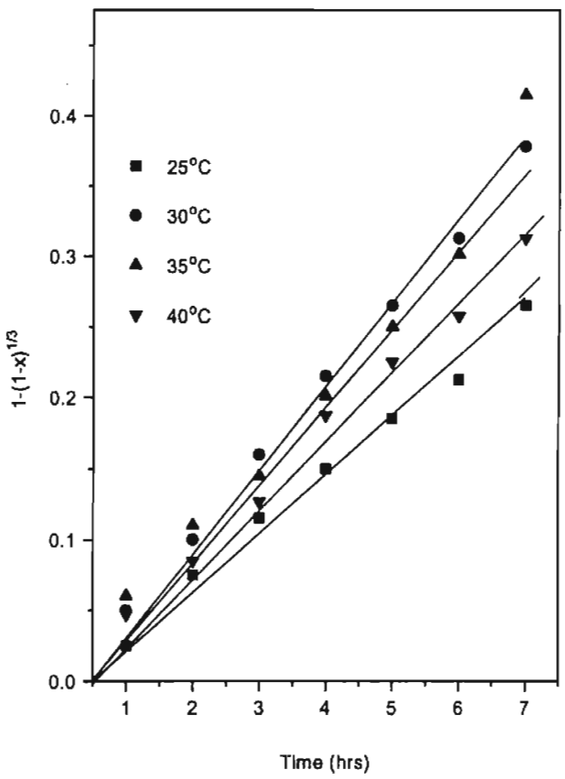

Fig-3.22 Plot of time vs-1-(1-x)$^{1/3}$ using NH_4Cl + glyoxal

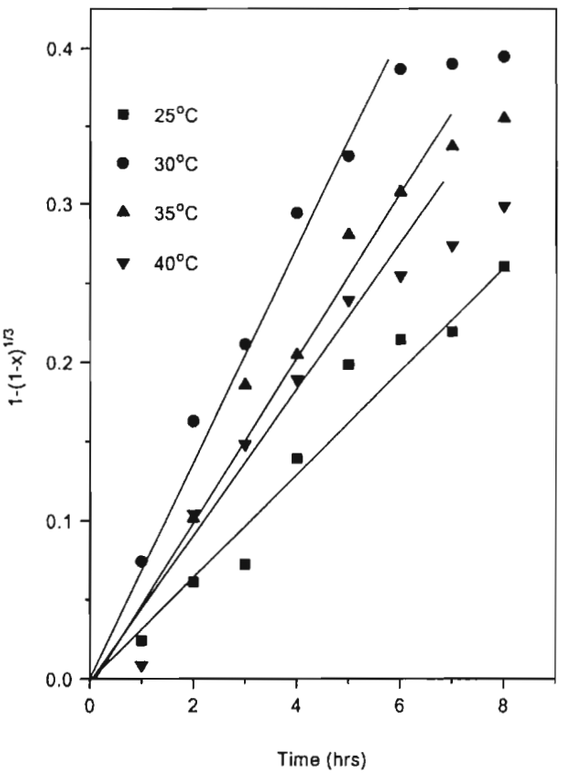

Fig. 3.23 Plot of time *vs.* $1-(1-x)^{1/3}$ using NH_4Cl + sucrose

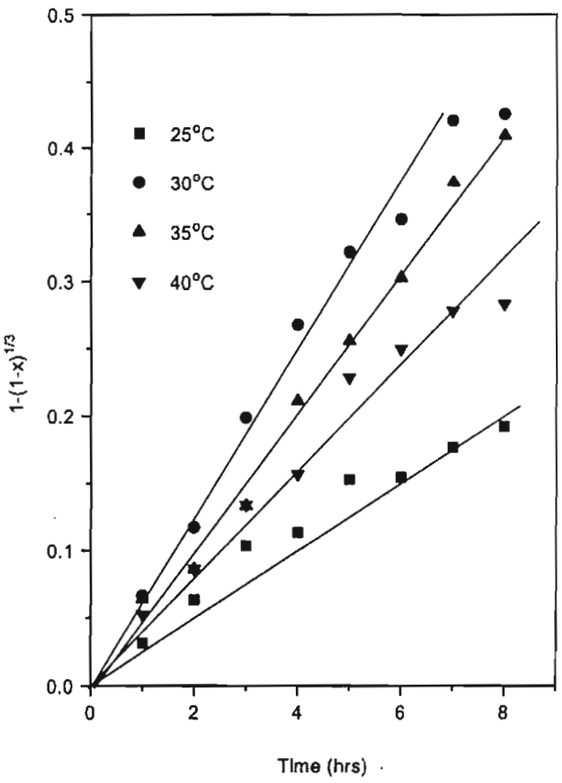

Fig-3.24 Plot of time vs-1-(1-x)$^{1/3}$ using NH_4Cl + starch

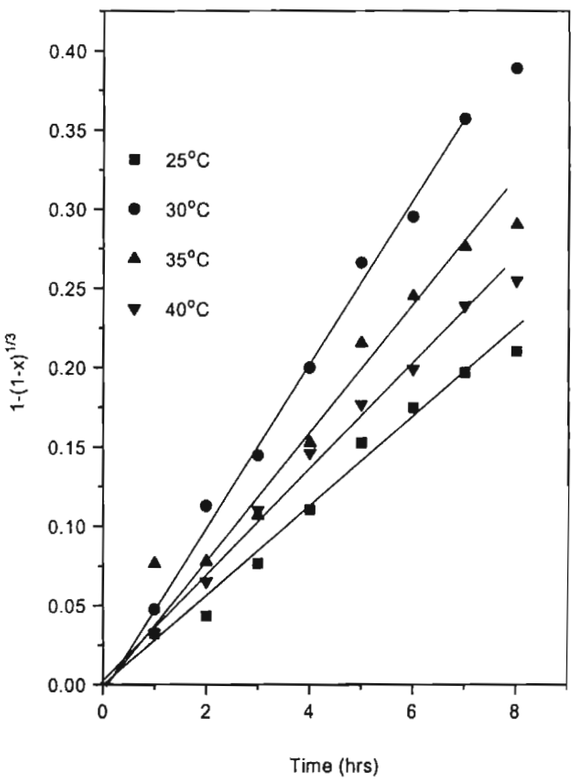

Fig. 3.25 Plot of time *vs.* $1-(1-x)^{1/3}$ using NH_4Cl + HCHO

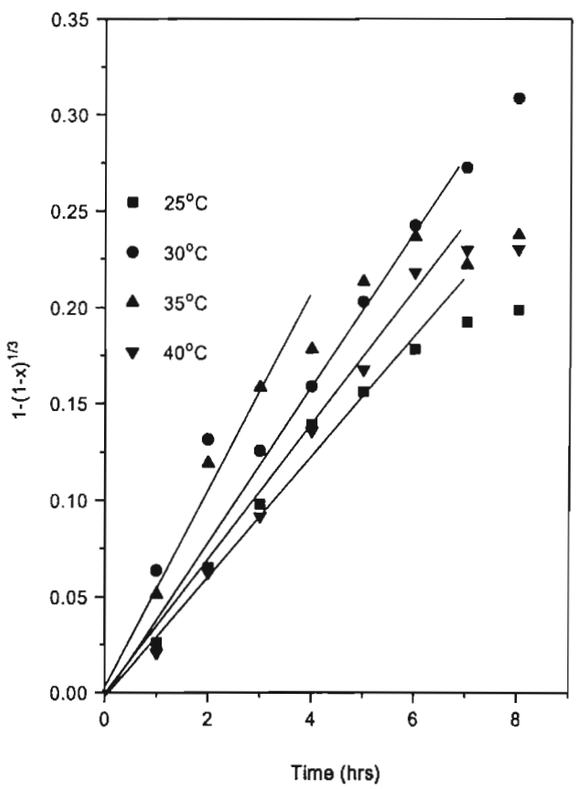

Fig. 3.26 Plot of time *vs.* $1-(1-x)^{1/3}$ using $NH_4Cl + CH_3CHO$

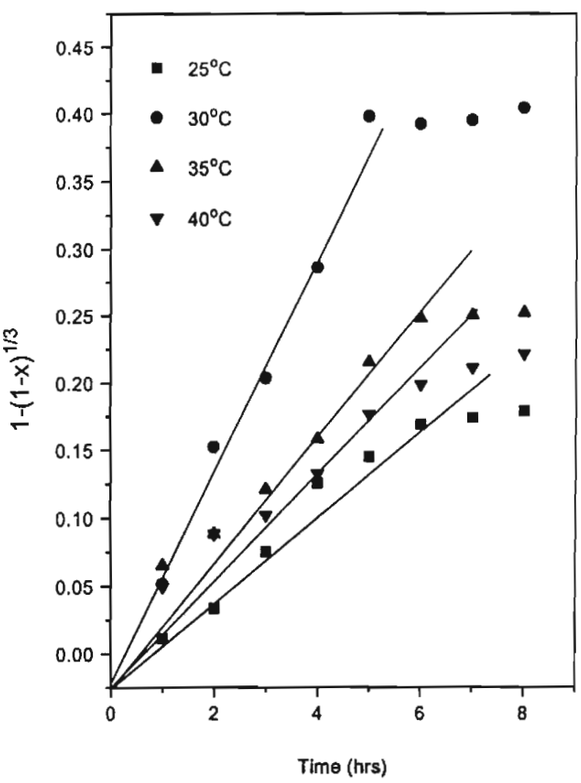

Fig. 3.27 Plot of time *vs.* $1-(1-x)^{1/3}$ using NH_4Cl + acetone

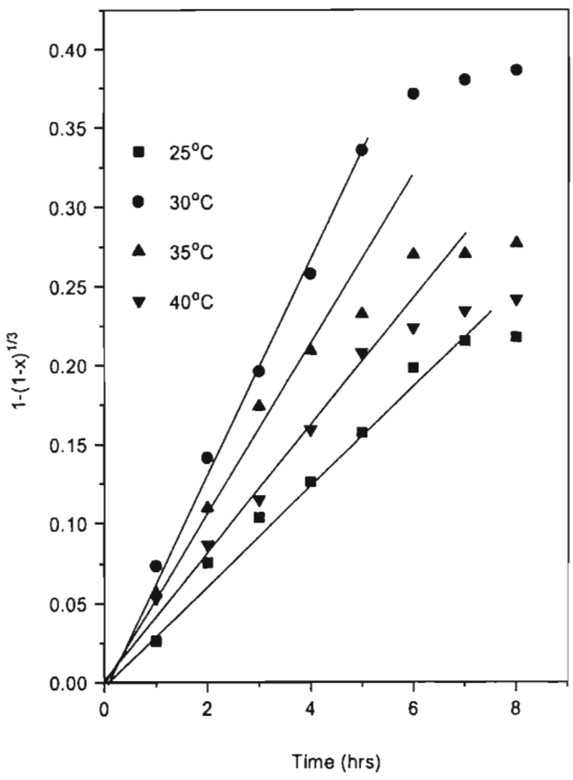

Fig-3.28 Plot of time vs-1-(1-x)$^{1/3}$ using NH_4Cl + methanol

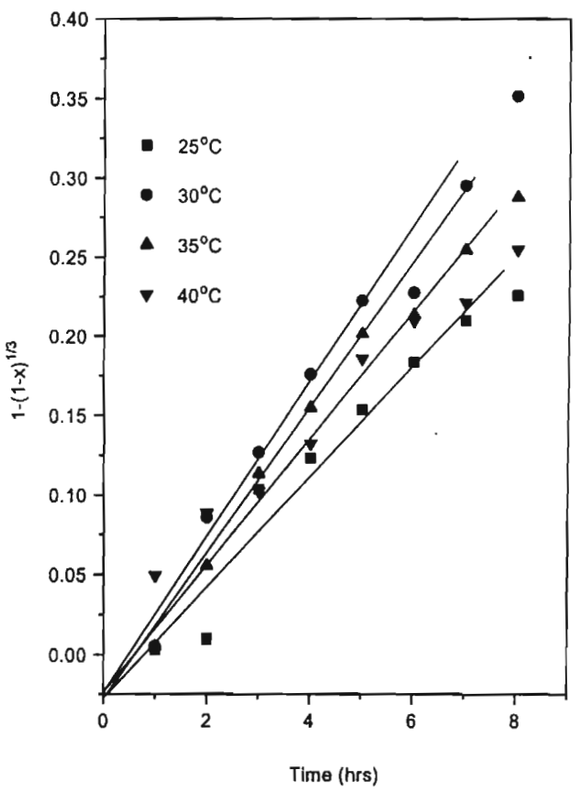

Fig. 3.29 Plot of time *vs.* $1-(1-x)^{1/3}$ using $NH_4Cl + CH_3COOH$

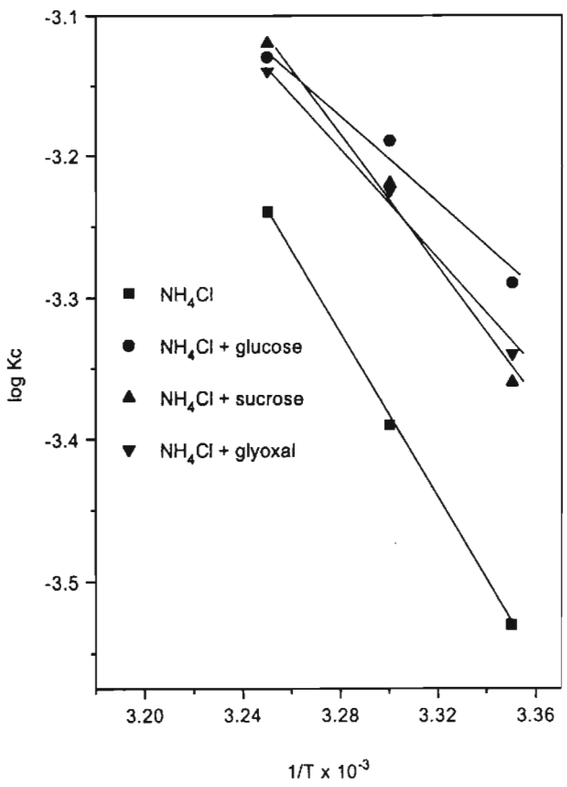

Fig.3.30 Arrhenius plots

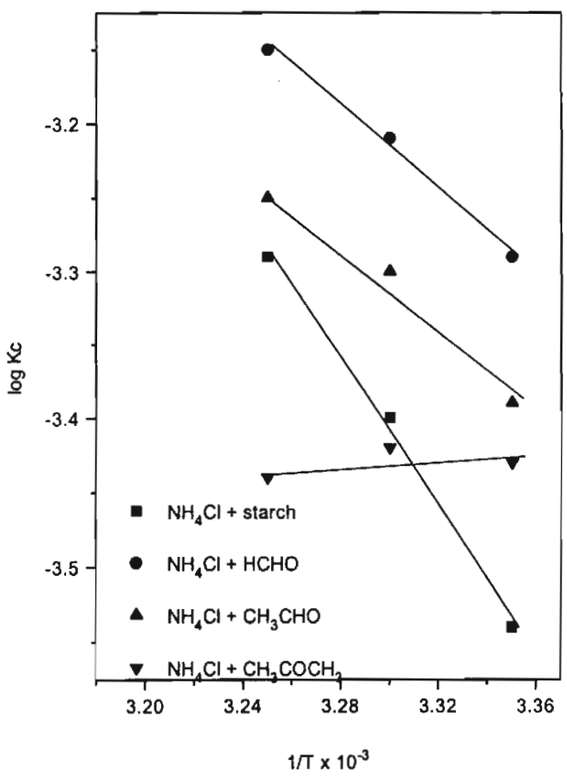

Fig. 3.31 Arrhenius plots

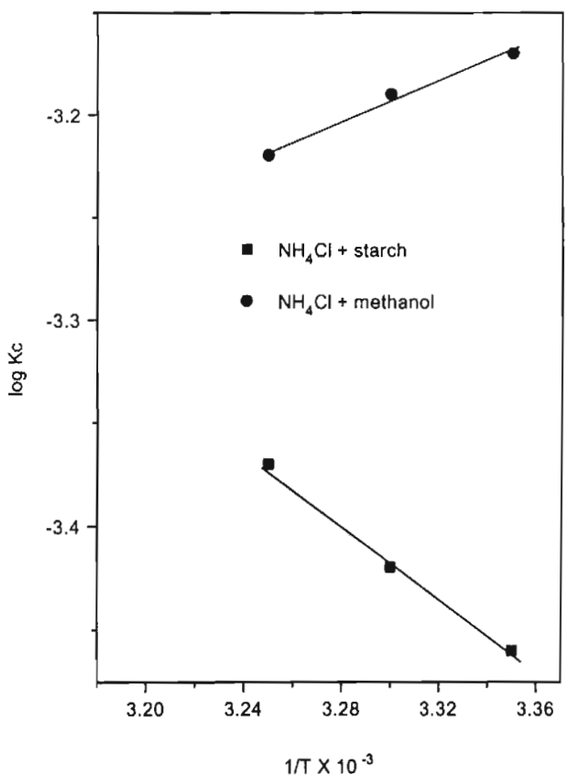

Fig. 3.32 Arrhenius plots

The activation energies calculated for all the above systems are from Arrhenius plots, which are shown in Figs. 3.30, 3.31 and 3.32. The Arrhenius plots for all the systems gave straight lines, which confirm that in presence of NH_4Cl + organic compounds rusting was controlled by surface chemical reactions. The activation energies for all the systems were less than that for NH_4Cl alone. So, it is obvious that the new compounds when added improve the rate of rusting reaction. Table 3.10 shows the activation energies in the descending order.

Table 3.10 Activation Energies calculated for different systems

No	Compounds used during rusting	Activation Energy KJ/ mol
1	NH_4Cl	63.82
2	$NH_4Cl + CH_3CHO$	54.71
3	NH_4Cl + sucrose	46.36
4	NH_4Cl + acetic acid	45.26
5	$NH_4Cl + HCHO$	42.80
6	NH_4Cl + glucose	41.78
7	NH_4Cl + acetone	28.22
8	NH_4Cl + glyoxal	28.07
9	NH_4Cl + starch	27.35
10	$NH_4Cl + CH_3OH$	17.78

It is observed that in all the cases when time is plotted against $1-(1-x)^{1/3}$ straight lines are obtained till major quantity of iron is removed from the system which takes 5-6 hours. After this a change in the trend is observed which could be due to the non-availability of iron on the surface of the particles. When glyoxal, acetone, starch and methanol are added along with NH_4Cl, the iron removal was fast enriching the TiO_2 content to 89% in 8 hrs.

From the above experiments it can be concluded that surface chemical reaction is the rate controlling step and this fact is further confirmed by rusting different sieve fractions of reduced ilmenite with NH_4Cl + glucose. For each sieve fraction rusting data $1-(1-x)^{1/3}$ is calculated and straight line graph is obtained by plotting time vs $1-(1-x)^{1/3}$. From this graph the slope is calculated and the inverse of slope when plotted against particle size a straight line is obtained Fig. 3.33, which further confirms the surface chemical hypothesis [181]. Table 3.11 shows the data of slope and average particle size.

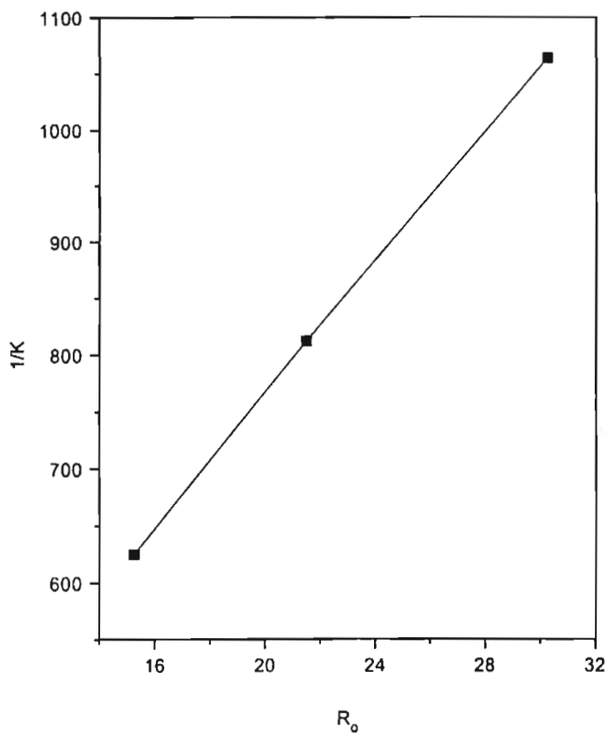

Fig. 3.33 Plot of average particle size (R_o) and inverse of slope

Table 3.11 Data of slope and average particle size

Sieve fractions	R_o (average particle size) microns	1/K (slope from $1-(1-x)^{1/3}$ graph)
-0.355 to + 0.25	30.25	1063.83
-0.25 to + 0.18	21.5	862.07
-0.18 to + 0.125	15.25	625

The following conclusions can be drawn from the above investigations.

1. Rusting reaction in presence of NH_4Cl is slow and incomplete.
2. When carbonyl compounds like methanol, acetone, glyoxal, glucose, sucrose etc are added along with NH_4Cl rusting reaction was more efficient.
3. Rusting in presence of organic compounds gave a product with about 90% TiO_2 compared to 75% for NH_4Cl alone.
4. The pH of the system was found varying below 4 during the rusting.
5. Quantity of dissolved oxygen, which is one of the important factors controlling rusting, was found to vary widely during the reaction.
6. XRD analysis showed the removal of metallic iron as well as the enrichment in anatase, rutile and pseudobrookite phases.
7. The surface morphology studied by SEM showed that the particles become highly porous during rusting due to removal of iron.
8. An increase in surface area of the particles was observed during rusting which is due to the removal of iron from the particles.
9. The activation energy of the reaction using carbonyl compounds + NH_4Cl was found to be very less compared to NH_4Cl alone which explains the higher efficiency of the reaction with these compounds.
10. The kinetics of rusting was controlled by surface chemical reactions.

CHAPTER 4

STUDIES ON RUSTING OF REDUCED ILMENITE USING MIXTURES OF CARBONYL COMPOUNDS ALONG WITH NH_4Cl

From the previous chapter it is clear that when certain carbonyl compounds are added along with NH_4Cl the efficiency of the rusting reaction was increased considerably. Rusting reaction was carried out as per the procedure given in chapter 2 section 2.3. Reaction conditions used were 125 g of reduced ilmenite suspended in 500 ml of water containing required quantity of the catalysts, a stirring rate of 800 rpm and an air flow rate of 4-5 lit/ min. The results are given in Figs. 4.1, 4.2, 4.3, 4.4 and 4.5 respectively. The effect of temperature on rusting using mixtures of compounds along with NH_4Cl was also investigated.

The results indicate that there is some marked improvement in the reaction when mixtures of carbonyl compounds were added during rusting. Most of the iron values were removed as iron oxide in about 5 hrs whereas 14-16 hrs were required when NH_4Cl alone was used and 8 hrs in the case of single compounds with NH_4Cl. It was hence thought worthwhile to investigate the effect of mixtures of some of these compounds as in combination they may perform better. Rusting reactions were carried out using mixtures of methanol + acetic acid + NH_4Cl, glyoxal + acetic acid + NH_4Cl, acetone + acetic acid + NH_4Cl, glyoxal + acetone + NH_4Cl, methanol + acetone + NH_4Cl, sucrose + acetic acid + NH_4Cl, ethyl alcohol + acetic acid + NH_4Cl, methanol + formic acid + NH_4Cl, acetic acid + formic acid + NH_4Cl, glyoxal + formic acid + NH_4Cl and urea + acetic acid + NH_4Cl. For comparing

the iron removal with respect to NH_4Cl and mixture of carbonyl compounds along with NH_4Cl, the % iron removal *vs*. time for NH_4Cl alone is plotted in Fig. 4.1. A graph showing the rusting behaviour of NH_4Cl alone, methanol + NH_4Cl, acetic acid + NH_4Cl and methanol + acetic acid +NH_4Cl is plotted in Fig. 4.2.

4.1.1 Rusting reaction carried out using methanol + acetic acid, glyoxal + acetone along with NH_4Cl

2% (v/v) methanol and 1% (v/v) acetic acid, 2% (v/v) glyoxal and 1% (v/v) acetone were added along with NH_4Cl to investigate the rusting reaction. The % iron removal *vs*. time is plotted in Fig. 4.1. In 5 hrs more than 75% iron removal was observed when methanol + acetic acid was used along with NH_4Cl whereas 80% iron removal was observed when glyoxal + acetone was added along with NH_4Cl during rusting.

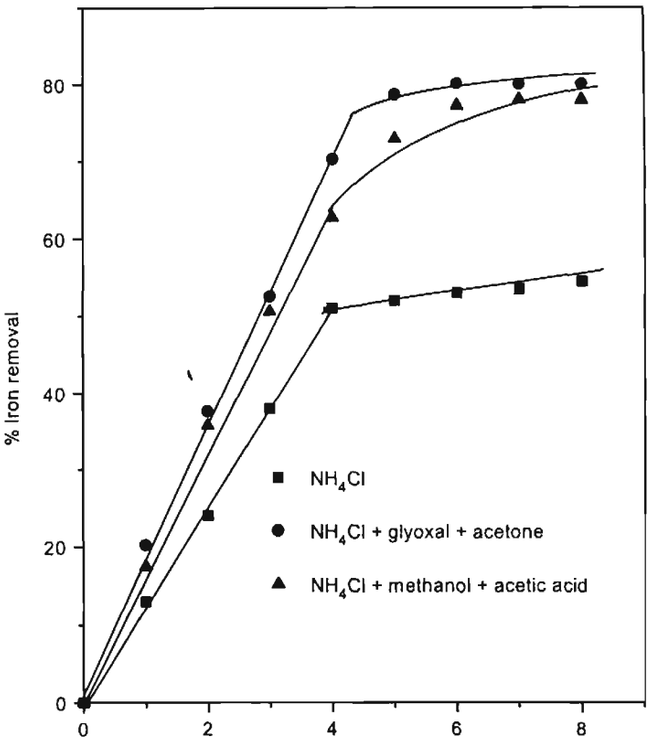

Fig-4.1 Plot of time vs-% iron removal

4.1.2 Discussion

When NH_4Cl alone was added during rusting an iron removal of about 50% was observed in 5 hrs. But when methanol and acetic acid were added along with NH_4Cl more than 75% of the iron was removed in 5 hrs and afterwards the reaction became slow reaching a value of 79% in 8 hrs. When mixture of glyoxal and acetone was added along with NH_4Cl, the rusting reaction was very fast and about 80% iron removal was observed in 5 hrs and afterwards it slowed down till 8 hrs. This may be due to the fact that almost all the metallic iron is

removed as iron hydroxide in 5 hrs and the rest of the iron present may be in the form of unreduced iron oxide or if the metallic iron is completely blocked with TiO_2 matrix, the diffusion of metal iron towards the reaction medium is restricted. Chemical anlysis of the 5 hrs rusted product shows that it contains only 1% metallic iron, which confirms that all the metallic iron except 1% has been removed in 5 hrs.

4.2.3 Comparison of rusting

Fig 4.2 gives a plot between % iron removal *vs.* time of rusting. The % iron removal during rusting, is a comparison of the efficiencies, of various systems namely NH_4Cl alone, NH_4Cl + methanol, NH_4Cl + acetic acid as well as NH_4Cl + methanol + acetic acid. This typical example was chosen to show the change in reaction efficiencies between the individual compounds and the mixtures when used for the rusting reactions. When NH_4Cl alone was used iron removal was slow giving only 54% removal in 8 hrs. When a mixture of NH_4Cl + acetic acid was added it was slightly better than NH_4Cl alone giving a value of about 50% removal up to 4 hrs after which it increased to about 70% in 8 hrs. The mixture of NH_4Cl + acetic acid system gave a value of about 70% in 5 hrs after which the reaction became slow giving a final value of 76% at 8 hrs. Rusting reaction using the mixture of methanol + acetic acid with NH_4Cl is found to be superior to the systems using NH_4Cl with or without single organic compound. In this case an iron removal of about 80% was obtained in 5 hrs after which it became very slow giving a final value of 80.5% in 8 hrs. This clearly shows that mixture of two carbonyl compounds is more efficient than single compounds. The same trend is observed in all the other systems.

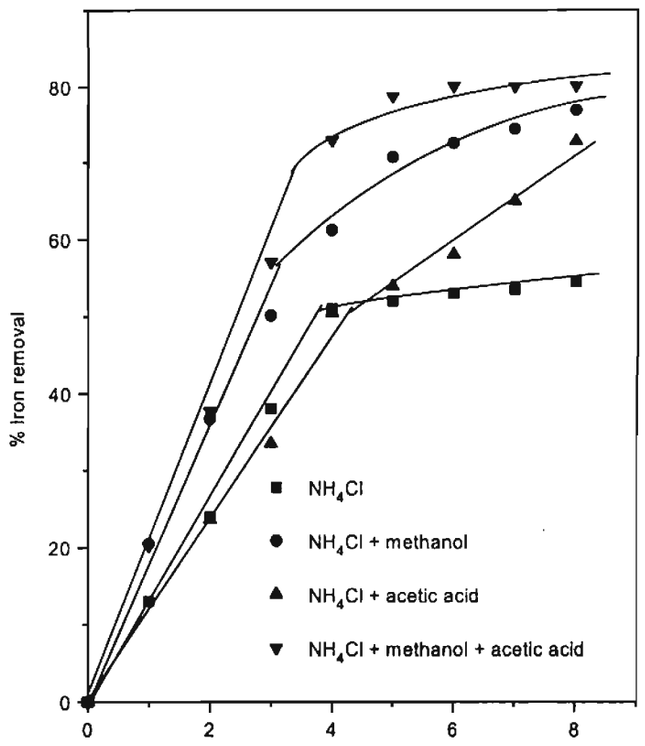

Fig-4.2 An Iron removal comparison

4.3.1 Rusting reaction carried out using mixture of methanol and acetone, acetone and acetic acid or sucrose and acetic acid along with NH_4Cl

Mixture of methanol and acetone was added along with NH_4Cl to find out the efficiency of rusting. Methanol added was 2% (v/v) and

acetone 1% (v/v). An iron removal of 75% was observed in 8 hrs. The quantity of acetone added was 2% (v/v) and acetic acid added was 1% (v/v) or sucrose added was 2% (w/v) and 1% (v/v) acetic acid. The

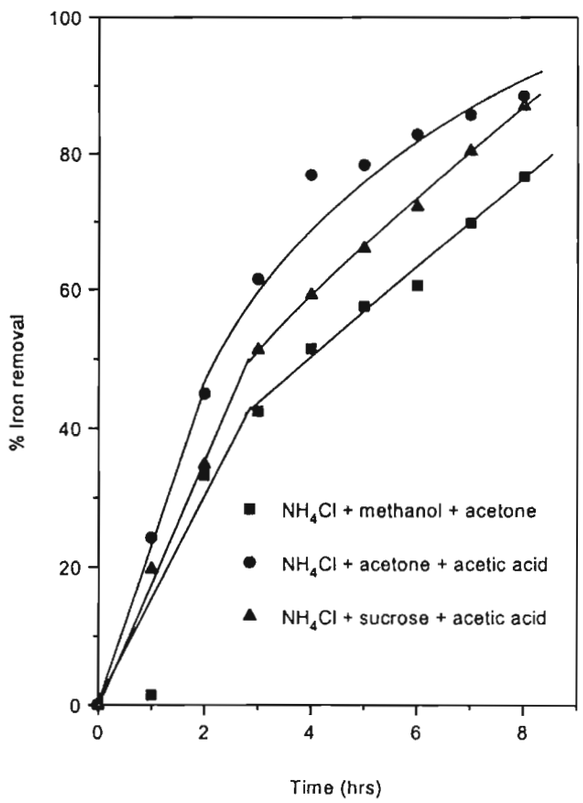

Fig-4.3. % iron removal vs. time

results are shown in Fig. 4.3.

4.3.2 Discussion

When methanol and acetone were added along with NH_4Cl about 40% iron removal was observed in 3 hrs. Then the reaction became slow reaching a value of 75% in 8 hrs. When acetone and

acetic acid were added along with NH_4Cl, the rusting reaction was very fast up to 4 hrs with an iron removal of 75% after which it became slow reaching a maximum of 90% removal in 8 hrs. About 94% TiO_2 was obtained after 8 hrs of reaction. About 4% of total iron was left behind after 8 hrs of reaction. The iron present may be in the form of oxide or may be entrapped in the TiO_2 matrix. When mixture of sucrose and acetic acid was added the reaction was fast up to 2 hrs with an iron removal of 35% after which it slowed down giving a value of 62% in 5 hrs. Finally it reached a value of 89% in 8 hrs.

4.3.3 Rusting reaction carried out using ethyl alcohol + acetic acid or methanol + formic acid along with NH_4Cl

Fig. 4.4 shows the result of rusting reaction carried out by adding mixture of 2% (v/v) ethyl alcohol and 1% (v/v) acetic acid or 2% (v/v) methanol and 1% (v/v) formic acid along with NH_4Cl.

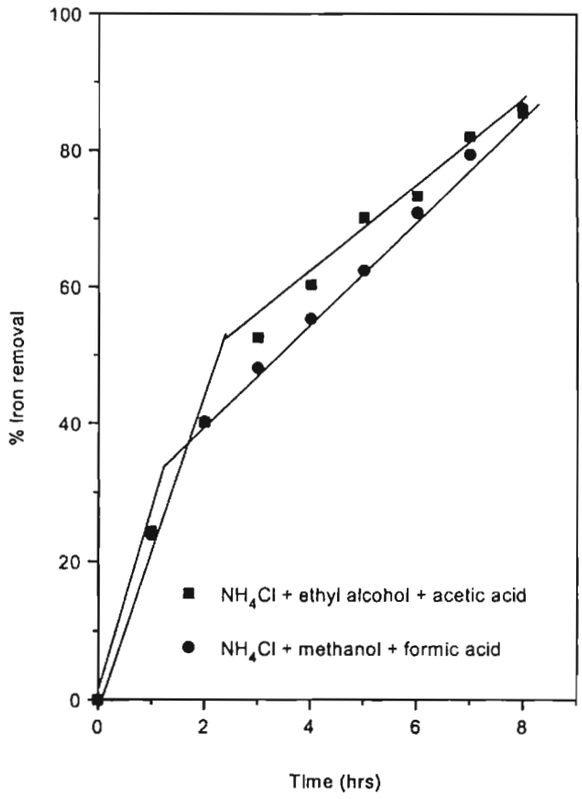

Fig-4.4. % Iron removal vs-time

4.3.4 Discussion

When ethyl alcohol and acetic acid were added along with NH_4Cl during the rusting reaction the iron removal was very fast up to 2 hrs giving a maximum iron removal of 45% after which the reaction became a little slow and gave a value of 85% iron removal in 8 hrs. When mixture of methanol and formic acid was added along with NH_4Cl about 40% of iron removal was obtained within 2 hrs and then the reaction steadily proceeded reaching a value of 85% iron removal in 8 hrs.

4.3.5 Rusting reaction carried out using glyoxal + acetic acid, mixture of acetic acid and formic acid, glyoxal + formic acid or urea + acetic along with NH_4Cl

Mixture of 2% (v/v) glyoxal and 1% (v/v) acetic acid, 1% (v/v) acetic acid + 1% (v/v) formic acid, 2% (v/v) glyoxal + 1% (v/v) formic acid or 2% (w/v) urea + 1% (v/v) acetic acid were added along with NH_4Cl to improve the rate of rusting reaction. The results are shown in Fig. 4.5

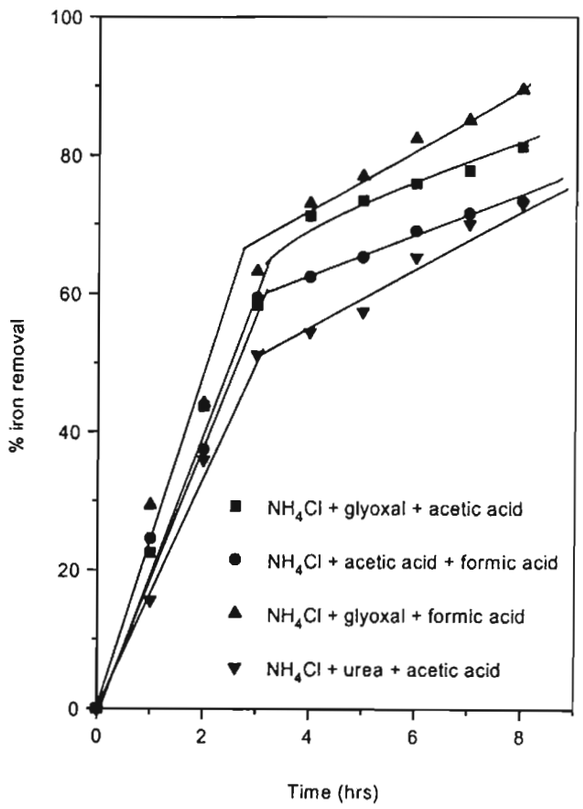

Fig-4.5. % Iron removal vs. time

4.3.6 Discussion

When mixture of glyoxal and acetic acid was added along with NH_4Cl, the rusting reaction was very fast up to 4 hrs where about 70% of iron removal was achieved. Then the reaction slowed down adding only 10% more during the next 4 hrs. When mixture of acetic acid and formic acid was added during rusting the reaction was fast during the first hour after which it became slow. The reason for this slowing down could be due to the fact that there is high degree of froathing during the reaction, which lifts the ilmenite particles from the reaction medium thus reducing physical contact between the particles and the medium. Only 35% iron removal was obtained in 2 hrs. After 8 hrs, the iron removal obtained was only 70%. When mixture of glyoxal and formic acid was added along with NH_4Cl during rusting reaction, the rusting was very fast in the initial hours. About 70% of iron removal was obtained in 4 hrs and then the reaction proceeded comparatively slow giving an iron removal of 85% in 8 hrs. When mixture of urea and acetic acid was added along with NH_4Cl during rusting the reaction was fast during the initial period. About 50% iron removal was obtained in 3 hrs and then the reaction became slow giving an iron removal of 70% in 8 hrs.

The fast reaction in the initial hours may be due to the presence of metallic iron on the outer surface of the individual grains where the reaction takes place fast. Another reason for slowing down may be passivation due to formation of oxide films on the surface or precipitation of hydroxides inside the pores that may hinder further reaction. As the reaction proceeds the availability of metallic iron on the surface is reduced and diffusion of metallic iron from the core of the reduced ilmenite particle has to take place. Because of diffusion

the synthetic rutile obtained after rusting is highly porous. The surface chemical reaction occurring during the initial hours is fast while the diffusion of metallic iron towards the rusting medium was very slow which may be the reason for slow reaction after the initial phase of rusting.

4.3.7 Dissolved Oxygen

As rusting reaction takes place in an electrochemical environment and the availability of oxygen to produce hydroxyl ions, the presence of oxygen in the rusting environment is one of the most important criteria for the reaction. The dissolved oxygen measured during the rusting reaction in the cases of NH_4Cl alone, NH_4Cl + methanol + acetone and NH_4Cl + sucrose + acetic acid are shown in Fig. 4.6, NH_4Cl + methanol + acetone and NH_4Cl + acetone + acetic acid are shown in Fig. 4.7 and NH_4Cl + ethyl alcohol + acetic acid and NH_4Cl + methanol + formic acid are shown in Fig. 4.8 respectively. Detailed analyses of the graphs show that no definite trend is observed in the dissolved oxygen in the systems. The values varied in a very irregular manner. But it is very clear that when NH_4Cl alone was added during the rusting reaction the dissolved oxygen measured initially was 6.5 ppm and as the reaction proceeded the concentration of dissolved oxygen in the medium got reduced and hence the rusting was also less. The dissolved oxygen measured during the starting stage of the reaction when the carbonyl compounds were added was above 8 ppm. When the rusting reaction proceeded there were narrow fluctuations but any time the measured dissolved oxygen was more than that of NH_4Cl alone.

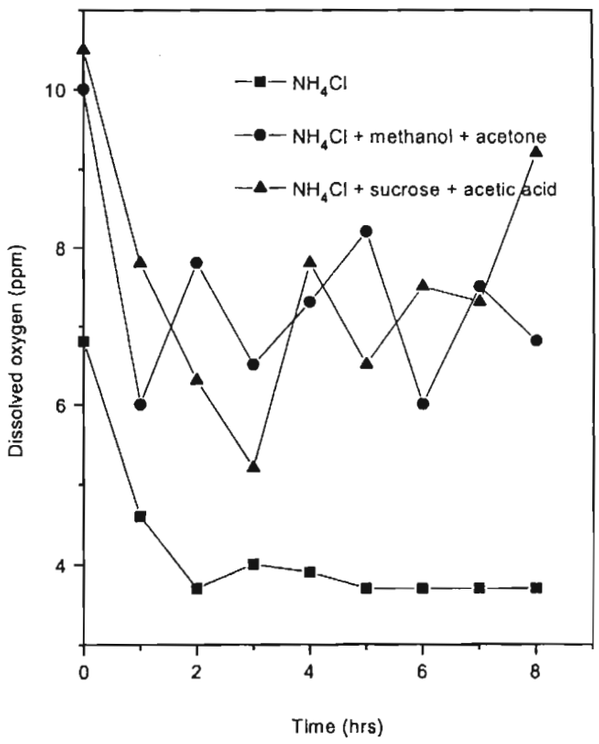

Fig-4.6. Variation in dissolved oxygen

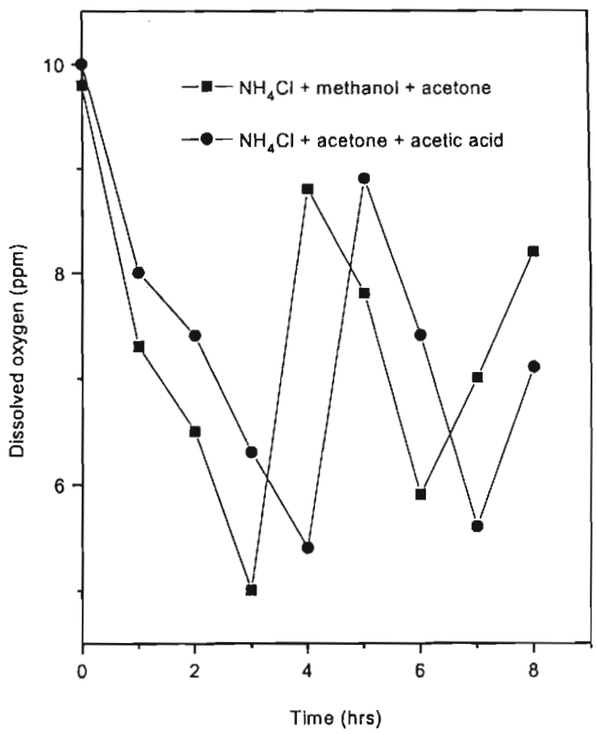

Fig-4.7. Variation in dissolved oxygen

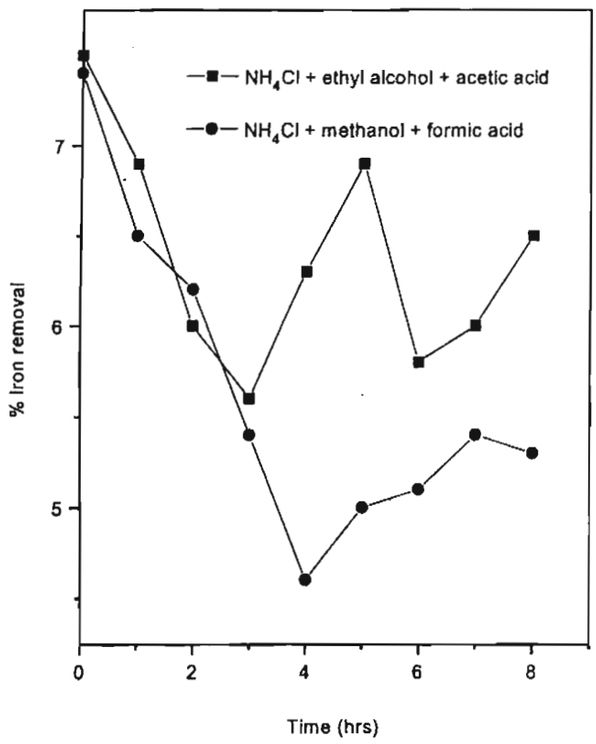

Fig-4.8. Variation in dissolved oxygen

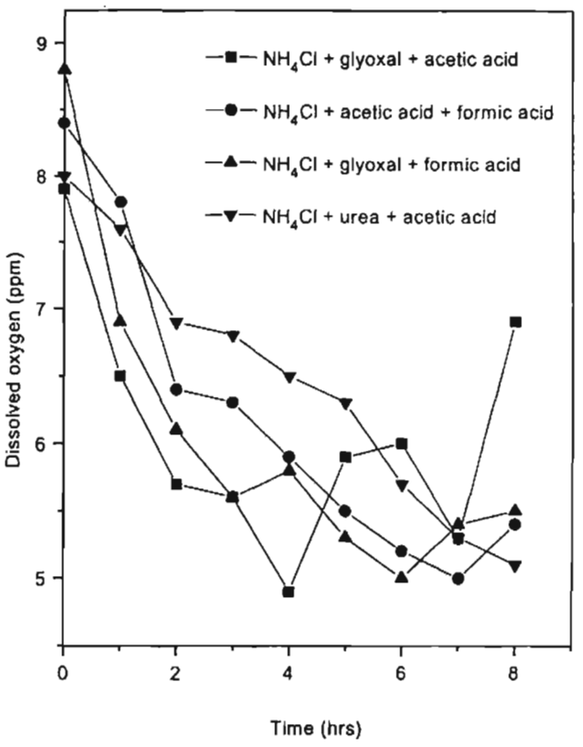

Fig-4.9. Variation in dissolved oxygen

4.3.8 Variation in pH

The rusting reaction of iron usually takes place below pH 4. Initial pH of the system may have a major influence on the progress of the reaction. The pH measured when NH_4Cl alone, NH_4Cl + methanol + acetic acid, NH_4Cl + acetone + acetic acid, NH_4Cl + methanol + formic acid and NH_4Cl + glyoxal + acetic acid are shown in Fig. 4.10. When NH_4Cl alone was added during rusting reaction the pH was adjusted to 4 using Con.HCl. As the rusting reaction progressed the pH of the system increased from 4 to 6. But when carbonyl compounds were added along with NH_4Cl during rusting the pH of the

system was already less than 4. As the reaction proceeded the pH fluctuated between 3 and 4 throughout the reaction till 8 hrs. At any time during the course of the reaction the pH was less than 4, which may be one of the reason for rusting using carbonyl compounds along with NH_4Cl. The acidic nature of the system through out the reaction may be due to the formation of carboxylic acids as a result of

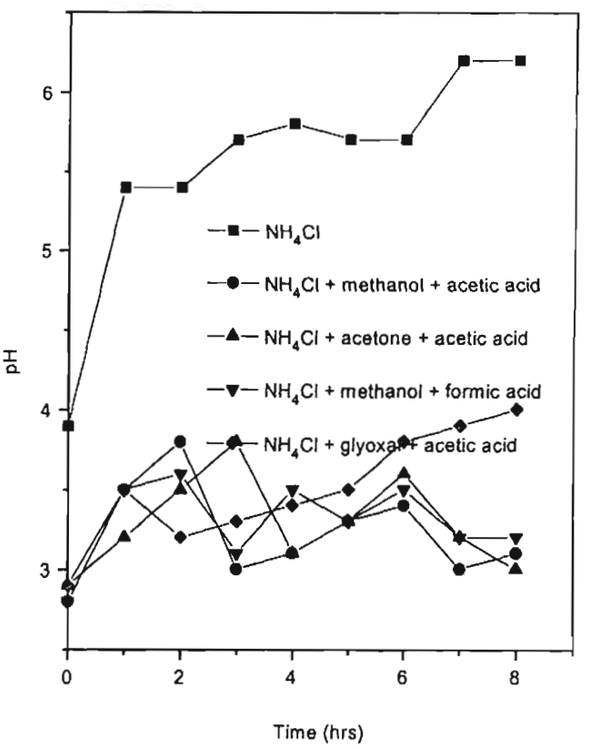

Fig·4.10. Variation in pH

oxidation during the rusting reaction.

4.4 Thermo Gravimetric Analyses

The samples obtained after rusting with NH_4Cl, mixtures of NH_4Cl + methanol + acetic acid, NH_4Cl + acetone + acetic acid or

NH_4Cl + ethyl alcohol + acetic acid were subjected to TGA after oven drying.

4.4.1 Synthetic rutile obtained by rusting with NH_4Cl alone

In the analysis of synthetic rutile obtained by rusting with NH_4Cl alone, a weight loss of 0.766% was observed up to 298.15°C. After that a weight gain of 3.874% was observed up to 999.39°C. TGA is shown in Fig. 5.1

The weight loss found up to 298.15°C may be due to the loss of adsorbed or absorbed water molecules in the pores of the rusted sample and may be due to the loss of hydroxide by the decomposition of ferrous and ferric hydroxide which might have got adsorbed on the surface or pores of the rusted ilmenite. The weight gain observed on heating up to 1000°C was 3.874%. Of this 3.874%, 3% may be due to the oxidation of 7% metallic iron remaining in the rusted ilmenite particles to form Fe_2O_3. The balance 0.874% may be because of oxidation of ferrous oxide present in the system. Theoretically 5% ferrous oxide, which is the difference between 7% metallic iron and 12.5% total iron, should give a weight gain of 1.1%. But the total weight gain was 0.874%. It may be possible that either all the remaining iron *ie.* 5% is not present as ferrous iron or all the ferrous was not getting oxidized.

The equations used for the calculation were

$$\begin{array}{lll} 2\,Fe & \longrightarrow & Fe_2O_3 \quad \text{----------(1)} \\ 111.7 & & 159.7 \\ 2\,FeO & \longrightarrow & Fe_2O_3 \quad \text{----------(2)} \\ 143.7 & & 159.7 \end{array}$$

Theoretical weight gain for 7% metallic iron on oxidation to Fe_2O_3 = 3%

Theoretical weight gain on oxidation of 5% ferrous iron = 1.1%

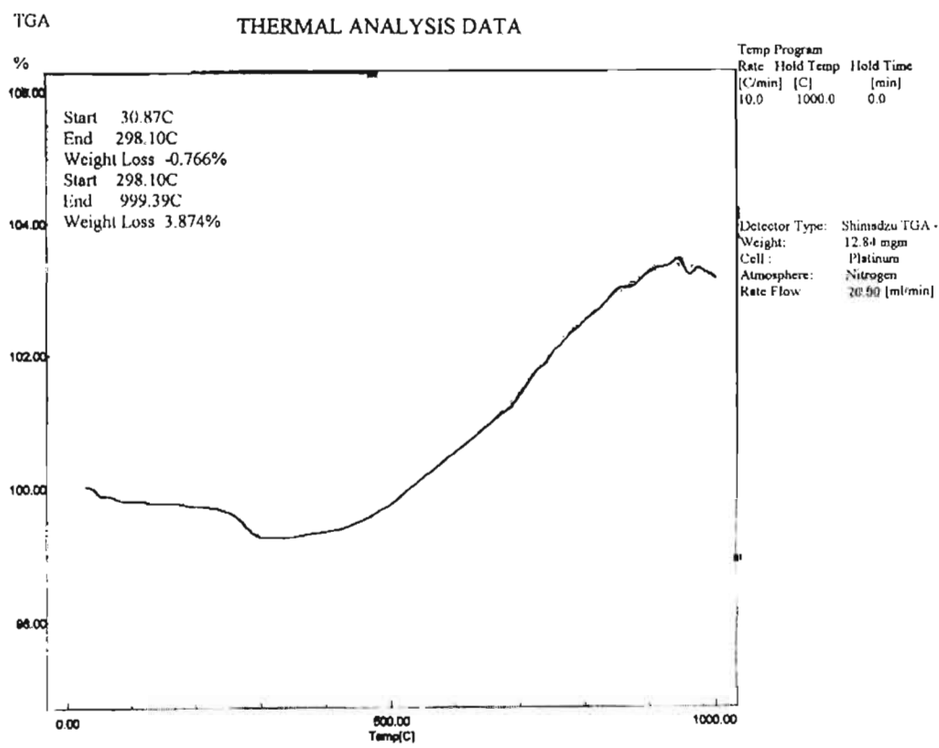

Fig. 5.1 Synthetic rutile obtained by rusting with NH_4Cl

4.4.2 Rusted ilmenite obtaind after rusting with mixture of NH_4Cl + methanol + acetic acid

On analysing the TGA graph of rusted ilmenite obtained by rusting with mixture of NH_4Cl + methanol + acetic acid a weight loss of 0.51% was observed up to 300.75°C, after which a weight gain of 2.037% was observed up to 653.39°C. Again on heating the sample to 999.15°C a further weight gain of 3.31% was obtained. The TGA is shown in Fig. 5.2.

Loss of small quantities of bound water molecules entrapped inside the pores of the rusted ilmenite and the hydroxide ions due to the decomposition of ferrous and ferric hydroxide could be the reasons for initial weight loss up to 300.75°C. The weight gain of 2.037% observed between 300.75°C to 653.39°C may be due to the oxidation of small amounts of metallic iron or ferrous oxide present in the sample. The total iron present after rusting was 4.5%. The metallic iron present was 1%, which was confirmed through analysis. So, the weight gain due to oxidation of 1% metallic iron should be 0.4297%. Deducting the metallic iron from the total iron gives a value of 3.5%, for the ferrous iron present, which should give a weight gain of 0.7875%. The total weight gain theoretically was 1.6489%. But the net gain observed was 2.037%, which shows that some other reactions are also taking place.

The weight gain observed up to 999.15% was 3.313%, which might be due to the oxidation of lower oxides of titanium present in the reduced ilmenite.

Apart from equations (1) and (2) the following equation was also considered for calculation

$$\underset{55.85}{Fe} \longrightarrow \underset{71.85}{FeO} \qquad \text{----------(3)}$$

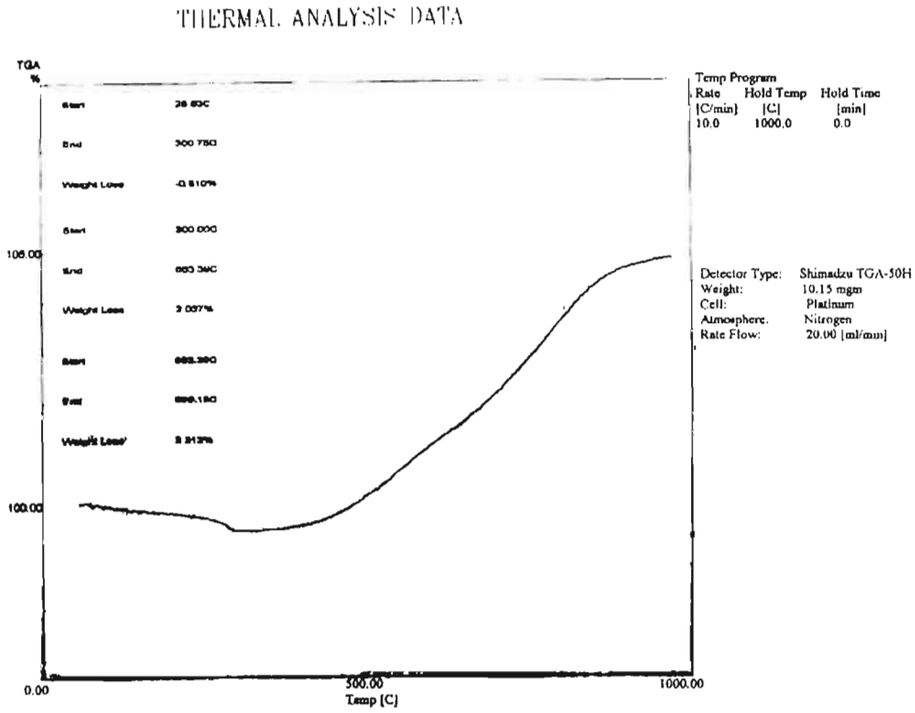

Fig. 5.2 Synthetic rutile obtained by rusting with NH_4Cl + methyl alcohol + acetic acid

4.4.3 TG of rusted ilmenite obtained by adding mixture of NH_4Cl + acetone + acetic acid

Fig. 5.3 shows the result of thermal analysis of rusted ilmenite obtained after rusting with mixture of NH_4Cl + acetone + acetic acid. Initially a weight loss was observed up to 302.23°C. On heating the sample up to 653.53°C a weight gain of 2.59% was observed. Again on heating the sample up to 999.36°C a weight increase of 3.129% was obtained.

The weight loss occurred initially up to 302.23°C may be due to the decomposition of hydroxides of ferrous and ferric and loss of bound water molecules which might have got adsorbed on the surface and the pores of the rusted particles. The weight gain of 2.59% obtained between temperatures 302.23°C to 653.53°C may be due to the oxidation of small amounts of metallic iron or ferrous oxide present in the rusted sample. The total iron present after rusting was 4.12%. The chemical analysis shows that the metallic iron present in the sample was 0.8%. So, the weight gain due to oxidation of 0.8% metallic iron to FeO should be 0.5708%. Deducting the metallic iron from the total iron, 3.32% is present in the form of ferrous which should give a weight gain of 1.4344%. But the net weight gain observed was 2.59%. The oxidation reactions were taking place in two steps, which show that some other reactions are also taking place.

The weight gain observed on heating the sample from 653.53°C to 999.36°C was 3.129%, which might be due to the oxidation of lower oxides of titanium.

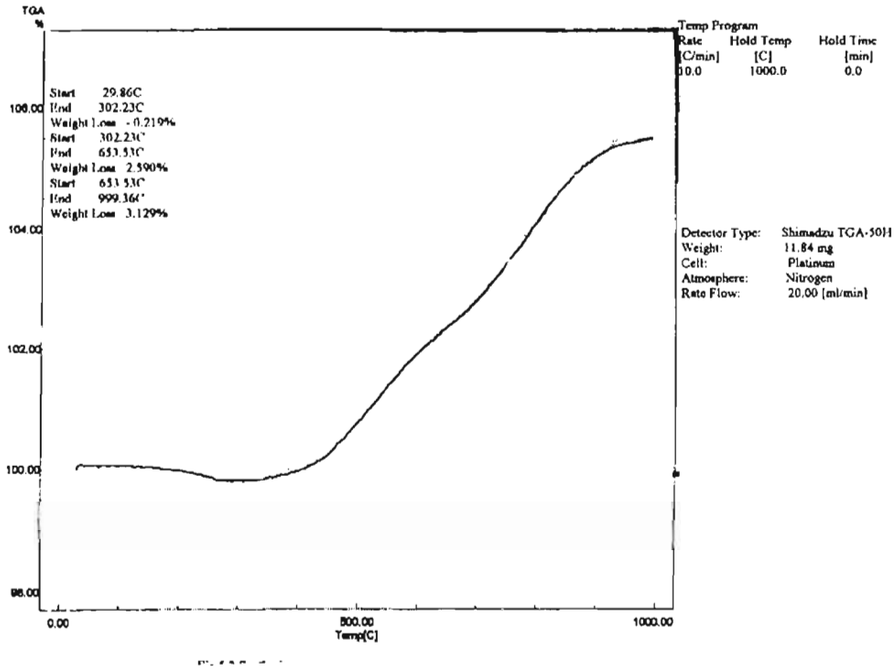

Fig. 5.3 Synthetic rutile obtained by rusting with NH_4Cl + acetone + acetic acid

4.4.4 Rusted ilmenite obtained after rusting with mixture of NH_4Cl + ethanol + acetic acid

On analysis of TGA graph of rusted ilmenite by rusting with mixture of NH_4Cl + ethanol + acetic acid a weight loss of 0.398% was observed up to 345.15°C. Again on heating the sample from 345.15°C to 999.47°C a further weight gain of 6.762% was obtained. The TG is shown in Fig. 5.4

Loss of small quantities of bound water molecules entrapped inside the pores of the rusted ilmenite and the hydroxide ions due to the decomposition of ferrous and ferric hydroxide could be the reason for initial weight loss up to 345.15°C. The weight gain of 6.762% observed between 345.15°C to 999.47°C may be due to the oxidation of metallic iron and ferrous iron present in the sample. The

total iron present in the sample was 4.53%. The oxidation of lower oxides of titanium present in the reduced ilmenite might also account for higher weight gain observed up to 999.47°C.

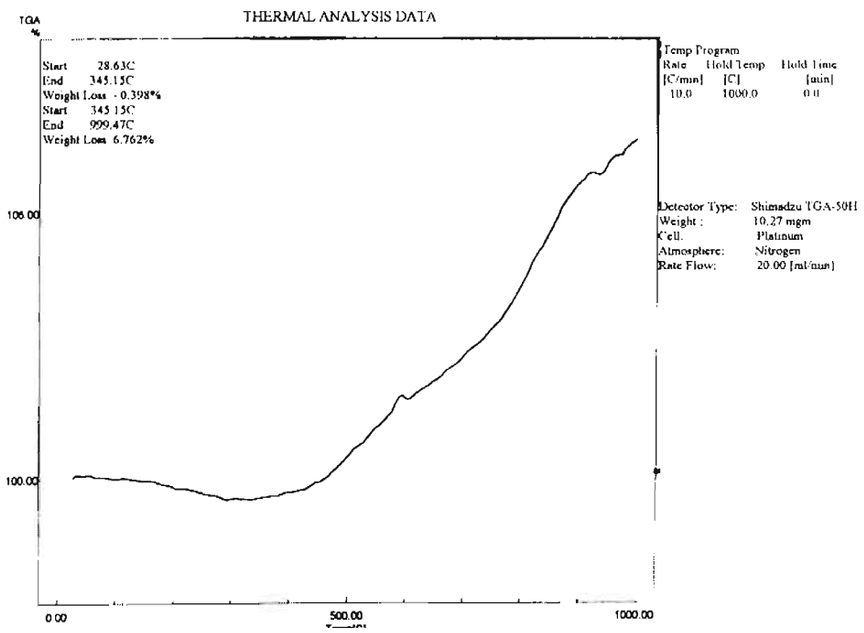

Fig. 5.4 Synthetic rutile obtained by rusting with NH_4Cl + ethyl alcohol + acetic acid

4.5 X- ray diffraction

The product obtained after rusting reduced ilmenite with NH_4Cl was analysed using XRD. The major phases observed are anatase, rutile and pseudobrookite along with small amounts of metallic iron.

4.5.1 XRD of synthetic rutile rusted with NH_4Cl alone

From TGA it is evident that up to 298.10°C there occurs weight loss and heating from 298.10°C to 999.39°C there occurs a weight gain. Hence these two temperatures were selected and the

samples were heated in a muffle furnace at these temperatures for 30 minutes. The XRD pattern is shown in Fig. 6.1. The sample heated at 298.17°C was analysed using XRD. Here also the major phases were anatase, rutile and pseudobrookite. The metallic iron peak was still observed which infers that it has not undergone any change during this heating. This shows that material remains the same without any major chemical or structural change even after heating to 298°C. When it was heated at 1000°C, rutile formation was clearly observed as the major phase. The occurrence of rutile as the major phase was due to the fact that anatase gets converted to rutile above 700°C.

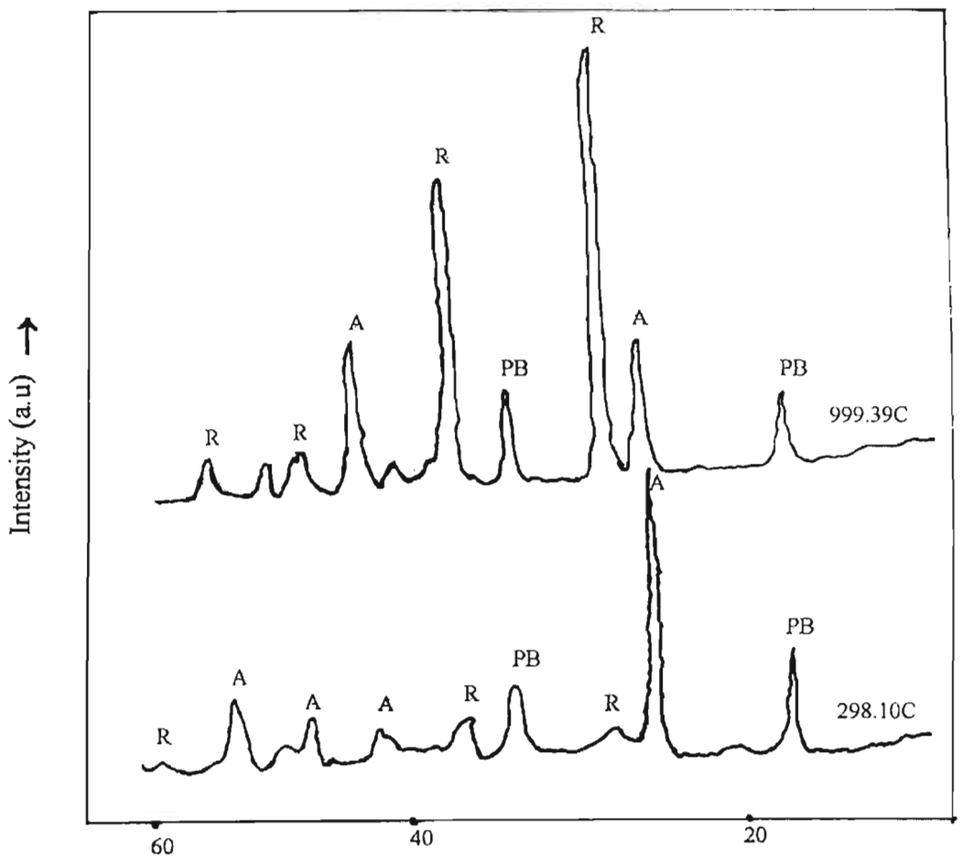

Fig. 6.1 XRD pattern of synthetic rutile obtained by rusting with NH_4Cl after heating at various temperatures (PB – Pseudo brookite, A – Anatase, R – Rutile)

4.5.2 XRD of synthetic rutile rusted with NH_4Cl + carbonyl compounds

The samples obtained by rusting using mixtures of NH_4Cl + methanol + acetic acid, NH_4Cl + acetone + acetic acid and NH_4Cl + ethyl alcohol + acetic acid were subjected for TGA and the temperatures up to which weight loss was observed and the temperatures up to which weight gain was observed were noted and

the samples were heated at that particular temperature in a muffle furnace. The samples were heated for 30 minutes at those particular temperatures. The XRD of these samples were analysed and are shown in Fig. 6.2,6.3 and 6.4 respectively.

The XRD patterns of samples obtained after heating at temperatures 300°C, 302°C and 345°C almost had similar trends. The major phases observed were anatase, rutile and pseudobrookite. The material has not undergone any major structural change or chemical change during this heating. When the samples were heated to 650°C oxidation of iron takes place. This is clearly observed in the XRD patterns. When the samples were heated at 1000°C rutile formation was clearly observed as the major phase. The occurrence of rutile as the major phase was due to the fact that anatase gets converted to rutile above 700°C.

In general when rusting reaction progressed the metallic iron peak diminished and the enrichment of anatase and rutile was observed from the XRD of rusted samples using NH_4Cl and NH_4Cl + carbonyl compounds.

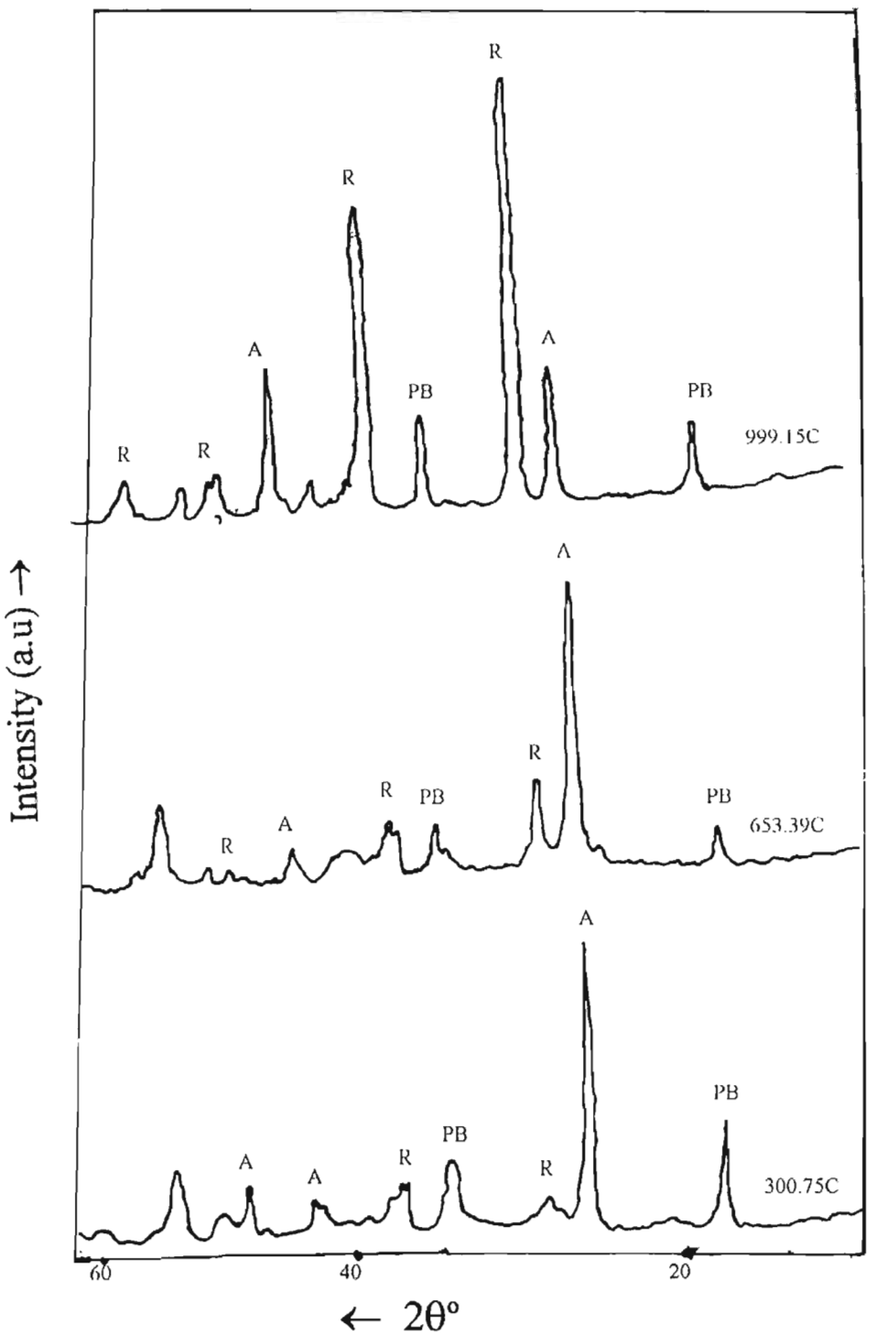

Fig. 6.2 XRD pattern of synthetic rutile obtained by rusting with NH_4Cl + methanol + acetic acid after heating at various temperatures (PB – Pseudo brookite, A – Anatase, R – Rutile)

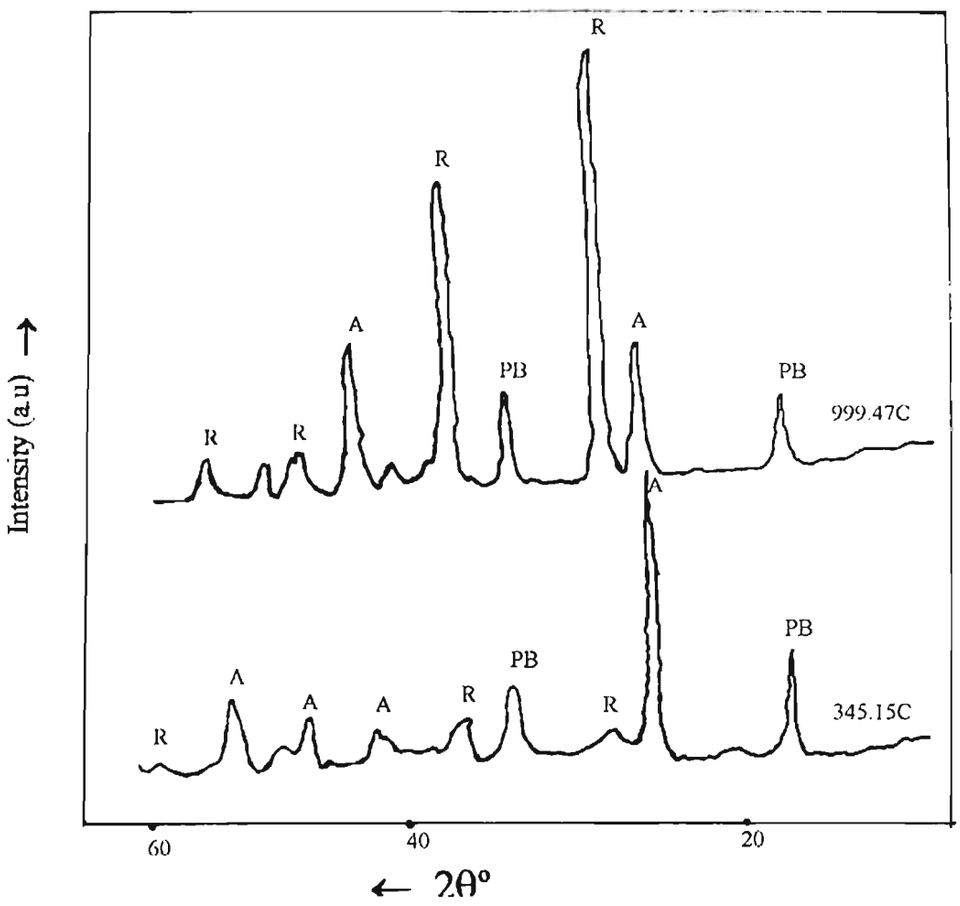

Fig.6.3 XRD pattern of synthetic rutile obtained by rusting with NH_4Cl + ethyl alcohol + acetic acid after heating at various temperatures (PB – Pseudo brookite, A – Anatase, R – Rutile)

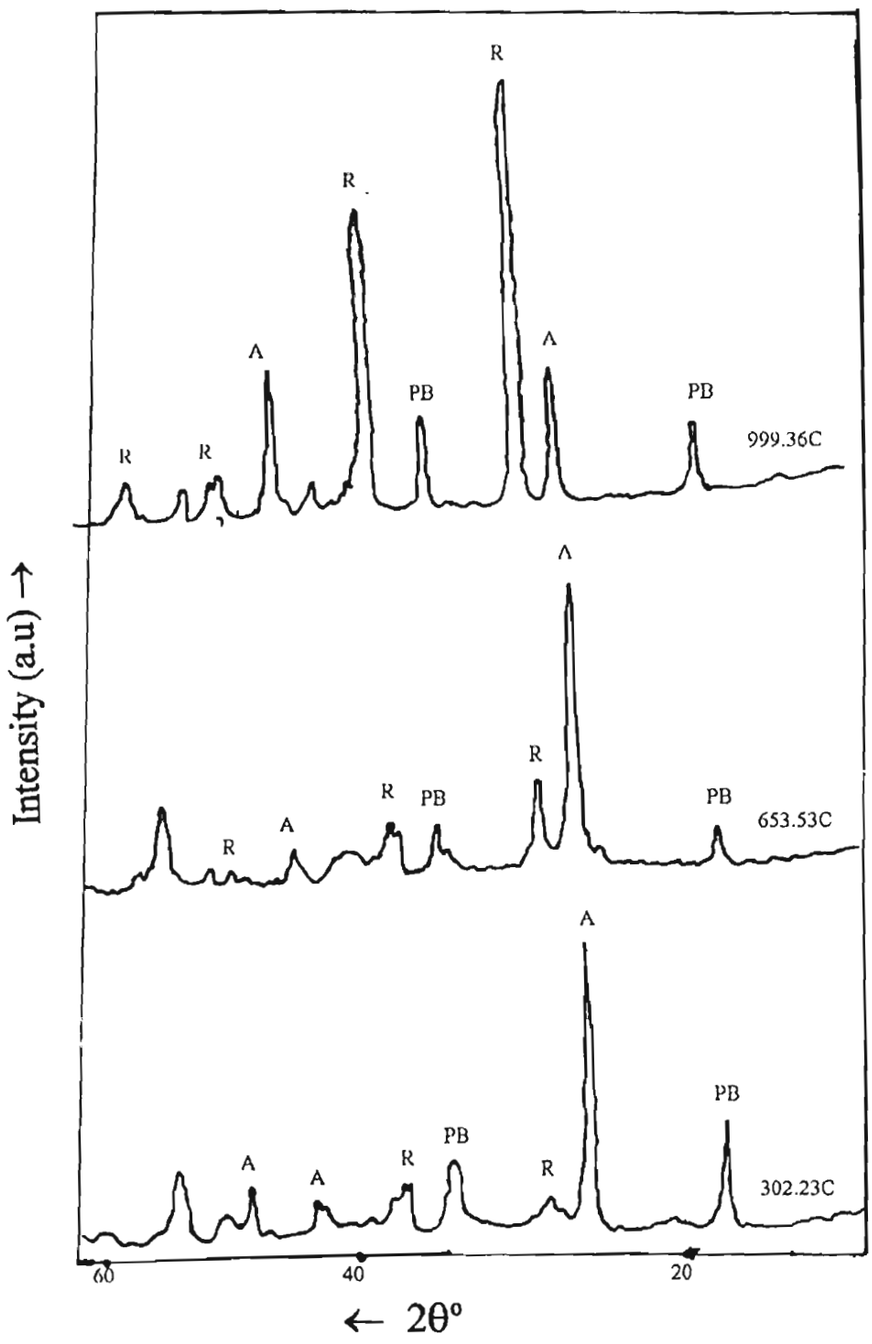

Fig. 6.4 XRD pattern of synthetic rutile obtained by rusting with NH_4Cl + acetone + acetic acid at various temperatures (PB – Pseudo brookite, A – Anatase, R – Rutile)

4.6 SEM

The surface morphology of the rusted ilmenite was investigated using SEM. The microstructures are shown in Figs. 7.1, 7.2, 7.3, 7.4 and 7.5 respectively. The metallic iron formed as a result of reduction of ilmenite gets agglomerated mainly on the surface of the particles. As, rusting reaction proceeds pores are formed on the surface of the particle due to the removal of metallic iron. When the metallic iron on the surface is removed the metallic iron present inside the core of the particle diffuses outside the particle and gets rusted so that more pores are developed. Finally the particle has the appearance of honeycomb.

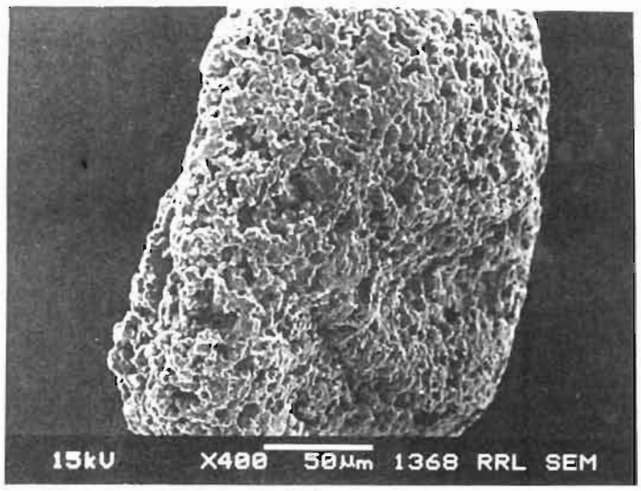

(a)

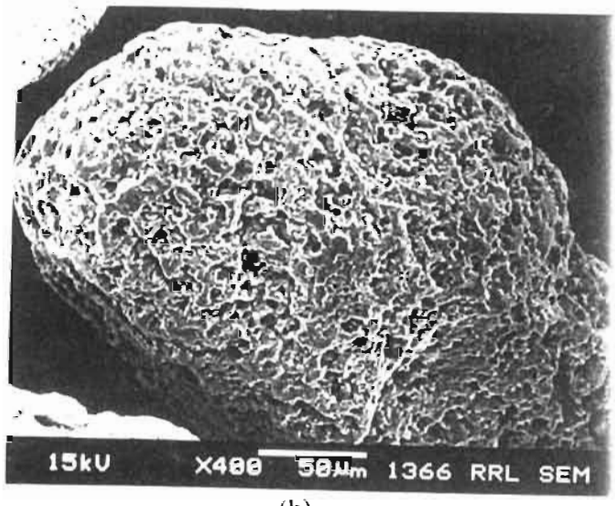

(b)

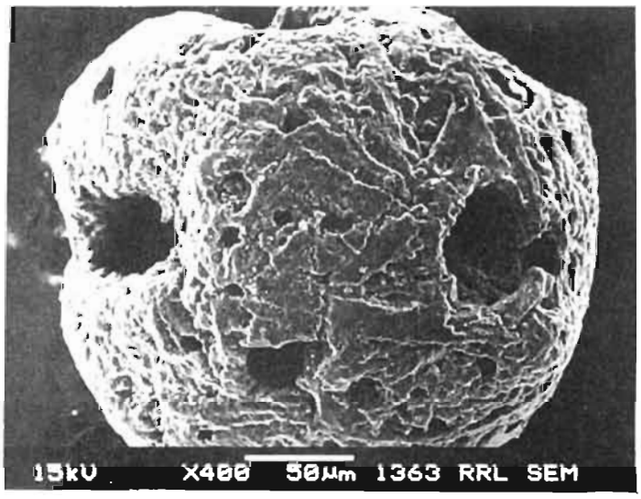

(c)

Fig. 7.1 SEM photograph of rusted ilmenite obtained by rusting with NH_4Cl + methanol + acetic acid (a) 3 hrs. (b) 5 hrs. (c) 8 hrs.

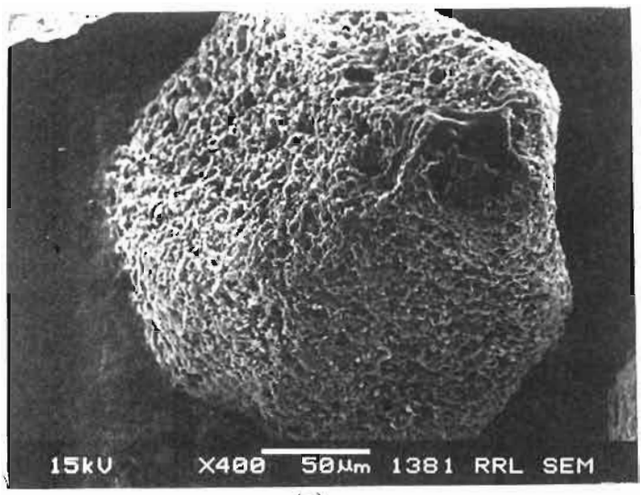

(a)

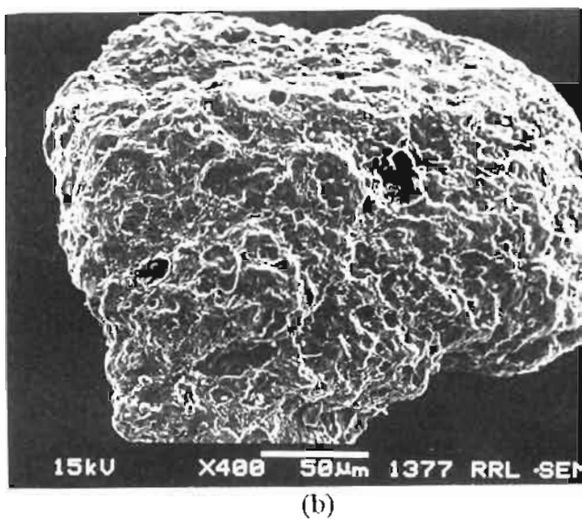

(b)

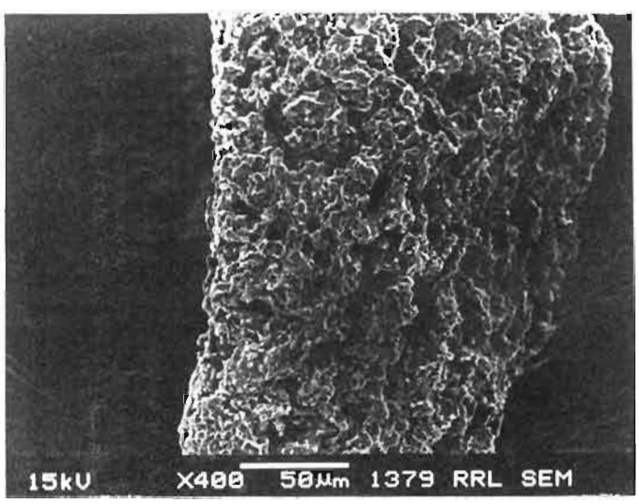

(c)

Fig. 7.2 SEM photograph of rusted ilmenite obtained by rusting with NH_4Cl + HCHO+ acetic acid (a) 3 hrs. (b) 5 hrs. (c) 8 hrs.

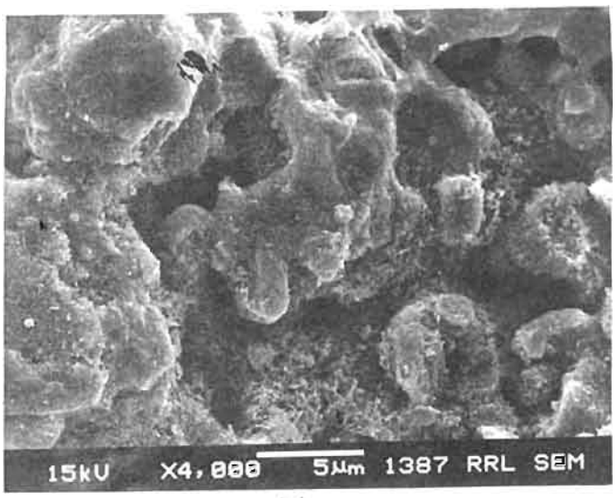

(a)

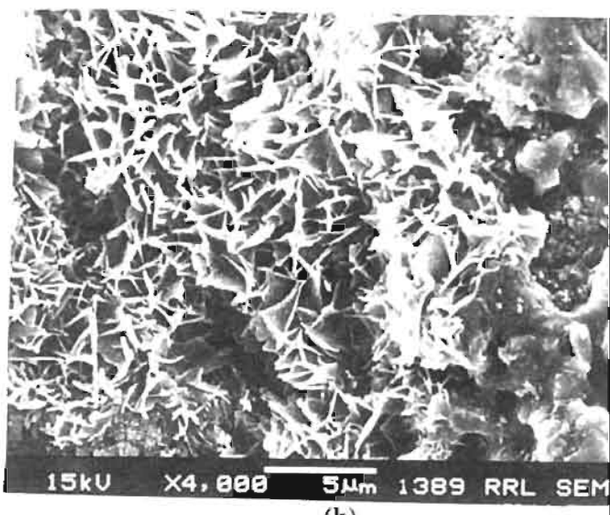

(b)

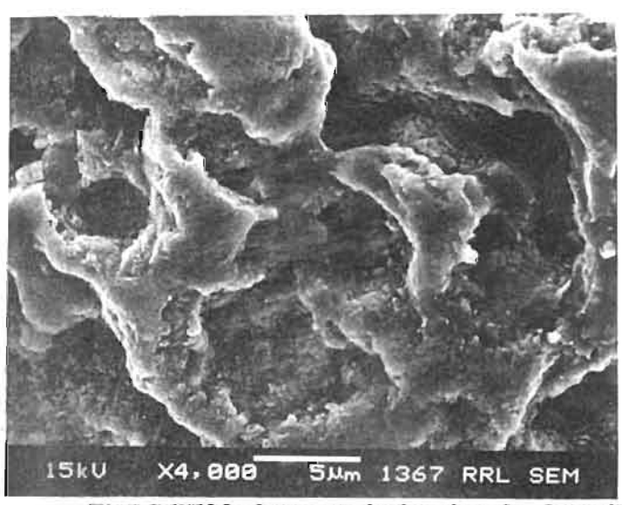

(c)

Fig7.3 SEM photograph showing the deposition of iron oxide into the pores during the progress of rusting. (a) & (b) Rusted ilmenite with $NH_4Cl + CH_3CHO$ + acetic acid (c) Rusted ilmenite with NH_4Cl + methanol + acetic acid

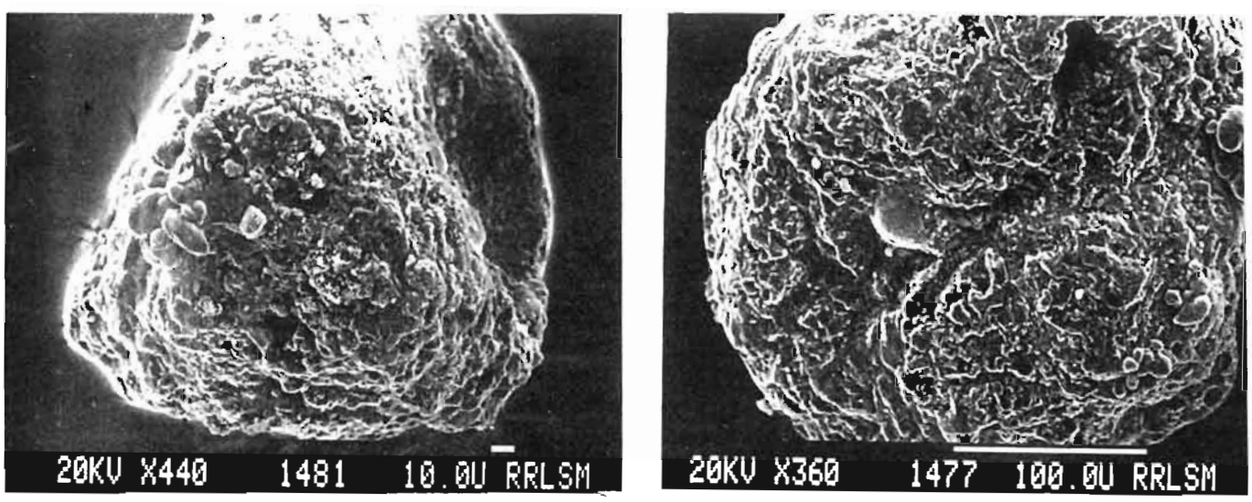
20KV X440 1481 10.0U RRLSM
20KV X360 1477 100.0U RRLSM

(a)

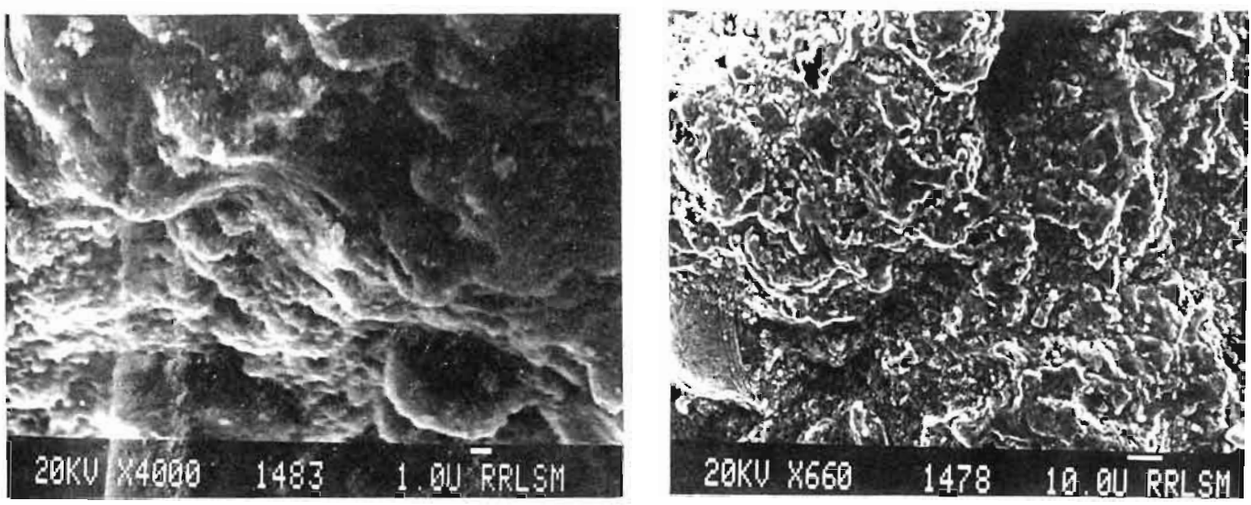
20KV X4000 1483 1.0U RRLSM
20KV X660 1478 10.0U RRLSM

(b)

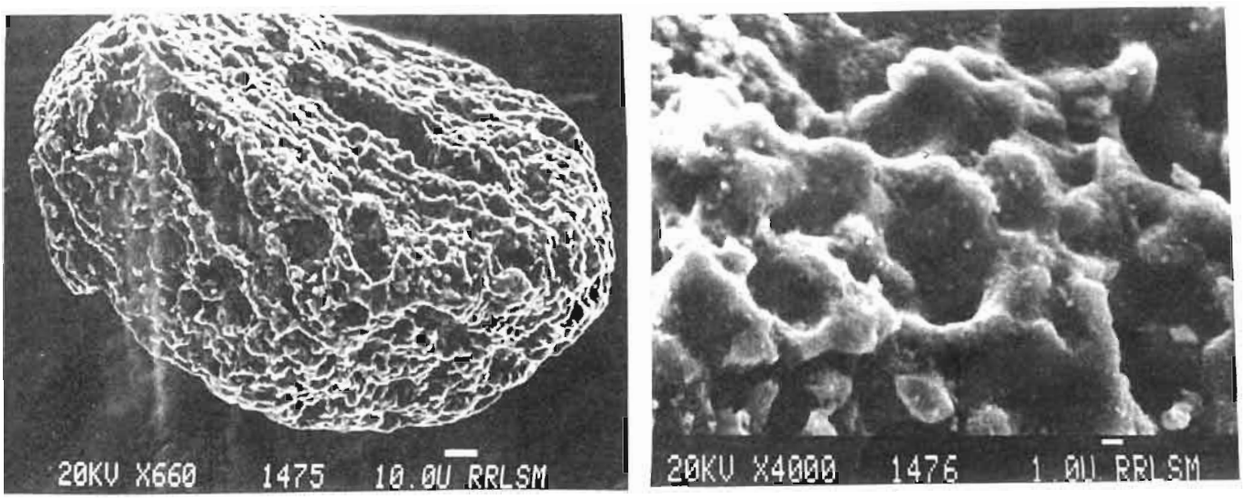

(c)

Fig. 7.4 SEM photograph of rusted ilmenite obtained by rusting with NH_4Cl + glyoxal + acetic acid (a) 3 hrs. (b) 5 hrs. (c) 8 hrs.

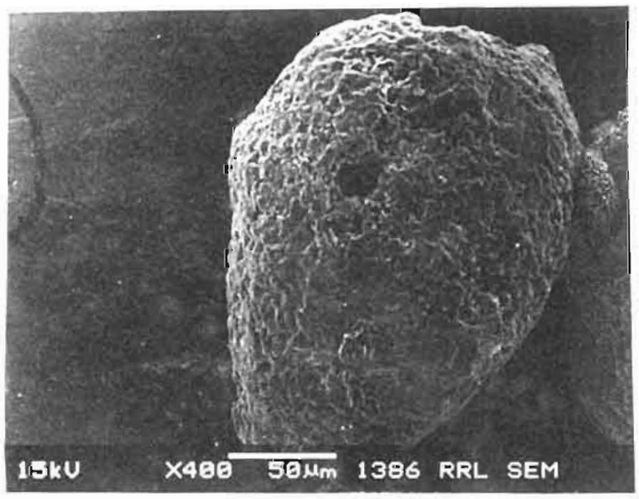

Fig. 7.5 SEM photograph of rusted ilmenite obtained by rusting with NH_4Cl + CH_3CHO+ acetic acid for 8 hrs.

4.7 Kinetics

The effect of temperature on rusting in presence of mixtures of carbonyl compounds along with NH_4Cl was studied at 25°C, 30°C, ,35°C and 40°C. Time *vs.* $1-(1-x)^{1/3}$ graphs were plotted to find out if the reaction was topochemical as in the case of single carbonyl compounds along with NH_4Cl. But the plots did not give straight lines. So, it is concluded that surface chemical reaction is not the rate determining step.

In a solid reaction, the product is formed on the reacting solid; the kinetics of the reaction may be governed by the factor of coating and the diffusion process. If the coating is very porous then there will be no resistance to reagents to react and hence coating will have no effect. In case the porosity is low or nonexistent then the reagent has to diffuse through the protective film either by pore diffusion or by lattice diffusion before it reaches the interface. In such cases the reaction rate decreases progressively because of gradual thickening of the product layer and hence the diffusion path increases. In the case of a spherical solid the decrease in rate would be enhanced if the area of the core interface decreases.

Considering all the above facts in mind the equation proposed by Crank – Ginstling and Brounshtein [182] for diffusion controlled reactions were applied. The plots obtained by plotting time *vs.* $1+2(1-x)-3(1-x)^{2/3}$ for all the systems gave straight lines. It is hence evident that when mixtures of carbonyl compounds were used along with NH_4Cl, the diffusion control mechanism is the rate determining step which is different from the system using NH_4Cl alone where it is controlled by surface chemical reaction. Arrhenius plots were drawn from the slopes of the diffusion control graphs and activation energies were calculated.

4.7.1 Rusting using NH_4Cl + actone + acetic acid

Fig. 8.1 shows the plot of time *vs.* $1+2(1-x)-3(1-x)^{2/3}$ when using NH_4Cl + actone + acetic acid for the rusting reaction. It is clear from the observation that the mechanism followed is the diffusion controlled one. The optimum temperature required for effective rusting was 30°C. The activation energy calculated from the Arrhenius plot is 17.41 KJ/mol, which is shown in Fig. 8.5.

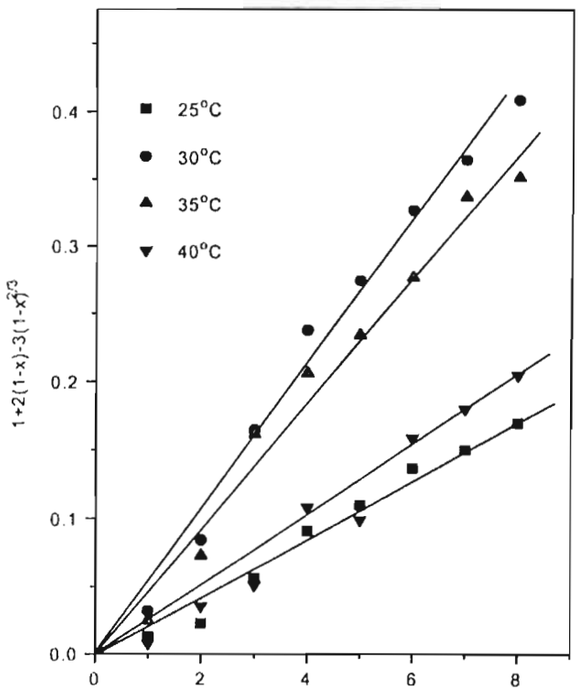

Fig. 8.1 Plot of time *vs.* $1+2(1-X)-3(1-X)^{2/3}$ using NH_4Cl + acetone + acetic acid

4.7.2 Rusting with NH_4Cl + methanol + formic acid

Plot of time *vs.* $1+2(1-x)-3(1-x)^{2/3}$ when adding NH_4Cl + methanol + formic acid is shown in Fig. 8.2. The optimum temperature for maximum rusting was found to be 30°C. The activation energy calculated for the above reaction was 21.54 KJ/mol. The Arrhenius plot is shown in Fig. 8.5.

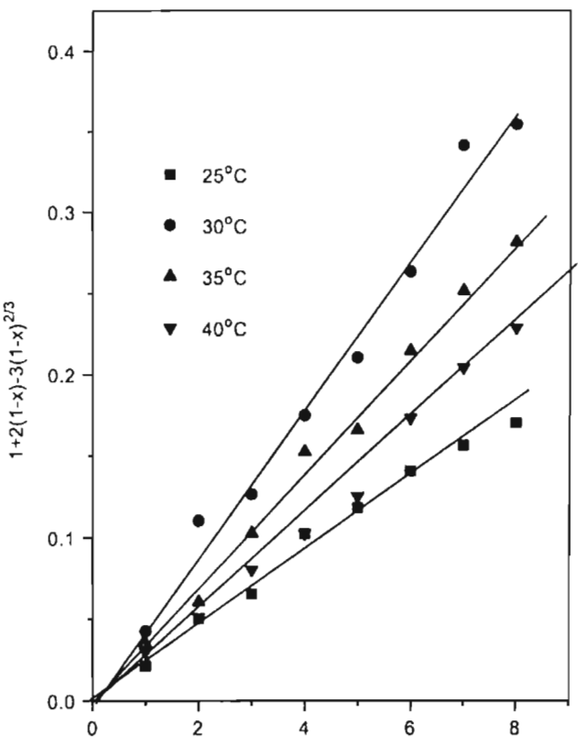

Fig. 8.2 Plot of time *vs.* $1+2(1-X)-3(1-X)^{2/3}$ using NH_4Cl + methanol + formic acid

4.7.3 Mixture of methanol and acetic acid along with NH_4Cl for rusting

The plot of time *vs.* $1+2(1-x)-3(1-x)^{2/3}$ obtained when mixture of NH_4Cl + methanol + acetic acid was added during rusting reaction is shown in Fig. 8.3. The optimum temperature for maximum rusting was found to be 30°C. From the Arrhenius plot the activation energy

calculated for the reaction was 38.29 KJ/mol, which is shown in Fig. 8.5.

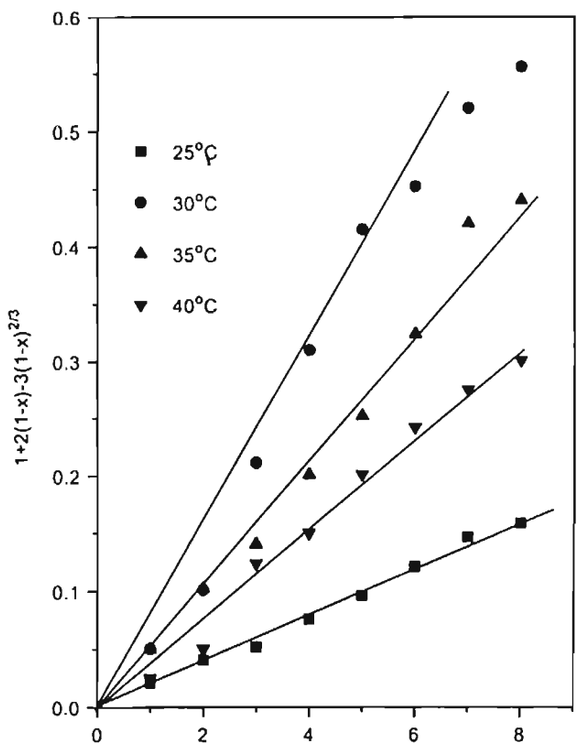

Fig. 8.3 Plot of time *vs.* $1+2(1-X)-3(1-X)^{2/3}$ using NH_4Cl + methanol + acetic acid

4.7.4 Mixture of ethanol and acetic acid added along with NH_4Cl during rusting

Fig. 8.4 shows the plot of time *vs.* $1+2(1-x)-3(1-x)^{2/3}$ when mixture of ethanol and acetic acid was added along with NH_4Cl. The

maximum rusting was observed at 30°C. The activation energy was found to be 46.22 KJ/mol. The Arrhenius plot is shown in Fig. 8.5.

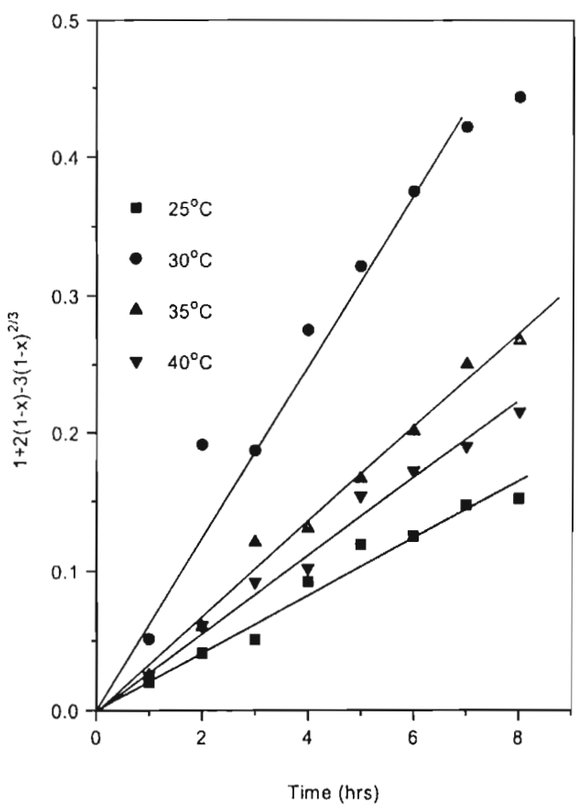

Fig. 8.4 Plot of time *vs.* $1+2(1-X)-3(1-X)^{2/3}$ using NH_4Cl + ethanol + acetic acid

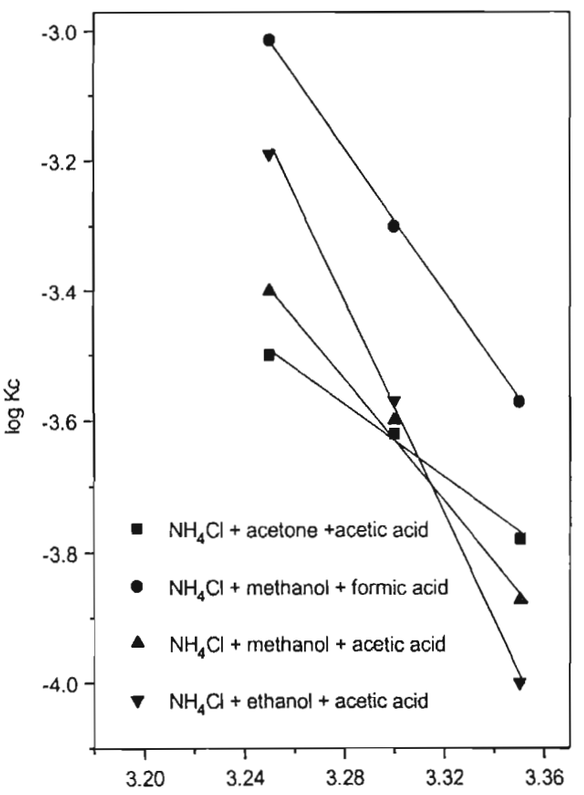

Fig-8.5 Arrhenius Plots

4.7.5 Mixture of NH_4Cl + glyoxal + acetic acid added during rusting

Fig. 8.6 shows the plot of time *vs.* $1+2(1-x)-3(1-x)^{2/3}$ when mixture of glyoxal and acetic acid was added along with NH_4Cl during the rusting reaction. The optimum temperature required for maximum rusting was found to be 30°C. The activation energy was

calculated from Arrhenius plot and it was found to be 47.87 KJ/mol and it is shown in Fig. 8.9.

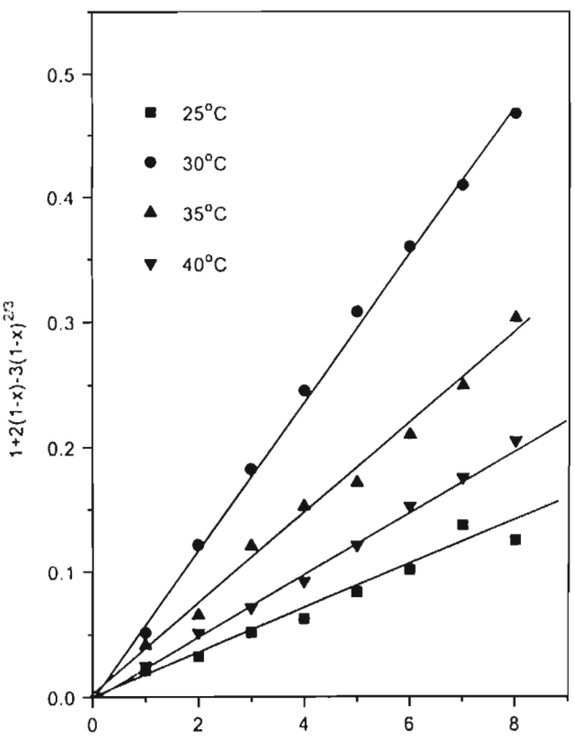

Fig. 8.6 Plot of time *vs.* $1+2(1-X)-3(1-X)^{2/3}$ using NH_4Cl + glyoxal + acetic acid

4.7.6 Mixture of acetic acid and formic acid added along with NH_4Cl during rusting

The results of time *vs.* $1+2(1-x)-3(1-x)^{2/3}$ is plotted in Fig 8.7 when NH_4Cl + acetic acid + formic acid were added during rusting reaction. The optimum temperature at which maximum rusting was found to be 30°C. The activation energy was calculated from

Arrhenius plot, which is shown in Fig. 8.9, and it was found to be 50.38 KJ/mol.

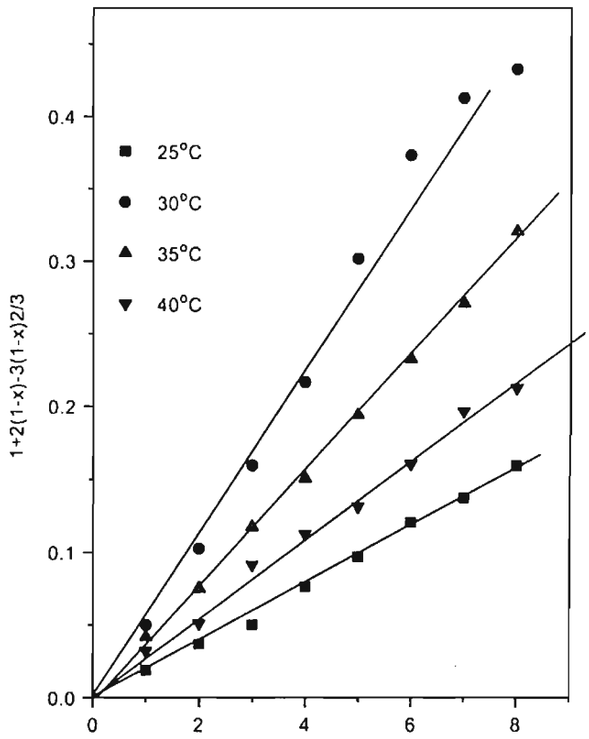

Fig. 8.7 Plot of time *vs.* $1+2(1-X)-3(1-X)^{2/3}$ using NH_4Cl + acetic acid + formic acid

4.7.7 Rusting with NH_4Cl + sucrose + acetic acid

Fig. 8.8 shows the results of time *vs.* $1+2(1-x)-3(1-x)^{2/3}$ when mixture of NH_4Cl + sucrose + acetic acid was added during rusting reaction. The optimum temperature required for maximum rusting was

found to be 30°C. The activation energy was calculated from Arrhenius plot which is shown in Fig. 8.9. The activation energy was found to be 54.23 KJ/mol.

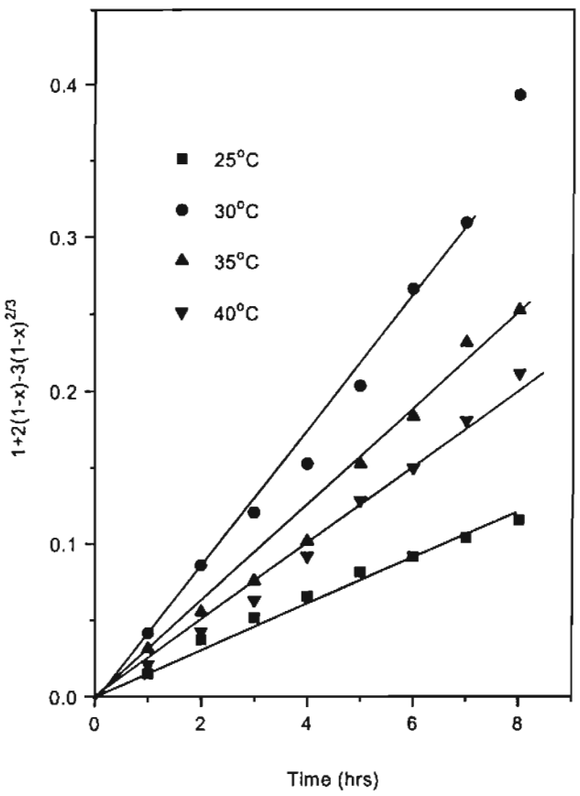

Fig. 8.8 Plot of time *vs.* $1+2(1-X)-3(1-X)^{2/3}$ using NH_4Cl + sucrose + acetic acid

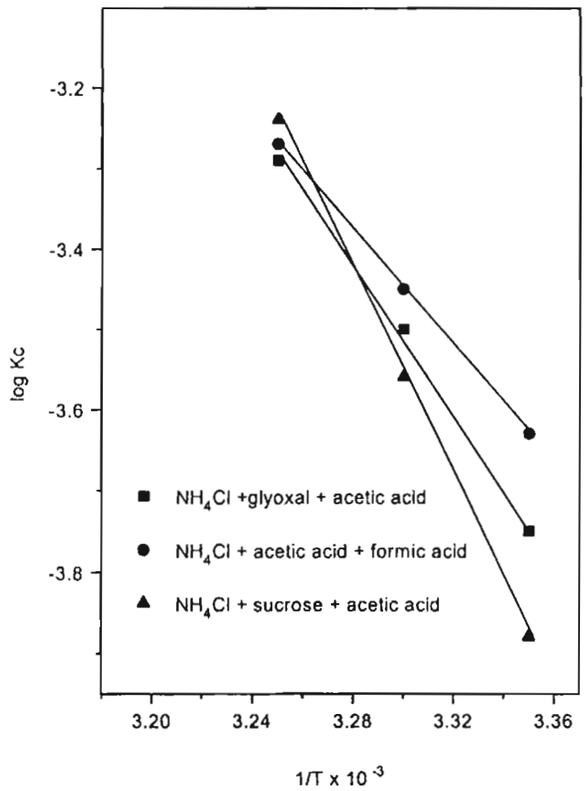

Fig.8.9 Arrhenius Plots

On analyzing the plots obtained by plotting time vs $1+2(1-x)-3(1-x)^{2/3}$, the rate of the reaction is found to be diffusion controlled one. When the diffusion through a product or residue layer becomes rate controlling the reaction should gradually decrease as the layer thickness increases. From the plots it is clear that as the temperature is increased from 25°C to 30°C the rate of the reaction is increased. Above 30°C the rate of the reaction was gradually decreased. So, the optimum temperature for maximum iron removal was found to be 30°C. The decrease in reaction rate above 30°C may be due to the evaporation of the carbonyl compounds. The activation energies

calculated using mixtures of NH_4Cl + acetone + acetic acid, NH_4Cl + methanol + formic acid, NH_4Cl + methanol + acetic acid, NH_4Cl + ethanol + acetic acid, NH_4Cl + glyoxal + acetic acid, NH_4Cl + acetic acid + formic acid and NH_4Cl + sucrose + acetic acid were 17.41 KJ/mol, 21.54 KJ/mol, 38.29 KJ/mol, 46.22 KJ/mol, 47.87 KJ/mol, 50.38 KJ/mol and 54.23 KJ/mol respectively. The maximum iron removal was also found for the system NH_4Cl + acetone + acetic acid where the activation energy is minimum and decreases in the order with increasing activation energy.

On examining the role of particle size, the reactions that are controlled by diffusion through product layer, the rate constant is proportional to $1/R_o^2$. If the particle size is reduced then the rate constant is increased more for the diffusion controlled process. Diffusion control is more sensitive to particle size because diffusion not only depends on available surface area through which the species move but also the length of the diffusion path. The dependence K on R_o can be a test for identification of reaction mechanism. When log K *vs.* log R_o [183] is plotted, slope 2 identifies the diffusion control. The plot of K` *vs.* $1/R_o^2$ is shown in Fig. 8.10 which is a straight line and confirms the reaction is a diffusion controlled one.

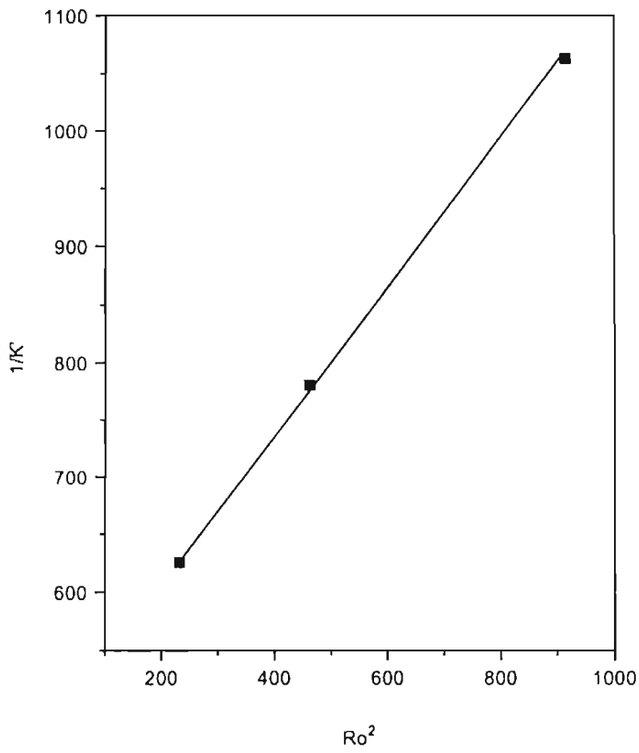

Fig.8.10 Plot of Rate constant 1/K vs R_o^2

4.8 Studies on Iron oxide

The iron hydroxide obtained after rusting with glyoxal and acetic acid was dried in an air oven at 105°C. The dried iron hydroxide was analyzed for total iron. The total iron content was found to be 56.42%. About 5 g of the dried iron oxide was dissolved in 100 ml of 5.31% HCl. Boiled well slowly to dissolve the iron oxide. Filtered through a filter paper and removed the synthetic rutile particles. Concentrated ammonia solution was then added slowly to precipitate iron as iron hydroxide. The precipitation was carried out between pH 3 and 4. Filtered through a filter paper and removed the synthetic rutile particles. The precipitate was dried in an air oven at 105°C. The XRD of iron oxide is shown in Fig. 9.1. The dried iron

hydroxide was powdered well in an agate mortar and oxidized at 800°C in a muffle furnace for half an hour. Then the purity was analysed as follows.

159.7 gms Fe_2O_3 contains 111.7 gms Fe

111.7/159.7 X x gms (Fe_2O_3)

Experiments were carried out by changing the concentration of HCl. But the purity of Fe_2O_3 was less. Only in the above explained method the maximum purity obtained was 99.3%.

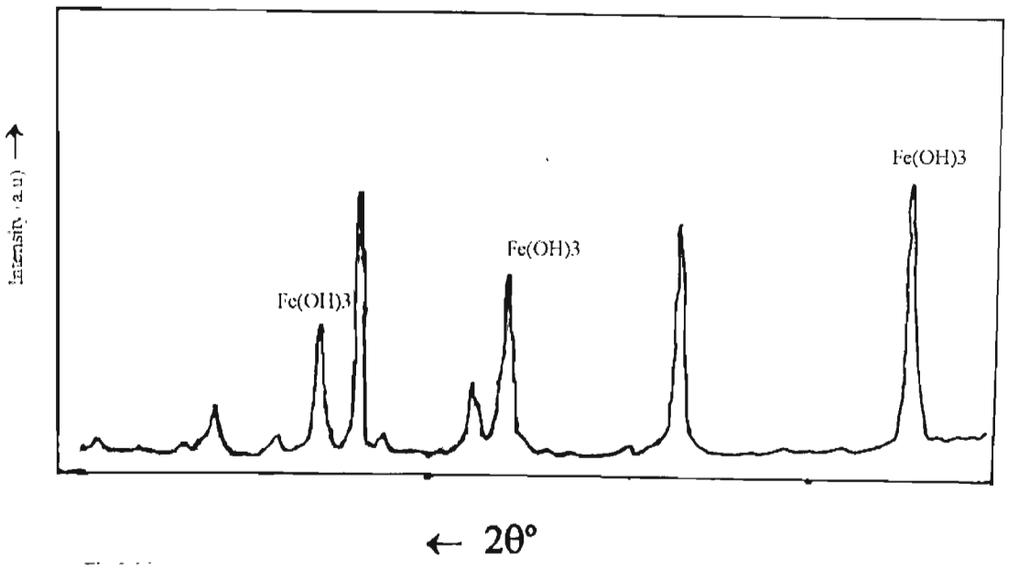

Fig. 9.1 XRD pattern of iron oxide obtained after rusting with glyoxal + acetic acid along with NH_4Cl

4.9 Conclusions

The following conclusions can be drawn from the above investigations.

- Rusting reaction is very efficient when mixture of carbonyl compounds like methanol + acetic acid, acetone + acetic acid, glyoxal + acetic acid, sucrose + acetic acid, etc added along with NH_4Cl.

- ❖ Rusting in presence of mixture of carbonyl compounds gave a product with about 93.4% TiO_2.
- ❖ The pH of the system was maintained below 4 when carbonyl compounds were added during rusting.
- ❖ Dissolved oxygen varied widely throughout the reaction.
- ❖ XRD analysis showed the removal of metallic iron phase as well as enrichment of phases like anatase, rutile and pseudo brookite.
- ❖ SEM analysis shows that the particles are highly porous like a honeycomb, which is due to the removal of iron from the particles.
- ❖ When mixture of carbonyl compounds were added during the rusting reaction the rate controlling step was diffusion control, which is proved through kinetic study.
- ❖ The activation energies calculated using mixtures of NH_4Cl + actone + acetic acid, NH_4Cl + methanol + formic acid, NH_4Cl + acetic acid, NH_4Cl + ethanol + acetic acid, NH_4Cl + glyoxal + acetic acid, NH_4Cl + acetic acid + formic acid and NH_4Cl + sucrose + acetic acid were 17.41 KJ/mol, 21.54KJ/mol, 38.29 KJ/mol, 46.22 KJ/mol, 47.87 KJ/mol, 50.38 KJ/mol and 54.23 KJ/mol respectively.

CHAPTER 5

OPTIMISATION OF REDUCTION FOR EFFICIENT RUSTING

It is very clear from the previous chapters that efficient rusting was observed when carbonyl compounds were added along with NH_4Cl during rusting. Hence it was decided to carry out investigations to find out the optimum metallisation at which maximum rusting was possible.

5.1 Reduction

Kerala ilmenite was reduced partially by carbothermically at 900, 950, 975, 1000 and 1050°C for 45 mts. The percentage metallisation obtained are given below in table 5.1

Table 5.1 Ilmenite reduced at different temperatures and their metallisation

Temperature (°C)	% Metallisation
900	10.38
950	56.87
975	64.87
1000	68.92
1050 (45mts)	75.91
1050 (4 hrs)	83.00

The ilmenite reduced at various temperatures was rusted for 5 hrs. by adding methanol + acetic acid along with NH_4Cl. The % iron removal was plotted against metallisation and it is shown in Fig. 5.1. From the plot it is very clear that optimum metallisation required for maximum iron removal was around 76%. For effective rusting the ilmenite has to be

reduced at 1050°C for 30-45 mts. and the optimum metallisation should be of above 75%.

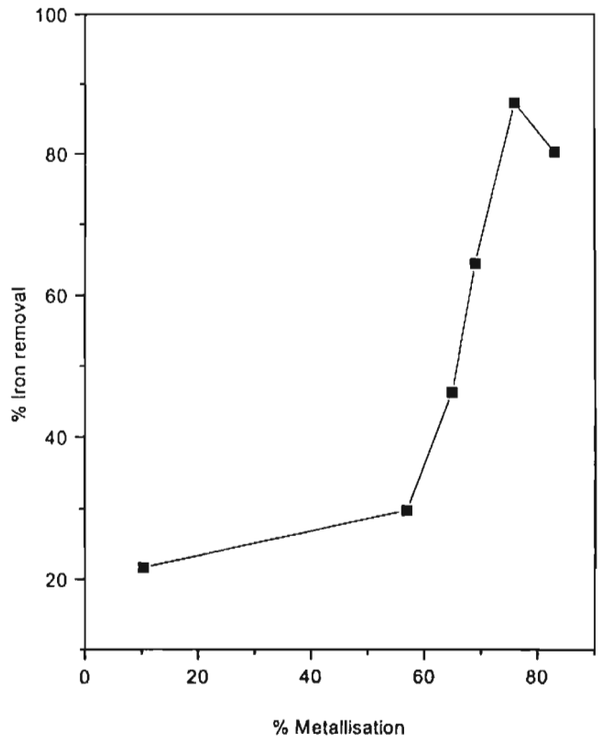

Fig. 5.1 Plot of % metallisation *vs.* iron removal

The table 5.2 shows the metallisation, % iron removal after 5 hrs and the % total iron present after 5 hrs.

% Metallisation	% Iron removal after 5 hrs	% Total iron present after 5 hrs
10.38	21.60	22.32
56.87	29.72	20.01
64.87	46.19	15.32
68.92	64.45	10.12
75.91	87.28	3.62
83.00	80.21	4.69

From the table 5.2 it is evident that 76% metallisation gave the maximum % iron removal in 5 hrs and the total iron left after 5 hrs of reaction was 3.62%. The reduced ilmenite having 76% metallisation was used for the rusting reaction throughout this series of the experiments.

5.2.1 Rusting reaction carried out by adding NH_4Cl alone

Reduced ilmenite was rusted with 1.5% (w/v) NH_4Cl solution. The results are shown in Fig. 5.2.

5.2.2 Rusting with mixtures of methanol and formic acid, methanol and acetic acid or acetone and formic acid along with NH_4Cl

The quantity of methanol added was 2% (v/v) and formic acid added was 1% (v/v) or 2% (v/v) methanol and 1% (v/v) acetic acid or 2% acetone and 1% formic acid. The results are plotted in Fig. 5.2.

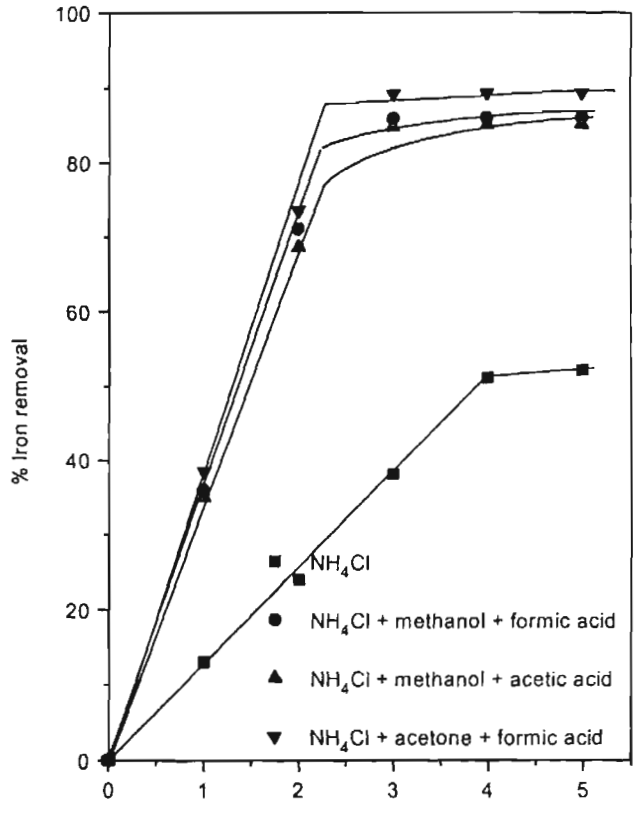

Fig. 5.2 Plot of time *vs* % iron removal

5.2.3 Discussion

When reduced ilmenite was subjected to rusting by adding NH_4Cl alone, about 50% iron removal was obtained up to 4 hrs after which the reaction became very slow and about 54% iron removal was obtained after 5 hrs.

When a mixture of methanol and formic acid was added along with NH_4Cl, the reaction was very fast. About 85% iron removal was observed in 3 hrs and then the reaction became comparatively slow since major quantities of the iron had been removed, and even after 5 hrs of rusting the amount of iron removal was only 85%.

In the case of methanol and acetic acid added along with NH_4Cl during rusting, an iron removal of more than 80% was observed in 3 hrs and then the reaction was slow reaching a value of 82% after 5 hrs of reaction.

During rusting using a mixture of acetone and formic acid along with NH_4Cl, the reaction was very fast and an iron removal of 90% was observed in 3 hrs. As major quantities of the iron were removed, there was no improvement further up to 5 hrs.

5.2.4 Rusting reaction carried out using mixture of NH_4Cl + glyoxal + formic acid, glyoxal + acetic acid + NH_4Cl or sucrose + formic acid + NH_4Cl

Rusting reaction was carried out by adding mixture of 2% (v/v) glyoxal and 1% (v/v) formic acid, 2% (v/v) glyoxal and 1% (v/v) acetic acid or 2% (w/v) sucrose and 1% (v/v) formic acid along with NH_4Cl. The % iron removal *vs.* time is plotted in Fig. 5.3.

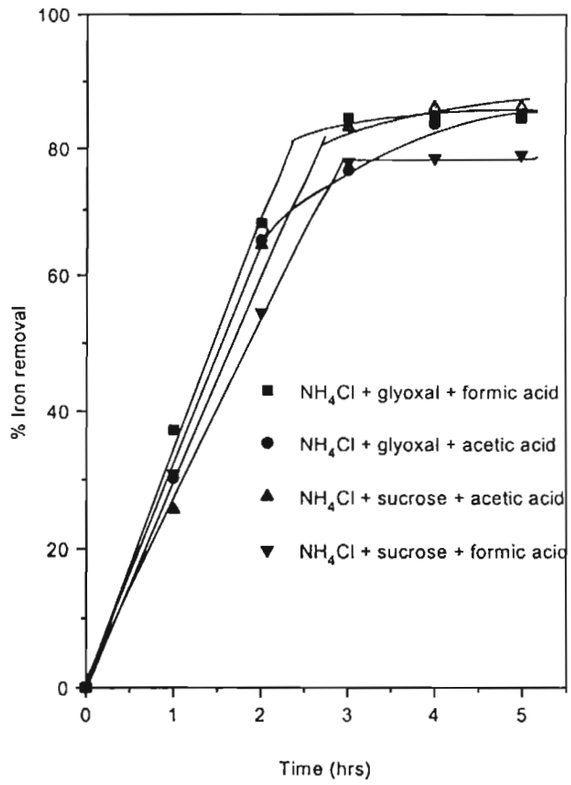

Fig. 5.3 Plot of iron removal vs. time

5.2.5 Discussion

When a mixture of glyoxal and formic acid was added along with NH_4Cl during rusting, the reaction was very fast and in 3 hrs about 85% iron removal was achieved. As major quantities of the iron were removed in 3 hrs there was not much improvement in the iron removal noticed even if the reaction was carried out further up to 5 hrs.

When a mixture of glyoxal, acetic acid and NH_4Cl were added during the rusting of partially reduced ilmenite the iron removal trend was almost similar to that of glyoxal and formic acid along with NH_4Cl. Within 3 hrs about 78% iron removal was obtained and when the reaction was continued up to 5 hrs the % iron removal was about 83%.

When rusting reaction was carried out by adding mixture of sucrose and acetic acid along with NH_4Cl, about 80% of iron removal was obtained in 3 hrs. As major quantities of the iron were removed in 3 hrs, the iron removal was slow afterwards giving a value of 88% after 5 hrs.

When a mixture of sucrose and formic acid was added along with NH_4Cl during the rusting reaction, about 75% of iron removal was obtained in 3 hrs after which the reaction was very slow giving an iron removal of 77% even after 5 hrs of rusting.

The reduced ilmenite, which was used for the rusting reaction, had a metallisation of 76%. So, the rest of the iron in the reduced ilmenite might be in the form of oxides. Also when pure reduced metal is exposed to atmosphere it easily forms metal oxide film on the surface [184]. The metallic iron on the surface of the reduced ilmenite when exposed to atmosphere will form metal oxide film. It is reported [185] that certain carbonyl compounds like aldehydes can reduce metal oxides like Ag, Cu, etc to the metal. It is not clear whether this is applicable in the case of iron oxide as it is not easy to reduce it. It is possible that these compounds can help along with the chloride ions in the removal of oxide layers from the surface, which may help the forward reaction. The maintenance of pH below 4 in all the cases when mixtures were used may also be helping the fast removal of iron from the particles. The lower pH may also help in avoiding the precipitation of the iron complexes inside the pores, which can hamper the forward reaction. In the case of NH_4Cl alone the pH goes on increasing from 4 to 6.6 during the progress of the reaction, whereas in the case of mixtures of compounds the pH was found to be below 4 throughout the reaction. Detailed investigations have shown that oxidation of the compounds to acids takes place but it was found difficult

to establish the exact mechanism by which the improvement in rusting takes place.

5.2.6 Dissolved Oxygen

The dissolved oxygen measured during the course of the reaction using NH_4Cl alone, NH_4Cl + methanol + formic acid, NH_4Cl + methanol + acetic acid, NH_4Cl + glyoxal + formic acid, NH_4Cl + glyoxal + acetic acid, NH_4Cl + sucrose + acetic acid, NH_4Cl + acetone + formic acid and NH_4Cl + sucrose + formic acid is plotted in Figs. 5.4 and 5.5 respectively.

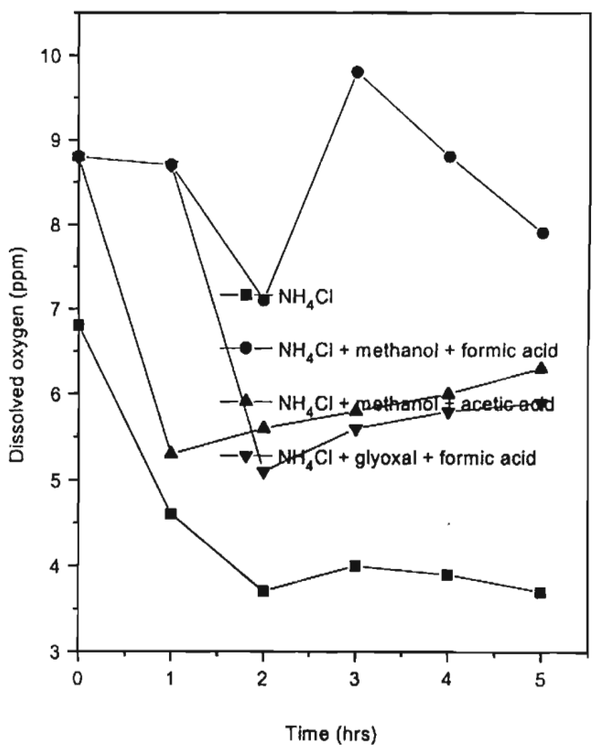

Fig. 5.4 Variation in dissolved oxygen

It is observed that the behaviour is entirely different from the system where 83% metallised ilmenite was used which is given in chapter 4. The observed values are higher in this case than the previous system. The reason for this is not obvious.

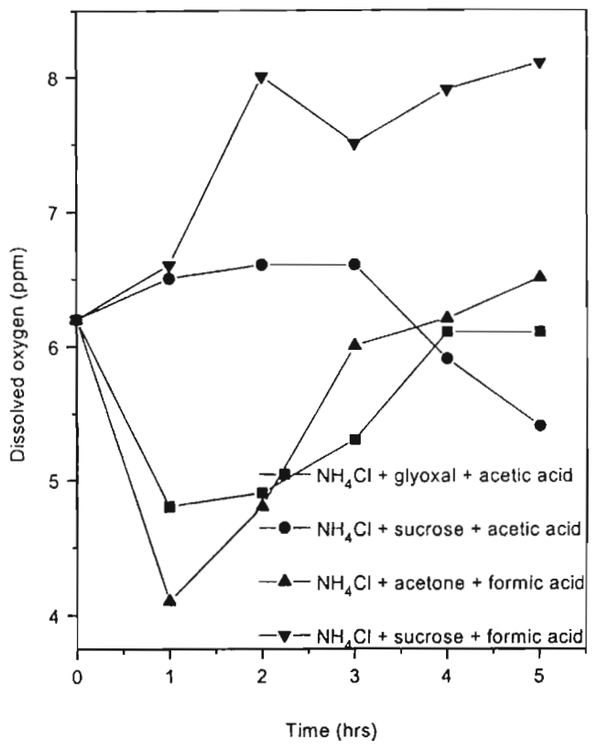

Fig. 5.5 Variation in dissolved oxygen

5.2.7 Discussion

When NH_4Cl alone was added during the rusting of reduced ilmenite, the dissolved oxygen measured initially at 0 hrs was 6.9 ppm. As the reaction proceeded after each hour the dissolved oxygen measured decreased and after 5 hrs it was 3.7 ppm.

When mixture of NH_4Cl, methanol and formic acid was added during rusting the dissolved oxygen measured initially was 8.8 ppm and in the second hour it decreased to 7 ppm, after which it increased to 9.8 ppm at 3 hrs and then decreased to 8 ppm in 5 hrs. In practice it was observed that almost 90% of total iron was removed in 3 hrs.

When mixture of NH_4Cl, methanol and acetic acid was added during rusting reaction, initially the measured oxygen was 8.8 ppm. After the reaction for one hour the measured dissolved oxygen was 5.2 ppm, which increased to 6.5 ppm in 5 hrs. Here also more than 90% iron removal was obtained within 3 hrs. There was no definite trend in the dissolved oxygen so as to make a definite conclusion.

When mixture of NH_4Cl, glyoxal and formic acid was added during rusting of reduced ilmenite the behaviour trend of dissolved oxygen was similar to that of the mixture of NH_4Cl, methanol and acetic acid. In this combination also about 90% iron removal was obtained in 3 hrs.

5.2.8 Variation in pH

The pH of the system was measured during the rusting of reduced ilmenite. The pH values obtained were plotted as a function of time, which is shown in Figs. 5.6 and 5.7 respectively. In the case of pH also the system behaves differently from that described in chapter 4 where 83% metallised ilmenite was used.

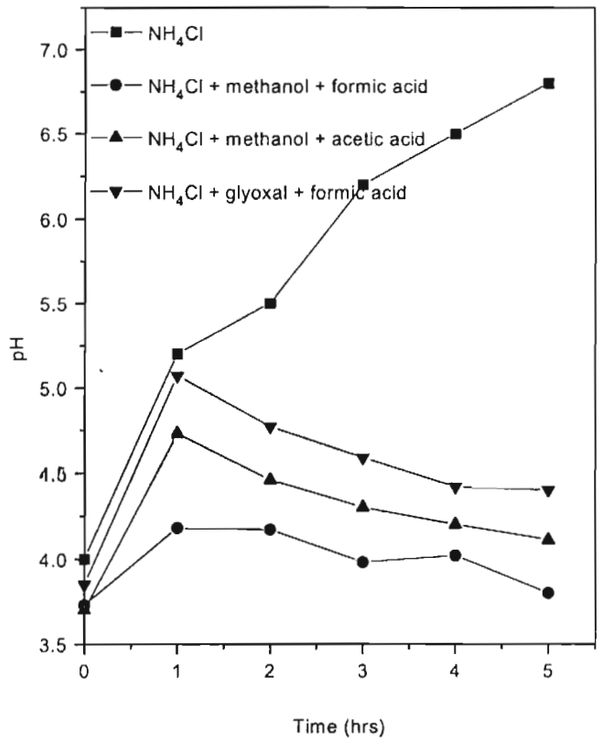

Fig. 5.6 Variation in pH

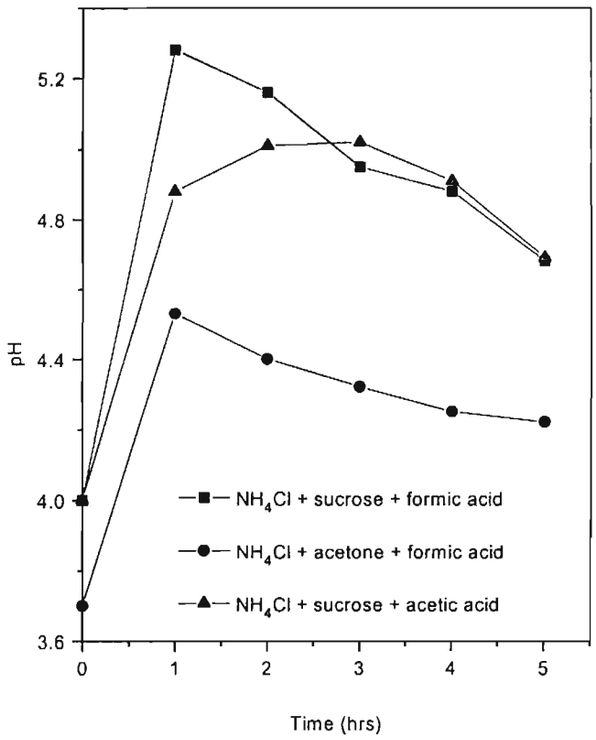

Fig. 5.7 Variation in pH

5.2.9 Discussion

When NH_4Cl alone was added during the rusting reaction, even though the pH was adjusted to 4 using con. HCl, the pH increased to 5.2, 5.4, 6.2, 6.4 and 6.6 as the reaction proceeded. While with mixtures of NH_4Cl and carbonyl compounds the initial pH itself was less then 4. A change in pH was observed throughout the whole reaction. Most of the time the pH was less than 4. This may be due to the oxidation of carbonyl compounds as the reaction proceeded. The rusting rate is also very high when the pH is maintained below 4.

5.3 Surface Area Measurments

The surface area measurment results of reduced ilmenite and rusted ilmenite are given in table 5.3

Table 5.3 Surface area measurements of reduced ilmenite and synthetic rutile

Name of the sample	Surface area (sq.m/ gm) using 76% metallised ilmenite	Surface area (sq.m/ gm) using 83% metallised ilmenite
Partially reduced ilmenite	2.3597	2.8757
Synthetic rutile with NH_4Cl + methanol + acetic acid	2.4742	3.2462
Synthetic rutile with NH_4Cl + sucrose + formic acid	3.1433	3.157
Synthetic rutile with NH_4Cl + acetone + formic acid	2.4824	3.2622

The 76% reduced ilmenite had a surface area of 2.3597 sq.m/ gm. As the rusting reaction proceeded the surface area increased slightly. the The synthetic rutile obtained with NH_4Cl + methanol or acetone + acetic acid or formic acid had a surface area of 2.4742 and 2.4824 sq.m/gm. When these compounds were used during the rusting reaction the reduced ilmenite grains did not crumble whereas the removal of reduced iron from the grains were observed. The values show that during rusting the increase in surface area is not much, which could be due to the fact that the particles keep their shape and size and there is no crumbling of the particles. The slight increase observed may be due to increase in porosity

due to removal of iron from the particles. In the case of formic acid and sucrose system there is a similarity in behaviour while in the case of other compounds the surface area are higher when 83% reduced ilmenite is used where corresponding iron removal was less. Crumbling of the particles may be one reason for this. The SEM and optical microscopic studies clearly reveals the nature of the particles after the iron was removed from the grains.

5.4 X – ray diffraction studies

XRD studies were carried out for partially reduced ilmenite, synthetic rutile obtained on rusting with NH_4Cl + methanol + acetic acid and NH_4Cl + acetone + formic acid. The XRD graphs are given in Figs 5.8, 5.9, 5.10 and 5.11. The XRD data shows that there is some structural difference with the 83% reduced and rusted materials, which is given in chapter 3. In 83% metallised ilmenite pseudo brookite was present where as in 76% reduced and rusted ilmenite pseudo rutile was prominent. The major phases observed in the partially reduced ilmenite was metallic iron, anatase, rutile, ilmenite and pseudo rutile. On analyzing the XRDs of synthetic rutile obtained by rusting with NH_4Cl + methanol + acetic acid or NH_4Cl + acetone + formic acid, the metallic iron peak has diminished and has no significance. But the peaks corresponding to anatase, rutile and pseudo rutile are predominant which confirms the enrichment of TiO_2. The metallic iron peak is usually observed at the 'd' value of 2.02. The growth of rutile peak at a 'd' value of 3.23 and anatase at a 'd' value of 3.48 confirms the enrichment in TiO_2.

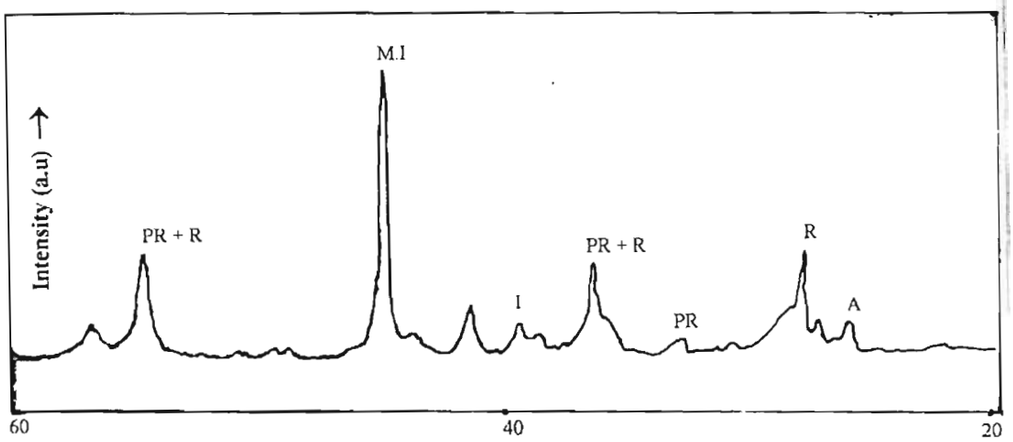

Fig. 5.8 Reduced ilmenite having 76% metallisation (M.I. - Metallic iron, A - Anatase, PR - Pseudo rutile, R - Rutile, I - Ilmenite)

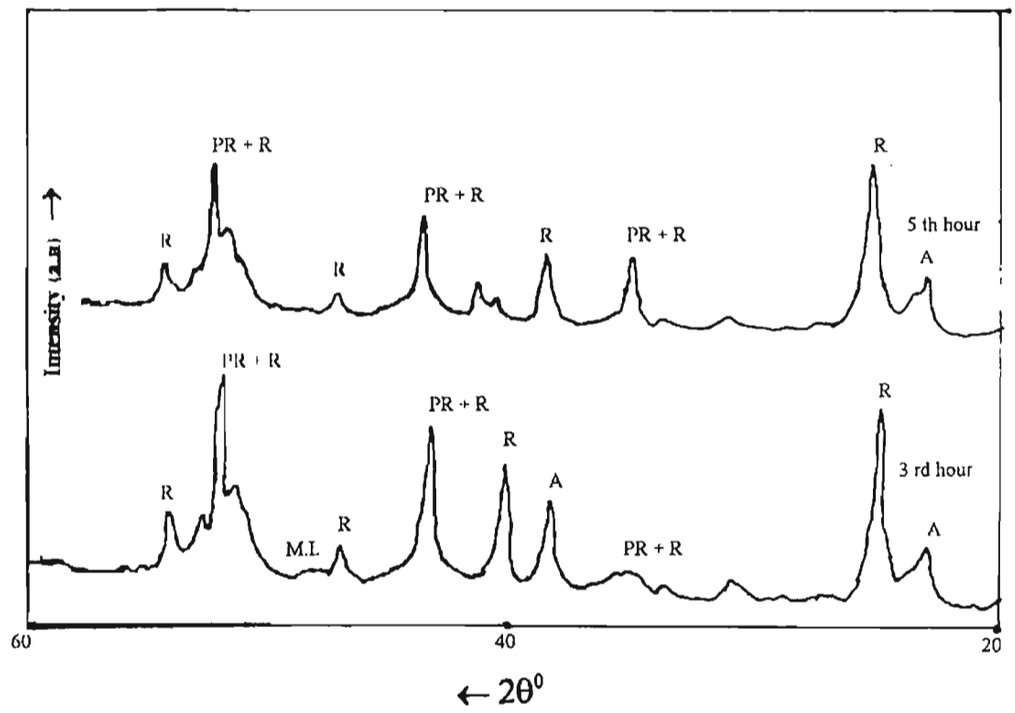

Fig. 5.9 XRD pattern of synthetic rutile obtained by rusting with Methanol + acetic acid along with NH4Cl (A - Anatase, R - Rutile, PR - Pseudo rutile, M.I. - Metallic iron)

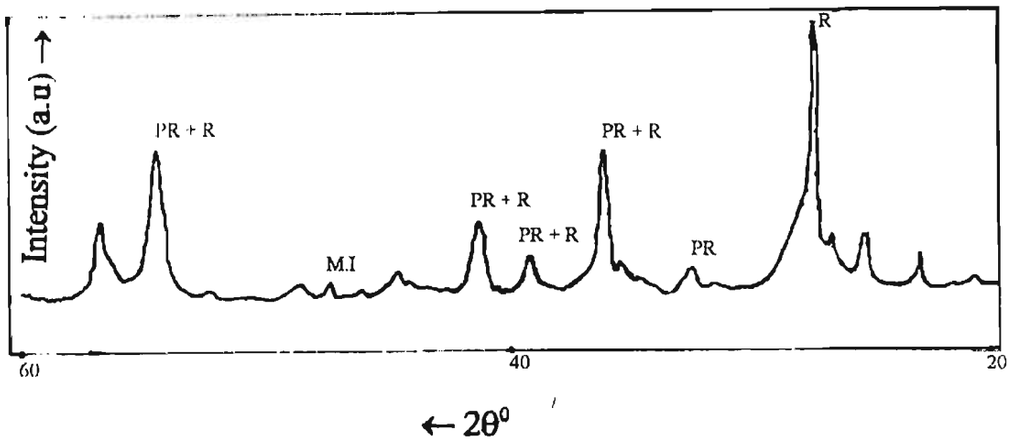

Fig. 5.10 XRD of synthetic rutile obtained by rusting with NH4Cl + sucrose + formic acid (A - Anatase, R - Rutile, PR - Pseudo rutile, M.I. - Metallic Iron)

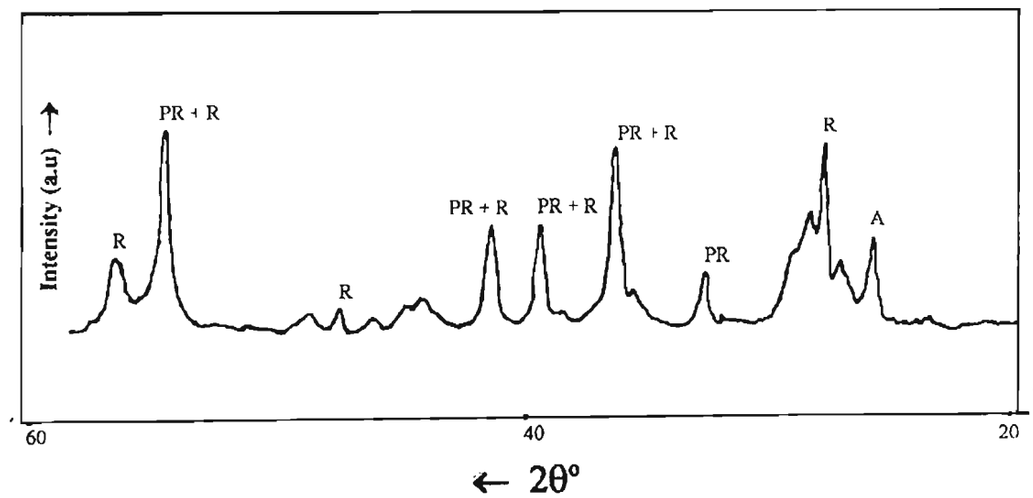

Fig. 5.11 XRD of synthetic rutile obtained by rusting with mixture of acetone + formic acid along with NH4Cl (A - Anatase, R - Rutile, PR - Pseudo rutile)

5.5 Scanning Electron Microscopy

The SEM micrograph of reduced ilmenite and synthetic rutile obtained by adding mixture of carbonyl compounds along with NH_4Cl are shown in Figs 5.12, 5.13 5.14, 5.15 and 5.16 respectively. The

morphological aspect of partially reduced ilmenite is quite interesting. The iron oxide present, in the ilmenite particles on account of reduction, blooms out, in the form of an attractive sunflower or rose buds. The morphology of synthetic rutile appears like separated sheet like structures. The metallic iron present between the cavities got removed as a result of rusting and sheet like structures are formed. This may be due to the fact that sintering has not taken place as the ilmenite was heated for lesser time (45 mts) and the reduction was partial. On heating for longer time the structure may change due to sintering as observed in the case of maximum reduced samples.

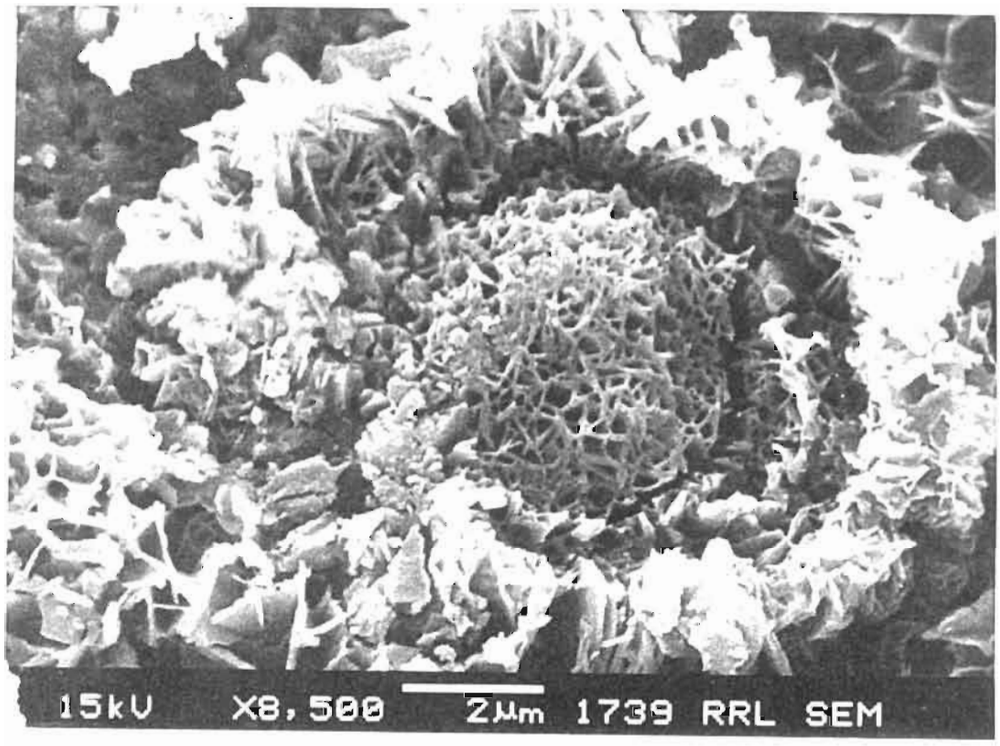

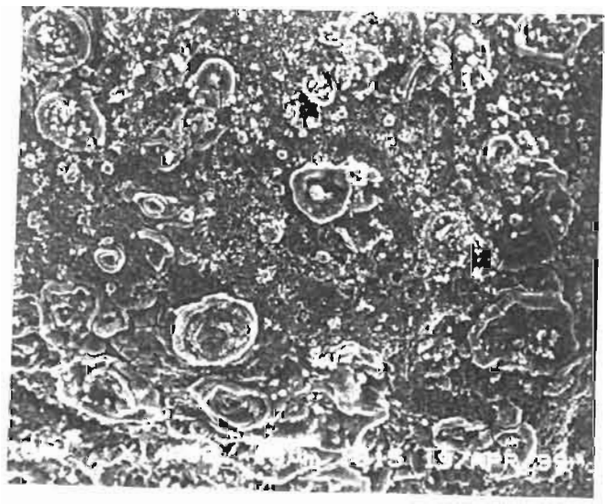

Fig. 5.12 SEM photograph of Reduced ilmenite having 76% metallisation

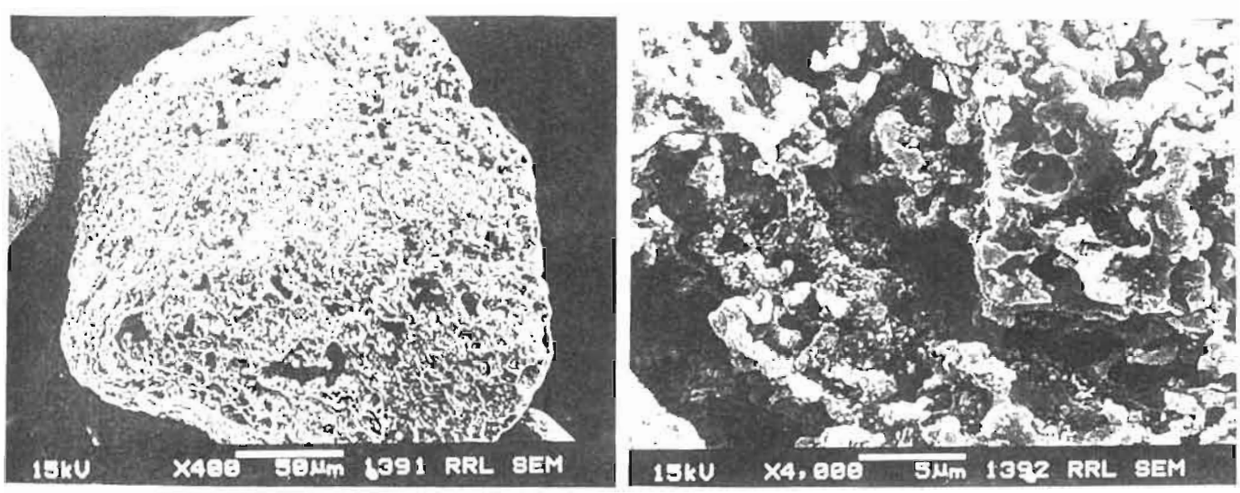

(a)

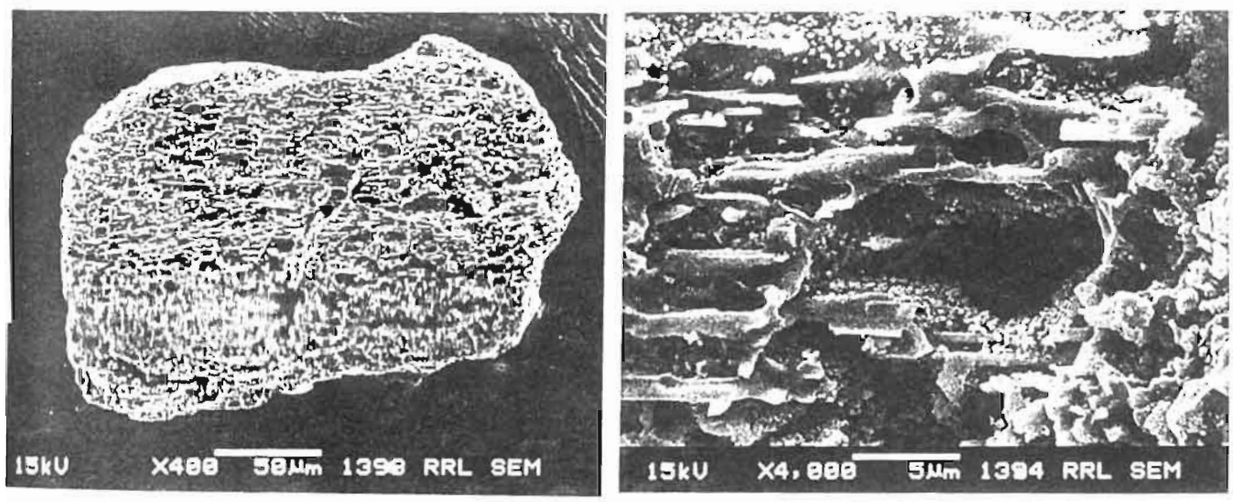

(b)

Fig. 5.13 SEM photograph of synthetic rutile obtained by rusting with (a) NH_4Cl + acetone + formic acid (b) NH_4Cl + glucose + acetic acid

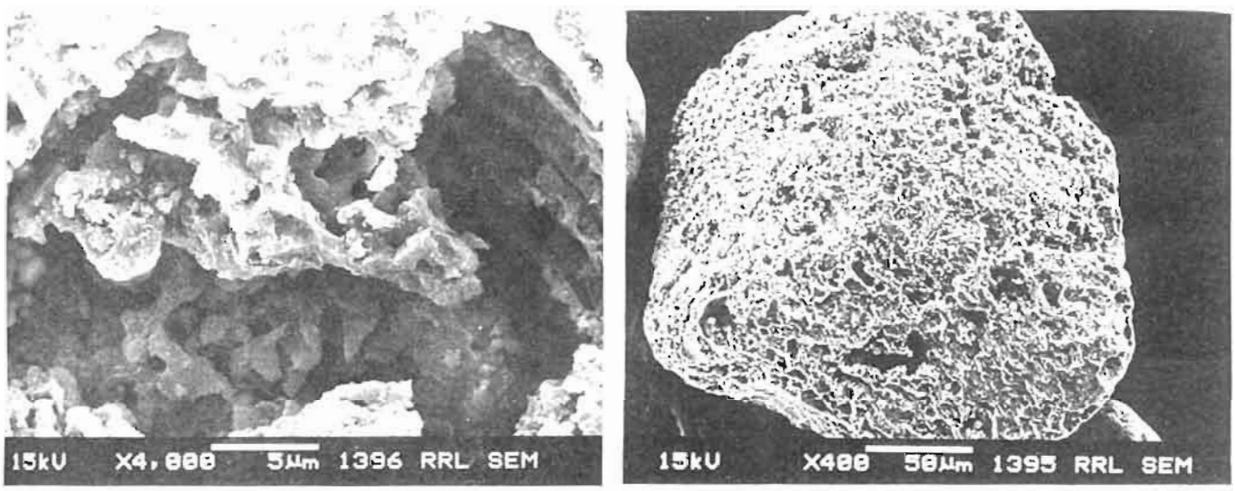

(a)

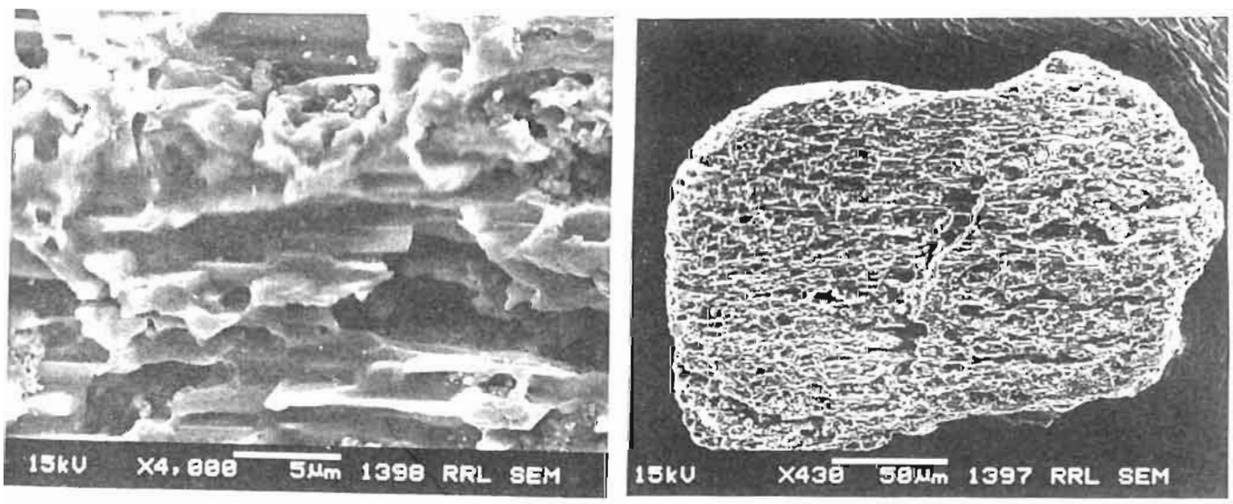

(b)

Fig. 5.14 SEM photograph of synthetic rutile obtained by rusting with
(a) NH_4Cl + sucrose + formic acid (b) NH_4Cl + methanol + formic acid

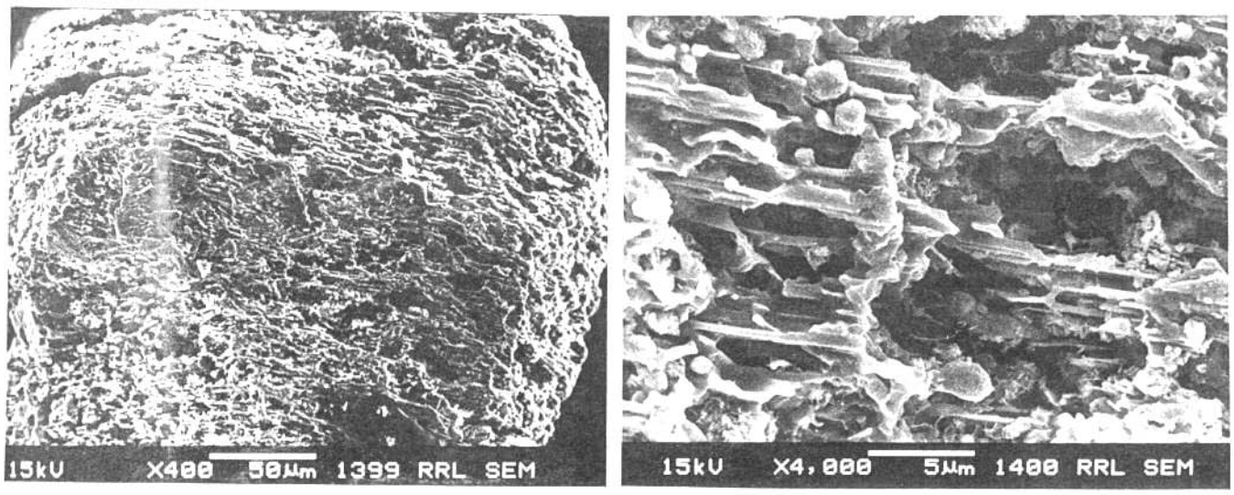

(a)

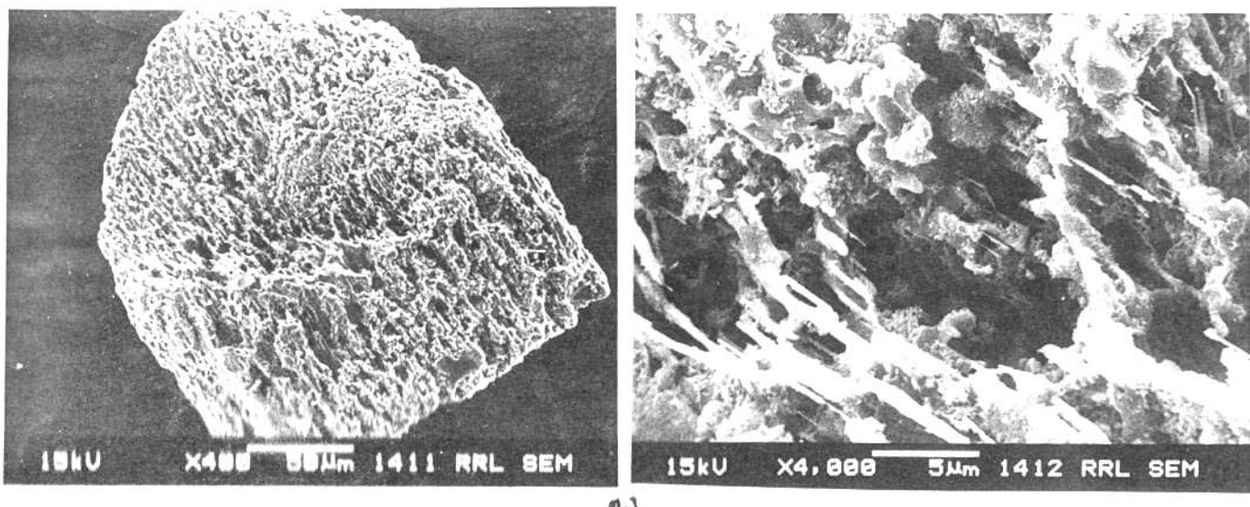

(b)

Fig. 5.15 SEM photograph of synthetic rutile obtained by rusting with
(a) NH_4Cl + methanol + acetic acid (b) NH_4Cl + acetone + acetic acid

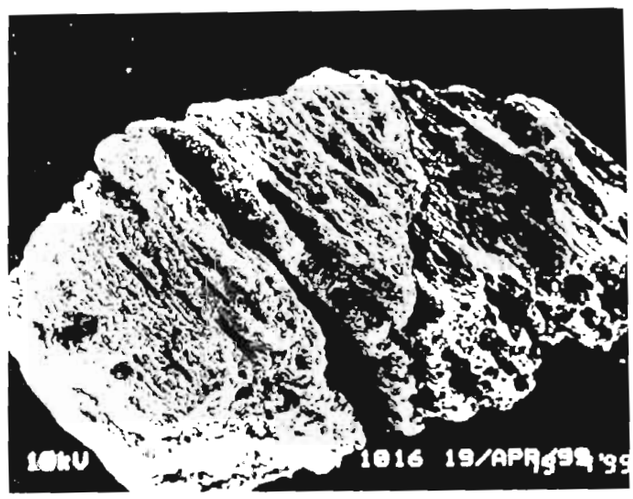

Fig. 5.16 SEM photograph of synthetic rutile obtained by rusting with NH_4Cl + glyoxal + acetic acid

5.6 Optical Microscopic Studies

Characterization of internal structure was carried out through optical microscopic studies. The micrographs obtained from optical microscopic studies are shown in Figs 5.17, 5.18, 5.19, 5.20 and 5.21 respectively. The bright and shinning area is the metallic iron deposited as a result of reduction. The white or grayish white areas, which are not shinning are due to oxides of titanium. It is clear from the optical photographs that the iron oxide present in the ilmenite particles gets reduced at 1050°C and forms a channel across the grains. As iron is removed, on rusting the channels are more porous and prominent.

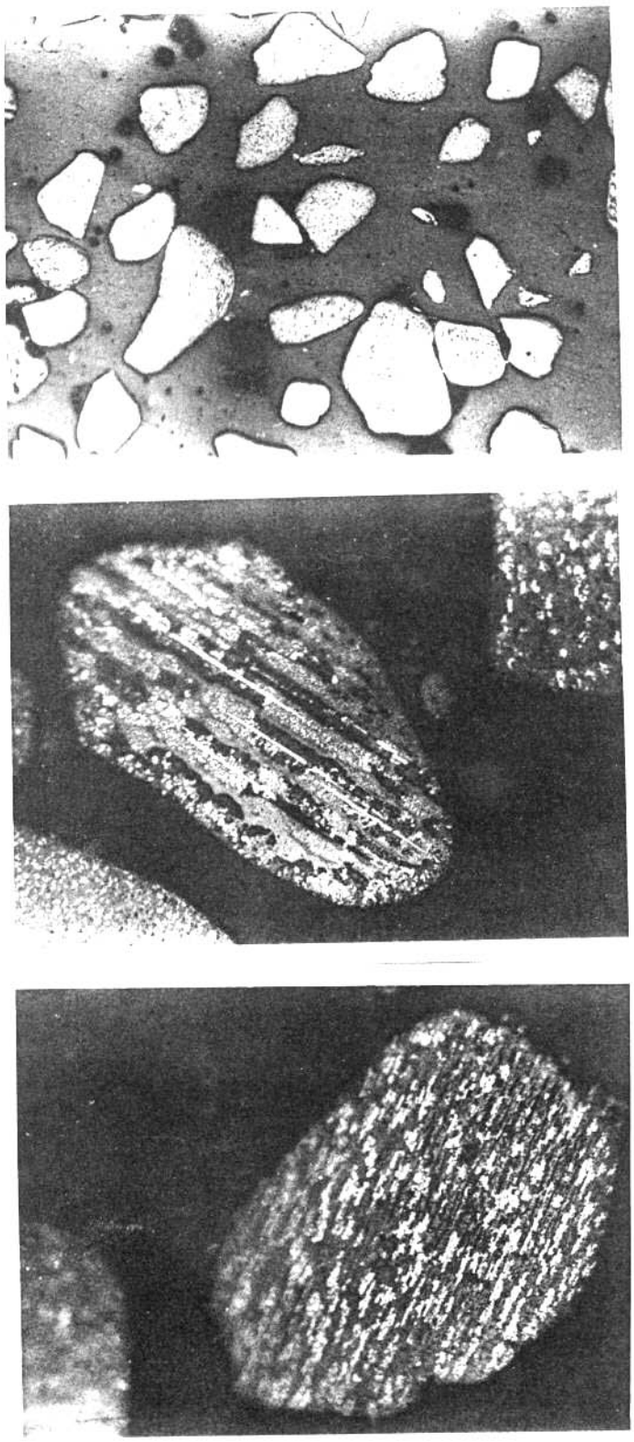

Fig. 5.17 Reduced Ilmenite having 76% metallisation

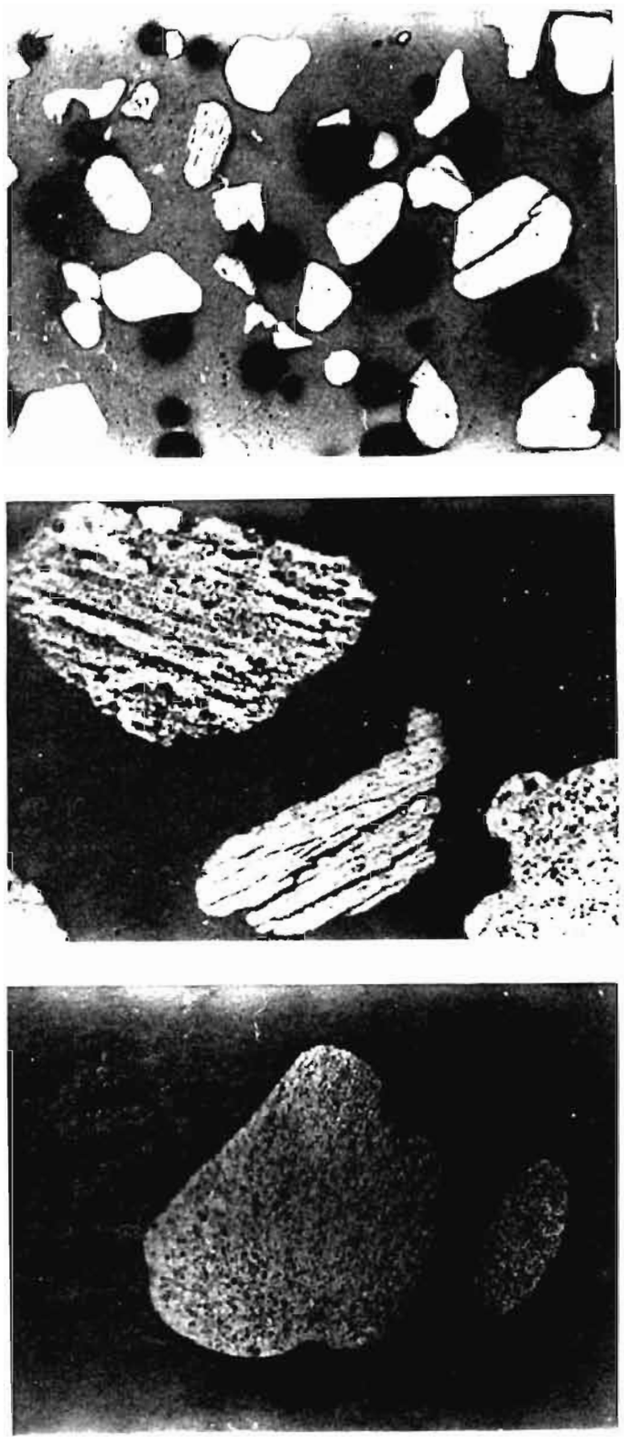

Fig. 5.18 Synthetic rutile obtained by rusting with NH_4Cl + methanol + acetic acid

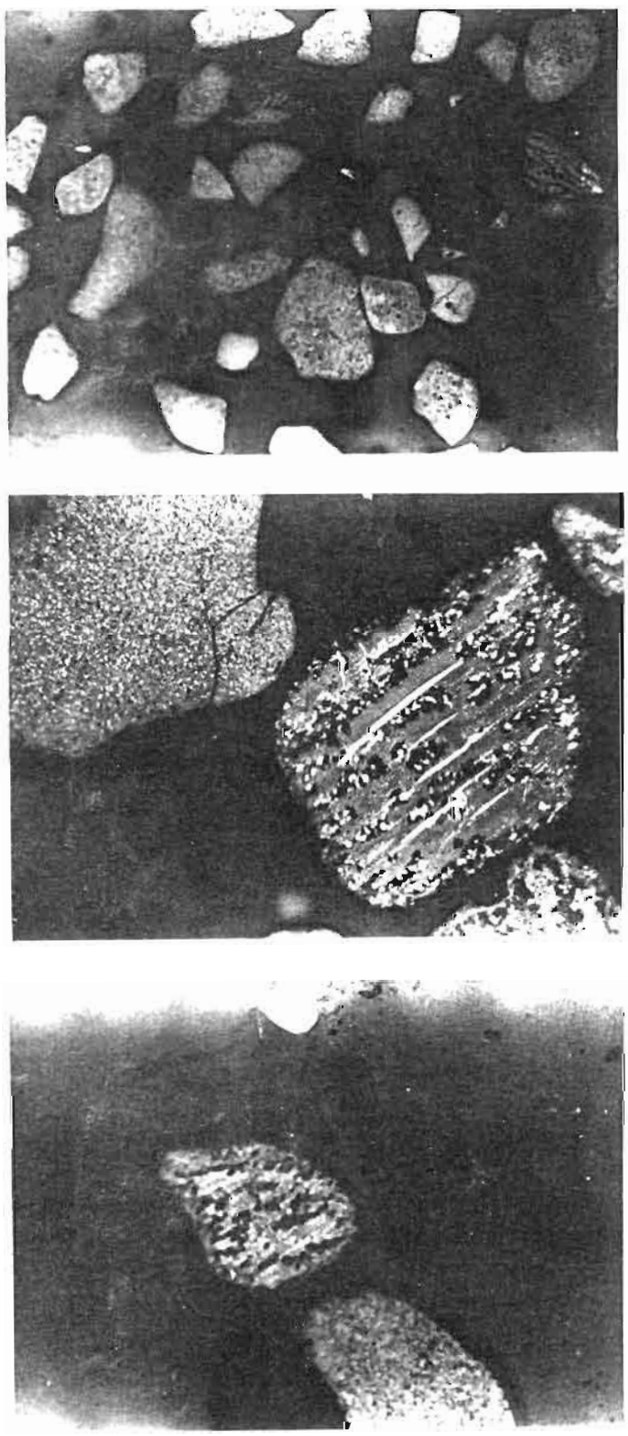

Fig. 5.19 Synthetic rutile obtained by rusting with NH_4Cl + sucrose + formic acid

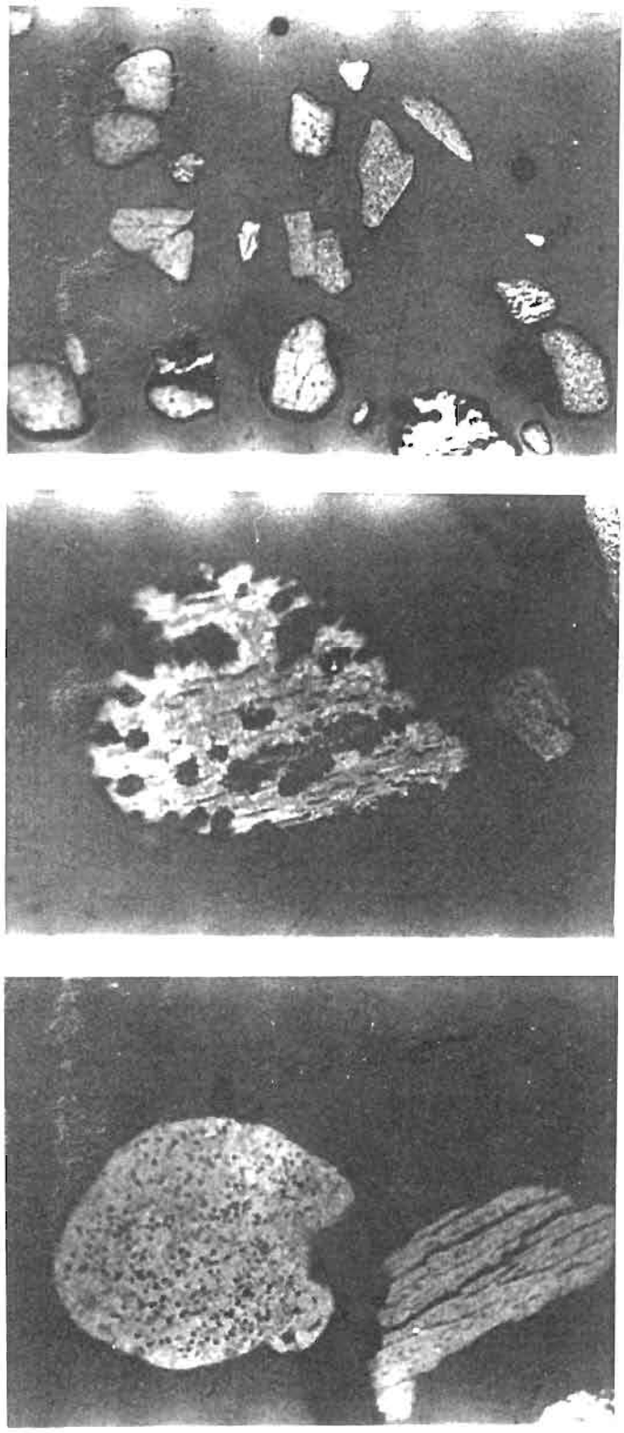

Fig. 5.20 Synthetic rutile obtained by rusting with NH_4Cl + acetone + formic acid

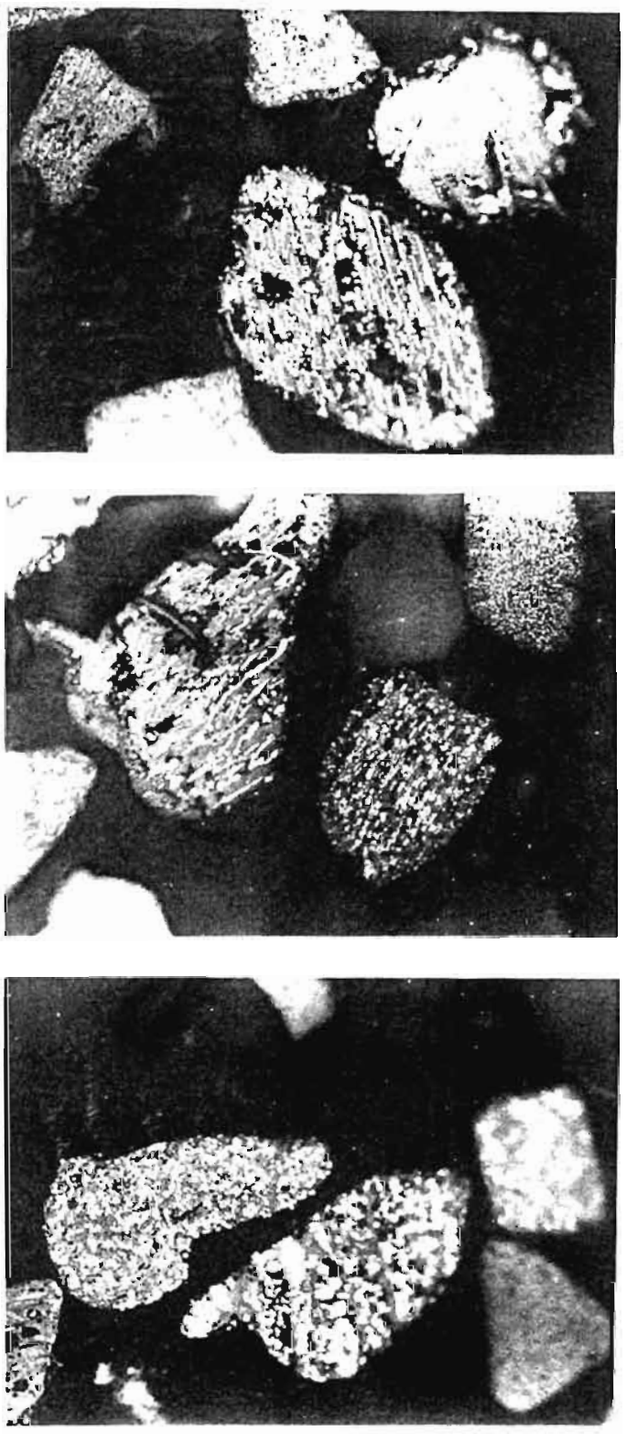

Fig. 5.21 Reduced ilmenite having 58% metallisation

5.7 Trace elements

The trace elements present in the reduced ilmenite and rusted ilmenite were analysed. In reduced ilmenite the $\%Cr_2O_3$ present was 0.1286 and %MnO present was 0.3120. In rusted ilmenite obtained by rusting with NH_4Cl + ethyl alcohol + acetic acid, the %Cr2O3 present was 0.1168 and % MnO present was 0.2049. It was observed that very small quantities of trace elements were also removed due to rusting.

5.8 Conclusions

The following conclusions can be arrived at from the above studies.

- Optimum metallisation required for efficient iron removal using carbonyl compounds as catalysts is around 76%.
- The non-sintering of the particles may be helpful for the fast removal of iron.
- When mixture of NH_4Cl + methanol + formic acid or NH_4Cl + methanol + acetic acid or NH_4Cl + acetone + formic acid or NH_4Cl + acetone + acetic acid were used the iron removal was very efficient giving a TiO_2 content of 96.7% in 3 hrs.
- When organic compounds are used for rusting the pH was found to remain below 4 throughout the reaction, which also may be assisting the fast removal of iron.
- The behaviour of the system in terms of dissolved oxygen, pH, structure and surface area were different from the one where 83% metallised ilmenite was used.

CHAPTER 6

DEVELOPMENT OF A STRUCTURAL MODEL FOR RUSTING REACTIONS CARRIED OUT USING REDUCED ILMENITE

In order to evaluate the mechanism for the rusting reaction carried out at optimised reduction conditions a structural model has been developed. The experimental values were tested with the values obtained through modelling.

6.1 Development of a Structural Model

A structural model was developed for the above reaction

6.2 Reactions in which a product layer is formed

The modeling of the reaction was carried out as follows.

$$A(fluid) + bB(solid) \rightarrow cC(fluid) + dD(solid)$$

In a porous solid the reaction occurs in a diffuse zone rather than a sharp interface. Let us assume the porous solid to be an aggregate of fine grains having the shape of spheres. There is a gradual change in conversion of solid over the pellet. The external layer will be completely reacted first and the thickness of the completely reacted layer will grow towards the interior of the porous solid.

When pore diffusion is fast compared with the rate of chemical reaction, the concentration of fluid is uniform throughout the pellet and the reaction

occurs at a uniform rate. If chemical kinetics is much faster than the rate of diffusion the reaction occurs in a narrow region between the unreacted and the completely reacted zones. We have formulated equations including both chemical kinetics and diffusion and derived the criteria for asymptotic regimes where a particular step controls the overall rate. The explanations and steps for modelling are as given below is in line with the work reported by Sohn and Szekely [186-189].

6.3 Mathematical formulation

Let us consider a porous pellet of volume Vp and of superficial area A, made up of individual particles (grains) having volume and surface area Vg and Ag respectively. The shape of the grains as well as the pellet is considered as spheres.

It is assumed that the solid pellet, which is an agglomeration of spherical grains, reacts with air in presence catalysts irrversibly.

A(gas + catalysts) + bB(solid) $\rightarrow$ Products

The additional assumptions are also made as

1. The pseudo-steady state approximation is valid for determining the concentration profile of the fluid reactant within the pellet.[190,191]
2. The resistance due to external mass transfer is negligible.

3. Intrapellet diffusion is either equimolar counter diffusion or occurs at low concentrations of diffusing species.
4. Diffusivities are constant throughout the pellet.
5. Diffusion throughout the product layer around the individual grains is not rate limiting.
6. The solid structure is macroscopically uniform and is unaffected by the reaction.

6.4 The assumptions

Assumption (1) is acceptable for gas solid system [192,193]. Ishida and Wen [194] have shown that external mass transfer is negligible if the pellet Sherwood number, kmR_0/De is greater than 100. The assumptions [3,4 and 6] are thought to be the problems of practical interest. It is safe to neglect the effect of diffusion through the product layer, because of small size of grains.

The conservation of fluid reaction is represented as

$$De\nabla^2 C_A - \upsilon_A = 0 \quad \text{----------[1]}$$

Where De is the effective diffusion co-efficient within the porous medium, CA is the reactant concentration and υA is the local rate of consumption of A

Within each grain, the conservation of solid reactant may be described as

$$-\rho_B \frac{\delta r_c}{\delta t} = bkC_A \quad \text{----------[2]}$$

Where ρ_B is the density of reduced ilmenite, r is the distance co-ordinate perpendicular to the moving reaction front, b is the stoichiometric factor and k is the reaction rate constant.

An expression for υA may be obtained by determining the surface area for reaction available per unit volume of the pellet.

$$\upsilon_A = \alpha_\beta \left(\frac{Ag}{Vg}\right) \left(\frac{Agr_c}{FgVg}\right)^{Fg-1} \quad \text{----------[3]}$$

where α_β is the volume fraction of the pellet occupied by solid B

Ag is the external surface of an individual grain

Vg is the volume of the grain

Fg is the shape factor

Shape factor for sphers is 3

Equation [1] and [2] can be expressed in dimensionless form for introducing dimensionless variables.

$$\Psi \equiv \frac{C_A}{C_{AB}} \quad \text{----------[4]}$$

$$\xi \equiv \frac{Agr_c}{FgVg} = \frac{r_c}{r_g} \quad \text{----------[5]}$$

$$t^* \equiv \left(\frac{bkC_{AB}Ag}{\rho_B FgVg}\right)t \quad \text{----------[6]}$$

$$\eta \equiv \frac{A_p R}{F_p V_p} = \frac{R}{R_p} \qquad \text{----------[7]}$$

$$\sigma \equiv \frac{F_p V_p}{A_p}\left(\frac{\alpha_\beta k A_g}{D_e V_g}\right)^{1/2} \qquad \text{----------[8]}$$

t is the total time of reaction

Fp Shape factor of the pellet ie 3

Ap external surface area of the pellet

($4\Pi r2 = 1$ already assumed)

Vp Volume of the pellet

R is the distance from the centre of symmetry in the pellet

The dimensionless form of equation [1] and [2] is

$$\nabla^{*2}\Psi - \sigma^2 \Psi \xi^{F_g - 1} = 0 \qquad \text{----------[9]}$$

$$\frac{\delta \xi}{\delta t^*} = -\Psi \qquad \text{----------[10]}$$

where $\nabla*$ is the Laplacian operator with η as the position co-ordinate.

The initial boundary conditions for equations [9] and [10] are

$$\xi = 1 \quad \text{at } t^* = 0 \qquad \text{----------[11]}$$

$$\Psi = 1 \quad \text{at } \eta = 1 \qquad \text{----------[12]}$$

$$\frac{\delta \Psi}{\delta \eta} = 0 \quad \text{at } \eta = 0 \qquad \text{----------[13]}$$

η is the length co-ordinate in ∇ operator [13].

In terms of the parameters used in the formulation the overall extent of the reaction is defined as

$$X = \int \frac{\eta^{F_p-1}(1-\xi^{F_g})\delta\eta}{\eta^{F_p-1}\delta\eta} \qquad \text{----------[14]}$$

The dimensionless representation governing equation shows the dependent variables ξ and Ψ are related to t* and η and the single parameter which appears in the formulation as σ.

The quanity of σ incorporates both structural and kinetic parameters.

6.5 Asymptotic Behaviour

(i) <u>When σ approaches zero</u>, the overall rate is controlled by chemical kinetics, and diffusion within the pellet is rapid compared with the rate of the chemical reaction. Further ξ is independent of η, although still a function t*. Under these conditions equation [10] is readily integrated to obtain

$$\xi = 1 - t^* \qquad \text{for } 0 \le t^* \le 1$$
$$\text{and} \quad \xi = 1 \qquad \text{for } t^* \ge \qquad \text{----------[15]}$$

Using equation [14] we get relationship between X and t*

$$t^* = 1 - (1-X)^{1/Fg} \equiv gFg(X) \qquad \text{----------[16]}$$

gFg(X) refers to the value of t* within asymptotic regime where $\sigma \rightarrow 0$. From experimental data it is understood that diffusion within the pellet was not rate controlling.

(ii) When σ approaches infinity

The overall rate is controlled by the diffusion of the gaseous reactant within the pellet. This corresponds to the shrinking core model.

$$P_{Fp}(X) = \frac{2F_p bDeC_{AB}}{\alpha_\beta \rho_B}\left(\frac{A_p}{F_p V_p}\right)^2 t \qquad \text{----------[17]}$$

$$= \frac{2F_g F_p}{\sigma^2} t^* = \frac{t^*}{\sigma^{\wedge 2}} \qquad \text{----------[18]}$$

where $\sigma^{\wedge 2} = \frac{\sigma^2}{2F_g F_p}$

Equation [17] provides a convenient means of determining the effective diffusivity by plotting experimental data obtained under diffusion control.

$$\sigma^{\wedge} = \frac{\sigma}{(2F_g F_p)^{1/2}} = \frac{V_p}{A_p}\left[\frac{\alpha_\beta kFp}{2De}\left(\frac{Ag}{FgVg}\right)\right]^{1/2} \qquad \text{-------[19]}$$

6.6 Analytical Solutions

Equation [16] and [18] correspond to asymptotic solutions for pure chemical control and pure diffusion control respectively.

Since the grains are spherical Fg =3 equation [9] becomes

$$\left(\frac{\delta^2}{\delta\eta^2} - \sigma\xi^2\right)\Psi = 0 \qquad \text{----------[9a]}$$

$$\Psi = \frac{\cosh(\sigma\xi\eta)}{\cosh(\sigma\xi)} \qquad \text{----------[20]}$$

$$\frac{\delta\xi}{\delta t^*} = -\Psi \qquad \text{----------[10]}$$

$$\xi = \frac{1-\cosh(\sigma\xi\eta)}{\cosh(\sigma\xi)} t^* \qquad \text{----------[21]}$$

The time required to achieve the complete reaction of the pellet is

$$t^*_{x=1} = 1+\sigma^{\wedge 2} \qquad \text{----------[22]}$$

The rate of reaction is independent of the solid reactant concentration.

The reaction of a porous solid with a fluid involves chemical reaction and intrapellet diffusion occurring in parallel. The grain model is the recent development in this area. The models have been tested against experiments and found to describe the reaction of porous solids reasonably well. A computer program was written for the above model.

The experimental values obtained were tested with the equations obtained through the development of structural model and was verified by plotting in the graphs. Figs. 6.1, 6.2 and 6.3 show, that the structural model goes in hand with the experimental value.

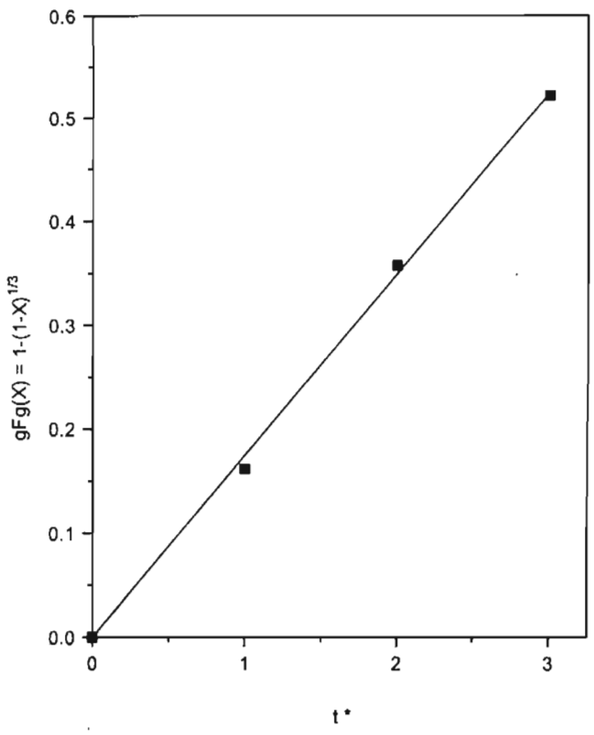

Fig. 6.1 Conversion function *vs.* reduced time for small values of σ

The straight line obtained on plotting t* *vs.* $gFg(X) = 1-(1-X)^{1/3}$ proves that the reaction is controlled by surface chemical or topochemical.

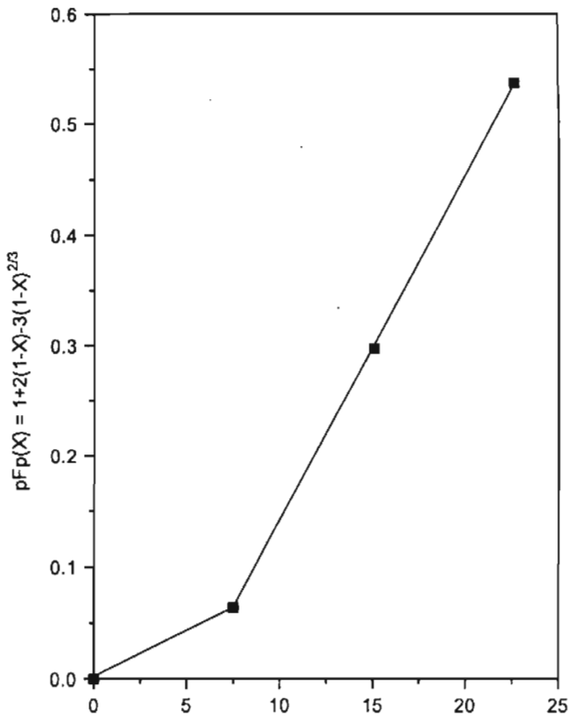

Fig. 6.2 Conversion function vs. reduced time for large values of σ

The graph obtained on plotting $t^*/\sigma^{\wedge 2}$ *vs.* $pFp(X) = 1+2(1-X)-3(1-X)^{2/3}$ is an evident of the diffusion controlled reaction. There is good agreement between the model developed and the experimental data, which shows that the model developed is correct and suitable.

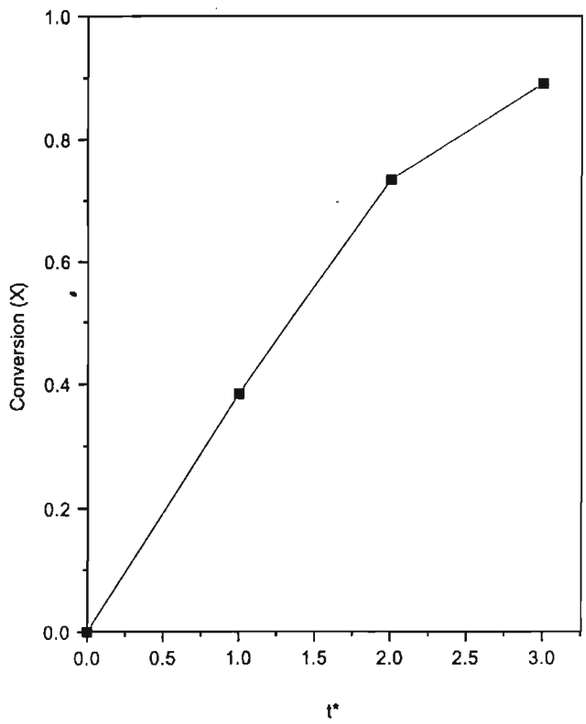

Fig. 6.3 Comparison of approximate solution with exact solution

The graph obtained by plotting t* *vs.* conversion (X) is also the same which we expect from the theoretical data.

6.7 Conclusion

The following conclusions can be arrived from the modeling studies

- ❖ The pellet grain model is a suitable model for the solid ilmenite and gas reactions.

- ❖ When σ approaches to 0, the overall rate is controlled by chemical kinetics, and diffusion within the pellet is rapid compared with the rate of the chemical reaction.
- ❖ When σ approaches to infinity, the overall rate is controlled by the diffusion of the gaseous reactant within the pellet.
- ❖ Analytical solutions were calculated for a pure chemical control and pure diffusion control.
- ❖ The rate of reaction is independent of the solid reaction concentration.
- ❖ All the plots obtained were in good agreement with the theoretical data.

6.8 Computer program

```
#include<iostream.h>
#include<stdio.h>
#include<conio.h>
#include<dos.h>
#include<string.h>
#include<graphics.h>

float P[4],xco,yco;
float x,y;
float xinc,yinc;
int gd=DETECT,gm;
char choice,chk,alt;

void calcvalue(void);
void convx(void);
void convx(void);
void surfchem(void);
void diffcon(void);

void main(void)
{
 initgraph(&gd,&gm,"c:\\tc\\bgi");
 x=getmaxx();
```

```
 y=getmaxy();
 do{
    clrscr();
    cleardevice();
    cout<<"\n Enter a choice";
    cout<<"\n Enter   1 : Calculation of values";
    cout<<"\n         2 : Conversion X Graph   ";
    cout<<"\n         3 : Surface Chemical Concentration Graph";
    cout<<"\n         4 : Diffusion Controlled Graph";
 choice=getch();
 cleardevice();
 switch(choice)
       {
        case '1' : calcvalue();
                   break;
        case '2' : convx();
                   break;
        case '3' : surfchem();
                   break;
        case '4' : diffcon();
                   break;
        default  : calcvalue();
       }
 }while((chk=getche())!='0');
 closegraph();
 restorecrtmode();
}

void calcvalue(void)
{
 int mul;
 char i,unit[5];
 float ilem,nh4cl,methanol,acetic;
 cout<<"\n\n\n\n\n Enter the corresponding value \n  ";
 cout<<"\n 1 : value of Ilemnite is in gram ";
 cout<<"\n 2 : value of Ilemnite is in kilogram ";
 cout<<"\n 3 : value of Ilemnite is in tonne ";
 cout<<"\n          Default value is in tonnes:";
 i=getche();
 cout<<i<<endl;
```

```
 switch(i)
 {
  case '1' : mul=1;
             strcpy(unit,"ml");
             break;
  case '2' : mul=1;
             strcpy(unit,"litre");
             break;
  case '3' : mul=1000;
             strcpy(unit,"litre");
             break;
  default  : mul=1000;
             strcpy(unit,"litre");
 }

 cout<<"\n \n \n Enter qty. of Ilemnite       : ";
 cin>>ilem;
 nh4cl=ilem*4;
 cout<<"\n Calculating values";
 delay(200);
 cout<<"\n\n\n Ammonium chloride required is :";
 cout<<nh4cl*mul<< unit;
 cout<<"\n Methanol required is         :";
 cout<<nh4cl*0.02*mul<< unit;
 cout<<"\n Acetic acid required is      :";
 cout<<nh4cl*0.01*mul<< unit;
 delay(2000);
 cout<<"\n Processing complete\n\n ";
 cout<<"\n Press Enter-key if you want to continue ";
 cout<<"\n or 0 key if you want to exit";
}

void callvalue(void)
{
 cleardevice();
 cout<<"\n \n \n Enter the values noted";
 cout<<"\n \n Enter the initial value :";
 cin>>P[0];
 cout<<"\n \n Enter the value at the end of first hour :";
 cin>>P[1];
```

```
  cout<<"\n \n Enter the value at the end of second hour :";
  cin>>P[2];
  cout<<"\n \n Enter the value at the end of third hour :";
  cin>>P[3];
 }

 void convx(void)
 {
  cleardevice();
  outtextxy(0.2*x,0.5*y,"Press 1 Key if you want to enter new values");
  outtextxy(0.2*x,0.55*y,"Press Enter-Key for standard values");
  alt=getch();
  if (alt=='1')
       { callvalue();}
  else
       {
         P[0]=0;
         P[1]=0.3934;
         P[2]=0.7376;
         P[3]=0.8887;
       }
   cleardevice();
   line(0.2*x,0.8*y,0.9*x,0.8*y);
   line(0.2*x,0.3*y,0.2*x,0.8*y);
   outtextxy(x/2-textwidth("Conversion Graph")/2,0.9*y-10,"Conversion
Graph");
   outtextxy(0.2*x,0.8*y+5,"0");
   outtextxy(0.4*x,0.8*y+5,"1");
   outtextxy(0.6*x,0.8*y+5,"2");
   outtextxy(0.8*x,0.8*y+5,"3");
   outtextxy(0.2*x-30,0.8*y,"0.0");
   outtextxy(0.2*x-30,0.6*y+2,"0.4");
   outtextxy(0.2*x-30,0.4*y+4,"0.8");
   outtextxy(0.2*x-30,0.3*y+5,"1.0");
   yco=0.8*y-P[0]*y/2;
   xinc=(0.2*x)/100;
   yinc=(P[1]-P[0])*y/200;
   for(xco=0.2*x;xco<=0.4*x;xco=xco+xinc)
   {
    putpixel(xco,yco,RED);
```

```
 delay(30);
 yco=yco-yinc;
}
 yco=yco+yinc;
 yinc=(P[2]-P[1])*y/200;
 for(xco=0.4*x;xco<=0.5*x;xco=xco+xinc)
{
 putpixel(xco,(yco-((xco-0.4*x)*0.005/(0.1*x))*y),GREEN);
 delay(30);
 yco=yco-yinc;
}
 yco=yco+yinc;
 for(xco=0.5*x;xco<=0.6*x;xco=xco+xinc)
{
 putpixel(xco,(yco-((0.6*x-xco)*0.005/(0.1*x))*y),GREEN);
 delay(30);
 yco=yco-yinc/2;
}
 yco=yco+yinc/2;
 yinc=(P[3]-P[2])*y/200;
 for(xco=0.6*x;xco<=0.65*x;xco=xco+xinc)
{
 putpixel(xco,(yco-((xco-0.6*x)*0.007/(0.05*x))*y),BLUE);
 delay(30);
 yco=yco-yinc/2;
}
 yco=yco+yinc/2;
 for(xco=0.65*x;xco<=0.7*x;xco=xco+xinc)
{
 putpixel(xco,(yco-0.007*y-((xco-0.65*x)*0.003/(0.05*x))*y),BLUE);
 delay(30);
 yco=yco-yinc/2;
}
 yco=yco+yinc/2;
 for(xco=0.7*x;xco<=0.75*x;xco=xco+xinc)
{
 putpixel(xco,(yco-0.007*y-((0.75*x-xco)*0.003/(0.05*x))*y),BLUE);
 delay(30);
 yco=yco-yinc/2;
}
```

```
    yco=yco+yinc/2;
    for(xco=0.75*x;xco<=0.8*x;xco=xco+xinc)
    {
    putpixel(xco,(yco-((0.8*x-xco)*0.007/(0.05*x))*y),BLUE);
    delay(30);
    yco=yco-yinc/2;
    }
    yco=yco+yinc/2;
    outtextxy(0.2*x,0.9*y,"Press Enter-key if you want to continue ");
    outtextxy(0.2*x,0.9*y+15,"or 0 key if you want to exit");
}

void surfchem(void)
{
    cleardevice();
    outtextxy(0.2*x,0.5*y,"Press 1 Key if you want to enter new values");
    outtextxy(0.2*x,0.55*y,"Press Enter-Key for standard values");
    alt=getch();
    if (alt=='1')
        { callvalue();}
    else
        {
          P[0]=0;
          P[1]=0.1735;
          P[2]=0.3598;
          P[3]=0.5190;
        }
    cleardevice();
    line(0.2*x,0.8*y,0.9*x,0.8*y);
    line(0.2*x,0.2*y,0.2*x,0.8*y);
    outtextxy(0.2*x,0.8*y+5,"0");
    outtextxy(0.4*x,0.8*y+5,"1");
    outtextxy(0.6*x,0.8*y+5,"2");
    outtextxy(0.8*x,0.8*y+5,"3");
    outtextxy(0.2*x-30,0.8*y,"0.0");
    outtextxy(0.2*x-30,0.6*y+3,"0.2");
    outtextxy(0.2*x-30,0.4*y+3,"0.4");
    outtextxy(0.2*x-30,0.2*y+3,"0.6");
    outtextxy(x/2-textwidth("Surface Chemical Concentration
Graph")/2,0.8*y+20,"Surface Chemical Concentration Graph");
```

```
  yco=0.8*y-P[0]*y;
  xinc=(0.2*x)/100;
  yinc=(P[1]-P[0])*y/100;
  for(xco=0.2*x;xco<=0.4*x;xco=xco+xinc)
  {
  putpixel(xco,yco,RED);
  delay(30);
  yco=yco-yinc;
  }
  yco=yco+yinc;
  yinc=(P[2]-P[1])*y/100;
  for(xco=0.4*x;xco<=0.6*x;xco=xco+xinc)
  {
  putpixel(xco,yco,GREEN);
  delay(30);
  yco=yco-yinc;
  }
  yco=yco+yinc;
  yinc=(P[3]-P[2])*y/100;
  for(xco=0.6*x;xco<=0.8*x;xco=xco+xinc)
  {
  putpixel(xco,yco,BLUE);
  delay(30);
  yco=yco-yinc;
  }
  outtextxy(0.2*x,0.9*y,"Press Enter-key if you want to continue ");
  outtextxy(0.2*x,0.9*y+15,"or 0 key if you want to exit");
}

void diffcon(void)
{
  cleardevice();
  outtextxy(0.2*x,0.5*y,"Press 1 Key if you want to enter new values");
  outtextxy(0.2*x,0.55*y,"Press Enter-Key for standard values");
  alt=getch();
  if (alt=='1')
       { callvalue();}
  else
       {
         P[0]=0.0;
```

```
            P[1]=0.0634;
            P[2]=0.2932;
            P[3]=0.5285;
          }
    cleardevice();
    line(0.2*x,0.8*y,0.9*x,0.8*y);
    line(0.2*x,0.2*y,0.2*x,0.8*y);
    outtextxy(0.2*x,0.8*y+5,"0");
    outtextxy(0.4*x,0.8*y+5,"1");
    outtextxy(0.6*x,0.8*y+5,"2");
    outtextxy(0.8*x,0.8*y+5,"3");
    outtextxy(0.2*x-30,0.8*y,"0.0");
    outtextxy(0.2*x-30,0.6*y+3,"0.2");
    outtextxy(0.2*x-30,0.4*y+3,"0.4");
    outtextxy(0.2*x-30,0.2*y+3,"0.6");
    outtextxy(x/2-textwidth("Diffusion Controlled
Graph")/2,0.8*y+20,"Diffusion Controlled Graph");
    yco=0.8*y-P[0]*y;
    xinc=(0.2*x)/100;
    yinc=(P[1]-P[0])*y/100;
    for(xco=0.2*x;xco<=0.25*x;xco=xco+xinc)
    {
    putpixel(xco,yco-((xco-0.2*x)*0.0005/(0.05*x))*y,RED);
    delay(30);
    yco=yco-yinc;
    }
    yco=yco+yinc;
    for(xco=0.25*x;xco<=0.3*x;xco=xco+xinc)
    {
    putpixel(xco,yco-0.0005*y-((xco-0.25*x)*0.0005/(0.05*x))*y,RED);
    delay(30);
    yco=yco-yinc;
    }
    yco=yco+yinc;
    for(xco=0.3*x;xco<=0.35*x;xco=xco+xinc)
    {
    putpixel(xco,yco-0.0005*y-((0.35*x-xco)*0.0005/(0.05*x))*y,RED);
    delay(30);
    yco=yco-yinc;
    }
```

```
yco=yco+yinc;
for(xco=0.35*x;xco<=0.4*x;xco=xco+xinc)
{
putpixel(xco,yco-((0.4*x-xco)*0.0005/(0.05*x))*y,RED);
delay(30);
yco=yco-yinc;
}
yco=yco+yinc;
yinc=(P[2]-P[1])*y/100;
for(xco=0.4*x;xco<=0.45*x;xco=xco+xinc)
{
putpixel(xco,yco-((xco-0.4*x)*0.0105/(0.05*x))*y,GREEN);
delay(30);
yco=yco-yinc;
}
yco=yco+yinc;
for(xco=0.45*x;xco<=0.5*x;xco=xco+xinc)
{
putpixel(xco,yco-0.0105*y-((xco-0.45*x)*0.012/(0.05*x))*y,GREEN);
delay(30);
yco=yco-yinc;
}
yco=yco+yinc;
for(xco=0.5*x;xco<=0.55*x;xco=xco+xinc)
{
putpixel(xco,yco-0.0105*y-((0.55*x-xco)*0.012/(0.05*x))*y,GREEN);
delay(30);
yco=yco-yinc;
}
yco=yco+yinc;
for(xco=0.55*x;xco<=0.6*x;xco=xco+xinc)
{
putpixel(xco,yco-((0.6*x-xco)*0.0105/(0.05*x))*y,GREEN);
delay(30);
yco=yco-yinc;
}
yco=yco+yinc;
yinc=(P[3]-P[2])*y/100;
for(xco=0.6*x;xco<=0.65*x;xco=xco+xinc)
{
```

```
 putpixel(xco,yco-((xco-0.6*x)*0.0215/(0.05*x))*y,BLUE);
 delay(30);
 yco=yco-yinc;
 }
for(xco=0.65*x;xco<=0.7*x;xco=xco+xinc)
 {
 putpixel(xco,yco-0.0215*y-((xco-0.65*x)*0.016/(0.05*x))*y,BLUE);
 delay(30);
 yco=yco-yinc;
 }
for(xco=0.7*x;xco<=0.75*x;xco=xco+xinc)
 {
 putpixel(xco,yco-0.0215*y-((0.75*x-xco)*0.016/(0.05*x))*y,BLUE);
 delay(30);
 yco=yco-yinc;
 }
for(xco=0.75*x;xco<=0.8*x;xco=xco+xinc)
 {
 putpixel(xco,yco-((0.8*x-xco)*0.0215/(0.05*x))*y,BLUE);
 delay(30);
 yco=yco-yinc;
 }
yinc=(0.565-P[3])*y/100;
for(xco=0.8*x;xco<=0.875*x;xco=xco+xinc)
 {
 putpixel(xco,yco,YELLOW);
 delay(30);
 yco=yco-yinc;
 }
 outtextxy(0.2*x,0.9*y,"Press Enter-key if you want to continue ");
 outtextxy(0.2*x,0.9*y+15,"or 0 key if you want to exit");
}
```

CHAPTER 7

AN ELECTROCHEMICAL INVESTIGATION ON RUSTING REACTION USING CYCLIC VOLTAMMETRY

Voltametry, a class of analytical techniques in which current at a working electrode is measured as a function of potential waveform applied to the electrode. In voltametry, the term "working electrode" is reserved for the electrode at which the reaction of interest occurs. The potential of this electrode serves as the driving force for the electrochemical reaction ie. It is the controlled parameter that causes the chemical species present in the solution to be electrolysed (reduced or oxidized) at the surface. The reducing or oxidizing strength of the electrode is controlled by the applied potential.

The resultant current – potential plot is called a voltammogram. It is a display of current versus potential.

Consider a solution of species 'Ox' which can be reduced to 'Red' with a characteristic potential E^{o} for the process. The experiment is begun by applying a potential E^{i}, so that no current flows and now, scan in the negative direction, is initiated. As the applied potential approaches E^{o} the current begins to increase and continues to do so until a peak is reached. Upon continued scanning, the current decays in a characteristic tailing fashion (E^{f}). At a point E^{f} the direction of sweep is changed and the reverse sweep begins which is again analogous to the forward sweep. This is shown in Fig 7.1.

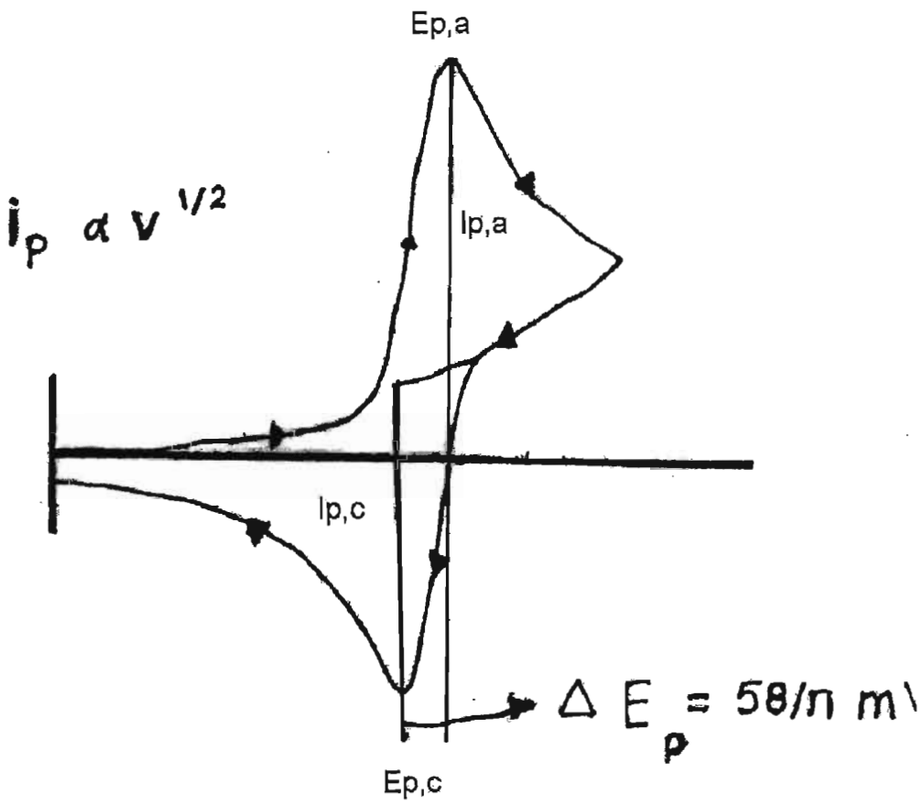

Fig 7.1 Cyclic voltammogram for a freely diffusing species

The anodic dissolution of reduced ilmenite has been studied using carbon paste electrode technique. To understand the polarization behaviour of reduced ilmenite carbon electrode has been prepared and used as 'working electrode'.

Reduced ilmenite is a unique mineral product, which is a heterogeneous agglomeration of a poorly conducting rutile phase and a conducting metallic iron phase.

A conventional three electrode cell was used with a platinum wire loop as a counter electrode and a saturated calomel electrode (E = + 0.2422) as the reference electrode. The electrochemical cell was similar in design to a Metrohm cell [195]. All potentials are measured using the above reference electrode. Current densities were calculated using the geometric surface area and all peak current densities are reported from zero current baseline.

7 .1 Investigations using reduced ilmenite

High anodic potentials were observed and the current increased in a non-linear way when reduced ilmenite was used or reduced ilmenite (RI) : carbon paste (CP) weight ratio was high. Due to high resistance, these electrodes preclude their use as electrodes. Hence electrodes were prepared with relatively low ratios. Reduced ilmenite (RI) and carbon paste (CP) were mixed in the ratio 1: 4 with tri-n-butyl phosphate as binder and packed in a 1.5 mm dia capillary tube and used as working electrode after compacting.

The working electrode was polished well using very fine emery paper. The working electrode was dipped in 20 ml of 1.5% NH_4Cl solution, which is slightly acidic (pH ~ 4) and as the electrolyte. Cyclic voltammograms were recorded by dipping the working electrode in the stationary elecrolyte and also by aerating the electrolyte. CV of working electrode by dipping in stationary electrolyte is shown in Fig 7.2 and aerating the electrolyte is shown in Fig 7.3 respectively. If both anodic peak and cathodic peak are displayed in a voltammogram then $I_p \alpha \upsilon^{1/2}$ and peak $E_p \alpha \log \upsilon$ is indicative

of a fully irreversible electron transfer reaction [196]. The open circuit potential was very stable and reproducible.

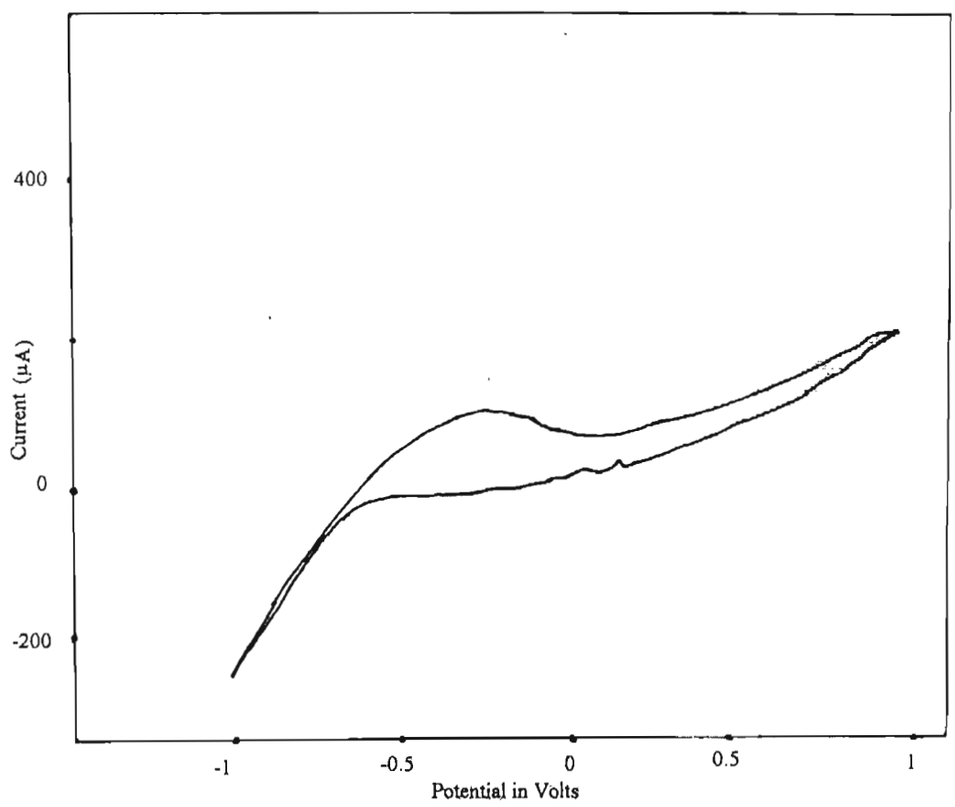

Fig 7.2 CV of reduced ilmenite electrode in stationary electrolyte

In the cyclic voltammogram Fig 7.2 the dissolution of iron (Fe^{2+}) is usually observed near 0.00 V. Scanning anodically from the open circuit potential the current increased immediately in an exponential manner at first up to –0.25 V; and then increased in a linear fashion up to 0 V. This is consistent with the formation of a partially passivating film. Above 0.00 V,

an abrupt increase in the current, which is associated with anode pitting, was observed.

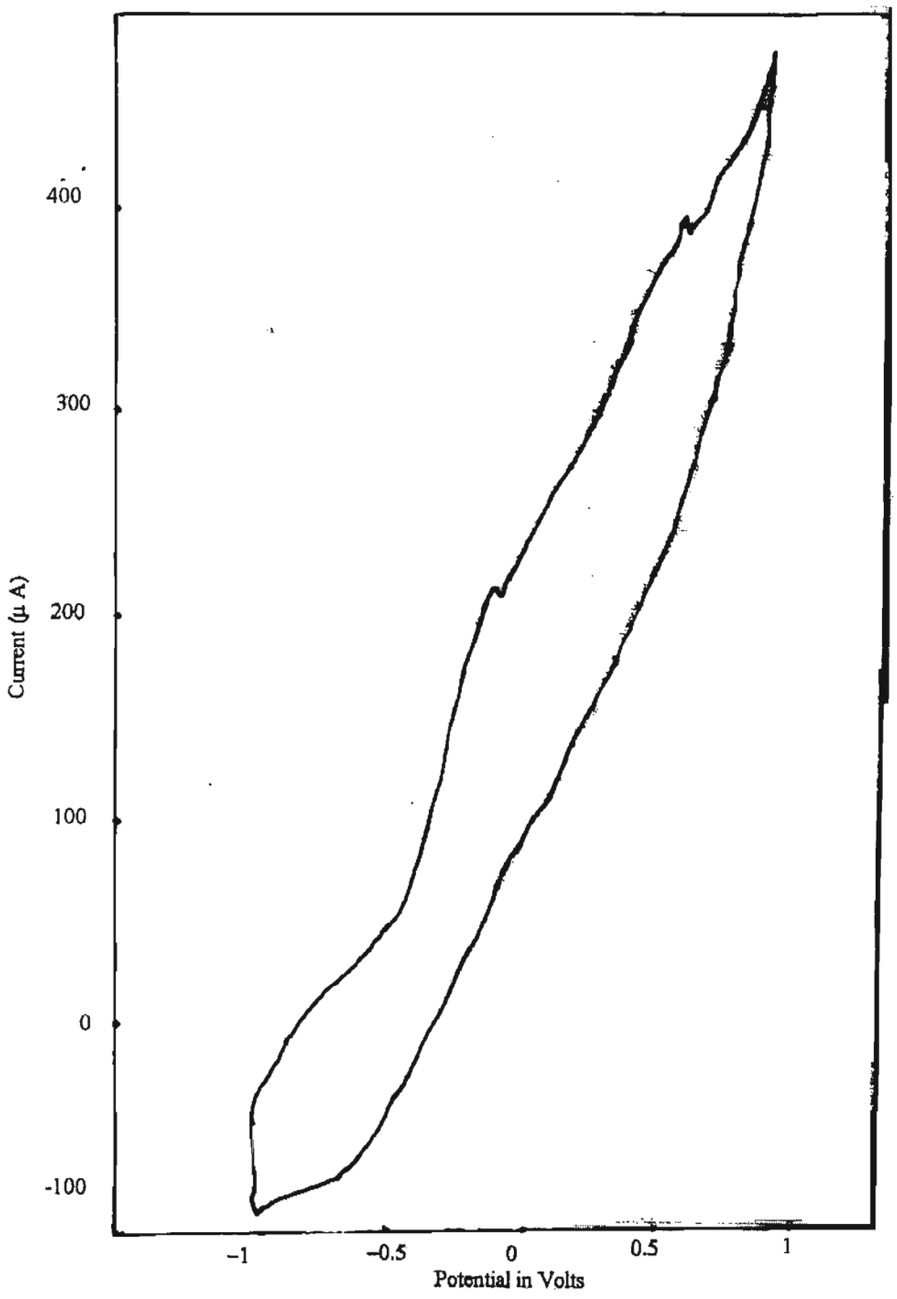

Fig7 .3 CV of reduced ilmenite electrode during aeration

However when the electrolyte is aerated the oxidation peak is observed (Fig 7.3) which is partially passivated. The observation may be interpreted if the dissolution reaction can be described in terms of a simple hydroxide mechanism [197].

$$Fe + H_2O \longrightarrow Fe(OH)_{(ad)} + H^+ + e^-$$

$$Fe(OH)_{(ad)} \longrightarrow FeOH^+_{(aq)} + e^-$$

$$FeOH^+_{(aq)} \longrightarrow Fe^{2+} + OH^-$$

The peaks obtained in the CV showed lot of shifts. This may be due to the presence of TiO_2 matrix in the reduced ilmenite.

7 .2 Investigations using partially rusted ilmenite

In order to study the mechanism of the rusting reaction carbon paste electrodes were developed using different rusted samples. During rusting reaction after every hour samples were withdrawn. For cyclic voltametry study carbon paste electrodes were made using rusted ilmenite obtained using NH_4Cl + sucrose as catalyst after one hour, 5 hours and 8 hours of rusting.

7 .2.1. With 1 hour rusted sample

Fig 7.4 shows the cyclic voltammogram of ilmenite after subjecting to rusting for 1 hour using NH_4Cl + sucrose. The scanning was carried out between –1 to +1 V. When scanned anodically nearly at 0.00 V a peak appeared which corresponds to the oxidation of metallic iron to Fe^{2+}. When scanning is continued another peak was obtained nearly at 0.9 V, which corresponds to the oxidation of Fe^{2+} to Fe^{3+} ion. In the reverse sweep there are no definite peaks observed. This may be due to the formation of FeOH adsorbed on the surface of the electrode. The reduction of FeOH is observed

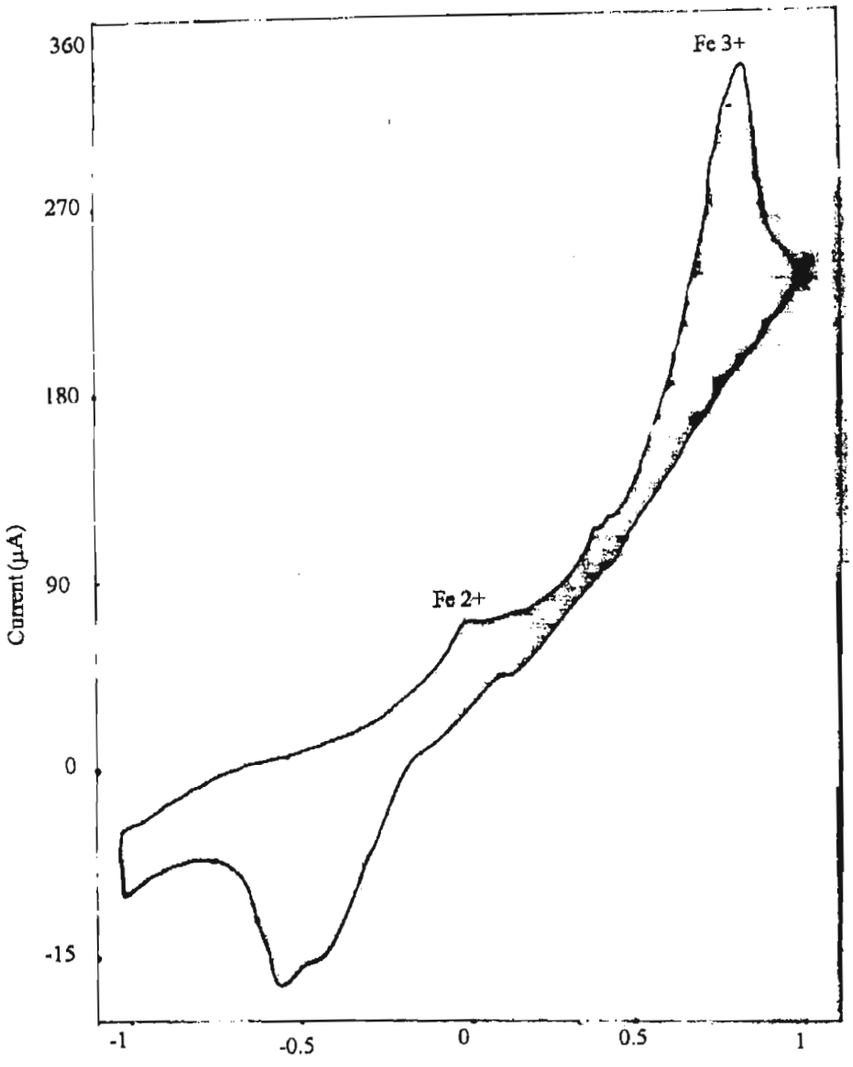

Fig. 7.4 CV of 1 hour rusted ilmenite

nearly at –0.48 V. So, during rusting the metallic iron obtained after reduction gets oxidized to Fe^{2+} and Fe^{3+}, which form their respective hydroxides in the oxidizing environment.

7 .2.2 Ilmenite for rusted for 5 hrs.

Carbon paste electrode was prepared using the 5 hrs. rusted ilmenite. The CV is shown in Fig 7.5. In this during the anodic sweep, the oxidation of Fe^{2+} is observed nearly at –0.8 V. The shift in the peak was mainly due to the presence of TiO_2 matrix. Nearly at 0.00 V the peak for immobile TiO_2 appears, as major portion of the iron is removed. TiO_2 is an insulator but it can be reduced so quickly. The formation of Magnelli phases (TiO_{2-x}) as a result of reduction of ilmenite is highly conducting [198]. So, near 0.00 V the lower oxides of titanium show peak. At 0.8 V the oxidation of Fe^{2+} to Fe^{3+} appears. Only in this CV the reverse peak is prominent and significant. Nearly at –0.1 V the reduction of Fe^{3+} to Fe^{2+} occurs. At –0.5 V the reduction of Fe^{2+} to metallic iron was observed.

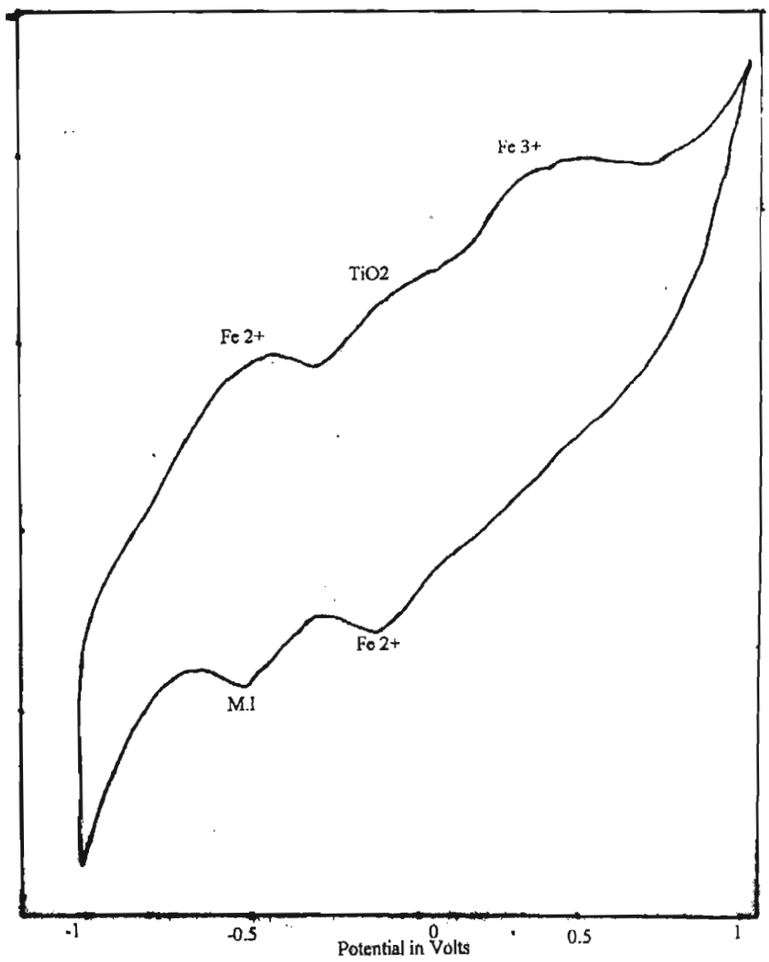

Fig. 7.5 CV of 5 hrs rusted ilmenite

7.2.3 Ilmenite rusted for 8 hrs.

Fig 7.6 shows the CV of ilmenite obtained after 8 hrs of rusting using NH_4Cl + sucrose. Carbon paste electrode was prepared using the above sample and CV was recorded. As major quantities of metallic iron was removed, a small peak was observed near –0.6 V which is due to the oxidation of ferrous iron. As TiO_2 matrix is enriched the shift in the Fe^{2+} peak is very much prominent. This is in agreement with the fact that 8 hrs rusted sample had got about 2% of metallic iron present in it. Nearly at –0.1 V the TiO_2 peak appears which is most significant and consistent.

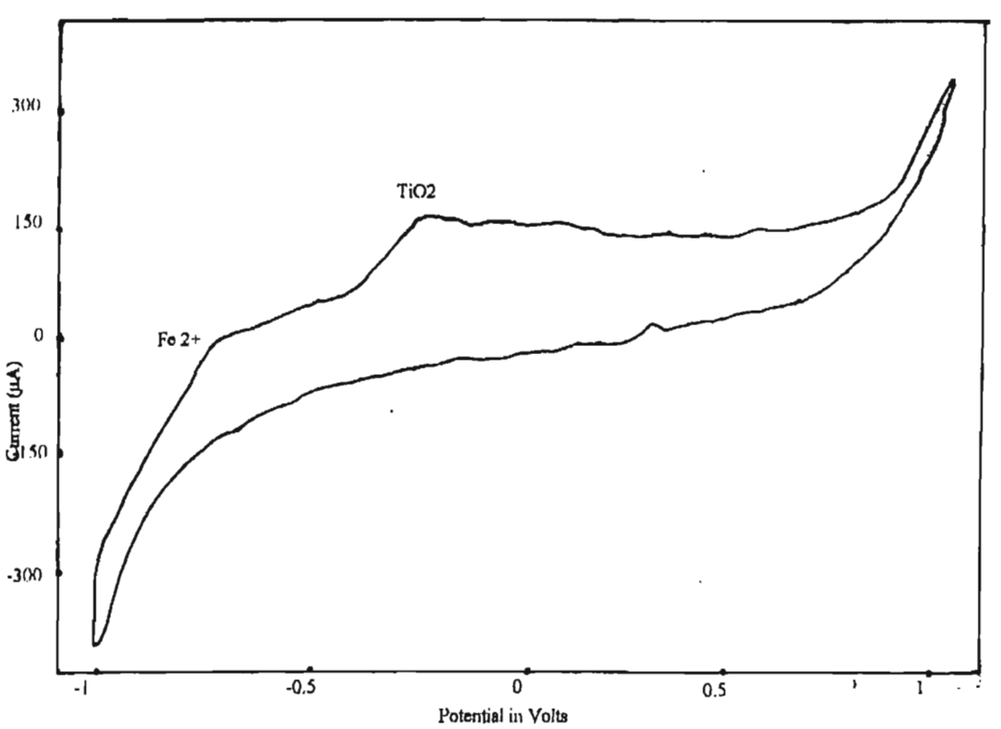

Fig. 7.6 CV of 8 hrs rusted ilmenite

7.3 Influence of TiO_2 matrix on the oxidation of Fe

It is reported that the rutile phase catalyses the anodic dissolution of iron [195]. A few experiments were carried out to prove the influence of the TiO2 matrix on the oxidation of iron present in reduced ilmenite. CV study of synthetic rutile where the iron content was negligible as well as that of synthetic rutile in presence of $FeSO_4$ solution was carried out.

7.3.1 Cyclic voltammogram of synthetic rutile

Carbon paste electrode was prepared using synthetic rutile and carbon powder. Fig 7.7 shows the CV of synthetic rutile. Nearly at 0.0 V the TiO_2 peak appears which is a significant one. In synthetic rutile only TiO_2 is present as the major constituent and hence the peak is assigned to TiO_2 only.

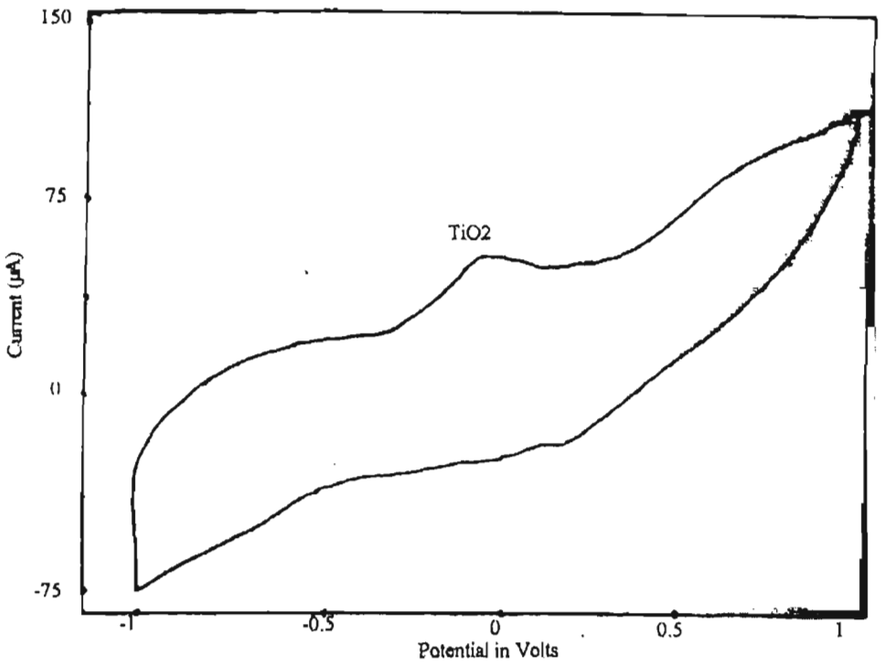

Fig. 7.7 CV of synthetic rutile

7.3.2 Cyclic voltammogram showing the catalytic activity of TiO_2 on iron

In order to prove the catalytic effect of TiO_2, along with 15 ml NH_4Cl and HCl about 5 ml of 0.01 N $FeSO_4$ was added. Fig 7.8 shows the CV of synthetic rutile in $FeSO_4$ solution. In this the solid electrode used was synthetic rutile and carbon powder. During the anodic sweep the peak, which appeared nearly at 0.00 V for synthetic rutile in Fig 7.7 disappeared where as the peak for Fe^{3+} appeared nearly at 0.8 V, which confirms the oxidation of Fe^{2+} to Fe^{3+} in the presence of TiO_2.

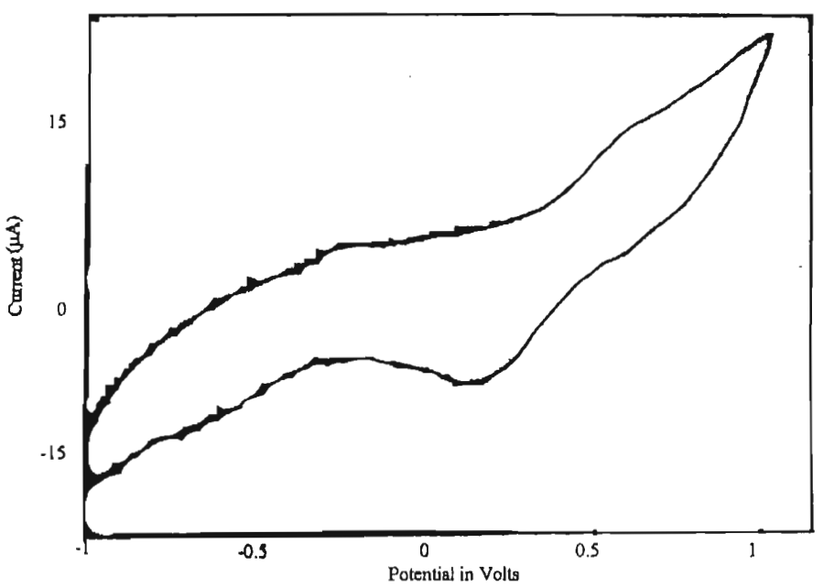

Fig. 7.8 CV showing the catalytic activity of TiO2 on iron

The electrochemical studies can be carried out to determine the mechanism of any type of reactions. Even if the reaction is an irreversible one electro-chemical studies gives a clear idea about the type of electron transfer taking place in the reaction.

The objective of this electro-chemical investigation was to understand the mechanism of the rusting reaction and a detailed electro-chemical investigation was not in the scope of this work. Hence further detailed electro-chemical studies were not carried out with the systems.

The following conclusions can be drawn from the above studies.

- An ilmenite : carbon paste electrode can be used as working electrode.

- When reduced ilmenite was used as an electrode in a stationary electrolyte passivating film was formed on the electrode surface.
- When the reduced ilmenite electrode was used and the electrolyte was aerated oxidation peak was observed which was partially passivated.
- The shifts in peak were mainly due to the presence of TiO_2 matrix.
- When partially rusted ilmenites were used as working electrode the peaks for Fe^{2+} and Fe^{3+} were observed.
- When major quantities of the iron were removed from the ilmenite particles the peak for immobile phase TiO_2 starts to appear.
- The TiO_2 present in the ilmenite particles catalyses the removal of iron, which was proved through cyclic voltammetry studies.

CHAPTER 8

SUMMARY AND CONCLUSION

The present work is concerned with the investigations carried out for the preparation of high grade synthetic rutile from Kerala ilmenite by an environment friendly process. The process consists of the following steps namely reduction, rusting, rutilation and leaching. In this process the second step rusting is the most time consuming step, which takes about 14-16 hrs. for completion. Investigations were carried out to improve the efficiency of the rusting reaction. The salient features of these investigations are summarized below.

RUSTING

The reduced ilmenite used for the study had a metallisation of 83%. 125 g of reduced Kerala ilmenite is suspended in 500 ml of 1.5% (w/v) NH_4Cl solution. Air at the rate of 4-5 lit./ min. was passed through the reaction. A mechanical stirrer was used to stir the solution continuously and the stirring rate was fixed as 800. Rusting is an electrochemical reaction in which separation of iron in the form of solid iron oxide takes place in the presence of NH_4Cl as catalyst. As the reaction was quite slow when NH_4Cl alone was used as the catalyst some additional compounds were added along with NH_4Cl to improve the efficiency of the reaction.

RUSTING REACTION WITH NH_4Cl + ADDITIONAL COMPOUNDS

Certain carbonyl compounds were added along with NH_4Cl to improve the efficiency of the rusting reaction. Compounds such as methanol, acetone, glyoxal, glucose, sucrose, starch, urea, saccharin, acetaldehyde, formaldehyde, ethanol and acetic acid when added along with NH_4Cl improved the rusting by reducing the reaction time to less than half of that of

NH_4Cl alone. The final product obtained after 8 hrs. of rusting with NH_4Cl + carbonyl compounds had a TiO_2 content of about 89% whereas a TiO_2 content of about 75% was achieved when NH_4Cl alone was used as the catalyst in 8 hrs.

The pH and the dissolved oxygen present in the system were measured during the progress of the reaction and a definite trend is not obvious in the case of dissolved oxygen whereas in the case of pH during the progress of the reaction the pH is maintained less than 4 which may be due to the oxidation of carbonyl groups during rusting which was confirmed through proper tests.

Kinetic study of the reaction was carried out at 25, 30, 35 and 40°C. As the temperature was increased the rate of rusting decreased when NH_4Cl + carbonyl compounds were added during the rusting reaction. Because of this only the above four temperatures were selected for the study. The optimum temperature at which maximum iron removal achieved was 30°. The studies reveal that the reaction followed is a topochemical or surface chemical one. The activation energies for the different systems were calculated, and for all the systems with carbonyl compounds had activation energy less than that of NH_4Cl alone as the catalyst.

The increase in surface area after rusting is noticed which might be due to the crumbling of particles during rusting. XRD studies reveal that as the rusting reaction proceeds the metallic iron peak diminishes and becomes insignificant because of the removal of iron from the particles. SEM studies reveal that the surface changes have occurred because of rusting and the particles are highly porous giving the structure of a honeycomb.

RUSTING REACTION CARRIED OUT WITH NH_4Cl + MIXTURE OF CARBONYL COMPOUNDS

In order to improve the efficiency of the rusting reaction further mixture of carbonyl compounds were added along with NH_4Cl during rusting. Mixtures like glyoxal + acetic acid, methanol + acetic acid, glyoxal + acetone, acetone + acetic acid, sucrose + acetic acid, methanol + acetone, acetone + acetic acid, ethyl alcohol + acetic acid, methanol + formic acid, glyoxal + formic acid, acetic acid + formic acid or urea + acetic acid with NH_4Cl were added during rusting. The reaction was very fast and maximum amount of iron removal was obtained in 8 hrs. After 5 hrs. of rusting the rusting reaction was very slow since major quatities of the iron removal was achieved in 5 hrs. After 8 hrs. of rusting, a TiO_2 content of 93.4% was achieved.

The dissolve oxygen and pH measured during the couse of the reaction were recorded. The pH is less than 4, which may be one of the reason for maximum rusting reaction.

The rusted ilmenite obtained after 8 hrs. of rusting was subjected to thermal analysis and the changes occurring temperatures were noted. The rusted samples were heated at those particular temperatures and the samples were subjected to XRD studies. The morphological changes were studied through SEM and it was found that the particles were highly porous as a result of rusting.

The kinetic studies were carried out for all the systems at 25, 30, 35 and 40°C. The optimum temperature for maximum rusting was observed at 30°. A detailed analysis shows that the reaction mechanism was diffusion controlled. The activation energies for all the systems were calculated.

OPTIMISATION OF REDUCTION FOR MAXIMUM RUSTING

As it was clear that 83% reduced ilmenite could give better iron removal with an enrichment of TiO_2 to 93.4%, it was thought worth while to optimize the reduction at which maximum rusting was possible. Experiments were carried out with reduced ilmenite having different metallisation and found that 76% metallisation was optimum for maximum iron removal. Studies were carried out using the 76% metallised ilmenite. Rusting was carried out by adding mixture of methanol and formic acid, methanol and acetic acid, acetone and formic acid, glyoxal and formic acid, glyoxal and acetic acid, sucrose and acetic acid or sucrose and formic acid along with NH_4Cl to reduced ilmenite. The reaction was very fast and major quantities of the iron were removed within 3 hrs. The rusted product had a TiO_2 content of 96.4%.

The dissolved oxygen and pH measured were different from that with 83% metallised ilmenite. The surface area of the rusted ilmenite is comparatively less when 76% metallised ilmenite was used for rusting. The particles did not crumble even after rusting. There were some structural changes observed in XRD. The phases present in the 76% metallised ilmenite were ilmenite, anatase, rutile and pseudo rutile. Pseudo brookite was observed in the case of 83% whereas pseudo rutile was observed in the case of 76% metallised ilmenite. The surface morphology shows that during reduction the iron agglomerates towards the periphery of the ilmenite grains and takes upcertain peculiar shapes. The rusted product had cell like or channel like structures which reveals that reduction had taken place in a particular fashion so that after the iron removal channel like structures were observed. The internal structure was studied through optical microscope.

The channel or cells like structures observed in the SEM were also seen in optical microscopic photographs.

A structural model was developed for the reaction considering the reaction as a gas solid one. A pellet grain model was used to establish the type of mechanism followed through out the reaction. It was found that the reaction was both surface chemical and diffusion controlled one. The experimental values were tested with the equations developed through the model.

ELECTROCHEMICAL INVESTIGATIONS ON RUSTING

Electrochemical investigations were carried out through cyclic voltammetric studies. A carbon paste electrode was prepared using ilmenite. During the progress of the rusting reaction it was found that the peaks observed for Fe^{2+} and Fe^{3+} ions disappeared and the peak for TiO_2 appeared on the removal of iron. The most interesting investigation was that the TiO_2 present in the ilmenite catalysed the removal of iron during rusting.

CONCLUSION

The investigations clearly prove the feasibility of accelerating the rusting reaction using some of the organic compounds as alone or as mixtures along with NH_4Cl. The studies were carried out in laboratory scale, which needs to be scaled up for commercialization. The problems araising during scaling up cannot be predicted at this level for which actual experiments have to be conducted. However it is quite clear that the time required for the reaction can be reduced to less than half, which will improve the economics of the process when commercialized.

References

1. Technology in Indian Titanium Dioxide Industry, DSIR, Govt. of India, P. 308 - 309,1993.

2. Technology in Indian Titanium Dioxide Industry, DSIR, Govt. of India, P.104, 1993.

3.Technology in Indian Titanium Dioxide Industry, DSIR, Govt. of India, P.105, 1993

4.Technology in Indian Titanium Dioxide Industry, DSIR, Govt. of India, P.106, 1993

5.Technology in Indian Titanium Dioxide Industry, DSIR, Govt. of India, P.76

6. Ginsca D. and Popscu I., Bull.Soc.roumaine phys; 1940,40, No: 73, 13 Chem.Abs.1940,34,7695.

7.Kroll W., Trans. Electrochem. Soci; 78(1940) 35

8.Moldovan, Iuliu, Wohl Andrei & Visa, Calin, Chem Abstr, 84 (1976) 78476p

9. Polorelov V.I., Baintenev N.A. & Burlibaev B.M., Chem Abstr, 85 (1976)

10. Bernard O. Wilcox, US 3, 159, 454 (Cl. 23 - 202), Dec.1, 1964 Appl. Sept. 26, 1960.

11. Laporte Titanium Ltd. (by Raymond J. Wigginton & John V. Bramely), Ger.1, 206, 412 (Cl. c01g), Dec. 9, 1965, Appl. Oct.15, 1962.

12. Tikkanen M.H., Tynela T. and Vuoristo, Met. Soc. Conf., 24 (1963) 269 - 282.

13. Williams F.R., Whitehead J., Marshall J., Conners A. and Gosden D.V. US 3677, 740 (Cl. 75 - I, C 216, C 22b) 18 Jul 1972, Brit. Appl. 38, 476 / 64, 31 Jul 1964.

14. Kino C., Takabatake T. and Okur M. Japan 73, 39, 157, (Cl. C01g, C

09c(s), (22b), 21 Nov 1973, Appl. 6468, 642, 08 Dec. 1964.

15. E.I.du pont de Nemours and co. (by James W. Reeves), Ger.1, 218, 734 (Cl. c 22b), June 8, 1966, US. Appl. April 29, 1964.
16. Samanta S., Sampath V.S. and Bhatnagar P.P., Indian Pat. 96, 661,04 Feb. 1967, Appl. Nov.1964.
17. Becher R.G., Canning R.G., Goodheart B.A. and Ulsra S., Australian Inst. Mining. Met. Proc., No. 214 (1965) 21-44.
18. Oceanic Process Corp., Neth. Appl. 6, 502, 141 (Cl, c22b) August 22, 1966, Appl. Feb. 19, 1965.
19. Fabriques de produits chemiques de Thann et de Mulhouse (by Maurice Figuet and Robert Mas), Fr.1, 456, 030 (Cl. c01g, c09c), Oct. 21, 1966, Appl. Sept. 6, 1965
20. Ruthner Industrie - Plangungs - A.G., Fr. 1, 484, 318 (Cl. c22b), June 9, 1967; Austrian - Appl. June 24, 1965.
21. Lo, Ching - Lung and Mackay T.S., Ger. 1, 300, 535 (Cl. c01g) 07 Aug. 1968, Appl. 5 May 1965.
22. Akio Yamaguchi, Masahide Harada and Joichiro Mariyama, Nippon Kogyo Kaishi, 81(7) (1965) 33-38; Chem. Abstr; 65 (1966) 363 C.
23. Khairy E.M., Kammal Hussein M. and El-Tawil S.Z., Tech.J. (Jamshedpur, India), 8(2), (1966) 10-14
24. Sehra J.C., and Jena J.B., Trans. Indian Inst. Metals, 19 (1966) 114-115.
25. Volk W., US 3,383, 200(Cl. 26-75), 14 May 1968, Appl. 13 Sep - 28 Nov. 1966.
26. Kammal Hussein M. and El-Tawil S.Z., Indian J. Technol; 5(3), (1967) 97-100.
27. Aravamuthan V., Prasad Rao Y.D. and Raghavan R., J. Proc. Inst. Chem. (India), 39(1), (1967) 23 -26.

28. Sinha H.N., and Waugh D.M., S. African pat. 6802, 407, 10 Sep. 1968, Australian, Appl.1 may 1967.

29. Aramendia M.M. and Armant D.L., US pat. 3457, 037 (Cl. 23-202, c01g, c22b), 22 Jul 1969, Appl. 15 Aug. 1967.

30. Madhavan Pillai K.S., Indian pat. 112, 041, 21 Feb. 1970, Appl. 21 Aug 1967.

31. O'Brien D.J. and Gain D., N.Z. J. Sci.; 10(3), (1967) 736 - 743.

32. Reeves J.W., US pat. 3850, 615 (Cl. 75-26; c22b) 26 Nov. 1974, Appl. 680,522, 3 Nov. 1967.

33. Safiullin N.Sh. and Belyaev E.K., Khim. Prom. Ukr. (Russ. Ed.), (1967) (4) 6-8; Chem. Abstr.; 68(1968) 23182d.

34. O'Brien D.J. and Marshall T., N.Z. J. Sci., 11(1) (1968) 159-169.

35. Suchil'nikov S.I., Pavlov V.A., Ponomarenko A.G. and Deryabin Y.A., Izv. Vyssh. Ucheb. Zaved; Chern. Met; 11(4), (1968) 56-59; Chem. Abstr.; 69 (1968) 453892.

36. Oster F., Fr. 1,566,670 (Cl. c22b, c01g), 9 May 1969, Appl. 26 Mar 1968.

37. Sankaran C., Misra R. N. and Bhatnagar P.P., Adv. Extr. Met., Proc. Symp; London 1967 (Pub. 1968) 480-500.

38. Mathew P.M., Indian pat. 123,319, 27 May 1972 Appl. 26 Sep. 1969.

39. Gokarn A.N. and Altekar V.A., Trans. Indian Inst. Metals, 22(1), (1969) 8-16

40.Reeves J.W., Ger. Offen. 1,941,509 (Cl. c22b) 3 Sep. 1970, US. Appl. 7 Feb. 1969.

41. Honchar A.P., US pat. 3,529,933 (Cl. 23-202, c01g) 22 Sep. 1970, Appl. 2 April 1969.

42. Chen J.H., Ger. Offen 2,004,878 (Cl. c22b), 6 May 1971, US Appl. 15 Oct. 1969.
43. Williams F.R., Whitehead J., Marshall J. Conners A. and Gosden D.V., Ger. Offen., 2,038,249 (Cl. c22b) 11 Feb. 1971, Brit. Appl. 31 Jul 1969.
44. Williams F.R., Whitehead J., Marshall J. and Conners A., Ger., Offen.2,038,247 (Cl. c22b c01g) 4 Mar. 1971, Brit. Appl. 31 Jul 1969.
45. Hi'ester N.K., US pat. 3560153 (Cl. 23-202; c01g), 2 Feb. 1971, Appl. 27 Feb. 1969
46. Bade H., Bellefontaine A. and Kienast G., S. African pat., 7007,971, 6 Jul 1971, Ger. Appl. P. 19603793, 2 Dec. 1969.
47. Kawai T., Shinozuka K. and Hashimoto Y., Japan pat., 7420688 (Cl. c22b, c01g) 27 May 1974, Appl. 6971,833, 10 Sep. 1969.
48. Benilite Corp. of America Jpn. Tokkyo koho 8008,572 (Cl.c22B 34/12), 5 Mar. 1980, US, Appl. 866548, 15 Oct 1969.
49. Jain S.K., Prasad P.M. and Jena P.K., Met. Trans.; (1970) 1, 1527-1530.
50. Meyer K., Reuter G. and Thumm W., Ger. Offen. 2008896 (Cl. c21c), 9 Sep.1971, Appl. 26 Feb. 1970.
51. Henkel H., Zirngibi H. and Rademachers J., Ger. offen. 2024907 (Cl. c01g) 9 Dec. 1971, Appl.22 May 1970.
52. Naguib A.G.E., US pat., 3660029 (Cl. 23/ 202 R; c01g) 2 May 1972, Appl. 62612, 10 Aug. 1970.
53. Soverini A., Sironi G. and Corbetta A., S. African pat., 710301803 Dec. 1971. Ital. Appl.24547 A/ 70 13 May 1970.
54. Soverini A., Sironi G. and Corbetta A., S. African pat., 7202621 (Cl. c01b) 5 Dec. 1972. Ital. Appl. 23449 A/ 71, 21 Apr. 1971.
55. Dunn Jr W.E., US pat., 4085189 (CL. 423-74; c01G 23/04), 18 Apr. 1978, Appl. 4563, 21 Jan. 1970

56. Yamada S., Naka H., Sasaki S. and Yoshida Y., Japan pat., 7437171 (Cl. c22b, c01g) 7 Oct. 1974, Appl. 7069382, 7 Aug 1970.

57. Robinson M., Wilson H.B. and Gray D.A., Brit. Pat., 1359882 (Cl. 022b), Jul. 1974, Appl. 3241 / 71, 27 Jan. 1971.

58. Fukushima S., Saito A. and Kaneko F., Japan, Kokai 7355,113 (Cl. 10E 11), 2 Aug, 1973, Appl. 7190342, 12 Nov 1971.

59. Dunn W.E., Jr., Ger. offen 2221006 (Cl. c21b), 16 Nov. 1972, US., Appl. 13846729 Apr.1971.

60. Chen J.H., Demande Fr., 2132755 (Cl. c22b), 29 Dec. 1972, US pat., Appl. 138467, 29 Apr. 1971.

61. Stickney W.A, Hunter W.L., Elger G.W. and Rhoads S.C., US. Pat.,, 3739061 (Cl. 423-610, c01g), 12 Jun 1973, Appl. 173334, 10 Aug. 1971.

62. Marshall J. and Mac Mahon D.M., Ger. offen. 2200954 (Cl. c22b), 7 Dec. 1972, Brit. Appl. 13606/71, 6 May 1971.

63. Stewart D.F. and Pollard L.J., Ger. offen. 2209795 (Cl. c21b), 21 Sep. 1972, Australian Appl. 4156 / 71, 1 Mar. 1971.

64. Iqubal S.H., Mahajan S.s. and Dadape V.V., Chem. Eng. World, 6(8), (1971) 81-83.

65. Camara E.G., Met. ABM (Ass. Brasil. Metals), 27(166), (1971) 665-669.

66. Moklebust O., US. Pat., 3765868 (Cl. 75/1, c01z, c22b), 16 OCt. 1973, Appl. 160449, 7 Jul. 1971.

67. Soverini A., Sironi G. and Corbetta A., Ital. 926454 (CL. c01G), 17 Aug. 1972, Appl. 21 Apr.1971.

68. Chen J.H., US. Pat., 3967954 (Cl. 75-1T; c22B1/ 00), 6 Jul. 1976, Appl. 132806, 9 Apr. 1971.

69. Iammartino N.R., Chem. Eng. (N.Y.), 79(9), (1972) 3-4.

70. Samanta S., Mishra R.N. and Bhatnagar P.P., Trans. Indian Inst. Metals, 25(1), (1972) 66-74.

71. Lailach G., Bayer E., Scharschmidt J. and Winter G, Ger offen. 2234843 (Cl. c22 C), 31 Jan. 1974, Appl. P 22348432, 15 Jul. 1972.

72.Katoka S. and Yamada S., Chem. Eng. (N.Y.), 80(7), (1973) 92-93.

73. Othmer D.F. and Nowak R. Chem. Eng. Progr 69(6), (1973) 113-114.

74. Komarov O.K., Doronin N.A. and Chistov L.B., Ts vet. Metal; (1973) (1), 49-52; Chem. Abstr. 79 (1973) 7455s.

75. Tittle K. and Foley E., Inst. Mining Met. Trans., Sect.C, 82 (Sept.), (1973) C 135 - C139.

76. Sinha H.N., Titanium Sci. Technol; Proc. Int. Conf. 2nd , 1972 (Pub. 1973) 233- 245

77. Balaszkiewics G., Borowiec K., Kepinski J. and Maternowski B., Pol. 84042 (Cl. c01G 23/04), 30 Sep. 1976, Appl. 166670, 20 Nov.1973.

78. Jena P.K., Jain S.K. and Prasad P.M., Banaras - Met., 5 (1973) 107-117.

79. Metallgesellschaft A. - G; Ger.offen, 2301355 (Cl. c01g), 18 Jul. 1974; Appl.P 2301355.0 12 Jan. 1973.

80. Sundaram M. and Aravamuthan V., Proc. Semin. Eletrochem. 14th, 1973 (Pub 1974) 127-134.

81. Mackey T.S., Light Metals, Proc., 103rd AIME, Annu. Meet 1974 (Pub. 1974) 2, 359-400.

82. Hiester N.K., Liston E.M. and Goerz D., Light Metals, Proc., 103rd AIME Annu. Meet. 1974 (Pub.1974) 2, 401-424.

83. Mackey T.S, Ind. Eng. Chem. Prod. Res. Develop., 13(1), (1974) 9-18.

84. Kurata T., Emi S., Ofuchi K., Takeuchi T. and Sone I., Ger. Offen. 2427947 (Cl. c01g) 2 Jan. 1975, Japan, Appl. 7365723, 11 Jun. 1974.

85. Glaeser H.H., US 3926614 (Cl. 75-1; c21B, c01G), 16 Dec. 1975, Appl. 462535, 19 Apr. 1974.

86. Kurata T., Emi S., Ofuchi K., Takeuchi T. and Sone I., Japan. Kokai 75148212 (Cl. c22B, c01G) 27 Nov. 1975, Appl. 7456909, 21 May 1974.

87. Pogorelov V.I., Baitenev N.A. and Klyashchitskaya N.D., USSR 560830 (Cl. c01G 23/04) 5 Jun.1977, Appl. 2177563, 2 Oct. 1975.

88. Allan B.W., Ger.offen. 2557411 (Cl. c22 B5/ 00) 30 Jun. 1977, Appl. 19 Dec. 1975.

89. Mori T., Kato A. and Kawakami N., Japan Kokai 77128817 (Cl. c22B 34/14), 28 Oct. 1977, Appl. 76/45, 34323, Apr. 1976.

90. Pollard L.J. and Stewart D.F., US 4047934 (Cl. 75-29; c21B 3/04) 13 Sep. 1977, Australian Appl. 75/1, 512, 7 May 1975.

91. Shiah C.D., US 4085190 (Cl. 423-80; c01 G 23/04), 18 Apr.1978, Appl. 572938, 29 Apr. 1975.

92. Reznichenko V.A., Solov'ev V.I., Karayazin I.A. and Bochkov B.A., Protessy Poluch. Rafinirovaniya Tugoplavkikh Met., (1975) 19-28, 253-260; Chem. Abstr., 84 (1976) 63066 f.

93. Moldovan I., Wohl A. and Visa C., Rev. Chim. (Bucharest) 26(9), (1975) 728-732; Chem. Abstr. 84 (1976) 78476 p.

94. Yamada S., Ind. Miner. (London), 100 (1976) 33-40.

95. Moldovan I., Wohl A. and Visa C., Rev. Chim. (Bucharest) 27(2), (1976) 109-112, Chem. Abstr. 85(1976) 35146 j.

96. Pogorelov V.I., Baintenev N.A. and Burlibaev B.M., Deposited Publ. 1973 VINITI, 6691-73.

97. Chen J.H. and Huntoon L.W., US. Pat., 4019898 (Cl. 75-101R; c22 B1/00), 26 Apr. 1977, Appl. 682099, 30 Apr. 1976.

98. Akashi K., Iszizuka R., Inoue M. and Wakasa R., Japan, Kokai, 77116711 (Cl. c22B 34/12), 30 Sep. 1977, Appl. 76/33, 103, 27 Mar. 1976.

99. Preston P.J., Roberts G.L., Jr., Fillmore D.A. and Sheehan G.M., Ger. Offen., 2744805 (Cl. c22B 3/00) 6 Apr. 1978.US, Appl. 729913, 5 Oct. 1976.

100. Awwal M.A., Rahman M., Tarafder S.A. and Huq A.M.S., At. energy. Cen. Dacca, AECD (Rep.) AECD/ CH/ 17, 1976.

101. Elger G.W., Kirby D.E. and Rhoads S.C., US, Bur. Mines, Rep. Invest. RI 8140 (1976)

102. USS Engineers and Consultants, Inc., Japan,Kokai 7801199 (Cl. c01G 23/04) 7 Jan. 1978, US, Appl., 696596, 16 Jun 1976.

103. Hashimoto Y., Itakura N. and Shinozuka K., Japan Kokai, 7852220 (Cl. c22B 34/12), 12 May 1978, Appl. 76/ 127, 423, 23 Oct. 1976.

104. Hockin H.W. and Rolfe P., S.African 7705662 (Cl. c22B), 23 Jun. 1978, Australian Appl. 76/7466, 22 Sep.1976.

105. Lakschevitz Jr. A., De Almeida N.N. and De Almeida A.L., Braz. Pedido PI 7608271 (Cl. c22 B 34/12), 4 Jul. 1978, Appl. 76/8271, 9 Dec. 1976.

106. Jones D.G., Inst. Inst. Mining Met. Trans., sect. c,83 Mar (1974) C1-C9; Izv. Akad. Nauk SSR, Ser.Khim. (1977), (2), 269-280; Chem. Abstr., 86 (1977).

107. O'Brien D.J., Shannon W.T, J. Finch and R. Mills, Proc. Australas. Inst. Min. Metal., 264 (1977) 45-54.

108. Burastero J.J., Rev. Ing. (Montevideo), 20 (1976) 53-65, Chem. Abstr., 86 (1977) 157669 y.

109.Tolley W.K., US. Pat., 4119697 (Cl. 423-82; c01 G 23/06), 10 Oct. 1978, Appl. 814506, 11Jul. 1977

110.Tolley W.K., US. Pat., 4178176 (USA), 19 Jul. 1978.

111. Jain S.K. and Jena P.K., Indian J. Technol., 15(9), (1977) 398-402.

112. Kwangtung Institute of Non-Ferrous Metals Research, Chinshu Hsuch Pao, 13(3), (1977) 161-168; Chem. Abstr., 88 (1978) 193793 j.

113. Burastero J.J., Rev. Ing. (Montevideo) 22 (1977) 37-48; Chem. Abstr., 88(1978) 75962 r.

114. Burastero J.J., Inf. Invest. - Cent. Invest. Technol; Pando, Urug.,980(1975) 58, Chem. Abstr. 89(1978) 63038 b

115. Hussein M.K., Kolta G.A. and El-Tawil S.Z., Egypt. J. Chem., 19(1), (1976) (Pub. 1978) 143-151.

116. Situmorang I. and Oteng S., Laporan - Lembaga Metall. Nas(Indones), 27/LMN/'78, (1978); Chem. Abstr., 91(1979) 160933 p.

117. Negoiu D., Panait C. and Bobirnac I. Rev. Chim. (Bucharest), 30(6), (1979) 546-548; Chem. Abstr., 91(1979) 17804.

118. Quaida M.B., Bonet C. and Foex M., Rev. Int. Hautes Temp. Refract., 15(2), (1978) 147-157; Chem. Abstr. 90(1979) 26779 u.

119. Swinden D.J., and Jones D.G., Trans. Inst. Min. Metall., Sect. C, 87 (June), (1978) 83-87.

120. Rado T.A, US. Pat.,, 4199552 (Cl. 423-83; c01G 23/04), 22 Apr. 1980, Appl. 910051, 26 May 1978.

121. Tolley W.K., US. Pat., 4202863 (USA), 27 Nov. 1980.

122. Bracanin B.F., Clements R.J. and Davey J.M., Proc. Australas. Inst. Min. Metall., 275(1980) 33-42.

123. Negoiu D., Panait C. and Negoiu M., Rev. Chim. (Bucharest), 31 (5), (1980) 451-453, Chem. Abstr., 93 (1980) 135708 c.

124. Borowiec K., Rudy Met. Niezelaz 25(5), (1980) 197-200; Chem. Abstr., 93 (1980) 153800 f.

125. Sinha H.N., Titanium' 80, Science and Technology, Vol. 3 (Proc. conf.), Kyoto, Japan, 19-22 May 1980, TMS / AIME, (1980), 1919-1926.

126. Brunsell D.A. and Riggs O.L., Jr., US 4272343 (USA), 9 Jan. 1980.

127. Mandil M.A. and Zein F.N., Titanium '80, Science and Technology, Vol 3 (Proc. conf.), Kyoto, Japan 19-22 May 1980, TMS / AMIE, (1980) 1983-1897.

128. Easteal A.J. and Morcom A.T., J.Chem. Technol. Biotechnol., 30 (9), (1980) 481-484.

129. Tolley W.K. and Stauter J.C., Ger offen. DE 3008911 (Cl. c22 B 34/12), 24 Sep. 1981, Appl. 7 Mar 1980.

130. Den G., T'U Liao Kung Yeh, 62 (1981) 19-22; Chem. Abstr., 96 (1982) 72375 f.

131. Tsuchida H., Narita E., Takeuchi H., Adachi M. and Okabe T., Bull. Chem. Soc. Jpn., 55(6), (1982) 1934-1938.

132. Duncan J.F. and Metson J.B., N.Z. J. Sci., 25(2), (1982) 111-116, 103-109.

133. Joedden K., Heymer G. and Stephen H.W., Ger. offen, DE 3203482 (Cl. c01 G 23/047), 11 Aug. 1983, Appl. 3 Feb. 1982.

134. Philips W.A. and Thomas J.A., Braz. Pedido, PIBR 8201050 (Cl. c01 G 23/04), 25 Oct. 1983, Appl. 82/1050, 1 Mar. 1982.

135. Brandstatter H.G., US 4521385 (Cl. 423-76; c01G 23/02), 4 Jun. 1985, GB Appl. 82/6846, 2 Mar 1982.

136. Solov'ev V.I., Reznichenko V.A. and Talmud N.I., Tsvetn Met., 12 (1982) 94-96, Chem. Abstr., 98(1983) 93214 j.

137. Yin Y., Xiyou Jinshu, 1(1), 1982 73-79; Chem. Abstr., 99(1983) 903111 y.

138. Ismail M.G.M.U., Amarasekera J. and Kumarasinghe J.S.N., Int. J. Miner.Process, 10(2), (1983) 161-164.

139. Malinsky I. and Castonguay G., CIM Bull; 76 (849), (1983) 136-140; Chem. Abstr., 98 (1983) 147157 p.

140. Girgin I., Madencilik 22(1), (1983) 43-56; Chem. Abstr., 99 (1983) 124913 p.

141. Levin M.I., Leonov A.M. and Titov A.A., Tsvetn. Met., 8(1983) 60-62; Chem. Abstr., 99(1983) 162000 w.

142. Poniatowski M. and Zielinski S., Pr. Inst. Metal. Zelaza in. stanislawa staszica, 35(3-4), (1983) 171-182; Chem. Abstr., 102 (1985) 29219 p.

143. Joedden K., Dorn F.W., Heymer G. and Stephen H.W., Ger offen; DE 3320641 (Cl. c22B 34/12), 13 Dec. 1984, Appl. 8 Jun. 1983.

144. Kahn J.A.; J. Met., 36(7), (1984) 33-38.

145. Sinha H.N., Symp. ser. - Australas. Inst. Min. Metall. (Extr. Metall. Symp.), 36(1984) 163-168.

146. Moles O.W., Ensley K.L. and Perkins H.A., US 4562048 (Cl. 423-81; c01G 23/00) 31 Dec. 1985, Appl. 605475, 30 Apr. 1984.

147. Kurihara J., Koike K. and Watanabe H., Kozangakubu Kenkyu Hokoku (Akita Daigaku) 5 (1984) 41-46, Chem. Abstr., 102(1985) 98886 r.

148. Lee H.C. and Park S.S., Nonmunji p-Sanop Kwahak Kisul Yonguso (Inha Taehakkyo), 13(1985) 257-261, Chem. Abstr. 104(1986) 133428 h.

149. Elger G.W., Wright J.B., J.E. Tress, H.E. Bell and R.R. Jordan, Rep. Invest.US Bur. Mines, RI. 9002, (1986).

150. Lemi Turker, Ismail Girgin and David Goodall, Min. Metall., Int. J. Min.Proc. 24(1988) 173-184.

151. Gauegen M., Ger offen. 1239018, 12 Jul. 1988.

152. Ismail Girgin, Hydro. Metallurgy, 24(1990) 127-134.

153. Grey I.E., Hollitt M.J., Obrien B.A. and O'Brien B.A., Aust. Pat. 9113180, 5 Sep. 1991.

154. Damodaran A.D., Mohan Das P.N., Sai P.S.T. and Surendar G.D., Proc. symp. held at the TMS Annual Meet. in San Diego, California, 1-5 Mar 1992, 1079-1089.

155. Warner N.A., US, Pat. 9324668, 9 Dec. 1993

156. Hoecker W., US, Pat. 612854, 31 Aug. 1994.

157. Mohan Das P.N., Rajeswari L.S., Raghavan P. and Damodaran A.D., Trans. Indian Inst. Met., 48(2), (1995) 97-102.

158. Mohan Das P.N., Damodaran A.D., Velusamy S. and Sasibhushanan S., Indian Patent No. 1033 / DEL/91.

159. Mohan Das P.N., Damodaran A.D., Bhat H.K., Velusamy S. and Sasibhushanan S., Indian Patent No. 1262 / DEL/97.

160. Damodaran A.D., MohanDas P.N., Bhat K.H., Mohanty B.C. and Mukerjee P.S., Indian Patent No. 804/DEL/97

161. Mohan Das P.N., Bhat K.H., Kochu Janaki M.E., Sasibhushanan S., Mukerjee P.S., Mohanty B.C. and Ray H.S., Indian Patent. No. 1578/DEL/99

162. Mohan Das P.N., Bhat K.H., Kochu Janaki M.E., Sasibhushanan S., Mukerjee P.S., Mohanty B.C. and Ray H.S., Canadian Patent (filed) 1998

163. Mohan Das P.N., Bhat K.H., Kochu Janaki M.E., Sasibhushanan S., Mukerjee P.S., Mohanty B.C. and Ray H.S., U.S. Patent (filed) 1998

164. Mohan Das P.N., Bhat K.H., Kochu Janaki M.E., Sasibhushanan S., Mukerjee P.S., Mohanty B.C. and Ray H.S., Australian Patent (filed) 1998

165. Mohan Das P.N., Bhat K.H., Kochu Janaki M.E., Sasibhushanan S., Mukerjee P.S., Mohanty B.C. and Ray H.S., Norwegian Patent No. 20001538 (2000)

166. Mohan Das P.N., Bhat K.H., Kochu Janaki M.E., Sasibhushanan S., Mukerjee P.S., Mohanty B.C. and Ray H.S., South African Patent No.20001497 (2000)

167. Mohan Das P.N., Jaya Kumari E. and Sasibhushanan S., Indian Patent No. 317/98

168. Nagamouri, Megaru and Shigen, Sozai, 114(13), (1998), 977 – 985 (Eng)

169. Bazin C., Girard B., Hodowin D., Powder Technol; (200), 108(2-3), 155-159 (Eng) Elseiver Science

170. Chen Y., Williams J.S., Campbell S.J. and Wang G.M., Mater. Sci. Eng., (1999) A 271 (1-2) 485-490 (Eng) Elseiver Science

171. Bradshaw S.M., S.Afr. J.Sci., 95(9), (1999), 395-396 (Eng)

172. Yang, Daoguang Peop. Rep. China. Faming Zhuanle Shenqing Gongkai Shuo mingshu CN 1,178,251 (8) Apr. 1998 Appl. 97,117,202 (8) Aug (1997)

173. Sahoo, Pravat Kumar, Galgali, Ramachandra Krishna Rao, Singh, Saroj Kumar, Bhattacharjee, Sarama, Mishra, Pratima Kumari, Mohanty and Bishnu Charanarbinda, Scand. J. Metall. 28 (6), (1999), 243-248 (Eng)

174. Technology in Indian Titanium Dioxide Industry, DSIR, Govt. of India, P. 110, 1993.

175. Ouseph C.C., Devassy C.P. and Thomas S.L., "A Text Book of Practical Physics", Viswanathan Publishers, Madras, (1970) P.43

176. Annie George Ph.D thesis, "Study of the Production of Synthetic Rutile from Ilmenite using Agricultural Wastes as Reductants", University of Kerala (1987)

177. Agarwal B.C. and Jain S.P., "A Text Book of Metallurgical Analysis" 3rd Ed. Khanna Publishers, Delhi (1976) P.21

178. Agarwal B.C. and Jain S.P., "A Text Book of Metallurgical Analysis" 3rd Ed. Khanna Publishers, Delhi (1976) P.25

179. Agarwal B.C. and Jain S.P., "A Text Book of Metallurgical Analysis" 3rd Ed. Khanna Publishers, Delhi (1976) P.111

180. Vogel's Textbook of Quantitative Chemical Analysis. ELBS 5th Ed. P.687

181. Han, K.N., Rubcumintara, T. and Fuerstenau, M.C., Metallurgical Transactions, **18B,** 1997, 325 –330

182. Kinetics of Metallurgical Reactions. Oxford & IBH publishing Co. PVT. LTD., 1993, P. 53, 78

183. Kinetics of Metallurgical Reactions., Oxford & IBH publishing Co. PVT. LTD., 1993, P.82

184. Dara S.S., Engineering Chemistry., S.Chand & company Ltd., IV Edn., 1994, P. 222

185. Organic Chemistry Vol. I The Fundamental Principles. ELBS 6th Ed. P. 220

186. Sohn H.Y. and Szekely, J. Chem.Engg. Sci. **27**, (1972) 763

187. Sohn H.Y. and Szekely, J. Chem.Engg. Sci. **28**, (1973) 1169

188. Szekely J., Lin C.I. and Sohn H.Y., Chem. Engg. Sci., **28**, (1973) 1975

189. Szekely J. and Sohn H.Y., Trans. Inst. Min. Met.,**82** (1973) C 92

190. Biscoff K.B., Chem.Engg. **18**, 711 (1963). **20**, (1965) 783

191. Luss D. Can. J. Chem.Engg., **46**, (1968) 154

192. Reid R.C and Sherwood T.K., Properties of gases and liquids, 2nd Ed; Mc Graw – Hill, New York (1966)

193. Smith J.M., Chemical Engg. Kinetics, 2nd Ed; Mc Graw – Hill, New York (1970)

194. Ishida M. and Wen C.Y.: A.I.Ch.E., J **14**, (1968), 311

195.Marinovich,S; Bailey, S; Avraamides J; and Jayasekera, S; The Aus. IMM Annual Conf. 237-241

196.Bard, A.J and Faulkner L.R.; 'Electrochemical Methods' John Wiley & Sons, New York (**1980**)

197.Sato,N; Corrosion, 45(**1989**) 354

198.George Zheng Chen, Derek J. Fray and Tom W. Farthing, Nature, Vol 407; Sep. (**2000**) 361-363